

DESIGN METHODS FOR DEEP FOUNDATIONS

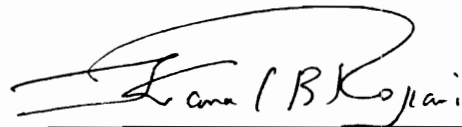
by

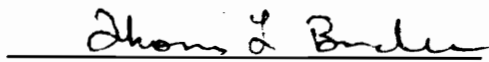
Phillip S.K. Ooi

Dissertation submitted to the Faculty of the
Virginia Polytechnic Institute and State University
in partial fulfillment of the requirement for the degree of
Doctor of Philosophy
in
Civil Engineering

Approved:


J.M. Duncan, Co-Chairman


K.B. Rojiani, Co-Chairman


T.L. Brandon


G.W. Clough


D. Frederick

February, 1991

Blacksburg, Virginia

DESIGN METHODS FOR DEEP FOUNDATIONS

by

Phillip S.K. Ooi

J. M. Duncan, Co-chairman

K. B. Rojiani, Co-chairman

CIVIL ENGINEERING

(ABSTRACT)

The first part of this study was the development of a simplified procedure for analyzing laterally loaded piles and drilled shafts. A computer program that can be used to estimate deflections and maximum bending moments in single fixed-head piles (or drilled shafts) and in groups of fixed-head piles (or drilled shafts) was developed. Using this program, charts were developed for estimating deflections and maximum bending moments directly in some of the more common types of single piles and drilled shafts.

The computer program was also used to perform parametric studies of groups of piles and drilled shafts, from which simple formulae for amplifying single pile (or drilled shaft) deflections and moments to those of the group were derived. These simple formulae enable the analysis and design of groups of deep foundations to be done more efficiently. The simplified procedure was used to analyze four well documented and well instrumented case histories of laterally loaded pile groups. Comparison of the predicted

and measured results indicate that the simplified procedure provides a method of analyzing laterally loaded groups of deep foundations that yield quite accurate predictions of group deflections and moments in some cases, and values that are conservative in other cases.

The second part of the research was to establish load factor design procedures for incorporating margins of safety for axially loaded deep foundations. Values of performance factors were developed for load factor design of axially loaded driven piles and drilled shafts. This was achieved by analyzing statistical information for loads and resistances, and determining the levels of reliability inherent in current designs, through the use of probability theory. Using these results, a target reliability level in the form of a reliability index was selected. Values of performance factors were then obtained for use with the current AASHTO (1989) code for bridges and the ASCE Standard 7-88 (1990) for buildings and other structures. The issues involved in a probabilistic analysis of groups of deep foundations were also discussed.

ACKNOWLEDGEMENTS

I would like to express my gratitude to my advisors, Professor J.M. Duncan and Professor K.B. Rojiani, for their helpful guidance, patience and support during the course of this study. I have learned a lot and benefited a great deal from working with them.

I would also like to thank the other members of my advisory committee: Professor T.L. Brandon, Dean G.W. Clough and Professor D. Frederick for their careful review of this dissertation and their valuable comments.

The research was funded by NCHRP Project 24-4. During the course of this research, the author has also worked with Professor R.M. Barker. His assistance and useful suggestions are greatly appreciated.

The author would also like to thank his co-workers C.K. Tan, S.G. Kim, and J.J. Chen for their assistance and useful discussions. Special thanks go to Clark Morrison for sharing his wealth of knowledge and experience on piles with me. The friendship shown by many fellow graduate students has made the stay in Blacksburg even more worthwhile.

For all their love and support, I dedicate this work to my parents and Lisa.

CHAPTER

PAGE

1.	INTRODUCTION	1
1.1	Objective and Scope	3
1.2	Organization	4
2.	REVIEW OF LITERATURE ON DESIGN OF DEEP FOUNDATIONS	6
2.1	Axial Loading	7
2.1.1	Bearing Capacity of Single Piles	8
2.1.1.1	α Method	9
2.1.1.2	β Method	11
2.1.1.3	λ Method	14
2.1.1.4	SPT Method	14
2.1.1.5	CPT Method	19
2.1.2	Bearing Capacity of Groups of Piles	21
2.1.3	Bearing Capacity of Single Drilled Shafts	25
2.1.3.1	Drilled Shafts in Cohesive Soils	25
2.1.3.2	Drilled Shafts in Cohesionless Soils	31
2.1.3.3	Drilled Shafts in Rock	35
2.1.4	Bearing Capacity of Groups of Drilled Shafts	44
2.2	Lateral Loading	47
2.2.1	Single Piles and Drilled Shafts	47
2.2.1.1	p-y Analysis	48
2.2.1.2	Evans and Duncan Procedure	50
2.2.2	Groups of Piles or Drilled Shafts	51
2.2.2.1	Factors That Affect Group Behavior	52
2.2.2.2	Methods of Predicting Lateral Behavior of Groups of Piles and Drilled Shafts	56
2.3	Methods of Incorporating Margins of Safety in Design	64
2.3.1	Design Criteria	64
2.3.2	Working Stress Design	65
2.3.3	Load (and Resistance) Factor Design	66
2.3.3.1	Load Factors and Load Combinations	69
2.3.3.2	Code Calibration	76
2.3.3.2.1	Calibration by Fitting with Working Stress Design	76
2.3.3.2.2	Calibration Using Reliability Methods	80
2.3.3.2.2.1	Steps in the Calibration Process	80

<u>CHAPTER</u>	<u>PAGE</u>	
2.3.3.2.2.2	Probability Theory and Computation of Reliability Indices	81
2.3.3.2.2.3	Computation of Performance Factors	91
2.3.4	Other Methods of Incorporating Margins of Safety in Designs	92
3.	SIMPLIFIED PROCEDURE FOR DESIGN OF PILES AND DRILLED SHAFTS TO RESIST LATERAL LOADS	96
3.1	Introduction	96
3.2	Single Piles and Drilled Shafts	97
3.2.1	Evans and Duncan Procedure	98
3.2.1.1	Lateral Deflection of Fixed-Head Piles or Drilled Shafts	98
3.2.1.2	Lateral Deflection of Free-Head Piles or Drilled Shafts	106
3.2.1.3	Bending Moments in Fixed-Head Piles or Drilled Shafts	114
3.2.1.4	Bending Moments in Free-Head Piles or Drilled Shafts	118
3.2.1.5	Deflections and Bending Moments in Piles or Drilled Shafts With Caps Above Ground	119
3.2.2	Simplified Procedure for Design of Single Fixed-Head Piles and Drilled Shafts to Resist Lateral Loads	124
3.3	Groups of Piles and Drilled Shafts	138
3.3.1	Focht and Koch's Procedure	139
3.3.2	Parametric Studies for Deflection of Groups of Piles and Drilled Shafts	144
3.3.3	Bending Moments in Groups of Piles and Drilled Shafts	152
3.3.4	Parametric Studies for Maximum Bending Moments in Groups of Piles and Drilled Shafts	154
3.4	Field Experiments	160
4.	DEVELOPMENT OF PERFORMANCE FACTORS FOR LOAD FACTOR DESIGN OF DEEP FOUNDATIONS	196
4.1	Single Piles	198
4.1.1	Introduction	198
4.1.2	Resistance Statistics	199
4.1.3	Load Statistics	208
4.1.4	Results of Calibration	213

<u>CHAPTER</u>	<u>PAGE</u>
4.1.4.1 Reliability Indices	213
4.1.4.2 Target Reliability Indices	216
4.1.4.3 Performance Factors	217
4.1.4.4 Other Performance Factors	224
4.2 Single Drilled Shafts	229
4.2.1 Introduction	229
4.2.2 Resistance Statistics	229
4.2.3 Results of Calibration	231
4.2.3.1 Reliability Indices	231
4.2.3.2 Target Reliability Indices	235
4.2.3.3 Performance Factors	235
4.2.3.4 Other Performance Factors	240
4.3 Groups of Piles or Drilled Shafts	245
5. SUMMARY AND CONCLUSIONS	262
5.1 Recommendations for Future Research	266
5.1.1 Deep Foundations Under Lateral Load	266
5.1.2 Deep Foundations Under Axial Load	267
REFERENCES	269
APPENDIX A PGROUPD: A Computer Program for Estimating Lateral Deflections and Maximum Bending Moments in Laterally Loaded Groups of Fixed-Head Piles and Drilled Shafts	279

LIST OF FIGURES

<u>Figure</u>	<u>Page</u>
2.1 Design Curves for Adhesion Factors for Piles Driven Into Clay Soils (After Tomlinson, 1987)	10
2.2 β Versus OCR for Full Displacement Piles (After Esrig and Kirby, 1979)	13
2.3 λ Coefficient for Driven Pipe Piles (After Vijayvergiya and Focht, 1972)	15
2.4 Relation Between Ultimate Point Resistance of Pile and Depth in Thin Sand Layer Overlying Weak Soil	18
2.5 Pile End-Bearing Computation Procedure After Begemann (After Nottingham and Schmertmann, 1975)	20
2.6 Shaft Friction Correction Factors (After Nottingham and Schmertmann, 1975)	22
2.7 Pile Group Acting as Block Foundation	24
2.8 Portions of Drilled Shafts not Considered in Computing Side Resistance (From Reese and O'Neill, 1988)	28
2.9 Elastic Settlement Influence Factor as a Function of Embedment Ratio and Modulus Ratio (After Donald, Sloan and Chiu, 1980, as presented by Reese and O'Neill, 1988)	38
2.10 Engineering Classification of Intact Rock (After Deere, 1968, and Peck, 1976, as presented by Reese and O'Neill, 1988)	39
2.11 Modulus Reduction Ratio as a Function of RQD (After Bieniawski, 1984, as presented by Reese and O'Neill, 1988)	41
2.12 Bearing Capacity Coefficient, K_{sp} (After Canadian Geotechnical Society, 1985)	43
2.13 p-y Curves for Analysis of Piles and Drilled Shafts Under Lateral Loading (After Reese, 1977)	49
2.14 Influence Factor $I_{\rho F}$ - Fixed-Head Floating Pile, Constant Soil Modulus (After Poulos and Davis, 1980)	59

<u>Figure</u>	<u>Page</u>
2.15 Interaction Factors, $\alpha_{\rho F}$ for Fixed-Head Piles or Drilled Shafts (After Poulos and Davis, 1980)	60
2.16 Frequency Distributions of Load Effect S and Resistance R	82
2.17 Definition of Safety Index β for Lognormal R and S	86
3.1 Lateral Load Versus Deflection for Fixed-Head Piles and Drilled Shafts in Sand (After Evans and Duncan, 1982)	100
3.2 Lateral Load Versus Deflection for Fixed-Head Piles and Drilled Shafts in Clay (After Evans and Duncan, 1982)	101
3.3 Modulus of Elasticity of Concrete (After PCI, 1985)	103
3.4 Resolution of Eccentric Load into a Lateral Load Acting on the Groundline and a Moment	107
3.5 Lateral Load Versus Deflection for Free-Head Piles and Drilled Shafts in Sand (After Evans and Duncan, 1982)	108
3.6 Lateral Load Versus Deflection for Free-Head Piles and Drilled Shafts in Clay (After Evans and Duncan, 1982)	109
3.7 Moment Versus Deflection for Free-Head Piles and Drilled Shafts in Sand (After Evans and Duncan, 1982)	111
3.8 Moment Versus Deflection for Free-Head Piles and Drilled Shafts in Clay (After Evans and Duncan, 1982)	112
3.9 Non-Linear Superposition (After Evans and Duncan, 1982)	113
3.10 Lateral Load Versus Moment for Fixed-Head Piles and Drilled Shafts in Sand (After Evans and Duncan, 1982)	115
3.11 Lateral Load Versus Moment for Fixed-Head Piles and Drilled Shafts in Clay (After Evans and Duncan, 1982)	116

<u>Figure</u>	<u>Page</u>
3.12 Idealized Shear Force and Bending Moment Diagram In a Pile That Can Translate But Not Rotate	122
3.13 Load Versus Deflection and Load Versus Moment for Prestressed Concrete Piles in Sand	125
3.14 Load Versus Deflection and Load Versus Moment for Prestressed Concrete Piles in Clay	126
3.15 Load Versus Deflection and Load Versus Moment for Steel-H Piles in Sand	127
3.16 Load Versus Deflection and Load Versus Moment for Steel-H Piles in Clay	128
3.17 Load Versus Deflection and Load Versus Moment for Drilled Shafts ($A_y/A_g = 1\%$) in Sand	130
3.18 Load Versus Deflection and Load Versus Moment for Drilled Shafts ($A_y/A_g = 2\%$) in Sand	131
3.19 Load Versus Deflection and Load Versus Moment for Drilled Shafts ($A_y/A_g = 4\%$) in Sand	132
3.20 Load Versus Deflection and Load Versus Moment for Drilled Shafts ($A_y/A_g = 8\%$) in Sand	133
3.21 Load Versus Deflection and Load Versus Moment for Drilled Shafts ($A_y/A_g = 1\%$) in Clay	134
3.22 Load Versus Deflection and Load Versus Moment for Drilled Shafts ($A_y/A_g = 2\%$) in Clay	135
3.23 Load Versus Deflection and Load Versus Moment for Drilled Shafts ($A_y/A_g = 4\%$) in Clay	136
3.24 Load Versus Deflection and Load Versus Moment for Drilled Shafts ($A_y/A_g = 8\%$) in Clay	137
3.25 Comparison of Values of Y_g/Y_s Calculated Using the Deflection Amplification Factor With Those Using PGROUPD for Groups of 14 in. Prestressed Concrete Piles in Sand	148
3.26 Comparison of Values of Y_g/Y_s Calculated Using the Deflection Amplification Factor With Those Using PGROUPD for Groups of 30 in. Drilled Shafts in Sand	149

<u>Figure</u>	<u>Page</u>
3.27 Comparison of Values of Y_g/Y_s Calculated Using the Deflection Amplification Factor With Those Using PGROUPD for Groups of 14 in. Prestressed Concrete Piles in Clay	150
3.28 Comparison of Values of Y_g/Y_s Calculated Using the Deflection Amplification Factor With Those Using PGROUPD for Groups of 30 in. Drilled Shafts in Clay	151
3.29 Comparison of Values of M_g/M_s Calculated Using the Moment Amplification Factor With Those Using PGROUPD for Groups of 14 in. Prestressed Concrete Piles in Sand	156
3.30 Comparison of Values of M_g/M_s Calculated Using the Moment Amplification Factor With Those Using PGROUPD for Groups of 30 in. Drilled Shafts in Sand	157
3.31 Comparison of Values of M_g/M_s Calculated Using the Moment Amplification Factor With Those Using PGROUPD for Groups of 14 in. Prestressed Concrete Piles in Clay	158
3.32 Comparison of Values of M_g/M_s Calculated Using the Moment Amplification Factor With Those Using PGROUPD for Groups of 30 in. Drilled Shafts in Clay	159
3.33 Pile Layout - Bucknell University Test Site (After Kim and Brungraber, 1976)	162
3.34 Soil Profile, Standard Penetration Test Data, Laboratory Test Results and Pile Driving Record for the Bucknell University Test Site (After Kim and Brungraber, 1976)	164
3.35 Load Test Setup at the Site of Lock and Dam 26 (After Holloway et al., 1981)	168
3.36 Timber Pile Instrumentation at the Site of Lock and Dam 26 (After Holloway et al., 1981)	170
3.37 Variation of Overconsolidation Ratio with Depth at the Site of Lock and Dam 26 (After Woodward-Clyde Consultants, 1979)	171

<u>Figure</u>	<u>Page</u>
3.38 Results of Cone Penetration Tests Before Pile Installation at the Site of Lock and Dam 26 (After Woodward-Clyde Consultants, 1979)	172
3.39 Lateral Load-Deflection Response of a Single Timber Pile at the Site of Lock and Dam 26 Predicted Using COM622	176
3.40 Comparison of Measured Values of Deflection of the Pile Group at the Site of Lock and Dam 26 with Values Calculated Using COM622 and the Simplified Procedure	179
3.41 Site Layout and Soil Strength Profile for the University of Houston Test Site of a Laterally Loaded Pile Group in Beaumont Clay (After Brown et al., 1987)	182
3.42 Lateral Load-Deflection Response of Piles in Beaumont Clay - University of Houston (After Brown et al., 1987)	184
3.43 Bending Moments in Piles in Beaumont Clay - University of Houston (After Brown et al., 1987)	185
3.44 Site Layout and Soil Strength Profile for the University of Houston Test Site of a Laterally Loaded Pile Group in Compacted Sand (After Brown et al., 1988)	190
3.45 Lateral Load-Deflection Response of Piles in Compacted Sand - University of Houston (After Brown et al., 1988)	191
3.46 Bending Moments in Piles in Compacted Sand - University of Houston (After Brown et al., 1988)	192
4.1 Reliability Index Versus Pile Length for Lognormally Distributed Load and Resistance	214
4.2 Reliability Index Versus Pile Length Using the Advanced Method	215
4.3 Comparison of Performance Factors for Building Code with Performance Factors for AASHTO - Driven Piles	223

<u>Figure</u>		<u>Page</u>
4.4	Reliability Index Versus Length of Drilled Shaft for Lognormally Distributed Load and Resistance	232
4.5	Reliability Index Versus Length of Drilled Shaft Using the Advanced Method	233
4.6	Comparison of Performance Factors for Building Code with Performance Factors for AASHTO - Drilled Shafts	239
4.7	Example Problem for Probability of Failure of Pile Groups	246
4.8	Clay: Driving Order and Load Level Effects on Load Distribution in Piles in Pile Groups (From O'Neill, 1983)	257
4.9	Sand: Driving Order Effects on Load Distribution in Piles in Pile Groups (From O'Neill, 1983)	260
A1	Flow Diagram for Program "PGROUPD"	283

LIST OF TABLES

<u>Table</u>	<u>Page</u>
2.1 Recommended Values of α for Drilled Shafts in Clay (After Reese and O'Neill, 1988)	27
2.2 Summary of Procedures for Estimating Side Resistance (q_s) of Drilled Shafts in Sand	32
2.3 Summary of Procedures for Estimating Base Resistance (q_p) of Drilled Shafts in Sand	34
2.4 Table of Coefficients of γ and β for Working Stress Design of Bridges - AASHTO (1989)	71
2.5 Table of Coefficients of γ and β for Load Factor Design of Bridges - AASHTO (1989)	72
2.6 Load Combinations for Working Stress Design of Buildings and Other Structures - ASCE Standard 7-88 (1990)	74
2.7 Load Combinations for Load Factor Design of Buildings and Other Structures - ASCE Standard (1990)	75
2.8 Values of Performance Factors Corresponding to Different Values of Safety Factor and Dead to Live Load Ratios	79
2.9 Relationship Between Probability of Failure and Reliability Index, β , Assuming Lognormal Loads and Resistances	87
2.10 Values of λ_1 and λ_2 for Different Failure Consequences (After Simpson et al., 1981)	94
3.1 R_I Values for Drilled Shafts with $E_c = 3500$ ksi, $E_s = 29000$ ksi and $c = 3$ in.	105
3.2 Approximate Location of the Maximum Bending Moment in Free-Head Piles or Drilled Shafts	120
3.3 Comparison of Predicted Versus Measured Values of Lateral Deflection of Pile Groups in the Bucknell University test (Kim and Brungraber, 1976)	166

<u>Table</u>	<u>Page</u>
3.4 Comparison of Predicted Versus Measured Values of Bending Moments of Piles in Pile Groups in the Bucknell University Test (Kim and Brungraber, 1976)	167
3.5 Comparison of Single Pile Deflections Predicted Using p-y Analysis with Those Using the Evans and Duncan Procedure for the Load Test Conditions in Lock and Dam 26, Alton, Illinois	174
3.6 Comparison of Maximum Moments in Single Piles Using p-y Analysis with Those Using the Evans and Duncan Procedure for the Load Test Conditions in Lock and Dam 26, Alton, Illinois	175
3.7 Comparison of Values of Maximum Bending Moment Calculated from p-y Analyses of (1) A Free-Head Pile, (2) A Fixed-Head Pile and (3) A Pile Fixed to a Cap 3 ft Above Ground	177
3.8 Comparison of Measured and Predicted Values of Maximum Bending Moment in the Pile Group at Lock and Dam 26, Alton, Illinois	180
3.9 Comparison of Predicted Versus Measured Values of Lateral Deflection of Pile Groups in Beaumont Clay at the University of Houston Test Site (Brown et al., 1987)	187
3.10 Comparison of Predicted Versus Measured Values of Bending Moments in Piles in Pile Groups in Beaumont Clay at the University of Houston Test Site (Brown et al., 1987)	188
3.11 Comparison of Predicted Versus Measured Values of Lateral Deflection of Pile Groups in Compacted Sand at the University of Houston Test Site (Brown et al., 1988)	193
3.12 Comparison of Predicted Versus Measured Values of Bending Moments in Piles in Pile Groups in Compacted Sand at the University of Houston Test Site (Brown et al., 1988)	194
4.1 Summary of Statistics for Axial Capacity of Friction Piles (After Sidi, 1986)	204

<u>Table</u>	<u>Page</u>
4.2 Summary of Statistics for Axial Capacity of Piles Using In Situ Test Results	206
4.3 Scale of Fluctuation and Point Coefficients of Variation for In Situ Soil Parameters	209
4.4 Statistics for Dead and Live Loads	210
4.5 Summary of Reliability Indices for Driven Piles	218
4.6 Performance Factors for Driven Piles	220
4.7 Summary of Performance Factors for Driven Piles Under Axial Load	226
4.8 Summary of Statistics for Axial Capacity of Drilled Shafts	230
4.9 Summary of Reliability Indices for Drilled Shafts	236
4.10 Performance Factors for Drilled Shafts Obtained from Reliability-Based Calibration with a Target Reliability Index of 2.5	237
4.11 Summary of Performance Factors for Drilled Shafts Under Axial Loads	241
4.12 Degree of Correlation Between Piles as Related to Pile Driving Order and Magnitude of Loads	258
A1 Regression Coefficients B_0 , B_1 , B_2 , B_3 and B_4	288

CHAPTER ONE

INTRODUCTION

The simplest type of foundations for buildings, bridges and other structures are spread footings. However, spread footings are not always suitable. For instance, when a structure is underlain by soft clay or loose sand, deep foundations may be needed to develop sufficient load-carrying capacity or to reduce settlements. Fleming et al. (1985) provided a detailed historical account of the evolution of deep foundations; some of the highlights are presented below.

Evidence exists in Europe that pile foundations were used as early as 4000 years ago to support ancient lakefront dwellings. The first recorded use of piles, dates back to the fourth century B.C. where an African tribe, the Peonians, lived on pile supported homes. One of the laws of the tribe was that prior to marriage, a man had to drive three piles into the ground. Being a polygamous tribe, a considerable number of piles must have been driven by their male citizens. In those days, piles were made from wood. Timber piles continued to be used by the Greeks, Romans, Egyptians and other civilizations, but they decay easily when subjected to alternate spells of wetting and drying, or when attacked by marine borers. Failure of piles by

degradation in these ways is known to have claimed many lives.

It was not until the mid 1830s that metal piles first appeared, in the form of cast iron pipes, and they were usually used for more important structures. In 1838, screw piles were employed for the first time in the construction of a lighthouse on the Thames river in England. The inventor of screw piles was Alexander Mitchell. At the end of the nineteenth century, highway bridges in the state of Nevada were the first structures to be founded on steel-I beam piles. Around 1908, steel-I beam piles were superceded by steel-H piles, marketed by Bethel Steel Co.

Joseph Aspdin patented Portland cement in 1824, but it was only in 1897 that A.A. Raymond developed the Raymond cast-in-place concrete pile system. Close-ended steel pipe piles that were filled with concrete after driving were developed in 1903 by R.J. Beale. In 1908, a Belgian by the name of E. Frankignoul invented the Franki driven-tube pile, and, with the addition of an expanded base, it later became the renowned Franki pile. Precast concrete piles also became available around the same time.

The earliest form of drilled shafts was called a "well foundation", where a hand-dug excavation or boring is filled with stone. This concept was used in the construction of the Taj Mahal in India from 1632 to 1650. The advent of

Portland cement in 1824, and the development of the percussion boring equipment used for sinking wells in the early 1900s led to the development of drilled shafts.

Over the years, research and development have produced a wealth of information on the design and construction of deep foundations. Deep foundations should be designed to resist both axial and lateral loads. Many reliable methods exist for the design of axially loaded deep foundations. However, the procedure for designing deep foundations under lateral loading are often very involved, and procedures for estimating lateral deflections and bending moments in groups of piles and drilled shafts are still evolving.

1.1 Objective and Scope

There are two main objectives in this study. The first is the development of a simplified method for estimating lateral deflections and maximum bending moments in single piles and drilled shafts and in groups of piles and drilled shafts. To facilitate this process, a computer program that can be used to estimate deflections and moments in individual piles and drilled shafts as well as groups of piles and drilled shafts is developed. Using this program, charts for estimating deflections and maximum bending moments in some of the more common types of single piles and

drilled shafts are developed. The computer program is also used to perform parametric studies of groups of piles and drilled shafts from which, simple formulae for amplifying single pile (or drilled shaft) deflections and moments to those for the group are derived.

The second objective of this study is to develop performance factors for design of axially loaded piles and drilled shafts using a reliability-based approach. This study begins with an analysis of load and resistance statistics. The mathematical formulation for computing reliability indices is also presented. This is followed by computing reliability indices for several state-of-the-art methods for predicting pile and drilled shaft capacities. The sensitivity of the reliability indices to dead to live load ratios and geometry of the deep foundations is also studied. Finally, target reliability indices are selected and used to determine the performance factors.

1.3 Organization

A review of literature on methods of designing piles and drilled shafts under axial and lateral loads is given in Chapter 2. Also included in Chapter 2 is a review of methods of incorporating margins of safety in the design of deep foundations.

The development of a simplified procedure for analyzing laterally loaded piles and drilled shafts is described in Chapter 3, accompanied by analyses of four well documented case histories using the newly developed simplified procedure. Comparisons are made between the predicted and actual behavior.

In Chapter 4, the reliabilities of existing methods of designing axially loaded piles and drilled shafts are assessed through an analysis of the statistics of loads, load tests on piles and drilled shafts, and soil parameters. Using probability theory, the level of reliability inherent in current design methods is determined, and recommendations for incorporating margins of safety in the design of axially loaded deep foundations are given in terms of performance factors, that account for the uncertainty in the resistance (eg. bearing capacity of foundations).

Chapter 5 presents a summary of the studies and recommendations for future research.

CHAPTER TWO

REVIEW OF LITERATURE ON DESIGN OF DEEP FOUNDATIONS

Deep foundations are columnar elements embedded in the soil beneath a structure for the purpose of transferring loads from the superstructure into the underlying soil or rock. Deep foundations must be designed to support the imposed axial and horizontal loads safely and with tolerably small movements. They can be divided into two classes: (i) piles which are installed by driving and (ii) drilled shafts which are installed by placing concrete in drilled holes.

The governing criterion in the design of vertically loaded piles or piers is usually the magnitude of settlement under load or safety against failure of the foundation soils. The structural capacity of the piles or piers may govern in cases where the foundation elements bear on sound rock.

The governing criterion in the design of laterally loaded piles and drilled shafts is usually either the maximum tolerable deflection or the structural capacity of the deep foundation itself. Mobilizing the ultimate lateral capacity of the soil requires such large displacements that this is not a realistic possibility, and ultimate soil failure does not control the design.

The current-state-of-the-art with respect to design of deep foundations as reflected in the literature is described in the following sections.

2.1 Axial Loading

Drilled shafts may be used individually or in groups. However, piles are usually driven in groups, and the most important consideration is the capacity of the pile group. At small spacings, especially in cohesive soils, groups of piles or drilled shafts may fail as a unit consisting of the piles and the soil between the piles. At large spacings, the group capacity is equal to the sum of the individual pile or drilled shaft capacities.

The bearing capacity of single piles is therefore important because it may relate directly to the group capacity, and it will be discussed in detail, followed by the bearing capacity of pile groups. Similar discussions are presented on the bearing capacity of single drilled shafts and groups of shafts.

2.1.1 Bearing Capacity of Single Piles

The ultimate bearing capacity of deep foundations is the sum of the shaft and point resistances, minus the weight of the pile or drilled shaft:

$$Q_{ult} = Q_s + Q_p - W \quad (2-1)$$

where Q_{ult} = total ultimate bearing capacity of a pile or a drilled shaft

Q_s = ultimate load carried in side resistance by piles or drilled shafts

$$= A_s q_s$$

Q_p = ultimate load carried in end bearing by piles or drilled shafts

$$= A_p q_p$$

A_s = surface area of the shaft of a pile or a drilled shaft

A_p = area of the tip of a pile or a drilled shaft

q_s = ultimate unit side resistance of a pile or a drilled shaft

q_p = ultimate unit tip resistance of a pile or a drilled shaft

W = weight of the pile or the drilled shaft

In practice, the weight of the pile or drilled shaft is small compared to the other terms, and is usually disregarded.

One rational method of estimating the bearing capacity of piles in compression is called the "static" approach. Static formulae are based on either classical soil mechanics theories or empirical correlations. These include the α , β and λ methods and methods based on in situ tests such as the cone penetration test (CPT) or the standard penetration test (SPT). The α , β and λ methods are more suited for piles in cohesive soils, while the SPT and CPT correlations are better suited for piles in cohesionless soils.

2.1.1.1 α -method

The α method relates the adhesion between the pile and the clay to the undrained shear strength of the clay. The ultimate unit skin friction, q_s , can be expressed by:

$$q_s = \alpha S_u \quad (2-2)$$

where S_u = mean undrained shear strength

α = adhesion factor applied to S_u

Tomlinson (1987) found that the value of the adhesion factor, α , varies with the value of the undrained shear strength, S_u , as shown in Fig. 2.1. Although not shown in

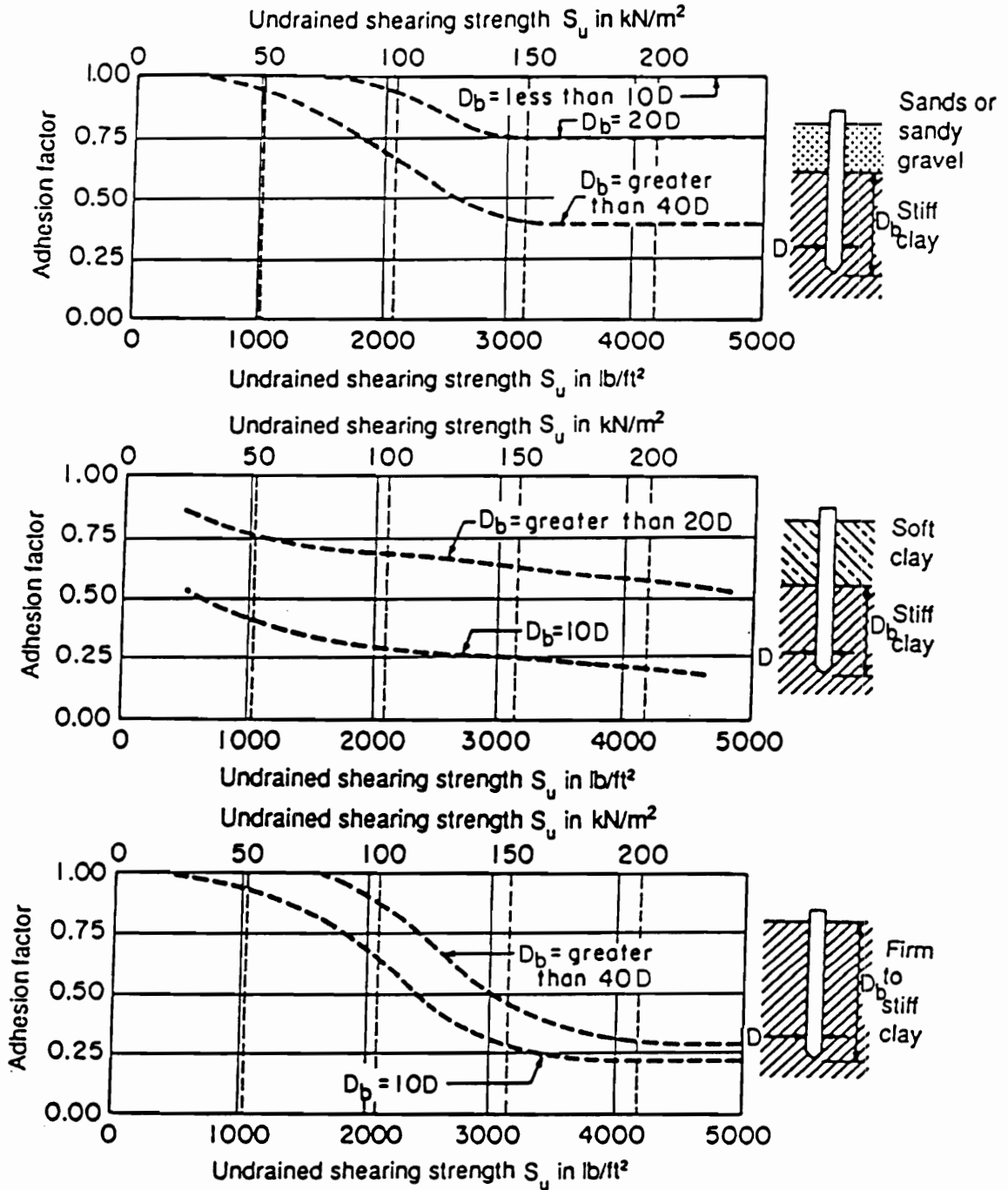


Figure 2.1 Design Curves for Adhesion Factors for Piles Driven Into Clay Soils (After Tomlinson, 1987)

the figure, there is considerable scatter around the curves because factors such as pile length, overconsolidation ratio and coefficient of lateral earth pressure are not represented, although these factors affect the pile capacity. Uncertainty in the undrained shear strength also contributes to the scatter. However, the α -method is used frequently in practice because it is simple, and because no method is available that fully reflects the effects of pile installation and all of the factors involved in the reconsolidation processes.

The value of the adhesion factor (α) also depends on the type of soil above the cohesive bearing stratum (Fig. 2.1). Soil from the upper layers may be carried down with the pile into the clay bearing stratum. Bringing down soft clay will tend to reduce adhesion while dragdown of cohesionless soil will increase adhesion in the lower cohesive stratum.

2.1.1.2 β -method

The β -method is an effective stress method for predicting skin friction of piles. The ultimate unit skin friction, q_s , is related to the effective stresses in the ground as follows:

$$q_s = \sigma_h' \tan \delta$$

$$\begin{aligned}
 &= K \tan \delta \sigma_v' \\
 &= \beta \sigma_v'
 \end{aligned}
 \tag{2-3}$$

where σ_h' and σ_v' are the horizontal and vertical effective stresses respectively, δ is the angle of shearing resistance between the soil and the pile, K is the coefficient of lateral earth pressure and β , equals $K \tan \delta$.

The value of the parameter K is very important. Kulhawy et al. (1983) noted that "the coefficient, K , is a function of the original in situ horizontal stresses and the stress changes caused in response to construction, loading and time." When a pile is first driven into the ground, the displaced soil exerts horizontal stresses on the pile. Excess pore pressures are generated and thus σ_v' is low, giving a high initial K value. As pore pressure dissipates, K changes with time. Depending on the overconsolidation ratio (OCR), the value of K may be higher or lower than the at-rest coefficient of lateral earth pressure, K_0 . Esrig and Kirby (1979) developed the relationship between β and OCR that is shown in Fig. 2.2.

The β -method has been found to work best for piles in normally consolidated and lightly overconsolidated clays. The method tends to overpredict skin friction of piles in heavily overconsolidated soils. Esrig and Kirby suggested that for heavily overconsolidated clays, the value of β should not exceed 2.

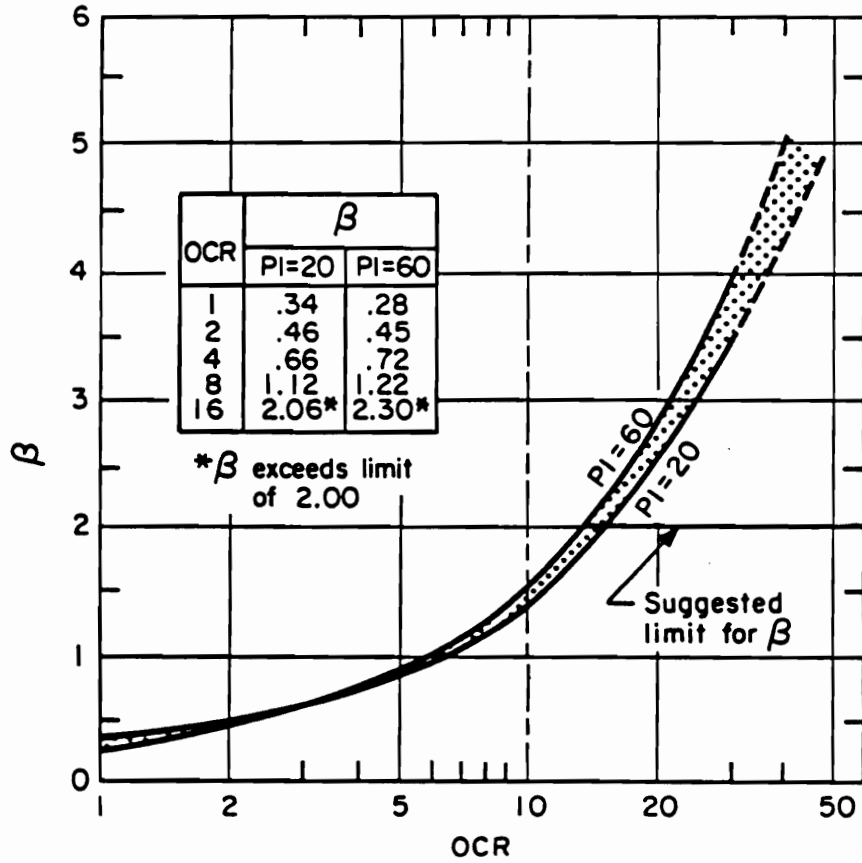


Figure 2.2 β Versus OCR for Full Displacement Piles
(After Esrig and Kirby, 1979)

2.1.1.3 λ -method

Vijayvergiya and Focht (1972) recognized that the passive lateral earth pressure ($\sigma_h' = \sigma_v' + 2S_u$) and the ultimate unit skin friction of a pile are related. They proposed the following relationship:

$$q_s = \lambda(\sigma_v' + 2S_u) \quad (2-4)$$

where λ is an empirical coefficient shown in Fig. 2.3. The value of λ decreases with pile length and was found empirically by examining the results of load tests on steel pipe piles.

2.1.1.4 SPT Method

In situ tests are widely used in cohesionless soils because obtaining good quality samples of cohesionless soils is very difficult. In situ test parameters may be used to estimate the tip resistance and skin friction of piles. Two frequently used in situ test methods for predicting pile capacity are the standard penetration test (SPT) method and the cone penetration test (CPT) method.

Meyerhof (1976) correlated the tip capacity and shaft resistance of piles with the SPT blow-count. This method applies only to sands and non-plastic silts.

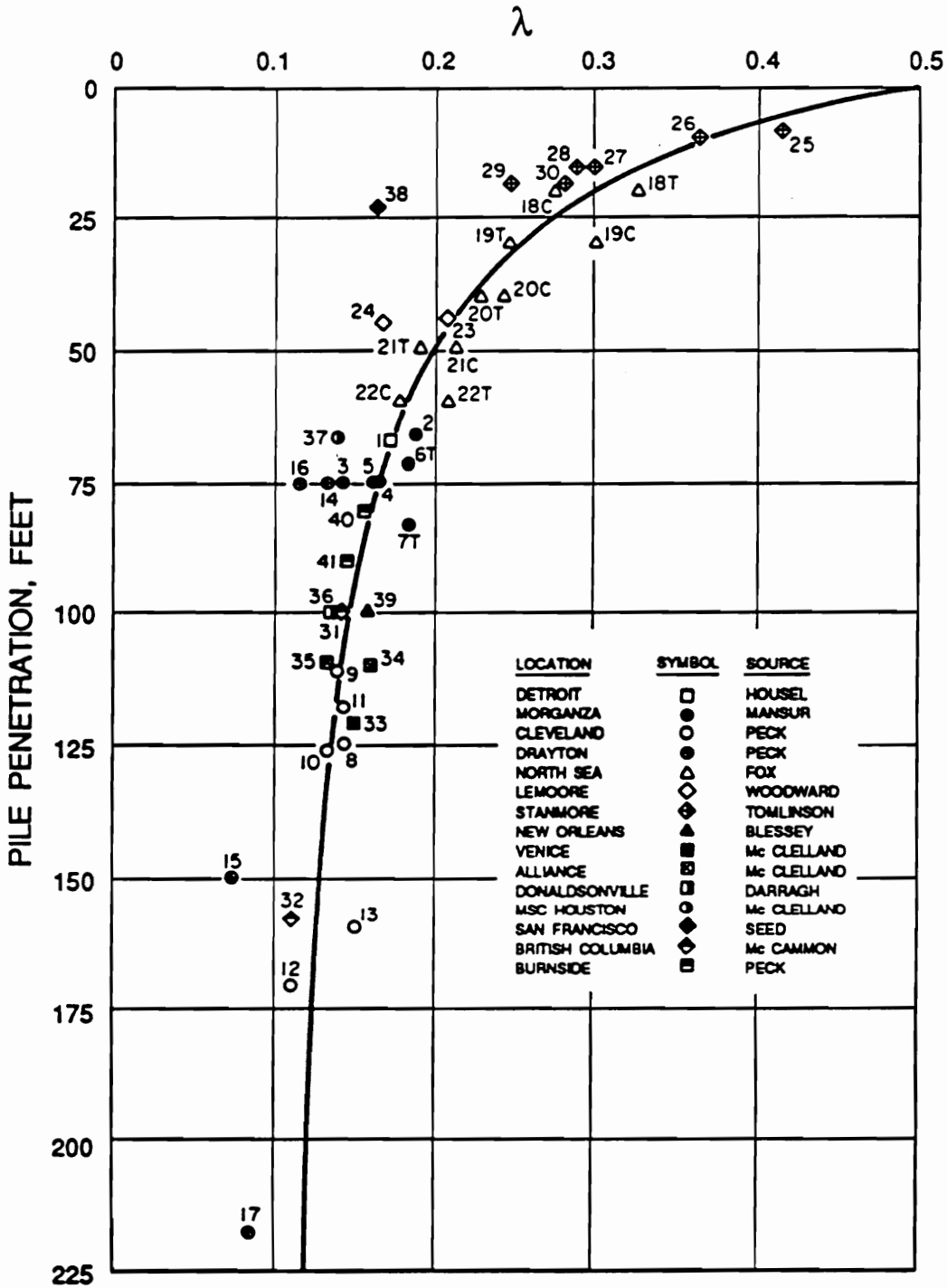


Figure 2.3 λ Coefficient for Driven Pipe Piles (After Vijayvergiya and Focht, 1972)

(a) Pile Tip Capacity - The ultimate unit tip resistance for piles, q_p (in tons per square foot) driven to a depth D_b into a cohesionless soil stratum can be approximated by:

$$q_p = \frac{0.4N_{\text{corr}}D_b}{D} \leq q_1 \quad (2-5)$$

where N_{corr} = average corrected SPT-N value near the pile tip

$$= [0.77 \log_{10} (20/\sigma_v')] N \quad (2-6)$$

N = measured SPT-N value

σ_v' = effective vertical stress at the pile tip (in tons/ft²)

D = pile width or diameter

q_1 = limiting point resistance (tons per square foot)

$$= 4N_{\text{corr}} \text{ for sands} \quad (2-7)$$

$$= 3N_{\text{corr}} \text{ for non-plastic silt} \quad (2-8)$$

The rationale behind Equation 2-5 is that the ultimate unit tip capacity in a cohesionless stratum increases linearly with the embedment ratio (D_b/D) up to a critical embedment ratio of 10 for sands, or 7.5 for silts. At higher embedment ratios, the tip capacity remains constant at its limiting value, q_1 .

In bearing strata with highly varying blow-counts, Meyerhof (1976) proposed that the average blow-count be

obtained within the range of depth from 4 pile diameters above to 1 pile diameter below the tip.

Piles bearing on a firm stratum overlying a weaker layer may punch into the lower stratum as shown in Fig. 2.4. Meyerhof (1976) suggested that if the distance between the pile tip and the weak deposit (H) is less than 10 pile diameters, the ultimate point resistance will be:

$$q_p = q_o + \frac{(q_1 - q_o)H}{10D} \leq q_1 \quad (2-9)$$

where q_1 is the limiting unit tip resistance in the upper stratum and q_o is the limiting unit tip resistance in the lower stratum.

(b) Skin Friction - The skin friction of piles in cohesionless soils may be estimated using the following equation (Meyerhof, 1976):

$$q_s = \frac{\bar{N}}{50} \text{ for driven displacement piles} \quad (2-10)$$

$$q_s = \frac{\bar{N}}{100} \text{ for non-displacement piles} \quad (2-11)$$

(eg. steel-H piles)

where q_s = unit skin friction for driven piles measured in
tsf

\bar{N} = average (uncorrected) SPT-blow count along the
pile shaft.

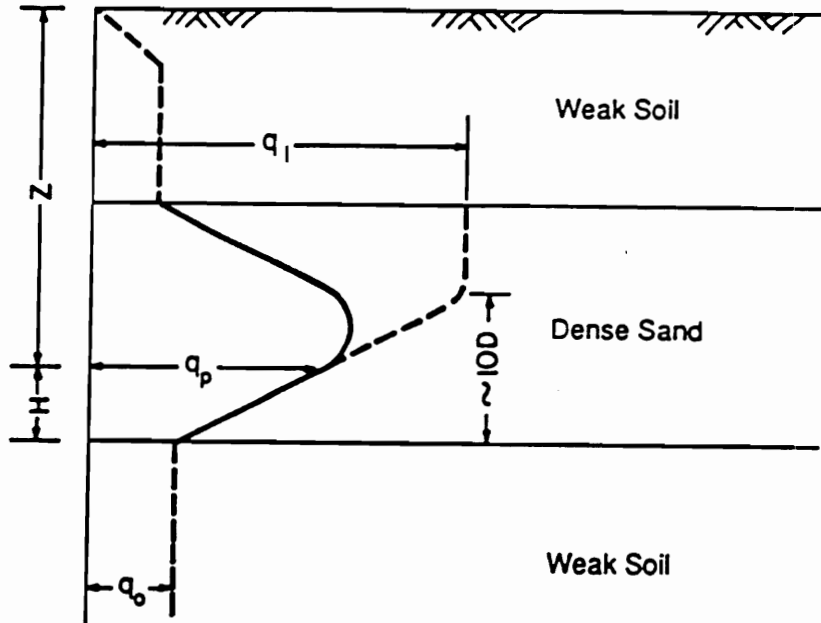


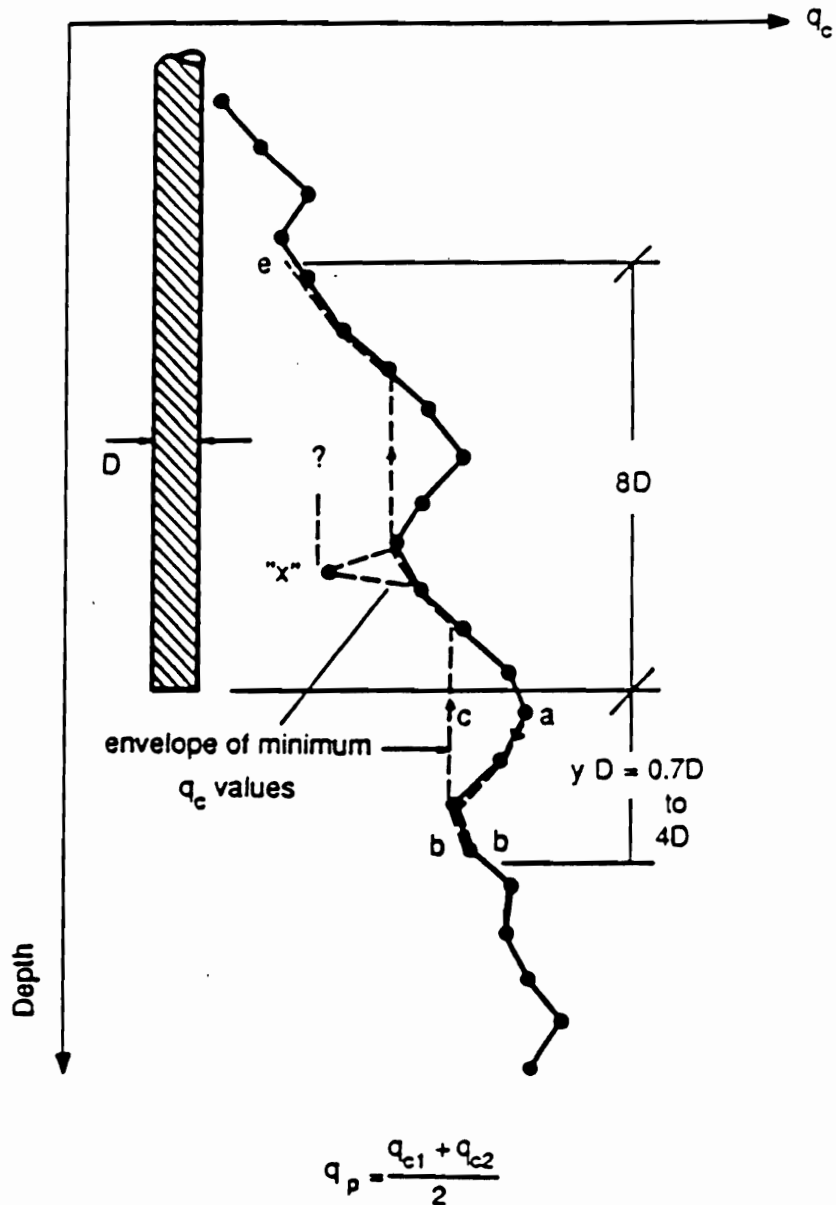
Figure 2.4 Relation Between Ultimate Point Resistance of Pile and Depth in Thin Sand Layer Overlying Weak Soil

2.1.1.5 CPT method

The cone penetration test yields two useful parameters that can be applied to pile capacity prediction: (i) the cone penetration resistance, q_c , which is related to the tip capacity of piles and (ii) sleeve friction, f_s , which can be used to estimate the skin friction capacity. Nottingham and Schmertmann (1975) developed the following procedure for estimating pile capacity:

(a) Pile Tip Capacity - Nottingham and Schmertmann (1975) found that a procedure that had been developed earlier by Begemann provided a good estimation of end bearing capacity in piles for all soil types. Begemann's procedure for estimating the tip resistance, q_p is outlined in Fig. 2.5. The minimum average cone resistance between 0.7 and 4 pile diameters below the elevation of the pile tip is obtained by a trial and error process, with the use of the minimum-path rule (see Fig. 2.5). The "minimum-path rule" developed by Begemann is also used to find the value of cone resistance for the soil for a distance of eight pile diameters above the tip. The two results are then averaged to give the pile tip resistance.

(b) Skin Friction - Nottingham and Schmertmann (1975) presented the following equation for computing the ultimate skin friction of piles:



q_{c1} = Average of all values of q_c along path a-b-c over a distance of yD below the pile tip. Sum q_c values measured at each elevation in the downward path a-b. Sum q_c values at every elevation where a cone resistance reading is made, along the upward path b-c, but at each elevation take the minimum of (i) the q_c value at that elevation or (ii) the lowest q_c value between that elevation and the elevation of point b. This method of determining q_c is called the "minimum path" rule. Compute q_{c1} for y -values from 0.7 to 4.0 and use the minimum q_{c1} value obtained.

q_{c2} = Average q_c over a distance of $8D$ above the pile tip (path c-e). Use the minimum path rule as for path b-c in the q_{c1} computations. Ignore any very extreme peaks or depressions (such as "x" in the diagram above) if the soil is a sand, but include these in minimum path if the soil is a clay.

Figure 2.5 Pile End-Bearing Computation Procedure After Begemann (After Nottingham and Schmertmann, 1975)

$$Q_s = K_{s,c} \left[\sum_{L_f=0}^{8D} (L_f/8D) f_s a_s + \sum_{L_f=8D}^Z f_s a_s \right] \quad (2-12)$$

where Q_s = ultimate skin friction capacity of the pile

$K_{s,c}$ = correction factors: K_c for clays and K_s for sands
(see Fig. 2.6)

L_f = depth to point considered

D = pile width or diameter

f_s = unit local sleeve friction resistance from CPT at
the point considered

a_s = pile perimeter

Z = total embedded pile length.

The advantages of using this method is that it (i) corrects for the type of cone penetrometer used (electrical versus mechanical), (ii) accounts for the material of the pile, (iii) considers the soil type, and (iv) corrects for depth of pile embedment.

2.1.2 Bearing Capacity of Groups of Piles

The ultimate bearing capacity of a pile group in sand is estimated by summing the capacities of all the piles in the group (Poulos and Davis, 1980). The group efficiency, defined as the ratio of the ultimate load capacity of the pile group to the sum of the ultimate capacities of the individual piles, is conservatively taken as unity.

Nottingham's (1975) factors K_s and K_c

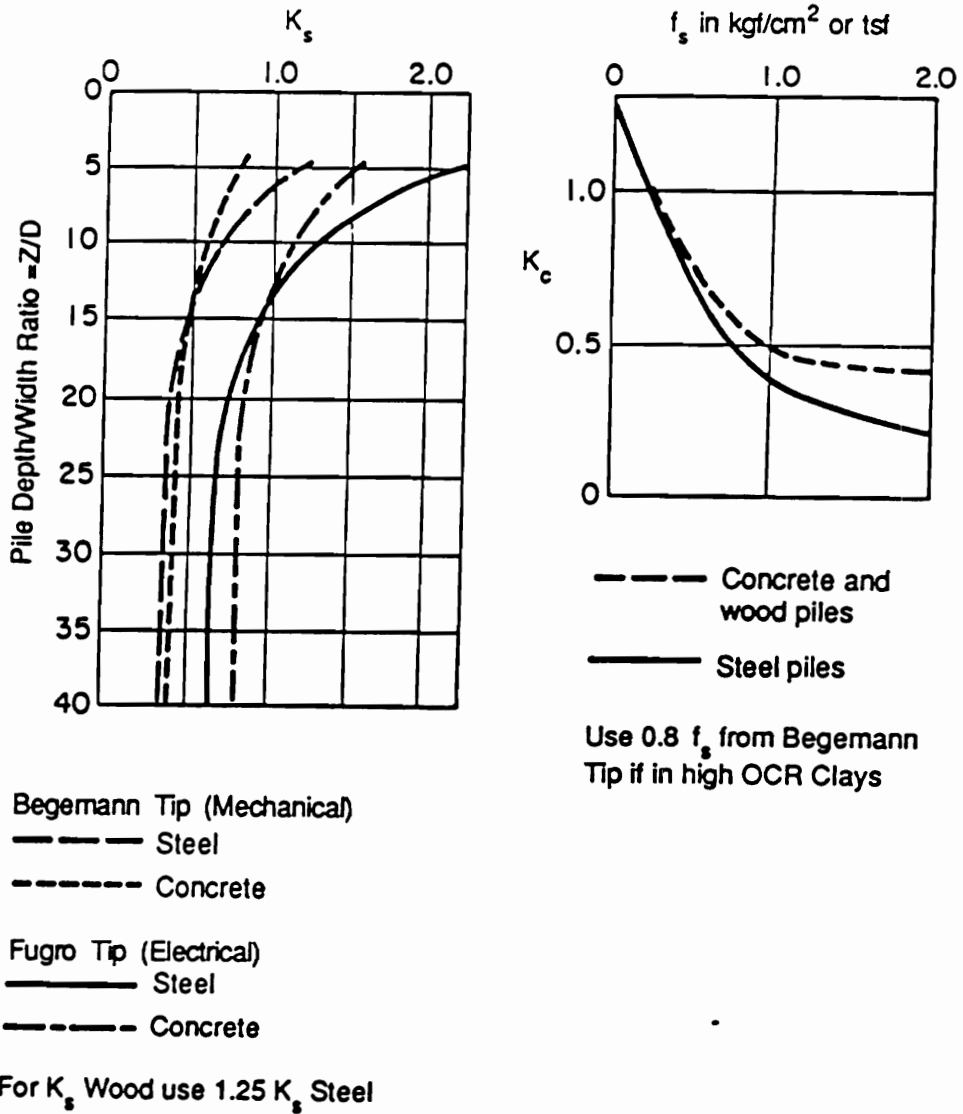


Figure 2.6 Shaft Friction Correction Factors
(After Nottingham and Schmertmann, 1975)

Evaluation of group capacity of piles in cohesionless soil is the same for the case when the pile cap is, and is not in contact with the ground.

For pile groups in cohesive soil, the presence and contact of the pile cap with the ground surface must be considered. Pile groups in clay with the cap in firm contact with the ground may fail as a unit consisting of the piles and the block of soil contained within the piles, and the ultimate bearing capacity in this case may be taken as the minimum of the following two values:

- (i) the sum of the individual pile capacities, or
- (ii) the bearing capacity for block failure of the group.

For a pile group of width X , length Y and depth Z (Fig. 2.7), the bearing capacity for block failure is given by:

$$Q_g = (2X + 2Y)Z\bar{S}_u + XYN_C S_u \quad (2-13)$$

where \bar{S}_u = average undrained shear strength along the depth of penetration of the piles

S_u = undrained shear strength at the base of the group

$$N_C = 5(1 + 0.2X/Y)(1 + 0.2Z/X) \quad \text{for } Z/X \leq 2.5 \quad (2-14)$$

$$N_C = 7.5(1 + 0.2X/Y) \quad \text{for } Z/X > 2.5 \quad (2-15)$$

If the pile cap is not in firm contact with the ground and the clay is normally or slightly overconsolidated or is sensitive, the individual pile capacity must be multiplied by an efficiency factor, η , where $\eta = 0.7$ for a pile spacing

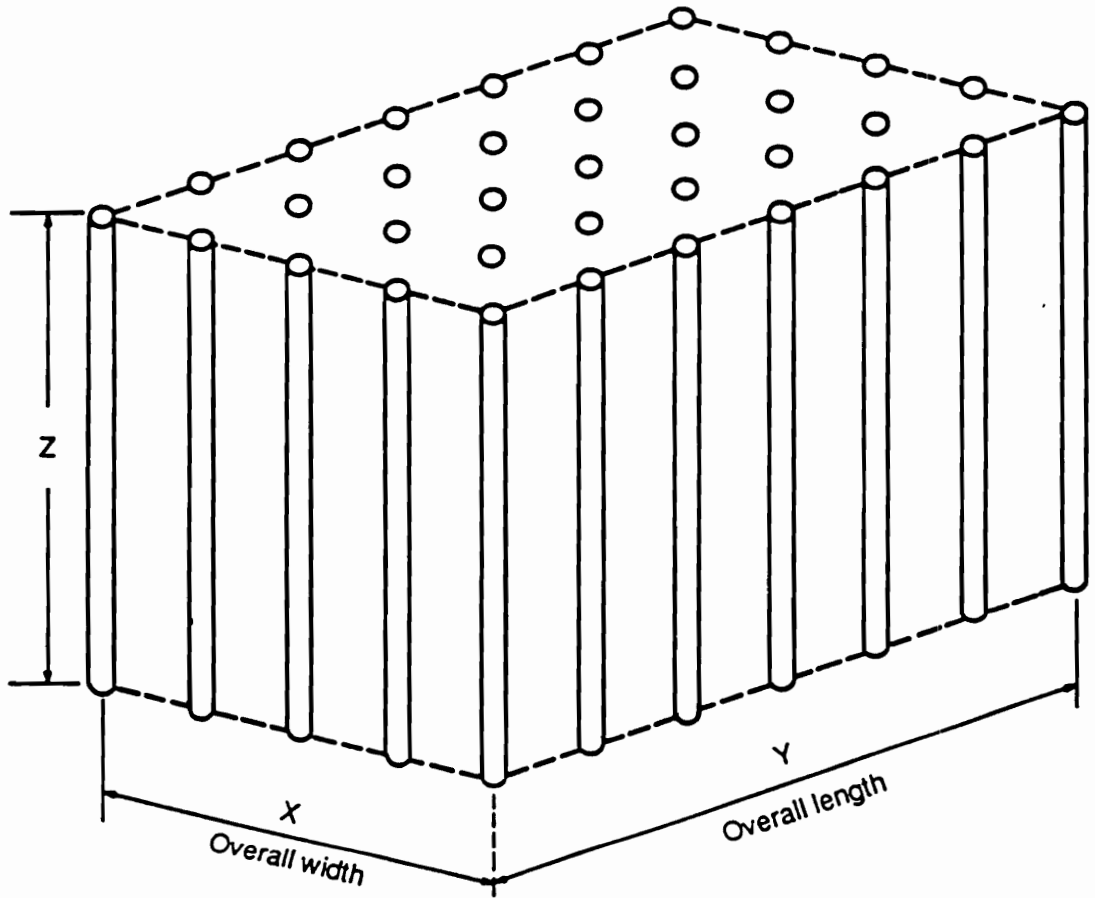


Figure 2.7 Pile Group Acting as Block Foundation

of $3D$ and $\eta = 1.0$ for a pile spacing of $6D$. The value of η may be linearly interpolated for intermediate spacings. The group capacity is then calculated as the minimum of:

- (i) the sum of the individual pile capacities multiplied by η , or
- (ii) the bearing capacity for block failure as described above.

If the clay is overconsolidated and insensitive, then the group should be treated as if the cap were in contact with the ground.

The vertical bearing capacity of a pile group containing batter piles may be estimated by treating the batter piles as vertical piles.

2.1.3 Bearing Capacity of Single Drilled Shafts

2.1.3.1 Drilled Shafts in Cohesive Soils

The ultimate capacities of drilled shafts in cohesive soils are usually governed by the conditions at the end of construction. Therefore, drilled shafts in clays are usually designed using total stress methods (eg. Reese and O'Neill, 1988). However, in some circumstances, the strength of the soil can change with time. These include shafts in expansive soils and shafts installed in cohesive soils that consolidate and move downward relative to the

shafts. In these cases, effective stress analyses (not discussed here) may be used.

(i) Shaft Resistance (α -method)

The α -method relates the adhesion between the drilled shaft and the clay to the undrained shear strength of the clay. The ultimate unit skin friction, q_s , can be expressed by:

$$q_s = \alpha S_u \quad (2-16)$$

where S_u = undrained shear strength and α = adhesion factor applied to S_u . Reese and O'Neill (1988) developed a procedure for prescribing α values along the length of drilled shafts in overconsolidated clays. Table 2.1 shows the values of α recommended by Reese and O'Neill. Fig. 2.8 shows the portions of the length of drilled shafts that are considered not to contribute to shaft adhesion.

The value of α is zero for the top 5 ft, consistent with findings from load tests. Load test data on instrumented drilled shafts have shown load transfer to be zero at the ground surface, increasing with depth. Because the rate of increase has not been determined with much certainty, Reese and O'Neill chose to use $\alpha = 0$ in the top 5 ft.

Table 2.1 Recommended Values of α for Drilled Shafts in Clay
(After Reese and O'Neill, 1988)

Location Along Drilled Shaft	Undrained Shear Strength	Value of α
From ground surface to depth along drilled shaft of 5 ft*	-	0
Bottom 1 diameter of the drilled shaft or 1 stem diameter above the top of the bell (if skin friction is being used)	-	0
All other points along the sides of the drilled shaft	< 2 tsf	0.55
	2 - 3 tsf	0.49
	3 - 4 tsf	0.42
	4 - 5 tsf	0.38
	5 - 6 tsf	0.35
	6 - 7 tsf	0.33
	7 - 8 tsf	0.32
	8 - 9 tsf	0.31
	> 9 tsf	Treat as Rock

* The depth of 5 ft may need adjustment if the drilled shaft is installed in expansive clays, or if there is substantial groundline deflection from lateral loading.

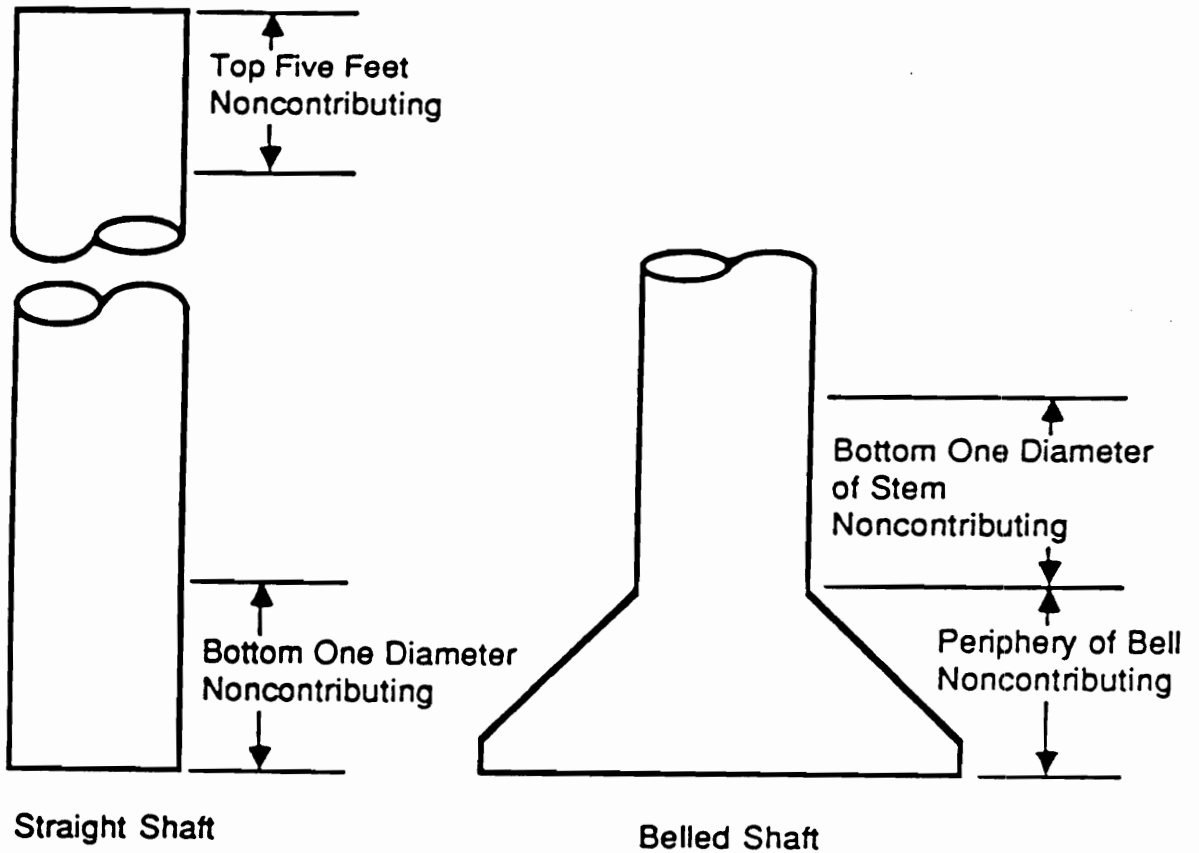


Figure 2.8 Portions of Drilled Shafts not Considered in Computing Side Resistance (From Reese and O'Neill, 1988)

The footnote in Table 2.1 accounts for the following:

(a) during dry weather, expansive soils shrink and move away from the shaft. A value of $\alpha = 0$ may be selected for a depth greater than 5 ft as indicated by the depth of seasonal moisture change in areas with expansive soil, and
(b) during lateral loading, the clay at the groundline may be pushed away due to lateral deflection of the shaft, especially if the loads are cyclic in nature, causing the shaft to be deflected back and forth.

The value of α is also zero for a distance of 1 diameter above the base of the shaft, because downward movement of the base can cause a tensile crack to develop in the soil near the base.

Based on load tests on drilled shafts in clay, Reese and O'Neill suggested the use of α values in Table 2.1 for the remaining portions of the drilled shaft. The value of α may be less than those in Table 2.1 in sensitive clays. In such soils, load tests should be conducted to establish appropriate values of α .

The data used in deriving this design method does not include clays with (a) S_u greater than 6 tsf, (b) OCR greater than 10, or (c) sensitivity greater than 4.

(ii) End Bearing

Reese and O'Neill (1988) applied Skempton's (1951) expression for end bearing of piles in clay, to drilled shafts as follows:

$$q_p = N_c S_u \leq 40 \text{ tsf} \quad (2-17)$$

where $N_c = 6(1 + 0.2Z/D_p) \leq 9$

S_u = average undrained shear strength of clay over a depth of one to two diameters below the base

Z = distance that the shaft extends into the ground

D_p = diameter of the base of the shaft

The limiting value of q_p (40 tsf) is based on the largest value measured in clays and is not a theoretical limit. Higher values of q_p may be used if indicated by load test results.

N_c should be reduced by 1/3 (i.e., use $2N_c/3$ in computations) in soft clays to account for large displacements prior to bearing capacity failure.

If D_p exceeds 75 in., the ultimate unit end bearing capacity of drilled shafts in stiff to hard clay should be reduced to q_{pr} as follows (Reese and O'Neill, 1988):

$$q_{pr} = F_r q_p \quad (2-18)$$

$$\text{where } F_r = \frac{2.5}{aD_p \text{ (in.)} + 2.5b} \leq 1.0$$

$$a = 0.0071 + 0.0021 Z/D_p \leq 0.015$$

$$b = 0.45\sqrt{S_u \text{ (ksf)}} \quad \text{where } 0.5 \leq b \leq 1.5$$

Equation 2-18 is based on load tests of large diameter underreamed drilled shafts in clay, and q_{pr} corresponds to a base settlement of 2.5 in.

2.1.3.2 Drilled Shafts in Cohesionless Soils

While many field load tests have been performed on drilled shafts in clays, very few have been performed on drilled shafts in sands.

The shear strength of cohesionless soils can be characterized by an angle of internal friction (ϕ') or empirically related to values of SPT blow count (N). Methods of estimating shaft resistance and end bearing using either ϕ' or N values are presented below.

(i) Shaft Resistance

Table 2.2 summarizes 5 methods of predicting shaft resistance of bored piles in sand. Quiros and Reese (1977) and Reese and O'Neill (1988) indicate that the unit side resistance should be limited to 2 tsf, corresponding to the

Table 2.2 Summary of Procedures for Estimating Side Resistance (q_s) of Drilled Shafts in Sand.

REFERENCE	DESCRIPTION
Touma and Reese (1974)	$q_s = K\sigma_v' \tan\phi' < 2.5 \text{ tsf}$ where $K = 0.7$ for $D_b \leq 25 \text{ ft}$ $K = 0.6$ for $25 \text{ ft} < D_b \leq 40 \text{ ft}$ $K = 0.5$ for $D_b > 40 \text{ ft}$
Meyerhof (1976)	$q_s \text{ (tsf)} = \frac{N}{100}$
Quiros and Reese (1977)	$q_s \text{ (tsf)} = 0.026N < 2 \text{ tsf}$
Reese and Wright (1977)	$q_s \text{ (tsf)} = \frac{N}{34}$ for $N \leq 53$ $q_s \text{ (tsf)} = \frac{N - 53}{450} + 1.6$ for $53 < N \leq 100$
Reese and O'Neill (1988)	$q_s \text{ (tsf)} = \beta\sigma_v' \leq 2 \text{ tsf}$ for $0.25 \leq \beta \leq 1.2$ where $\beta = 1.5 - 0.135\sqrt{z}$

where N = uncorrected SPT blow count

σ_v' = vertical effective stress

ϕ' = friction angle of sand

K = load transfer factor

D_b = embedment of drilled shaft in sand bearing layer

β = load transfer coefficient

z = depth below ground in feet

maximum value ever measured, and Touma and Reese (1974) suggest an upper limit of 2.5 tsf. These values however, are not theoretical limits. Higher values can be used if they are verified by load tests.

It may be noted that the side resistance of drilled shafts in sand can be estimated using (a) the friction angle [Touma and Reese (1974)] or (b) the SPT blow count [Meyerhof (1976), Quiros and Reese (1977) & Reese and Wright (1977)]. Reese and O'Neill (1988) proposed a method for uncemented sands that uses a different approach in that the shaft resistance is independent of the soil friction angle and the SPT blow count. They suggested that the friction angle approaches a common value for uncemented sands due to high shearing strains in the sand and stress relief that occurs during drilling.

(ii) End Bearing

Load tests show that large settlements are required to mobilize the maximum end bearing resistance of drilled shafts in sands. Since large settlements are not tolerable in most structures, the procedures presented in Table 2.3 for calculating the ultimate unit end bearing capacity (q_p) are based on a downward movement equal to either 1 inch [Touma and Reese (1974) and Quiros and Reese (1977)] or 5%

Table 2.3 Summary of Procedures for Estimating Base Resistance (q_p) of Drilled Shafts in Sand.

REFERENCE	DESCRIPTION
Touma and Reese (1974)	<p>Loose q_p (tsf) = 0</p> <p>Medium Dense q_p (tsf) = $\frac{16}{k}$</p> <p>Very Dense q_p (tsf) = $\frac{40}{k}$</p> <p> $\left\{ \begin{array}{l} k = 1 \text{ for } D_p < 1.67 \text{ ft} \\ \text{ \& } k = 0.6D_p \\ \text{ for } D_p \geq 1.67 \text{ ft.} \end{array} \right.$ </p> <p>Applicable only if $D_b > 10D$</p>
Meyerhof (1976)	$q_p \text{ (tsf)} = \frac{2N_{\text{corr}}D_b}{15D_p} < \begin{cases} \frac{4}{3} N_{\text{corr}} \text{ for sand} \\ N_{\text{corr}} \text{ for nonplastic silts} \end{cases}$
Quiros and Reese (1977)	Same as Touma and Reese (1974)
Reese and Wright (1977)	$q_p \text{ (tsf)} = \frac{2}{3} N \quad \text{for } N \leq 60$ $q_p \text{ (tsf)} = 40 \quad \text{for } N > 60$
Reese and O'Neill (1988)	$q_p \text{ (tsf)} = 0.6N \quad \text{for } N \leq 75$ $q_p \text{ (tsf)} = 45 \quad \text{for } N > 75$

where N_{corr} = SPT blow count corrected for overburden pressure
 $= [0.77 \log_{10}(20/\sigma_v')] N$

N = uncorrected SPT blow count

D_p = base diameter of drilled shaft in ft

D_b = embedment of drilled shaft in sand bearing layer

of the base diameter [Reese and Wright (1977) and Reese and O'Neill (1988)].

Reese and O'Neill (1988) recommend that for base diameters greater than 50 in., q_p should be reduced to q_{pr} as follows:

$$q_{pr} = \frac{50}{D_p} q_p \quad (2-19)$$

where q_{pr} = reduced base resistance for $D_p > 50$ in.

D_p = diameter of the base of the shaft (in.)

q_p = ultimate unit end bearing resistance calculated using one of the methods in Table 2.3.

Meyerhof's expression for base resistance stems from the idea that the point resistance increases linearly with embedment up to a limiting depth of 10 shaft diameters; thereafter, the point resistance remains constant with depth.

2.1.3.3 Drilled Shafts In Rock

Drilled shafts socketed in rock derive their axial capacities from end bearing and/or side resistance. The depth of the socket is typically one to three times the diameter (Canadian Geotechnical Society, 1985). The design procedure presented in this section assumes that: (a) the

rock strength measured during site investigation will not deteriorate during construction when water or drilling fluids are used, (b) the drilling fluid used will not form a lubricated film on the sides of the excavation, and (c) the bottom of the excavation is properly cleaned out. This is especially important if the capacity of the drilled shaft is based on end bearing.

The design procedure proposed by Reese and O'Neill (1988) for bearing capacity of drilled shafts socketed in rock assumes that the load is carried entirely by the shaft if the computed settlement is less than 0.4 in. Conversely, loads that cause settlements greater than 0.4 in. are assumed to be carried entirely by the base of the drilled shaft. This method is conservative since loads are assumed to be carried entirely in side resistance or entirely in end bearing, and no allowance is made for the loads to be carried by a combination of side resistance and end bearing. The steps in the design procedure are as follows:

1. Estimate the settlement of the portion of the drilled shaft that is socketed in rock. This consists of two components:
 - (a) the elastic shortening of the socketed portion of the drilled shaft, ρ_e , which can be computed as follows:

$$\rho_e = \frac{(\Sigma P_i) H_S}{A_{SOC} E_C} \quad (2-20)$$

where H_S = depth of the socket

ΣP_i = working load at the top of the socket

A_{SOC} = cross-sectional area of the socket

E_C = Young's modulus of concrete in the socket, considering the stiffness of any steel reinforcement, and

(b) settlement of the base of the drilled shaft, ρ_{base} , which can be computed as follows:

$$\rho_{base} = \frac{(\Sigma P_i) I_\rho}{D_S E_R} \quad (2-21)$$

where I_ρ = influence coefficient obtained from Fig. 2.9

D_S = diameter of the base of the drilled shaft socket

E_R = modulus of the in situ rock, taking the joints and their spacing into account.

The Young's modulus of the in situ rock, E_R , can be estimated as follows:

$$E_R = K_E E_i \quad (2-22)$$

where E_i = intact rock modulus found either by testing or by means of Fig. 2.10

K_E = modulus modification ratio, related to the

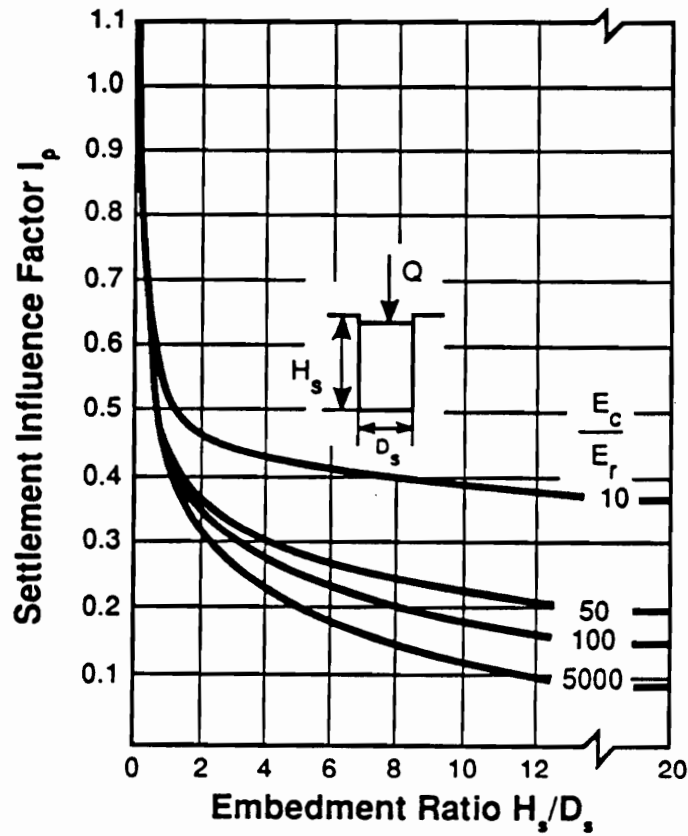


Figure 2.9 Elastic Settlement Influence Factor as a Function of Embedment Ratio and Modulus Ratio (After Donald, Sloan and Chiu, 1980, as presented by Reese and O'Neill, 1988)

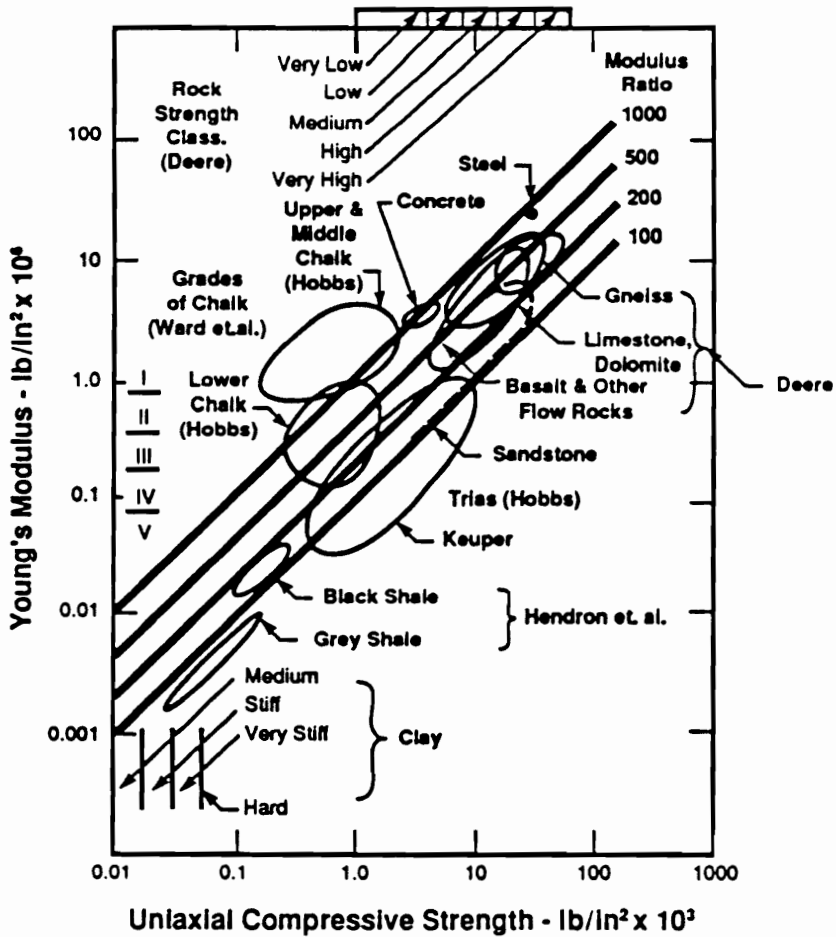


Figure 2.10 Engineering Classification of Intact Rock (After Deere, 1968, and Peck, 1976, as presented by Reese and O'Neill, 1988)

rock quality designation (RQD), as shown in Fig. 2.11

2. Calculate $\rho_e + \rho_{\text{base}}$. If the sum is less than 0.4 in., compute the ultimate capacity based on shaft resistance alone (Paragraph 3). If the sum is greater than 0.4 in., compute the ultimate capacity based on base resistance alone (Paragraph 4).
3. Estimate the side resistance of drilled shafts socketed in rock as follows: if the uniaxial compressive strength of the rock is less than or equal to 280 psi, then the ultimate unit side resistance (q_s) is given by (Carter and Kulhawy, 1987):

$$q_s = 0.15q_u \quad (2-23)$$

where q_u is the uniaxial compressive strength of the rock. If the uniaxial compressive strength of the rock or concrete (in the drilled shaft), whichever is less, is greater than 280 psi, then q_s is given by (Horvath and Kenney, 1979):

$$q_s = 2.5\sqrt{q_u} \quad (2-24)$$

where q_s and q_u are in psi.

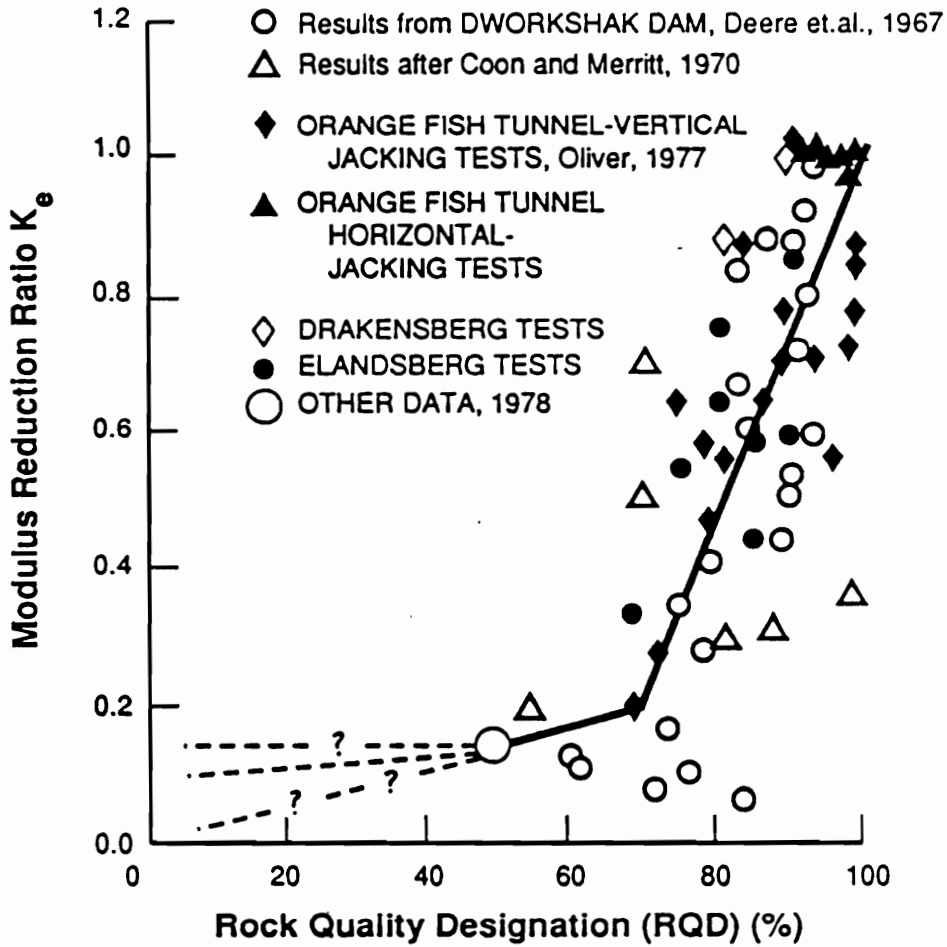


Figure 2.11 Modulus Reduction Ratio as a Function of RQD (After Bieniawski, 1984, as presented by Reese and O'Neill, 1988)

4. Estimate the base resistance of the drilled shaft socket from the uniaxial compression strength as follows (Canadian Geotechnical Society, 1985):

$$q_p = 3q_u K_{sp} d \quad (2-25)$$

where q_u = average uniaxial compression strength of the rock core

K_{sp} = dimensionless bearing capacity coefficient

$$K_{sp} = \frac{3 + s_d/D_s}{10[1 + 300t_d/s_d]^{0.5}} \quad (\text{See Fig. 2.12}) \quad (2-26)$$

d = dimensionless depth factor

$$d = 1 + 0.4H_s/D_s \leq 3.4$$

s_d = spacing of discontinuities

t_d = width or thickness of discontinuities

D_s = diameter of drilled shaft socket

H_s = depth of embedment of drilled shaft socket

= 0 for drilled shafts resting on top of bedrock.

This method is not applicable to soft stratified rocks, such as shale or limestone. When this method is applicable, the rocks are usually so sound that the structural capacity will govern the design (Fellenius et al., 1989). This method is applicable only if (a) $s_d > 1$ ft, (b) $t_d < 0.25$ in. for unfilled discontinuities or $t_d < 1$ in. for discontinuities

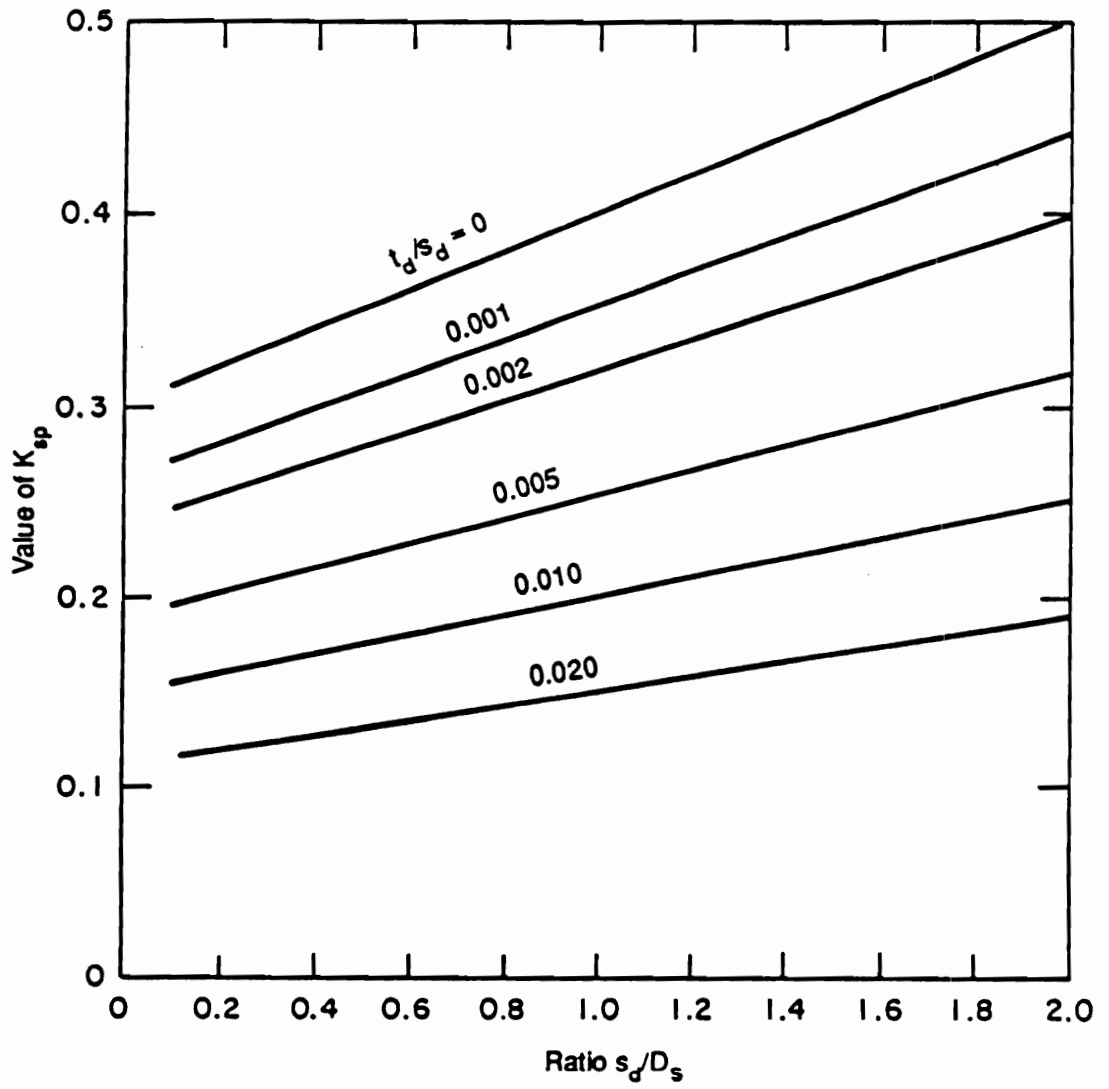


Figure 2.12 Bearing Capacity Coefficient, K_{sp}
(After Canadian Geotechnical Society, 1985)

filled with soil or rock debris, and (c) $D_S > 1$ ft. For drilled shafts socketed in soft rock, treat the rock as soil and design the drilled shaft using the methods described in Section 2.1.3.1 if the material is cohesive or Section 2.1.3.2 if the material is cohesionless. This procedure can also be used to estimate the tip resistance of driven piles bearing on rock; in this case, $H_S = 0$.

2.1.4 Bearing Capacity of Groups of Drilled Shafts

For groups of drilled shafts in cohesive soil, the mode of behavior depends on whether or not the cap is in contact with the ground. If the cap is in contact with the ground, groups of shafts may fail as a unit consisting of the shafts together with the block of soil contained within the shafts. The ultimate bearing capacity in this case should be taken as the minimum of the following two values:

- (i) the sum of the individual capacities of the drilled shafts, or
- (ii) the bearing capacity for block failure of the group.

For a group of drilled shafts of width X , length Y and depth Z , the bearing capacity for block failure in cohesive soils is given by Equation 2-13.

If the cap is not in firm contact with the ground and the clay is normally consolidated or slightly overconsolidated or is sensitive, the individual capacity of the drilled shaft must be multiplied by an efficiency factor, η , where $\eta = 0.7$ for a center-to-center spacing of $3D$ and $\eta = 1.0$ for a spacing of $6D$ (Reese and O'Neill, 1988). The value of η may be linearly interpolated for intermediate spacings. The group capacity is then calculated as the minimum of:

- (i) the sum of the individual capacities of the drilled shaft multiplied by η or
- (ii) the bearing capacity for block failure as described above.

If the cap is not in firm contact with the ground, and the clay is heavily overconsolidated and insensitive, then the group capacity should be estimated in a similar manner as the case where the cap is in contact with the ground.

Installation of drilled shafts in cohesionless soils results in stress relief. Therefore, the density of the sand may decrease during construction of drilled shafts. The ultimate bearing capacity of a group of drilled shafts in sand is estimated by multiplying the sum of the capacities of all the shafts in the group by a group efficiency factor. The group efficiency factor, defined as the ratio of the ultimate load capacity of the group to the

sum of the ultimate capacities of the individual shafts, is 0.7 for a center-to-center spacing of three diameters and 1.0 for a spacing of six diameters (Reese and O'Neill, 1988). The value of the efficiency factor can be interpolated for intermediate spacings. Evaluation of group capacity of drilled shafts in cohesionless soil is the same whether the cap is or is not in firm contact with the ground.

Block failure can also occur when the base of a group of shafts overlies a layer of soil very much weaker than the layer in which they terminate. The bearing capacity of the base of the equivalent pier, q_p can be computed as follows:

$$q_p = q_o + \frac{(q_1 - q_o)H}{10X} \leq q_1 \quad (2-27)$$

where q_o = bearing capacity of base if it were at the top of the lower (weak) soil

q_1 = bearing capacity of base in the upper soil in the absence of the softer lower soil

H = vertical distance from the base of the shafts in the group to the top of the weak layer

X = width (least horizontal dimension) of group.

2.2 Lateral Loading

Lateral loads on deep foundations arise due to wind, earthquake, water pressures, earth pressures, and live loads. Deep foundations must be designed to withstand such forces without failing and without deflecting excessively.

Mobilizing the ultimate lateral capacity of the soil requires such large displacements that this is not a realistic possibility, and ultimate soil failure does not usually control the design. Of interest to a designer of a laterally loaded deep foundation is the deflection of the pile or pier and the maximum bending moment in it. Estimating these quantities requires analysis of the interaction between the foundation and the surrounding soil.

2.2.1 Single Piles and Drilled Shafts

The behavior of single piles or drilled shafts under lateral loads can be analyzed using (a) elastic analysis, (b) subgrade reaction analysis, and (c) p-y analysis. Elastic analyses and subgrade reaction analyses approximate the soil behavior as linear. Since soil behavior is seldom linear especially at high stress levels, non-linear p-y analysis will form the basis of the theory for laterally loaded deep foundations considered here.

2.2.1.1 p-y Analysis

The p-y method, devised by McClelland and Focht (1958), appears to be the most rational procedure for the design of deep foundations under lateral loading. It was initially developed from full scale load tests data for design of offshore platforms.

The procedure involves solving the beam equation for a laterally loaded pile as follows:

$$E_p I_p \frac{d^4 y}{dz^4} + E_s y = 0 \quad (2-28)$$

where $E_p I_p$ = flexural stiffness of the pile (FL^2), E_p and I_p are the Young's modulus (FL^{-2}) and moment of inertia (L^4) of the pile, y = deflection of the pile (L), z = depth (L), E_s = $-p/y$ = subgrade (soil) modulus (FL^{-2}), and p = soil reaction (FL^{-1}).

The magnitude of the soil modulus E_s varies with the soil displacement (y) due to the nonlinearity of the stress-strain behavior of soils. Because of the inhomogeneity of the soil and because the soil reaction varies with depth in a laterally loaded deep foundation, the soil modulus is best described by a family of p-y curves as shown in Fig. 2.13. Recommendations for computing p-y curves for various soil types and groundwater conditions are given by Reese (1984).

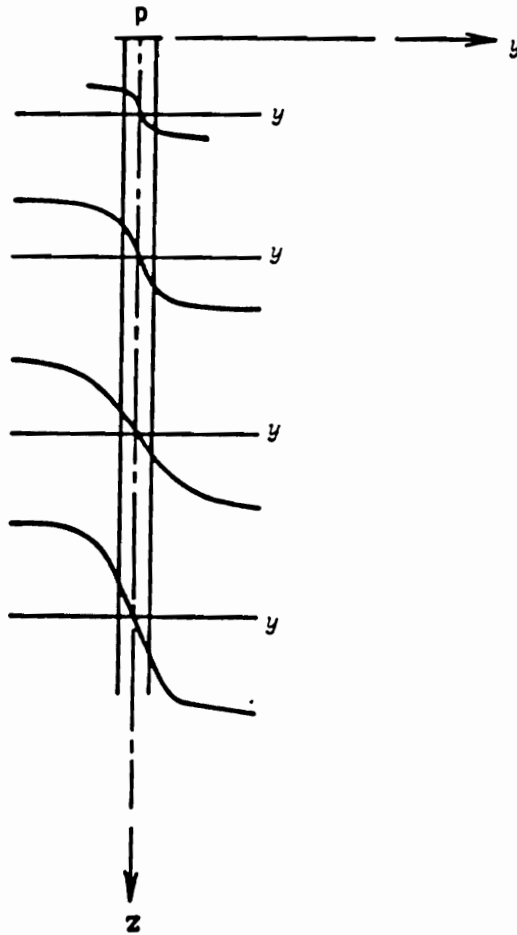


Figure 2.13 p-y Curves for Analysis of Piles and Drilled Shafts Under Lateral Loading (After Reese, 1977)

The solution to the problem of a laterally loaded pile or drilled shaft requires the use of computer programs and involves considerable engineering time. However, non-linear analysis can be greatly simplified if generalized, dimensionless forms of p-y curves capable of representing a wide variety of soil types, soil strengths, pile sizes, pile stiffnesses and different loading conditions can be derived. This is possible since only the soil close to the ground surface is important with regard to lateral loads. A non-dimensional technique has been developed by Evans and Duncan (1982).

2.2.1.2 Evans and Duncan Procedure

Through the use of dimensional analyses, Evans and Duncan (1982) developed a simple procedure for analyzing the nonlinear behavior of laterally loaded piles, capable of predicting lateral deflections and bending moments as would a p-y analysis. It is based on a large number of p-y analyses of both free-head and fixed-head piles in cohesive and cohesionless soils. Their study resulted in the following useful dimensionless relationships: (1) lateral load versus lateral deflection, (2) moment versus lateral deflection, and (3) lateral load versus moment. Using these charts, it is possible to predict deflections and moments in

laterally loaded piles without the need for a computer. Details of the procedure will be presented in Chapter 3.

2.2.2 Groups of Piles or Drilled Shafts

Drilled shafts may be used either individually or in groups. Piles however, are usually driven in groups. Procedures for analyzing group behavior of piles (or drilled shafts) should ideally be capable of estimating (i) group deflections, (ii) load distribution among piles or drilled shafts in the group, and (iii) the maximum bending moment induced in the group. This section will review some of the techniques available for such analysis.

Pile group problems can be divided into two categories: (i) groups of widely spaced piles and (ii) groups of closely spaced piles. The first category consists of piles that are spaced far enough apart that the deflection of one pile in the group will not affect the other piles, and that the piles interact only through the pile cap. It suffices to analyze this category of pile groups by distributing the lateral loads equally among all the piles in the group, and considering the behavior of any one pile. Conversely, in groups of closely spaced piles, the response of one pile in a group will influence the nearby piles through the soil between them. This behavior is termed pile-soil-pile

interaction. This category of pile groups will be studied more closely in Chapter 3.

2.2.2.1 Factors That Affect Group Behavior

Factors that affect single pile behavior such as pile size, pile stiffness and soil strength also affect the behavior of pile groups. Pile length is not a consideration here as the discussion is limited only to long piles, i.e. piles which would show little or no reduction in lateral displacement under the same lateral load if the pile embedment was increased. However, several important differences exist between single pile behavior and the behavior of pile groups. They include: (i) pile-soil-pile interaction, (ii) presence of a pile cap, (iii) effect of installation on adjacent piles, and (iv) rotational restraint afforded by the pile cap (Brown and Reese, 1985).

(i) Pile-soil-pile Interaction

The deflection of any pile in a group causes deflection of the surrounding soil and piles, thus leading to larger deflection for the pile group than for single piles subjected to the same load per pile. Pile-soil-pile interaction is one of the most significant differences in the behavior of pile groups as compared to single piles.

Therefore, reliable methods of predicting pile group behavior should account for this effect.

(ii) Effect of Pile Cap

The presence of a cap connection to a group of piles can increase the restraint of the piles to lateral displacement provided the soil surrounding the cap remains in contact with the cap throughout the life of the structure. However, the effects of settlement of the soil around the piles, or scour, can cause a loss of cap-soil contact. For this reason, and the fact that it is difficult to model the behavior of a cap under lateral load, the resistance contribution of the cap to lateral loads is usually neglected in practice.

(iii) Effect of Installation on Adjacent Piles

Deep foundations can be installed by means of the following procedures: (a) driving (eg. driven piles), (b) boring and casting in situ (eg. drilled shafts), (c) driving a casing and casting in situ (egs. cast-in-shell piles or filled pipe piles), and (d) screwing (eg. screw piles).

Pile installation effects are difficult to quantify and model accurately, and are usually neglected. Installation of deep foundations can lead to: (a) a change in consistency

of the soil and (b) a change in the state of stress in the ground.

Installation by driving displacement piles in loose sands causes soil densification and possibly particle crushing. When piles are driven in groups in loose cohesionless soils, the soil around the piles becomes highly compacted, and this can lead to an increase in the lateral resistance of the piles. Driving piles in cohesive soils causes remolding of the soil and consequently, a loss in shear strength. As consolidation progresses, pore pressures dissipate and the shear strength increases. The original in situ shear strength may or may not be surpassed depending on the stress history and sensitivity of the soil. Pore pressures dissipate more slowly in pile groups than around single piles (O'Neill, 1983).

Installation by driving causes a displacement of a volume of soil equal to the volume of the pile. Displacement of the soil causes a change in the magnitude and direction of the principal stresses. If the piles are spaced close together, there would be an overlap of the zones of stress increase in the soil between the piles.

Where the pile is installed in a prebored hole such as in the construction of a bored pile, stress relief occurs in the soil. Moreover, migration of water from wet concrete into the soil can further soften the soil. As a result, the

lateral resistance computed using the shear strength of the ground prior to installation may be less than the lateral resistance available to the bored pile.

The soil strength that governs the behavior of pile groups under lateral load is that of the soil after installation and reconsolidation. Present methods of lateral load analysis of deep foundations do not involve adjustments to account for installation effects because rational assessment of installation effects would require better understanding of soil behavior than is characteristic of the current state-of-the-art. The effects of installation can at best be treated only qualitatively. A better understanding of installation effects could help pave the way for the evolution of more reliable methods of predicting group behavior of deep foundations under lateral loads.

(iv) Effect of Rotational Restraint at the Pile Cap

Piles that are embedded in reinforced concrete pile caps are effectively restrained from rotation at the top, and they thus deflect laterally with negligible rotation at the top of the pile. It is convenient in analytical techniques to represent the pile-to-pile cap connection as fixed, pinned or free. Brown and Reese (1985) argued that these assumptions are not strictly correct. However, the

degree of rotational restraint afforded by typical pile caps is sufficiently close to the fixed-head case so that that condition affords an accurate approximation, accurate enough for practical purposes.

2.2.2.2 Methods of Predicting Lateral Behavior of Groups of Piles and Drilled Shafts

The lateral behavior of pile groups can be predicted through the use of experimental techniques (such as model tests or full scale load tests) or analytical methods. Although model tests are inexpensive to run, they are incapable of representing correctly the soil stresses in the prototype. Kulkarni et al. (1985) have overcome this particular difficulty by carrying out centrifugal modelling of pile groups under lateral load. Full scale load tests, on the other hand, are extremely expensive.

In general, analytical models available for predicting lateral behavior of pile groups can be divided into five categories (O'Neill, 1983):

1. finite element method
2. continuum model
3. modified continuum model
4. modified unit load transfer and

5. hybrid model.

(i) Finite Element Method

With the present pace of advancement in computer hardware technology, 3-D finite element analysis of pile groups may prove to be a promising tool in analyzing laterally loaded pile groups, especially in highly stratified soils. Moreover, the finite element method is capable of accounting for the presence and stiffnesses of the piles and the soil correctly. However, disadvantages of 3-D finite element analysis include: (i) the problem is complex, (ii) high quality and extensive soil test data is required to fully describe the soil behavior, and (iii) it is not able to model installation effects.

(ii) Continuum Model

The continuum model includes the approach of Poulos (1971), which assumes the soil to be elastic. Poulos used Mindlin's three dimensional elasticity equations to solve for stresses and displacements due to horizontal point loads applied in an elastic half space. The solution can be used to evaluate the influence of one pile on other piles in the group through the use of elastic influence factors.

Poulos' (1971) procedure can be used to estimate the elastic groundline deflection of a pile within a group as follows:

$$\rho_k = \bar{\rho}_F \left[\sum_{\substack{j=1 \\ j \neq k}}^{N_{\text{pile}}} (P_j \alpha_{\rho F k j}) + P_k \right] \quad (2-29)$$

where ρ_k = lateral deflection of pile k (L)

$\bar{\rho}_F$ = unit elastic displacement of a single pile under unit horizontal load (LF^{-1})

$$= I_{\rho F} / E_s Z$$

$I_{\rho F}$ = influence factor (Fig. 2.14)

E_s = Young's modulus of soil (FL^{-2})

Z = length of the pile (L).

N_{pile} = number of piles in the group

P_j = lateral load on pile j (F)

$\alpha_{\rho F k j}$ = elastic interaction factor for determining the influence of pile j on pile k, based on the spacing between piles j and k and the angle θ

θ = angle between direction of loading and the line joining the centers of piles j and k, and

P_k = lateral load on pile k (F)

The interaction factor, $\alpha_{\rho F k j}$, can be obtained from Fig. 2.15 for fixed-head piles. $\alpha_{\rho F k j}$ is a function of the spacing to diameter ratio (s/D), θ and K_R , where s = center-

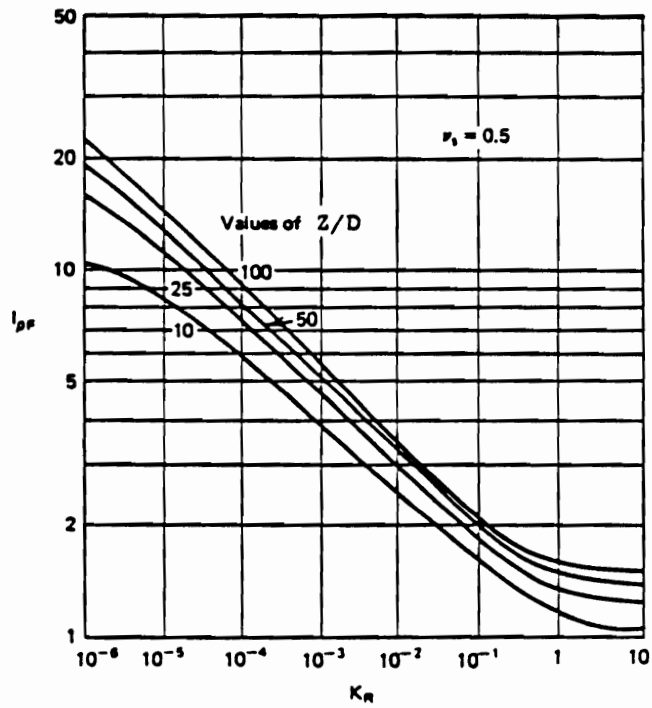
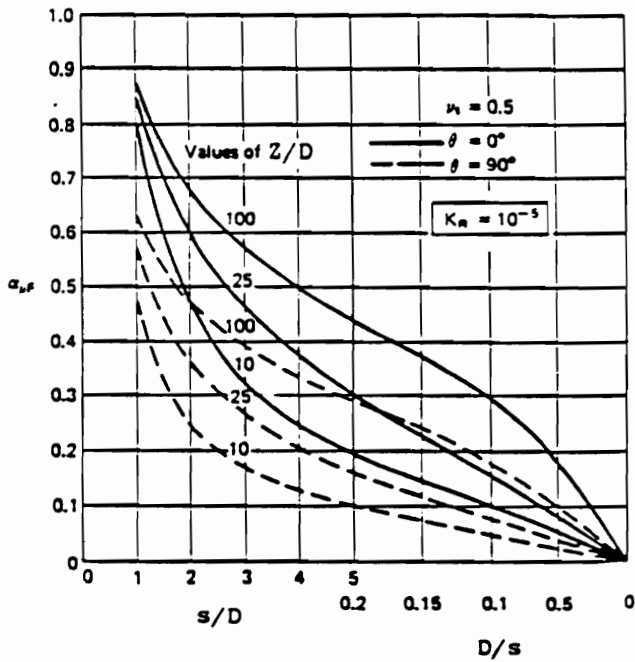
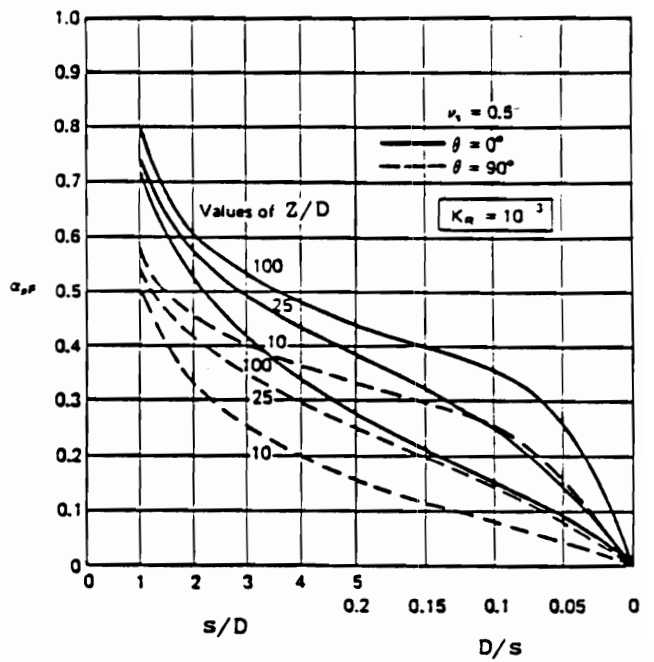


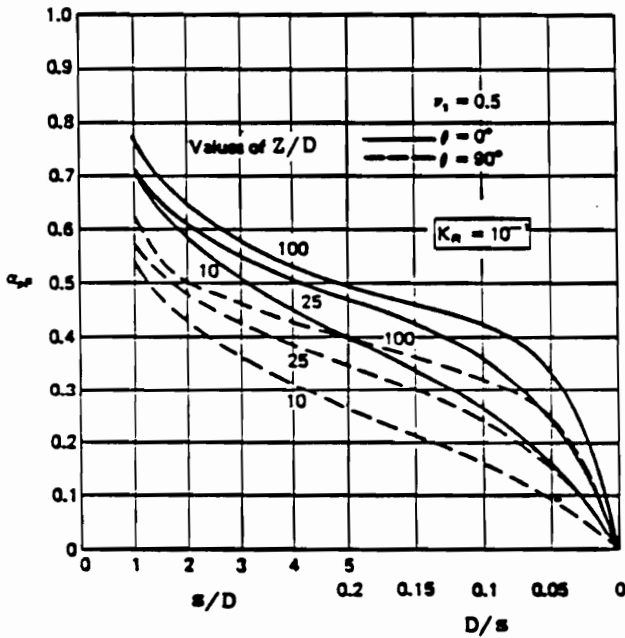
Figure 2.14 Influence Factor $I_{\rho F}$ - Fixed-Head Floating Pile, Constant Soil Modulus (After Poulos and Davis, 1980)



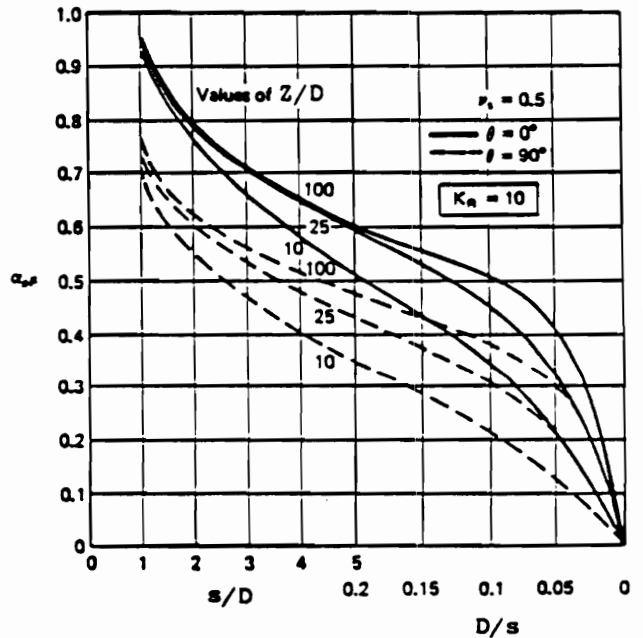
$\alpha_{\rho F}$ for $K_R = 10^{-5}$.



$\alpha_{\rho F}$ for $K_R = 10^{-3}$.



$\alpha_{\rho F}$ for $K_R = 10^{-1}$.



$\alpha_{\rho F}$ for $K_R = 10$.

Figure 2.15 Interaction Factors, $\alpha_{\rho F}$ for Fixed-Head Piles or Drilled Shafts (After Poulos and Davis, 1980)

to-center pile spacing, D = pile width or diameter and K_R is the pile flexibility factor defined as follows:

$$K_R = \frac{E_p I_p}{E_s Z^4} \quad (2-30)$$

where E_p = Young's modulus of pile (FL^{-2}) and I_p = moment of inertia of pile (L^4).

If the piles are connected by a cap, then the piles will all deflect equally. Equation 2-29 yields a set of N_{pile} equations but there are a total of $(N_{pile} + 1)$ unknowns; N_{pile} unknown values of reaction in each pile, and one unknown value of group deflection, $Y_G = \rho_1 = \rho_2 = \dots = \rho_{N_{pile}}$. The remaining equation needed in order to solve for the set of $(N_{pile} + 1)$ unknowns is the requirement that the sum of the individual pile loads must equal the load on the group, P_g , i.e.

$$\sum_{j=1}^{N_{pile}} P_j = P_g \quad (2-31)$$

Shortcomings of Poulos' elastic procedure include: (i) real soils do not behave elastically, and (ii) the method cannot account for more than one soil type.

(iii) Modified Continuum Approach

Belonging to this category of analysis is the Winkler model for pile groups, introduced by Nogami (1980, 1983). The soil is modelled by a network of springs, thereby allowing pile-soil-pile interaction [Nogami and Chen (1984) and Randolph and Wroth (1979)]. The Winkler model for a pile group however, allows soil response only in the horizontal direction, and ignores the interconnection among elements in the vertical direction throughout the soil mass (Poulos and Davis, 1980). However, this method is advantageous because of computational simplicity and the ease of accounting for several soil types.

(iv) Modified Unit Load Transfer

This method involves the development of p-y (unit load transfer) curves for a group of piles considered as a single pile. The modified single pile, whose diameter is equal to the width of the group, consists of the piles in the group and the soil in between the piles. Bogard and Matlock (1983) used this procedure on a circular group of piles assuming that the lateral resistance is equally distributed among all piles in the group. This method is more difficult to apply to non-circular groups of piles.

(v) Hybrid Model

Proposed by Focht and Koch (1973), the hybrid model combines the use of Poulos' elastic interaction coefficients and non-linear p-y analysis to predict pile group behavior. They assumed that non-linear soil behavior occurs only close to the individual piles, and that pile-soil-pile interaction is linear and can be predicted through the use of Poulos' elastic interaction coefficients.

Focht and Koch (1973) modified Poulos' (1971) procedure of Equation 2-29 as follows:

$$\rho_k = \frac{-}{\rho_F} \left[\sum_{\substack{j=1 \\ j \neq k}}^{N_{\text{pile}}} (P_j \alpha_{\rho} F_{kj}) + R P_k \right] \quad (2-32)$$

where R is the relative stiffness factor defined as follows:

$$R = Y_S / \rho \quad (2-33)$$

where Y_S = non-linear p-y deflection of a single pile at the mudline

ρ = elastic deflection of a single pile at the mudline

$$= \bar{\rho}_F P_S$$

In computing Y_S and ρ , the lateral load on the single pile is computed as the total lateral load on the group divided by the number of piles or drilled shafts ($P_S = P_g / N_{\text{pile}}$).

The hybrid model has the advantage that different values of stiffness are used to represent the single pile behavior and the pile-soil-pile interaction (O'Neill, 1983). This enables adjustments to be made for the plastic deformation of the soil around individual piles through the use of the relative stiffness factor, R . This ability to account for different stiffnesses in individual pile behavior and in pile-soil-pile interaction is not possible with the elastic continuum model.

O'Neill et al. (1977) and O'Neill and Tsai (1984) have developed a hybrid model in three dimensions, where every pile in a group is discretized into elements. Each element represents a Mindlin point load in computing the pile-soil-pile interaction. The p - y curves at every location in each pile are individually modified to account for the effects of all other piles. An iterative process is required. One difference between this model and Focht and Koch's procedure is that the unit load transfer (p - y) curves are modified individually to account for the loads from adjacent piles.

2.3 Methods of Incorporating Margins of Safety in Design

2.3.1 Design Criteria

Structures should desirably be designed to be safe, economical and aesthetically pleasing. Safety cannot be

compromised. On the other hand, overconservatism can lead to wastefully expensive designs. A balance must be struck by the engineer to design structures that are safe and also economically efficient.

From a safety standpoint, structures should be designed so that they are able to support loads without reaching a "limit state". A limit state is reached when the structure no longer fulfills one of its design requirements. There are two types of limit states:

(i) An ultimate limit state corresponds to the maximum load carrying capacity of the structure, and reaching this limit state usually leads to complete collapse. An example is the bearing capacity failure of a foundation.

(ii) A serviceability limit state corresponds to loss of serviceability, and occurs before collapse. A serviceability limit state involves unacceptable deformations or undesirable damage levels. This may be reached in foundations through excessive settlement or lateral displacement, or structural deterioration of the foundations.

2.3.2 Working Stress Design

Foundations are conventionally designed using working stress design (WSD) methods. The approach in WSD is

different for the ultimate and the serviceability limit states. In an ultimate limit state design, safety is achieved by ensuring that the magnitude of the resistance divided by a factor of safety ($FS > 1$) is greater than or equal to the magnitude of the loads. The WSD checking format is as follows:

$$R_N/FS \geq S_D + S_L + S_E \quad (2-34)$$

where R_N is the nominal resistance, S_D and S_L are nominal values of dead and live load effects, S_E is an environmental load such as wind, earthquake, etc. and FS is the factor of safety. The disadvantage of this method is its inability to account for the different degrees of uncertainties associated with the various types of loads.

In serviceability limit state design, unfactored loads are usually used to calculate deformations, and these are compared to the maximum tolerable values.

2.3.3 Load (and Resistance) Factor Design

In load (and resistance) factor design (LFD), it is recognized that the loads and resistances are probabilistic in nature. Different types and magnitudes of loads have varying probabilities of occurrence. In order to account for their differing probabilities of occurrence, each load

component is amplified by a load factor, the value of which depends on the level of uncertainty of the load component.

The factored loads are compared to the design strengths or resistances to evaluate the adequacy of the design. The design resistances are obtained by multiplying nominal values of resistance by performance factors (or resistance factors), usually denoted as ϕ . According to AASHTO (1989), ϕ should "provide for the probability that small adversion in material strength, workmanship and dimensions, while individually within acceptable tolerance and limits of good practice, may combine to result in understrength."

The objective of design is to ensure that the design resistance is greater than or equal to the sum of the factored loads, i.e.

$$\phi R_n \geq \sum \gamma_i S_i \quad (2-35)$$

where ϕ is the performance factor, S_i is the load effect due to load component i and γ_i is the load factor for load component i .

The potential advantages of LFD over WSD include the following:

- 1) It accounts for the variability in loads and resistances.
- 2) Consistent margins of safety may be achieved in both structural and foundation designs.

3) More economical use of materials may result because a more rational basis is used to set safety margins.

Using reliability theory, values of performance factors can be derived for ultimate limit states, provided sufficient statistical data is available. For cases where sufficient data is not available, performance factors can be calculated by matching the margin of safety with that of working stress design, which has usually been established through experience. Since the factors of safety and the statistics for the resistance vary for different methods of analysis, the values of performance factors are method dependent. One shortcoming of the LFD method is that since the performance factors are method dependent, there may be a variety of performance factors for just one limit state consideration.

In serviceability limit state design using LFD, loads and resistances are unfactored, and the design procedures resemble those used in conventional WSD.

Load factor design of foundations is currently implemented in the Danish Code (1985) and the Ontario Highway Bridge Design Code (1983). The use of LFD for foundations in the current AASHTO code (1989) for bridges, and for the ASCE Standard (1990) for buildings and other structures will be examined in the following sections.

2.3.3.1 Load Factors and Load Combinations

Bridges

Loads acting on bridge superstructures include one or more of the following: dead load, live and impact loads, thrust due to earth pressures, buoyancy, wind load, longitudinal and centrifugal forces caused by moving vehicles, earthquake loads, stream and ice flow forces, and forces induced by changes in the dimensions of the structure, such as shrinkage and temperature effects.

One difference between the loads acting on the bridge superstructure and those that act on the foundation is that impact loads are usually assumed to be fully dissipated before reaching the foundation. However, bent piers and integral abutments are usually designed to carry impact loads, and these are the most common substructures in which drilled shafts are used. The load combinations and load factors for the design of the superstructure, as given in the 1989 AASHTO specifications, can be used for the design of foundations as follows:

$$\begin{aligned} \text{Total Load} = & \gamma[\beta_D D + \beta_L L + \beta_C C F + \beta_E E + \beta_B B + \beta_{S F} S F + \beta_W W + \\ & \beta_{W L} W L + \beta_{L F} L F + \beta_R (R + S + T) + \beta_{E Q} E Q + \\ & \beta_{I C E} I C E] \end{aligned} \quad (2-36)$$

where γ = load factor (see Tables 2.4 and 2.5)

β = coefficient (see Tables 2.4 and 2.5)

D = dead load

L = live load

E = earth pressure

B = buoyancy

W = wind load

WL = wind load on live load - 100 pounds per linear ft.

LF = longitudinal force from live load

CF = centrifugal force

R = rib shortening

S = shrinkage

T = temperature

EQ = earthquake

SF = stream flow pressure

ICE = ice pressure

The factored load combinations considered by AASHTO are shown in Table 2.5. Each line in the table, designated by loading group numbers I through IX, gives the values of the load factors, γ , and the coefficients, β , that govern the contributions to the total load. For example in group (load combination) I, total load = $1.3(D + 1.67L_n + CF + \beta_E E + B + SF)$.

Table 2.4 Table of Coefficients of γ and β for Working Stress Design of Bridges (After AASHTO, 1989)

Col.No.	1	2	3	3A	4	5	6	7	8	9	10	11	12	13	14
	β -FACTORS														
GROUP	γ	D	(L+I) _n	(L+I) _p	CF	E	B	SF	W	WL	LF	R+S+T	EQ	ICE	%
I	1	1	1	0	1	β_E	1	1	0	0	0	0	0	0	100
IA	1	1	2	0	0	0	0	0	0	0	0	0	0	0	150
IB	1	1	0	1	1	β_E	1	1	0	0	0	0	0	0	**
II	1	1	0	0	0	1	1	1	1	0	0	0	0	0	125
III	1	1	1	0	1	β_E	1	1	0.3	1	1	0	0	0	125
IV	1	1	1	0	1	β_E	1	1	0	0	0	1	0	0	125
V	1	1	0	0	0	1	1	1	1	0	0	1	0	0	140
VI	1	1	1	0	1	β_E	1	1	0.3	1	1	1	0	0	140
VII	1	1	0	0	0	1	1	1	0	0	0	0	1	0	133
VIII	1	1	1	0	1	1	1	1	0	0	0	0	0	1	140
IX	1	1	0	0	0	1	1	1	1	0	0	0	0	1	150

(L+I)_n - Live load plus impact for AASHTO Highway H or HS loading
 (L+I)_p - Live load plus impact consistent with the overload criteria of the operation agency.

** Percentage = $\frac{\text{Maximum Unit Stress (Operating Rating)}}{\text{Allowable Basic Unit Stress}} \times 100$

% in Column 14 is the maximum permissible percentage of basic unit stress for load group indicated

No increase in allowable unit stresses shall be permitted for members or connections carrying wind loads only.

$\beta_E = 1.0$ for vertical and lateral loads on all structures except reinforced concrete boxes.

$\beta_E = 1.0$ and 0.5 for lateral loads on rigid frames (check both loadings to see which one governs)

Table 2.5 Table of Coefficients of γ and β for Load Factor Design of Bridges (After AASHTO, 1989)

Col.No.	1	2	3	3A	4	5	6	7	8	9	10	11	12	13
	β -FACTORS													
GROUP	γ	D	$(L+I)_n$	$(L+I)_p$	CF	E	B	SF	W	WL	LF	R+S+T	EQ	ICE
I	1.3	β_D	1.67	0	1	β_E	1	1	0	0	0	0	0	0
IA	1.3	β_D	2.2	0	0	0	0	0	0	0	0	0	0	0
IB	1.3	β_D	0	1	1	β_E	1	1	0	0	0	0	0	0
II	1.3	β_D	0	0	0	β_E	1	1	1	0	0	0	0	0
III	1.3	β_D	1	0	1	β_E	1	1	0.3	1	1	0	0	0
IV	1.3	β_D	1	0	1	β_E	1	1	0	0	0	1	0	0
V	1.25	β_D	0	0	0	β_E	1	1	1	0	0	1	0	0
VI	1.25	β_D	1	0	1	β_E	1	1	0.3	1	1	1	0	0
VII	1.3	β_D	0	0	0	β_E	1	1	0	0	0	0	1	0
VIII	1.3	β_D	1	0	1	β_E	1	1	0	0	0	0	0	1
IX	1.2	β_D	0	0	0	β_E	1	1	1	0	0	0	0	1

$(L+I)_n$ - Live load plus impact for AASHTO Highway H or HS loading
 $(L+I)_p$ - Live load plus impact consistent with the overload criteria of the operation agency.

$\beta_E = 1.3$ for lateral earth pressure for retaining walls and rigid frames.

$\beta_E = 0.5$ for lateral earth pressure when checking positive moments in rigid frames.

$\beta_E = 1.0$ for vertical earth pressure

$\beta_D = 1.0$ for flexural and tension members

For Column Design

$\beta_D = 0.75$ when checking member for minimum axial load and maximum moment or maximum eccentricity

$\beta_D = 1.0$ when checking member for maximum axial load and minimum moment

Loading groups I, II and III usually apply to the design of the superstructures and substructures, groups IV, V and VI apply usually to the design of arches and frames, while groups VII, VIII and IX apply usually to the design of substructures (Heins and Firmage, 1979). The fourteenth column of Table 2.4 lists the percentage increase in allowable stresses permitted in the load combinations, and is mainly used in working stress design. The increase in allowable stresses accounts for the fact that the probability of the load components reaching their maximum values simultaneously varies from one load combination to another.

ASCE Standard for Buildings and Other Structures

Loads acting on buildings include one or more of the following: dead load, live load, roof live load, snow load, rain load, wind load, earthquake load, thrust due to water and earth pressures, loads due to fluids, loads due to ponding, and loads due to changes in the dimensions of the structure such as shrinkage, temperature effects and settlement.

The load combinations used in designing buildings and other structures are shown in Table 2.6 for WSD and Table 2.7 for LFD [ASCE Standard 7-88, (1990) formerly ANSI A58.1]. One apparent difference between the two codes is

Table 2.6 Load Combinations for Working Stress Design of Buildings and Other Structures (After ASCE Standard 7-88, 1990)

2.3 Combining Loads Using Allowable Stress Design

2.3.1 Basic Combinations. Except when applicable codes provide otherwise, all loads listed herein shall be considered to act in the following combinations, whichever produces the most unfavorable effect in the building, foundation, or structural member being considered. The most unfavorable effect may occur when one or more of the contributing loads are not acting.

1. D
2. $D + L + (L_r \text{ or } S \text{ or } R)$
3. $D + (W \text{ or } E)$
4. $D + L + (L_r \text{ or } S \text{ or } R) + (W \text{ or } E)$

The most unfavorable effects from both wind and earthquake loads shall be considered, where appropriate, but they need not be assumed to act simultaneously.

2.3.2 Other Load Combinations. The structural effects of F , H , P , or T shall be considered in design.

2.3.3 Load Combination Factors. For the load combinations in 2.3.1 and 2.3.2, the total of the combined load effects may be multiplied by the following load combination factors:

1. 0.75 for combinations including, in addition to D :
 $L + (L_r \text{ or } S \text{ or } R) + (W \text{ or } E)$
 $L + (L_r \text{ or } S \text{ or } R) + T$
 $(W \text{ or } E) + T$
2. 0.66 for combinations including, in addition to D :
 $L + (L_r \text{ or } S \text{ or } R) + (W \text{ or } E) + T$

2.2 Symbols and Notation

D = dead load consisting of: (a) weight of the member itself; (b) weight of all materials of construction incorporated into the building to be permanently supported by the member, including built-in partitions; and (c) weight of permanent equipment;

E = earthquake load;

F = loads due to fluids with well-defined pressures and maximum heights;

L = live loads due to intended use and occupancy, including loads due to movable objects and movable partitions and loads temporarily supported by the structure during maintenance. L includes any permissible reduction. If resistance to impact loads is taken into account in design, such effects shall be included with the live load L ;

L_r = roof live loads (see 4.11).

S = snow loads;

R = rain loads, except ponding;

H = loads due to the weight and lateral pressure of soil and water in soil;

P = loads, forces, and effects due to ponding;

T = self-straining forces and effects arising from contraction or expansion resulting from temperature changes, shrinkage, moisture changes, creep in component materials, movement due to differential settlement, or combinations thereof;

W = wind load;

Table 2.7 Load Combinations for Load Factor Design of Buildings and Other Structures (After ASCE Standard 7-88, 1990)

2.4 Combining Loads Using Strength Design

2.4.1 Applicability. The load combinations and load factors given in 2.4.2 and 2.4.3 shall be used only in those cases in which they are specifically authorized by the applicable material design standard.

2.4.2 Basic Combinations. Except where applicable codes and standards provide otherwise, structures, components, and foundations shall be designed so that their design strength exceeds the effects of the factored loads in the following combinations:

1. $1.4D$
2. $1.2D + 1.6L + 0.5(L_r \text{ or } S \text{ or } R)$
3. $1.2D + 1.6(L_r \text{ or } S \text{ or } R) + (0.5L \text{ or } 0.8W)$
4. $1.2D + 1.3W + 0.5L + 0.5(L_r \text{ or } S \text{ or } R)$
5. $1.2D + 1.5E + (0.5L \text{ or } 0.2S)$
6. $0.9D - (1.3W \text{ or } 1.5E)$

Exception: The load factor on L in combinations (3), (4), and (5) shall equal 1.0 for garages, areas occupied as places of public assembly, and all areas where the live load is greater than 100 lb/ft² (pounds-force per square foot).

Each relevant strength limit state shall be considered. The most unfavorable effect may occur when one or more of the contributing loads are not acting.

2.4.3 Other Combinations. The structural effects of F, H, P , or T shall be considered in design as the following factored loads: $1.3F$, $1.6H$, $1.2P$, and $1.2T$.

2.2 Symbols and Notation

D = dead load consisting of: (a) weight of the member itself; (b) weight of all materials of construction incorporated into the building to be permanently supported by the member, including built-in partitions; and (c) weight of permanent equipment;

E = earthquake load;

F = loads due to fluids with well-defined pressures and maximum heights;

L = live loads due to intended use and occupancy, including loads due to movable objects and movable partitions and loads temporarily supported by the structure during maintenance. L includes any permissible reduction. If resistance to impact loads is taken into account in design, such effects shall be included with the live load L ;

L_r = roof live loads (see 4.11).

S = snow loads;

R = rain loads, except ponding;

H = loads due to the weight and lateral pressure of soil and water in soil;

P = loads, forces, and effects due to ponding;

T = self-straining forces and effects arising from contraction or expansion resulting from temperature changes, shrinkage, moisture changes, creep in component materials, movement due to differential settlement, or combinations thereof;

W = wind load;

that the load factors for the building code are less than those for the bridge code.

2.3.3.2 Code Calibration

Code calibration is the process of assigning values of code parameters such as performance factors or load factors. For a given set of load factors such as those in the AASHTO code or in the ASCE Standard 7-88, the codes can be calibrated by fitting with working stress design or by a more formal process using reliability analysis.

2.3.3.2.1 Calibration by Fitting with Working Stress Design

For cases where there is insufficient statistical data, performance factors can be determined using judgment and by fitting with working stress design specifications.

In LFD format, nominal loads are related to the nominal resistance by the following equation:

$$\phi R_n \geq \sum_{i=1}^n \gamma_i S_i \quad (2-37)$$

where R_n = nominal resistance (eg. pile capacity), S_i = load effect due to load component i (eg. dead and live loads), γ_i

= load factor for load component i , ϕ = performance factor and, n = number of load components.

In the WSD format, nominal loads are related to the nominal resistance by the following equation:

$$\frac{R_n}{FS} \geq \sum_{i=1}^n S_i \quad (2-38)$$

where FS is the factor of safety. Dividing Equation 2-37 by Equation 2-38 gives:

$$\phi \geq \frac{\sum_{i=1}^n \gamma_i S_i}{FS \sum_{i=1}^n S_i} \quad (2-39)$$

If the loads consist of dead load, S_D , and live load, S_L , then Equation 2-39 becomes:

$$\phi \geq \frac{\gamma_D S_D + \gamma_L S_L}{FS(S_D + S_L)} \quad (2-40)$$

Dividing both numerator and denominator by S_L , Equation 2-40 may be written as:

$$\phi \geq \frac{\gamma_D S_D / S_L + \gamma_L}{FS(S_D / S_L + 1)} \quad (2-41)$$

Values of performance factor obtained from Equation 2-41 for a range of safety factors and dead to live load ratios are shown in Table 2.8. The ratio of dead to live load depends on the construction material (steel, concrete or timber) and the type of structure. The dead load will be less in a steel structure than in a concrete structure. The dead to live load ratio is also different in bridges as opposed to buildings.

Below is an example (for the foundations of a steel bridge) of a calibration by fitting with working stress design, based on information obtained from the literature. In a bridge, the ratio of dead load to live load increases with increasing span length. Hansell and Viest (1971) recommended the following relationship for steel bridges:

$$\frac{S_D}{S_L + S_I} = 0.0132W \quad (2-42)$$

where S_I = impact load and W = span length in ft. Impact loads are seldom considered in foundation design except in bent piers and integral abutments. The impact load, S_I , in Equation 2-42 can be eliminated by substituting the following equation from AASHTO:

$$S_I = \frac{50S_L}{W + 125} \leq 0.3 \quad (2-43)$$

Table 2.8 Values of performance factors corresponding to different values of safety factor and dead to live load ratios

1) AASHTO ($\gamma_D = 1.3$ and $\gamma_L = 2.17$)

Safety Factor	Performance Factors			
	$S_D/S_L = 1.0$	$S_D/S_L = 2.0$	$S_D/S_L = 3.0$	$S_D/S_L = 4.0$
1.5	1.16	1.06	1.01	0.98
2.0	0.87	0.80	0.76	0.74
2.5	0.69	0.64	0.61	0.59
3.0	0.58	0.53	0.51	0.49
3.5	0.50	0.45	0.43	0.42
4.0	0.43	0.40	0.38	0.37

2) Building Code ($\gamma_D = 1.2$ and $\gamma_L = 1.6$)

Safety Factor	Performance Factors			
	$S_D/S_L = 1.0$	$S_D/S_L = 2.0$	$S_D/S_L = 3.0$	$S_D/S_L = 4.0$
1.5	0.93	0.89	0.87	0.85
2.0	0.70	0.67	0.65	0.64
2.5	0.56	0.53	0.52	0.51
3.0	0.47	0.44	0.43	0.43
3.5	0.40	0.38	0.37	0.37
4.0	0.35	0.33	0.33	0.32

The resulting equation was derived by Snyder and Moses (1978):

$$\frac{S_D}{S_L} = \left[1 + \frac{50}{W + 125} \right] 0.0132W \quad (2-44)$$

Yokel (1989) recommended that the design factors should be calibrated for span lengths of about 200 ft. For a bridge span of 200 ft, the approximate dead to live load ratio is 3.05. Substituting $\gamma_D = 1.3$ and $\gamma_L = 2.17$ into Equation 2-41, the performance factor, ϕ is related to the factor of safety as follows:

$$\phi \geq \frac{1.52}{FS} \quad (2-45)$$

Calibrating by fitting with working stress design is useful for transferring experience from working stress design to load factor design.

2.3.3.2.2 Calibration Using Reliability Methods

2.3.3.2.2.1 Steps in the Calibration Process

The procedure for estimating performance factors corresponding to a given set of load factors consists of the following steps:

- 1) Estimate the level of reliability inherent in current design methods.
- 2) Observe the variation of the reliability levels with different span lengths, dead load to live load ratios, geometry of the foundation, methods of predicting capacities and load combinations.
- 3) Select a target reliability index based on the margin of safety implied in current designs.
- 4) Calculate performance factors consistent with the selected target reliability index. It is also important to couple experience and judgment with the calibration results in the decision process.

2.3.3.2.2 Probability Theory and Computation of Reliability Indices

Probability theory has been widely used to model uncertainties in engineering design, where design parameters such as loads and resistances are treated as random variables. Fig. 2.16 shows the frequency distributions of the load effect (S) and the resistance (R) for a hypothetical circumstance. A value of R that is greater than S implies that the structure is safe. However, since R and S are random variables, there is a possibility that the

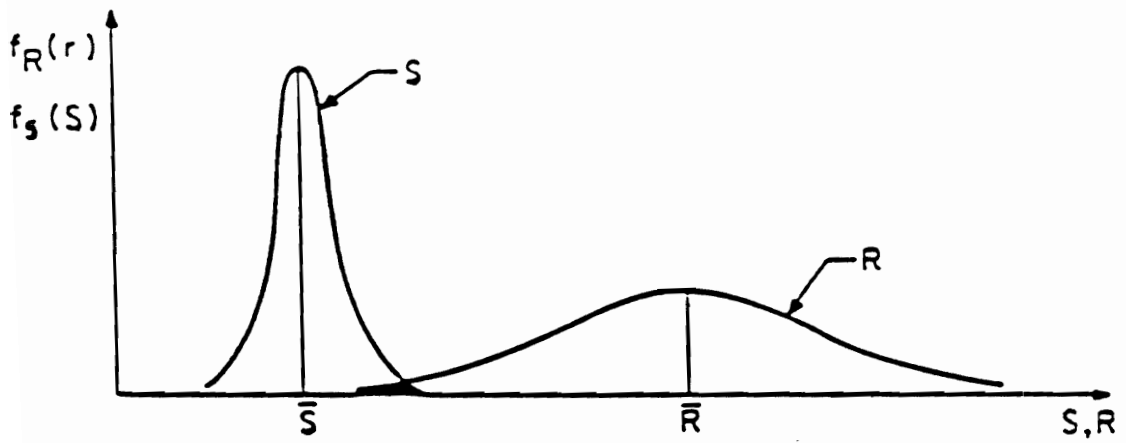


Figure 2.16 Frequency Distributions of Load Effect S and Resistance R

load effect S may be greater than R (shaded area in Fig. 2.16).

The safety of a structure can be measured in terms of the probability of failure, which is defined as the probability that the structure ceases to perform its intended function. Meyerhof (1970) indicated that the lifetime probability of failure of foundations should be between 10^{-3} and 10^{-4} .

Reliability of foundations can be expressed using a performance function or a limit state function. If the loads and resistance are normally distributed, the performance function can be written as:

$$g(R,S) = R - S \quad (2-46)$$

where $g()$ is the margin of safety, R is the resistance and S is the load.

If R and S are lognormally distributed, the performance function can be written as:

$$g(R,S) = \ln(R/S) \quad (2-47)$$

In this case, failure occurs when $R/S < 1$ or $g() < 0$.

The probability of failure, p_f for both cases of R and S being normal, and R and S being lognormal, can be written as follows:

$$p_f = P[g() < 0] \quad (2-48)$$

or

$$p_f = 1 - F_u(\bar{g}/\sigma_g) \quad (2-49)$$

where $F_u()$ is the standard normal distribution function, \bar{g} , and σ_g are the mean and standard deviation of the performance function defined as follows:

$$\bar{g} = \ln \left[\frac{\bar{R}}{\bar{S}} \sqrt{\frac{1 + V_S^2}{1 + V_R^2}} \right] \quad (2-50)$$

and

$$\sigma_g = \sqrt{\ln[(1 + V_R^2)(1 + V_S^2)]} \quad (2-51)$$

where \bar{R} and \bar{S} are the mean values of R and S respectively, and V_R and V_S are the coefficients of variation (standard deviation divided by the mean) of R and S respectively.

It can be shown that the probability density function of $g()$ is lognormal if R and S are lognormal. The probability of failure for lognormal R and S is given by:

$$p_f = 1 - F_u \left[\frac{\ln[(\bar{R}/\bar{S})\sqrt{(1 + V_S^2)/(1 + V_R^2)}]}{\sqrt{\ln[(1 + V_R^2)(1 + V_S^2)]}} \right] \quad (2-52)$$

The parenthetic term in F_u is the reliability index, β , i.e.

$$\beta = \frac{\ln[(\bar{R}/\bar{S})\sqrt{(1 + V_S^2)/(1 + V_R^2)}]}{\sqrt{\ln[(1 + V_R^2)(1 + V_S^2)]}} \quad (2-53)$$

The reliability index is the number of standard deviations that separates the mean value of the safety margin from the failure limit (Fig. 2.17).

If the bias is defined as the mean value divided by the nominal value, and if the loads consist of only dead and live loads, Equation 2-53 simplifies to:

$$\beta = \frac{\ln \left[\frac{\lambda_R FS (S_D/S_L + 1)}{\lambda_D S_D/S_L + \lambda_L} \sqrt{\frac{1 + V_D^2 + V_L^2}{1 + V_R^2}} \right]}{\sqrt{\ln[(1 + V_R^2)(1 + V_D^2 + V_L^2)]}} \quad (2-54)$$

where FS is the factor of safety, λ_R , λ_D and λ_L are the bias for resistance, dead load and live load respectively, V_R , V_D and V_L represent the coefficients of variation for the resistance, dead load and live load respectively, and S_D and S_L denote the nominal values of dead load and live load. The reliability index is related to the probability of failure as shown in Table 2.9 for the case of lognormal loads and resistances.

The method described above is called a First Order Second Moment Method - first order because only the first order terms of a Taylor series expansion for $g()$ are involved, and second moment since only the first and second moments (mean values and variances) of the random variables are used in the formulation. One drawback of this method is that the performance function, $g()$, is linearized at the

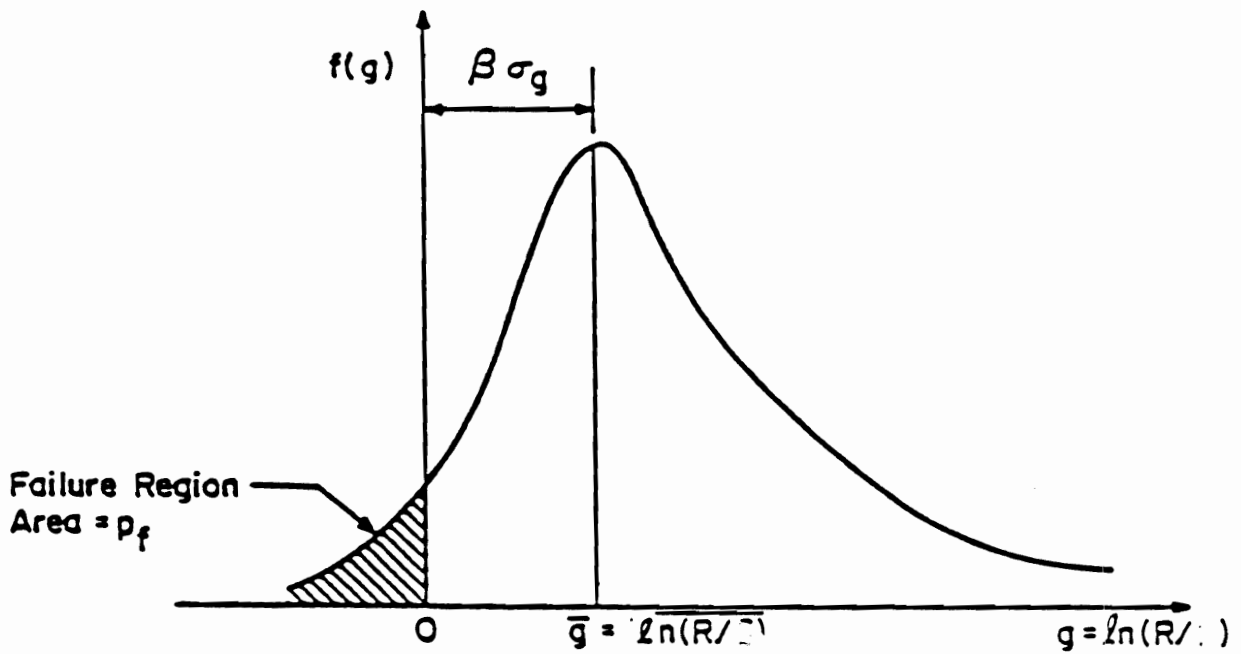


Figure 2.17 Definition of Safety Index β for Lognormal R and S

Table 2.9 Relationship between probability of failure and reliability index, β assuming lognormal loads and resistances*

β	Pf	β	Pf
2.5	9.86×10^{-3}	1.96	10^{-1}
3.0	1.15×10^{-3}	2.50	10^{-2}
3.5	1.34×10^{-4}	3.03	10^{-3}
4.0	1.56×10^{-5}	3.57	10^{-4}
4.5	1.82×10^{-6}	4.10	10^{-5}
5.0	2.12×10^{-7}	4.64	10^{-6}
5.5	2.46×10^{-8}	5.17	10^{-7}

* The numbers in the table are calculated using the simple approximate relationship between β and p_f given by Rosenbleuth and Esteva (1972) as follows:

$$p_f = 460 \exp(-4.3\beta)$$

mean values of the random variables. If $g()$ is nonlinear, neglecting the higher order terms can result in significant errors.

Dead loads in bridges and buildings are usually time invariant and normally distributed while live loads and resistances can be treated as lognormal variables. To circumvent the problems that arise with the first order second moment method when the distributions are mixed, the reliability index can be evaluated by transforming the nonnormal variables to equivalent normal variables. With these equivalent normal variables, the reliability index is calculated using the same procedure as for normal variables i.e. the performance function becomes:

$$g() = \bar{R}^N - \bar{D}^N - \bar{L}^N \quad (2-55)$$

and the reliability index, β , is calculated using the following equation:

$$\beta = \frac{\bar{R}^N - \bar{D}^N - \bar{L}^N}{\sqrt{(\sigma_R^N)^2 + (\sigma_D^N)^2 + (\sigma_L^N)^2}} \quad (2-56)$$

where the superscript N denotes the equivalent normal distribution for the mean values and standard deviations.

According to Ang and Tang (1984), the equivalent normal distribution of a nonnormal variable must be obtained such that "the cumulative probability as well as the probability

density ordinate of the equivalent normal distribution are equal to those of the corresponding nonnormal distribution at the appropriate point on the failure surface." A lognormally distributed random variable (eg. R) will have an equivalent normal mean and standard deviation as follows (Ang and Tang, 1984):

$$\bar{R}^N = r^* [1 - \ln r^* + \ln \bar{R} - 0.5 \ln(1 + V_R^2)] \quad (2-57)$$

and

$$\sigma_R^N = r^* \sqrt{\ln(1 + V_R^2)} \quad (2-58)$$

where \bar{R} and V_R are the mean value and c.o.v. of R respectively, and r^* is the value of R at the failure point. Similar expressions can be derived for the live load assuming that it too is lognormally distributed:

$$\bar{L}^N = l^* [1 - \ln l^* + \ln \bar{L} - 0.5 \ln(1 + V_L^2)] \quad (2-59)$$

and

$$\sigma_L^N = l^* \sqrt{\ln(1 + V_L^2)} \quad (2-60)$$

Although the performance function (Equation 2-55) is linear, the mean values and standard deviations required change with the failure point values. Hence, an iterative process is required to solve for β .

The iteration procedure is as follows:

1. Define the performance function; $g(X_1, X_2, X_3, \dots, X_n) = 0$ where the X_i 's are the design random variables.

2. Guess a value for the reliability index.
3. For the first iteration, equate the initial checking point $(X_1^*, X_2^*, X_3^*, \dots, X_n^*)$ to the point at the mean values $(\bar{X}_1, \bar{X}_2, \bar{X}_3, \dots, \bar{X}_n)$.
4. For all nonnormal variables, calculate the mean and standard deviation $(\bar{X}_i^N$ and $\sigma_i^N)$ of the equivalent normal distribution.
5. Evaluate $\partial g/\partial X_i$ for all values of X_i that are nonnormal at the checking point, X_i^* .
6. Calculate the direction cosines for all values of X_i that are nonnormal as follows:

$$\alpha_i^* = \frac{\partial g/\partial X_i}{\sqrt{[\sum(\partial g/\partial X_i)^2]}} \quad (2-61)$$

7. Calculate the new checking point for all values of X_i that are nonnormal from:

$$X_i^* = X_i^N - \alpha_i^* \beta \sigma_i^N \quad (2-62)$$

and repeat steps 4 to 7 until the value of β remains constant.

The reliability index can be calculated with the aid of a computer program that incorporates the above methodology.

To summarize, two methods of calculating reliability indices have been described. Both the FOSM and the iterative (or advanced) procedures can be used to calculate

β generically, using only the values of the bias and the coefficients of variation of the resistance and the loads.

2.3.3.2.2.3 Computation of Performance Factors

Once the reliability levels inherent in current design methods have been calculated, a target reliability index that reflects an acceptable margin of safety is selected. Performance factors can now be calculated using the selected target reliability index.

The expression for the performance factor can be derived by substituting $R_n = \bar{R}/\lambda_R$ into Equation 2-46, and expressing \bar{R} in terms of β , V_R , V_S and S through the use of Equation 2-53. The resulting expression for the performance factor, ϕ , is as follows:

$$\phi = \frac{\lambda_R(\sum \gamma_i S_i)}{\bar{S} \sqrt{\frac{1 + V_R^2}{1 + V_S^2}} \exp[\beta_T \sqrt{\ln(1 + V_R^2)(1 + V_S^2)}]} \quad (2-63)$$

where β_T is the target reliability index. When only dead and live loads are considered, Equation 2-63 simplifies to:

$$\phi = \frac{\lambda_R(\gamma_D S_D/S_L + \gamma_L)}{(\lambda_D S_D/S_L + \lambda_L) \sqrt{\frac{1 + V_R^2}{1 + V_D^2 + V_L^2}} \exp[\beta_T \sqrt{\ln(1 + V_R^2)(1 + V_D^2 + V_L^2)}]} \quad (2-64)$$

2.3.4 Other Methods of Incorporating Margins of Safety in Designs

Apart from working stress design and load factor design, there are at least two other methods of ensuring acceptable levels of risk in design. They include the following:

- (1) Bolton's worst attainable value approach, and
- (2) the λ approach

1. Bolton's Worst Attainable Value Approach

No safety factors are used in Bolton's (1981) worst attainable value approach. Instead, the approach assumes the worst set of values for the design parameters. An advantage of this method is that it forces the designer to think about the worst possible scenario. Disadvantages of this method include the following:

- (a) The determination of the margin of safety is left entirely to the judgment ("pessimism" or "optimism") of the engineer.
- (b) There may be one parameter which is very sensitive to the resistance while the other parameters are trivial in their contribution.
- (c) The soil exploration must be deemed to be as "inferior"

in quality as is attainable.

- (d) The occurrence of the worst condition scenario may be highly unlikely.

2. The λ Approach

Proposed by Simpson et al. (1981), this method of assigning a margin of safety also does not use a factor of safety per se. This approach is similar to load and resistance factor design in that the load is increased, and the parameters that contribute to resistance are decreased by a certain amount. The methodology is as follows:

- (a) Identify all limit states applicable to the structure.
- (b) Select the method(s) of analysis and determine all relevant variables (V). V should include all different load components, resistance parameters such as cohesion, angle of internal friction, etc.
- (c) Estimate the expected values of the variables (V_e).
- (d) Establish the worst credible values (V_{WC}) of each variable.
- (e) For each limit state, select from Table 2.10 the severity of consequence, and obtain the appropriate values of λ_1 and λ_2 .
- (f) Calculate the limit state value of each variable (V^*) as follows:

Table 2.10 Values of λ_1 and λ_2 for different failure consequences (After Simpson et al., 1981)

CLASS	SEVERITY OF CONSEQUENCE	λ_1	λ_2
1	Disappointing	-0.5	-0.8
2	Significant repairs	0.0	-0.6
3	Major damage or possible casualty	0.5	-0.4
4	Catastrophic	1.0	-0.2

$$V^* = V_{WC} + \lambda \Delta V \quad (2-65)$$

where V_{WC} = worst credible value

ΔV = uncertainty of V (positive for adverse effects such as loads and negative for beneficial effects such as cohesion in a bearing capacity problem)

$$\Delta V = V_{WC} - V_e \quad (2-66)$$

V_e = expected value of V

λ = values of λ_1 or λ_2 obtained from Table 2.10 corresponding to the severity of the consequence of reaching the limit state

- (g) Apply λ_1 to one variable and λ_2 to the other variables, and check the design without using any factor of safety.
- (h) Repeat step (g) with λ_1 applied to a different variable and λ_2 to all other variables, and check the design. Repeat this process until λ_1 is applied to all variables.
- (i) Select the case that yields the most conservative design from steps (g) and (h).

One advantage of this method is that it systematically considers the effects of each variable in the limit state. The use of the values of λ to calculate the limit state values (V^*) however, masks the role of the expected values, which usually govern the design in most cases.

CHAPTER THREE

SIMPLIFIED PROCEDURE FOR DESIGN OF PILES AND DRILLED SHAFTS TO RESIST LATERAL LOADS

3.1 Introduction

Lateral loads on deep foundations arise due to wind, earthquake, water pressures, earth pressures, and live loads. Deep foundations must be designed to withstand such forces without failing (i.e. without reaching the ultimate limit state), and without deflecting excessively (i.e. without reaching the serviceability limit state).

The governing criterion in the design of laterally loaded piles and drilled shafts is almost always the maximum tolerable deflection or the structural capacity of the pile or drilled shaft. Ultimate soil failure usually does not control the design, since mobilizing the ultimate lateral capacity of the soil requires such large displacements that this is not a realistic possibility in most cases.

Batter piles are frequently used to resist lateral loads. However, constructing batter drilled shafts is difficult. Construction problems include maintaining hole stability during excavation, installing casing and rebar cages in inclined holes, concrete placement in inclined holes, and availability of suitable construction equipment. Because of these difficulties, batter drilled shafts are

used infrequently. The discussion of lateral loading of deep foundations will be limited to only vertical piles and drilled shafts.

In designing vertical piles and drilled shafts to resist lateral loads, both lateral deflection and structural capacity should be considered. Procedures for estimating (1) lateral deflections of single piles and drilled shafts, (2) lateral deflections of groups of piles and drilled shafts, (3) maximum bending moments in single piles and drilled shafts, and (4) maximum bending moments in groups of piles and drilled shafts are addressed in the following sections.

3.2 Single Piles and Drilled Shafts

The procedure for estimating lateral deflections and bending moments in single piles and drilled shafts described here is the one developed by Evans and Duncan (1982). The Evans and Duncan procedure was derived from a large number of p-y analyses, and the method models non-linear behavior of the soil. Unlike p-y analyses, the Evans and Duncan procedure has the advantage of computational simplicity in that it does not require the use of a computer.

3.2.1 Evans and Duncan Procedure

Evans and Duncan (1982) related lateral deflections of deep foundations to the lateral loads using what they called a characteristic load (P_C). The characteristic load (P_C) embodies the important properties of the pile or drilled shaft (diameter, stiffness) and the soil (strength, stiffness) that determine the way that the pile or drilled shaft and soil respond to lateral loads. The larger the value of P_C , the greater is the capacity of the pile or drilled shaft to carry lateral loads, and the smaller is its deflection under a given lateral load. Procedures for calculating values of P_C are described in a subsequent section.

3.2.1.1 Lateral Deflection of Fixed-Head Piles or Drilled Shafts

The condition of restraint against rotation at the top of a pile or drilled shaft has a strong effect on the magnitude of its lateral deflection under load. Piles and drilled shafts that are embedded in reinforced concrete caps are effectively restrained from rotation at the top, and they deflect laterally with negligible rotation at the top. On the other hand, drilled shafts (and less frequently

piles) may be used individually by connecting directly to the structure without a cap, in which case they may be essentially free to rotate at the groundline. The lateral deflection of a fixed-head shaft is approximately one-fourth that of a free-head shaft subjected to the same load.

The procedures and charts discussed in this section are for fixed-head piles and drilled shafts. Charts in dimensionless form were developed by Evans and Duncan (1982) for sand and clay (Figs. 3.1 and 3.2). These charts show the variation of P_S/P_C with Y_S/D . P_S is the lateral load, P_C is the characteristic load, Y_S is the groundline lateral displacement, and D is the width or diameter of the single pile or drilled shaft. These charts model the same non-linear behavior of soil as the p-y method of analysis. The procedure for determining the lateral deflection of a pile or drilled shaft, using Figs. 3.1 and 3.2, is as follows:

- 1) For a pile, determine the width or diameter, D , the Young's modulus, E_p , and the moment of inertia I_p . Section and material properties of driven piles can usually be obtained from the manufacturer's literature.

In the case of a drilled shaft, select the diameter D , the concrete modulus E_c , and the steel reinforcement. The quantities needed for analysis of drilled piers are the flexural stiffness, $E_p I_p$ and R_I , the ratio of the moment of

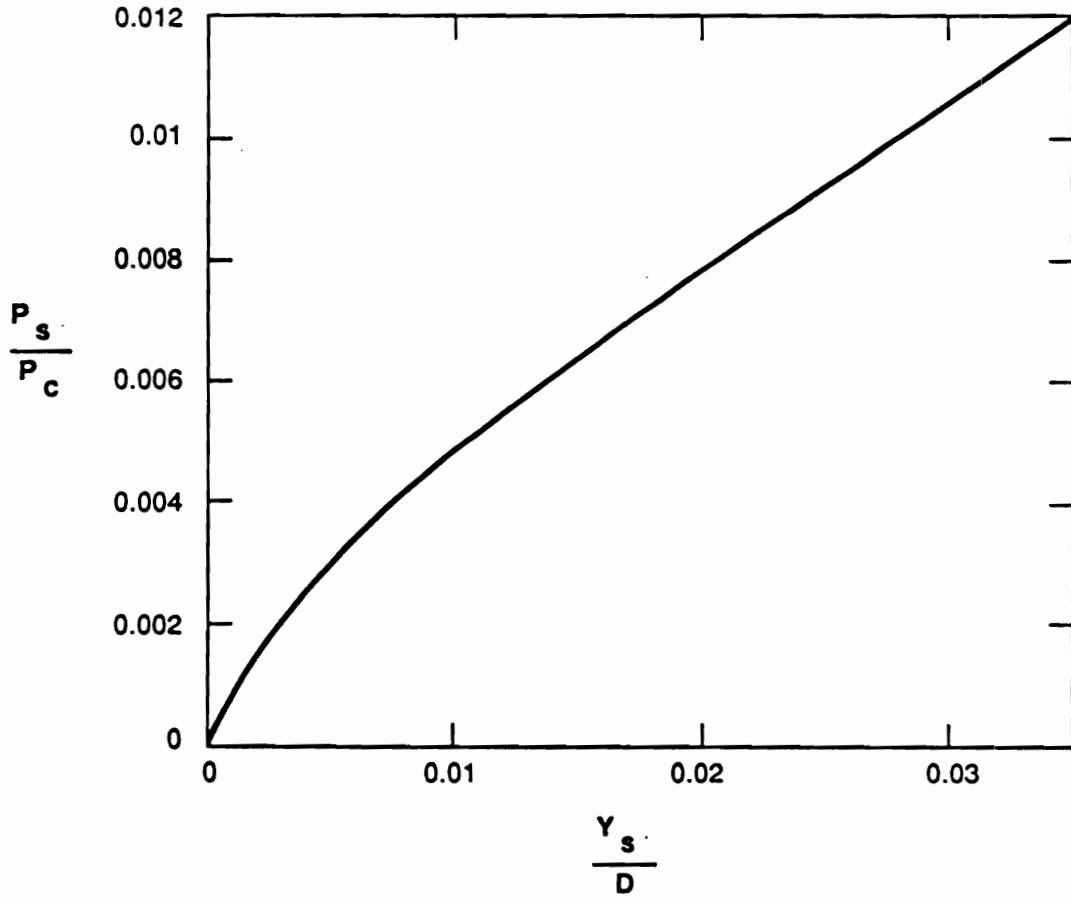


Figure 3.1 Lateral Load Versus Deflection for Fixed-Head Piles and Drilled Shafts in Sand (After Evans and Duncan, 1982)

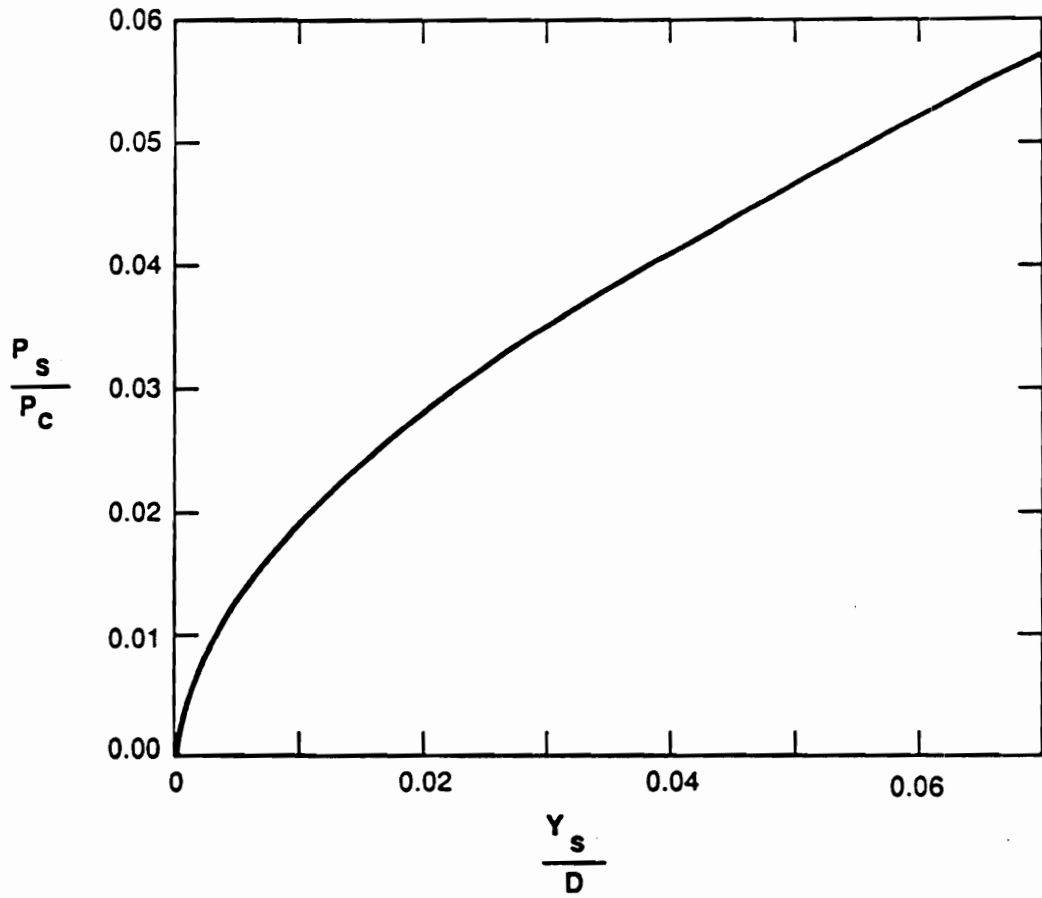


Figure 3.2 Lateral Load Versus Deflection for Fixed-Head Piles and Drilled Shafts in Clay (After Evans and Duncan, 1982)

inertia of the shaft to the moment of inertia of a solid, unreinforced, circular section. The moment of inertia of the shaft can be calculated considering the separate contribution of the concrete and the steel. The Young's modulus of the shaft (E_p) is conveniently taken as being equal to the Young's modulus of concrete (E_c), which can be related to the concrete compressive strength and density, as shown in Fig. 3.3. The modulus of steel can be taken as 29×10^6 psi.

2) Estimate the average undrained shear strength (S_u) for clays, or the average angle of internal friction (ϕ') for sands.

The behavior of the soil close to the ground surface is the most important with regard to lateral loads. The properties (S_u for clays, ϕ' and unit weight, γ' , for sands) should be averaged over a depth extending about eight pile or shaft diameters below the top of the pile or drilled shaft. Buoyant unit weights for sands are used below the water table.

3) Determine the characteristic load (P_C), which is defined by the following equations:

$$\text{For clay} \quad P_C = 7.34 D^2 (E_p R_I) (S_u / E_p R_I)^{0.683} \quad (3-1)$$

$$\text{For sand} \quad P_C = 1.57 D^2 (E_p R_I) (\gamma' D \phi' K_p / E_p R_I)^{0.57} \quad (3-2)$$

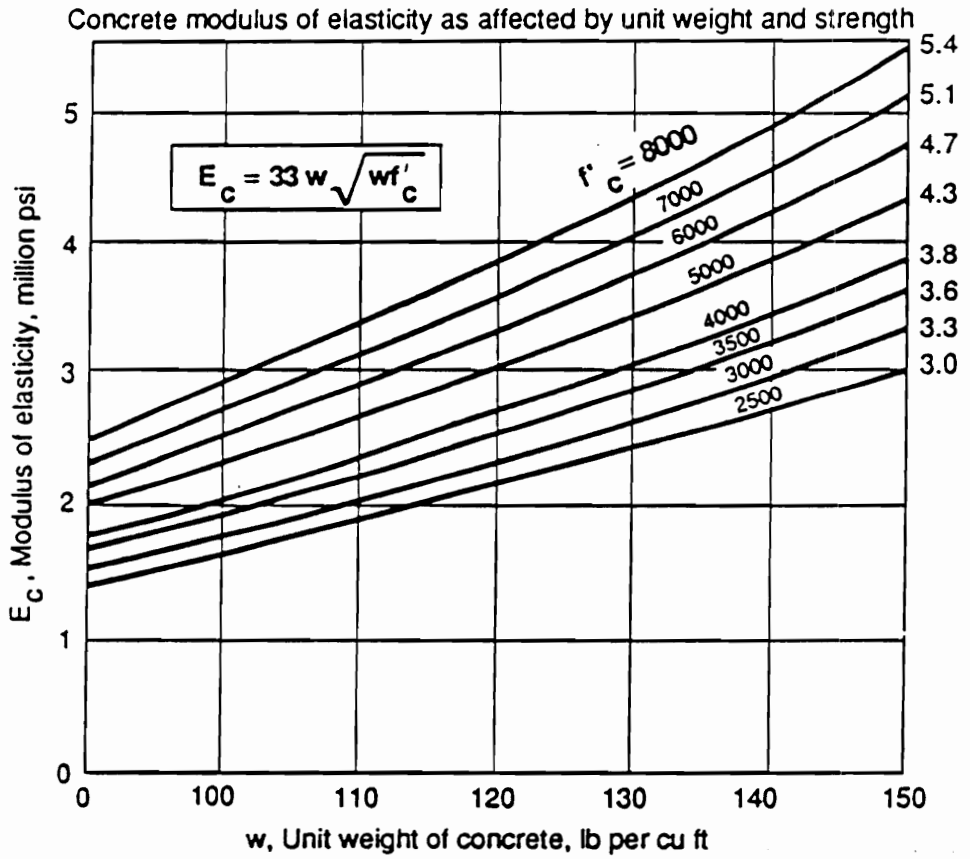


Figure 3.3 Modulus of Elasticity of Concrete (After PCI, 1985)

where R_I = moment of inertia ratio

$R_I = I_p/I_{\text{solid}}$ (See Table 3.1 for values of R_I for drilled shafts of various diameters and percentages of steel area)

I_{solid} = moment of inertia of a solid circular cross-section

$$I_{\text{solid}} = \pi D^4/64$$

Thus $E_p R_I = (E_p I_p)/(\pi D^4/64)$

γ' = effective unit weight of soil

K_p = Rankine passive earth pressure coefficient

$$K_p = \tan^2(45^\circ + \phi'/2)$$

ϕ' = angle of internal friction for sand (in degrees)

Consistent units must be used for all the terms in Equations 3-1 and 3-2.

4) Calculate the value of the load ratio, P_S/P_C .

5) Use Fig. 3.1 for piles or shafts in sand, or Fig. 3.2 for piles or shafts in clay to determine the value of Y_S/D .

6) Calculate $Y_S = D (Y_S/D)$.

Table 3.1: R_I values for drilled shafts with $E_C = 3500$ ksi,
 $E_S = 29\,000$ ksi and $c = 3$ in.

A_S/A_g	DIAMETER OF DRILLED SHAFT			
	18 in.	24 in.	30 in.	36 in.
0.01	1.06	1.07	1.09	1.09
0.02	1.11	1.14	1.16	1.18
0.04	1.21	1.27	1.31	1.34
0.08	1.38	1.50	1.58	1.63

where A_S = area of steel

A_g = gross cross-sectional area of drilled shaft

c = cover

3.2.1.2 Lateral Deflection of Free-Head Piles or Drilled Shafts

A lateral load (P_S) acting at a distance (e) above the ground, can be resolved into two components as shown in Fig. 3.4: a lateral load with the same magnitude (P_S) acting at the groundline, plus a bending moment (M_e) equal to the lateral load multiplied by the eccentricity (i.e. $M_e = P_S e$). Evans and Duncan showed that the lateral displacement of a free-head pile or drilled shaft can be estimated using nonlinear superposition of the deflection caused by the lateral load (Y_{SP}) and the deflection caused by the bending moment (Y_{SM}).

The component of the lateral displacement (Y_{SP}) due to the groundline lateral load can be estimated using Figs. 3.5 and 3.6. The procedure is the same as described in connection with fixed-head piles and drilled shafts in Section 3.2.1.1.

The component of the lateral displacement (Y_{SM}) due to the bending moment can be estimated as follows:

- 1) Calculate the bending moment $M_e = P_S e$
- 2) Determine the characteristic moment (M_C), which is defined by the following equations:

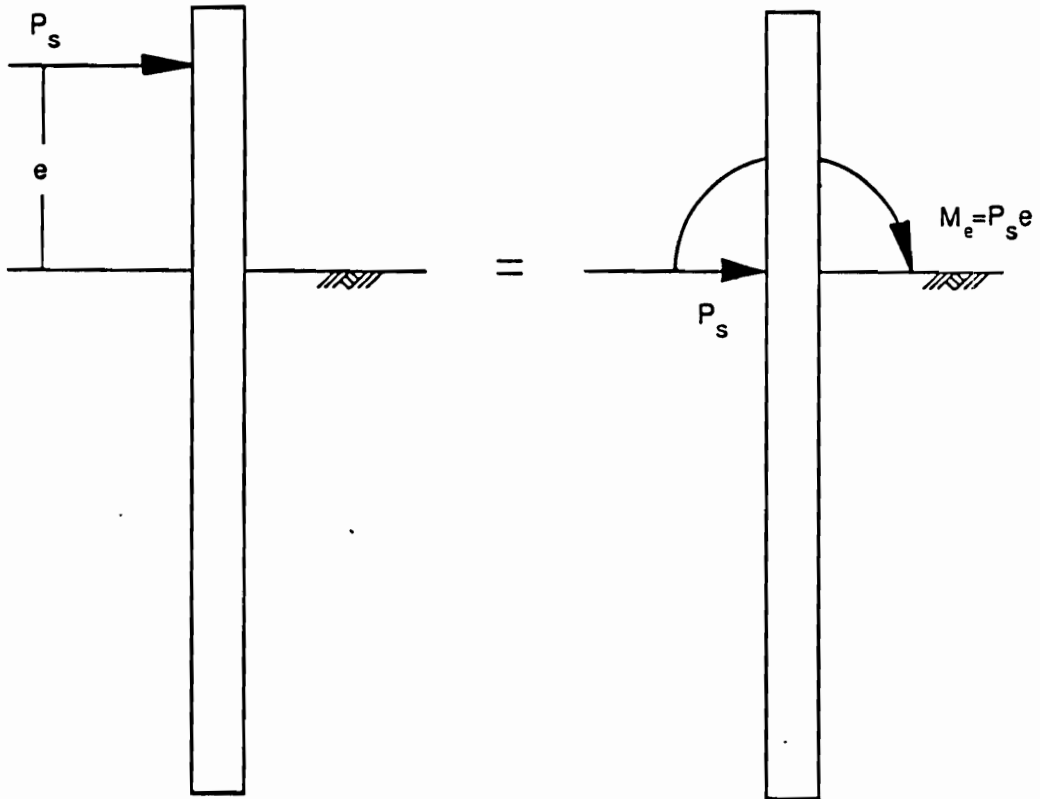


Figure 3.4 Resolution of Eccentric Load into a Lateral Load Acting on the Groundline and a Moment

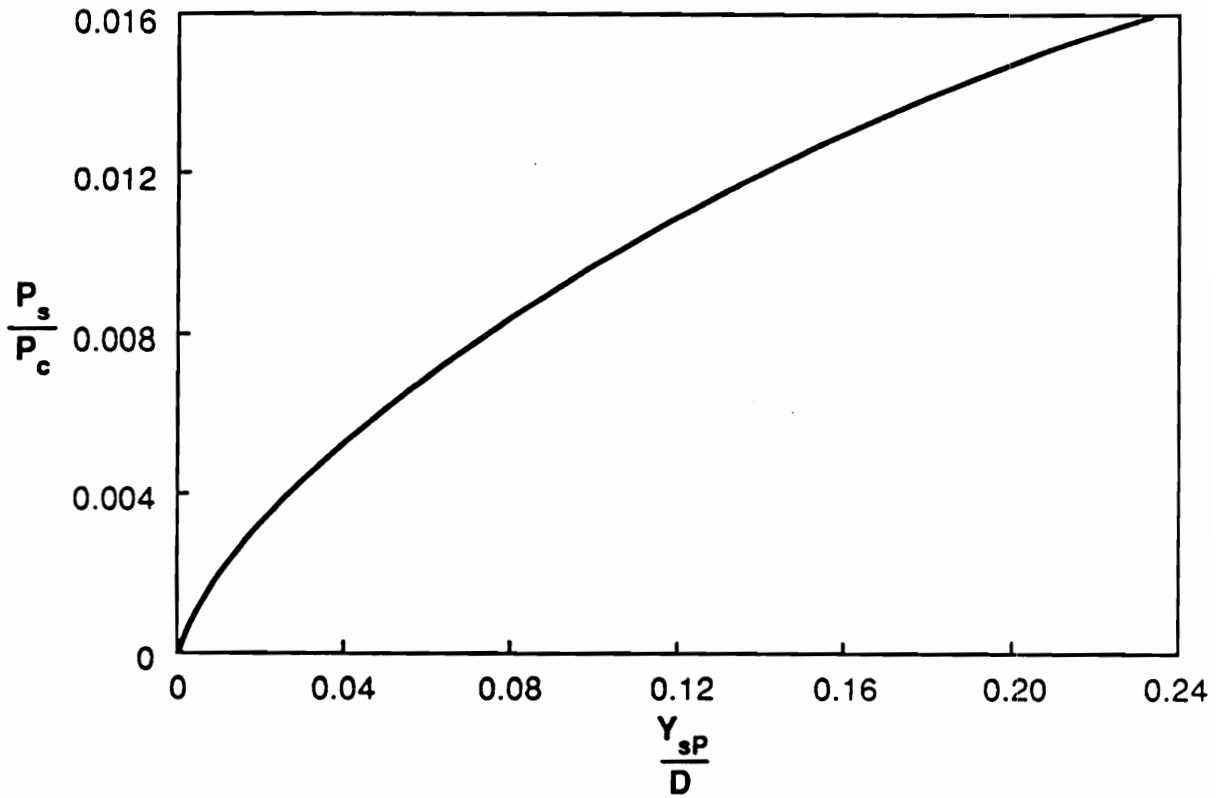


Figure 3.5 Lateral Load Versus Deflection for Free-Head Piles and Drilled Shafts in Sand (After Evans and Duncan, 1982)

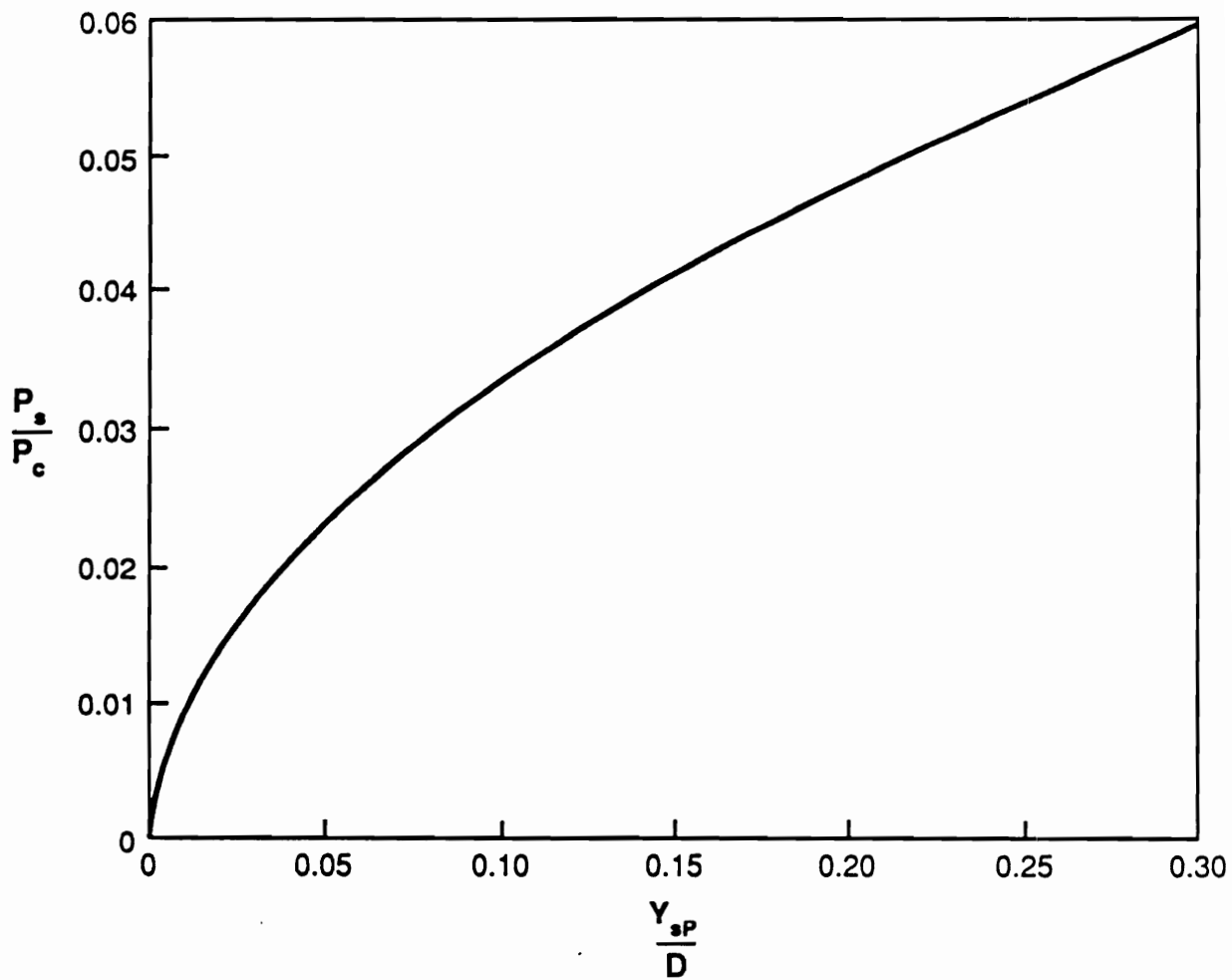


Figure 3.6 Lateral Load Versus Deflection for Free-Head Piles and Drilled Shafts in Clay (After Evans and Duncan, 1982)

$$\text{For clay} \quad M_C = 3.86 D^3 (E_p R_I) (S_u / E_p R_I)^{0.46} \quad (3-3)$$

$$\text{For sand} \quad M_C = 1.33 D^3 (E_p R_I) (\gamma' D \phi' K_p / E_p R_I)^{0.4} \quad (3-4)$$

where R_I , K_p , γ' , and ϕ' are as defined previously. Consistent units must be used in all the terms in Equations 3-3 and 3-4.

3) Calculate the ratio M_e/M_C .

4) Use Fig. 3.7 for piles or shafts in sand and Fig. 3.8 for piles or shafts in clay to determine the value of Y_{SM}/D .

5) Calculate $Y_{SM} = D(Y_{SM}/D)$.

Knowing Y_{SP} and Y_{SM} , the total lateral deflection of a free-head pile or drilled shaft can then be estimated using nonlinear superposition as follows (Evans and Duncan, 1982):

1) Using Y_{SM} and Fig. 3.5 for piles or shafts in sand, or Fig. 3.6 for piles or shafts in clay, calculate P_M as shown in Fig. 3.9b.

P_M is the equivalent lateral load that would cause the deflection Y_{SM} .

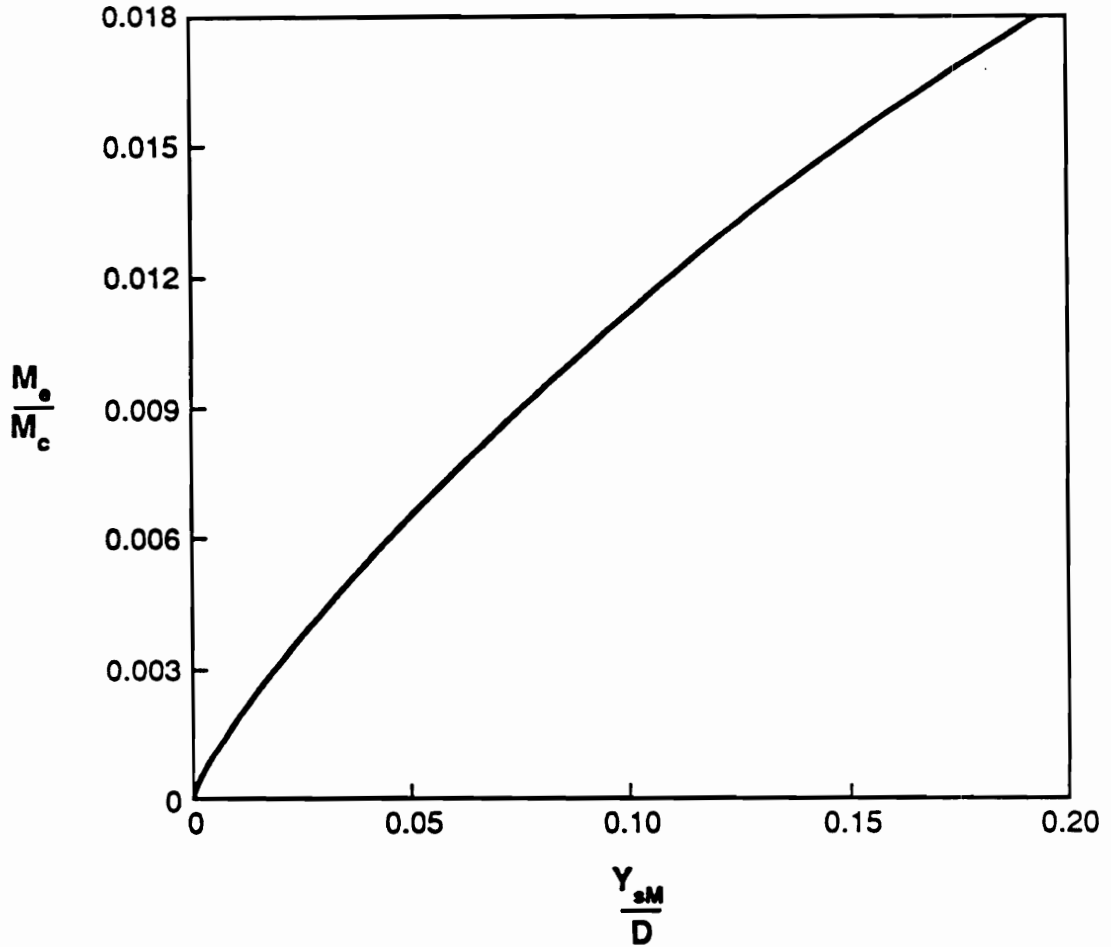


Figure 3.7 Moment Versus Deflection for Free-Head Piles and Drilled Shafts in Sand (After Evans and Duncan, 1982)

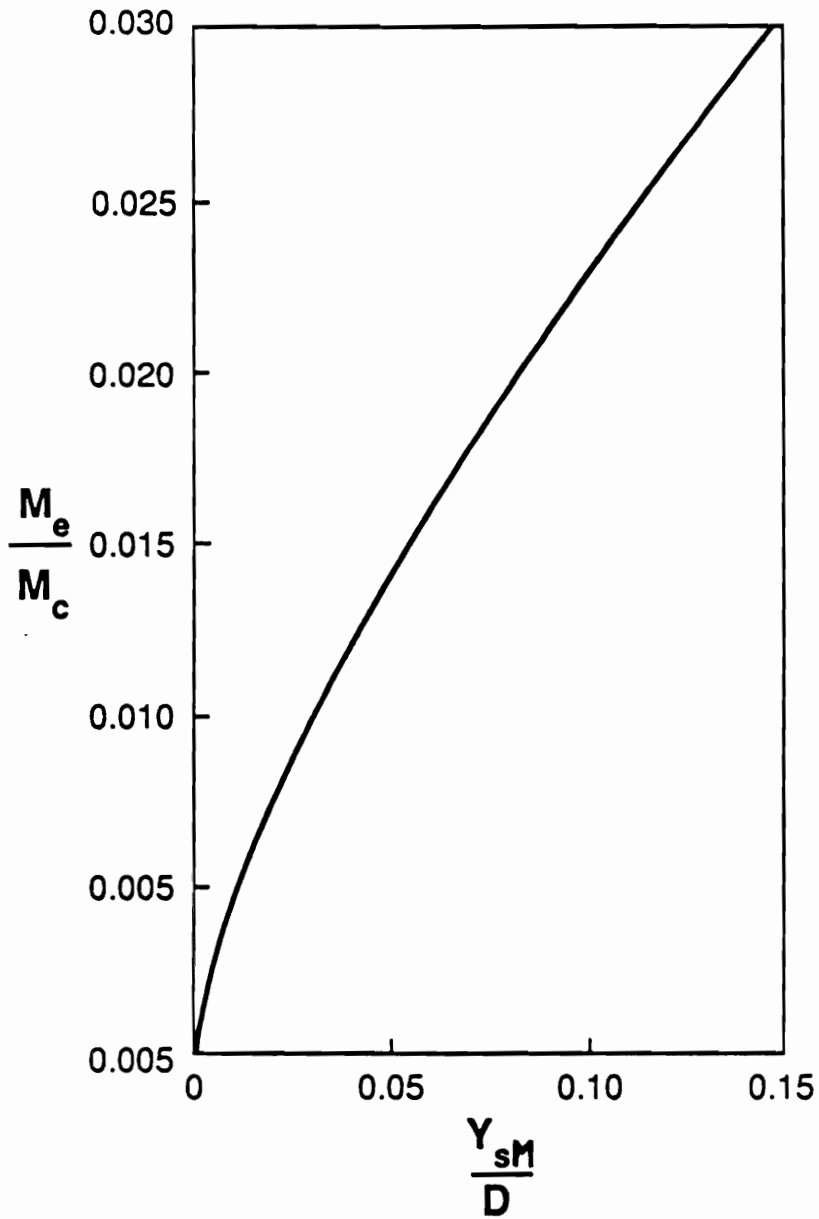


Figure 3.8 Moment Versus Deflection for Free-Head Piles and Drilled Shafts in Clay (After Evans and Duncan, 1982)

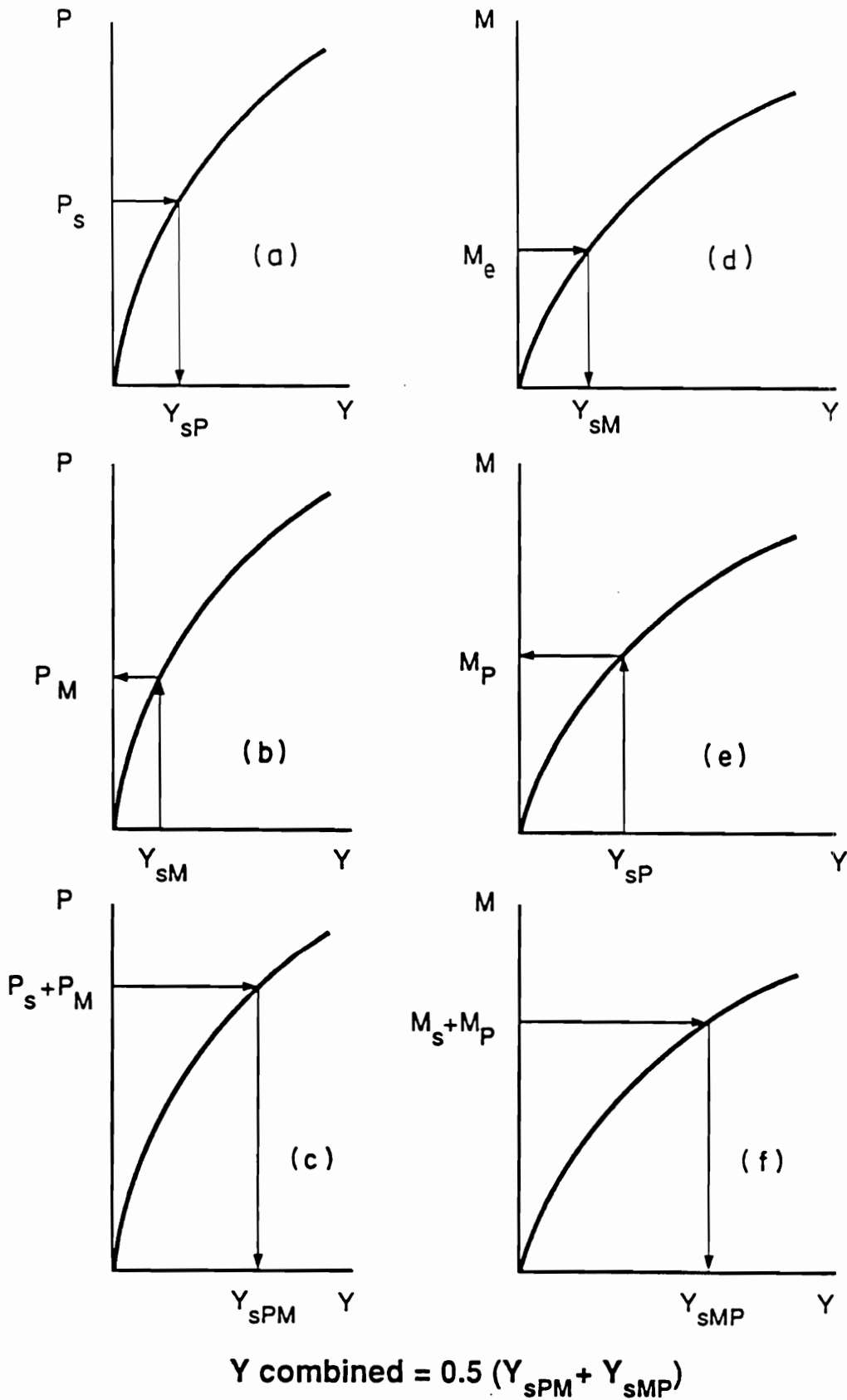


Figure 3.9 Non-Linear Superposition (After Evans and Duncan, 1982)

2) Using Y_{SP} and Fig. 3.7 for piles or shafts in sand and Fig. 3.8 for piles or shafts in clay, calculate M_p as shown in Fig. 3.9e.

M_p is the equivalent moment that would cause the deflection Y_{SP} .

3) Determine the deflection Y_{SPM} caused by the lateral load ($P_S + P_M$) as shown in Fig. 3.9c. Y_{SPM} is the deflection caused by the sum of the real load plus the equivalent load.

4) Determine the deflection Y_{SMP} caused by the moment ($M_S + M_p$) as shown in Fig. 3.9f. Y_{SMP} is the deflection caused by the sum of the real moment plus the equivalent moment.

5) Estimate the total deflection (Y_S) using the equation $Y_S = 0.5(Y_{SPM} + Y_{SMP})$

3.2.1.3 Bending Moments in Fixed-Head Piles or Drilled Shafts

Evans and Duncan (1982) developed a simple procedure for estimating the maximum bending moment induced in single piles and drilled shafts (M_S) due to a lateral load at the top of the pile or drilled shaft. They developed the design charts shown in Figs. 3.10 and 3.11 for fixed-head piles and

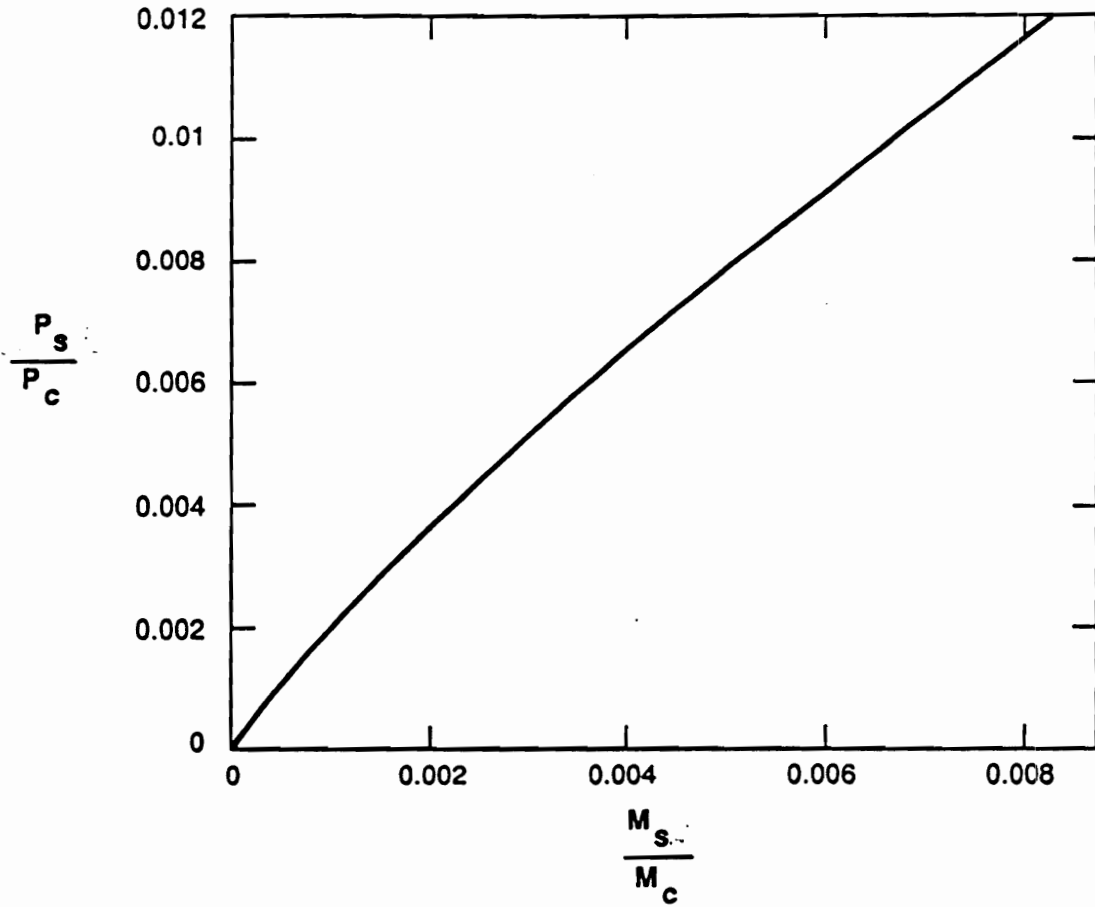


Figure 3.10 Lateral Load Versus Moment for Fixed-Head Piles and Drilled Shafts in Sand (After Evans and Duncan, 1982)

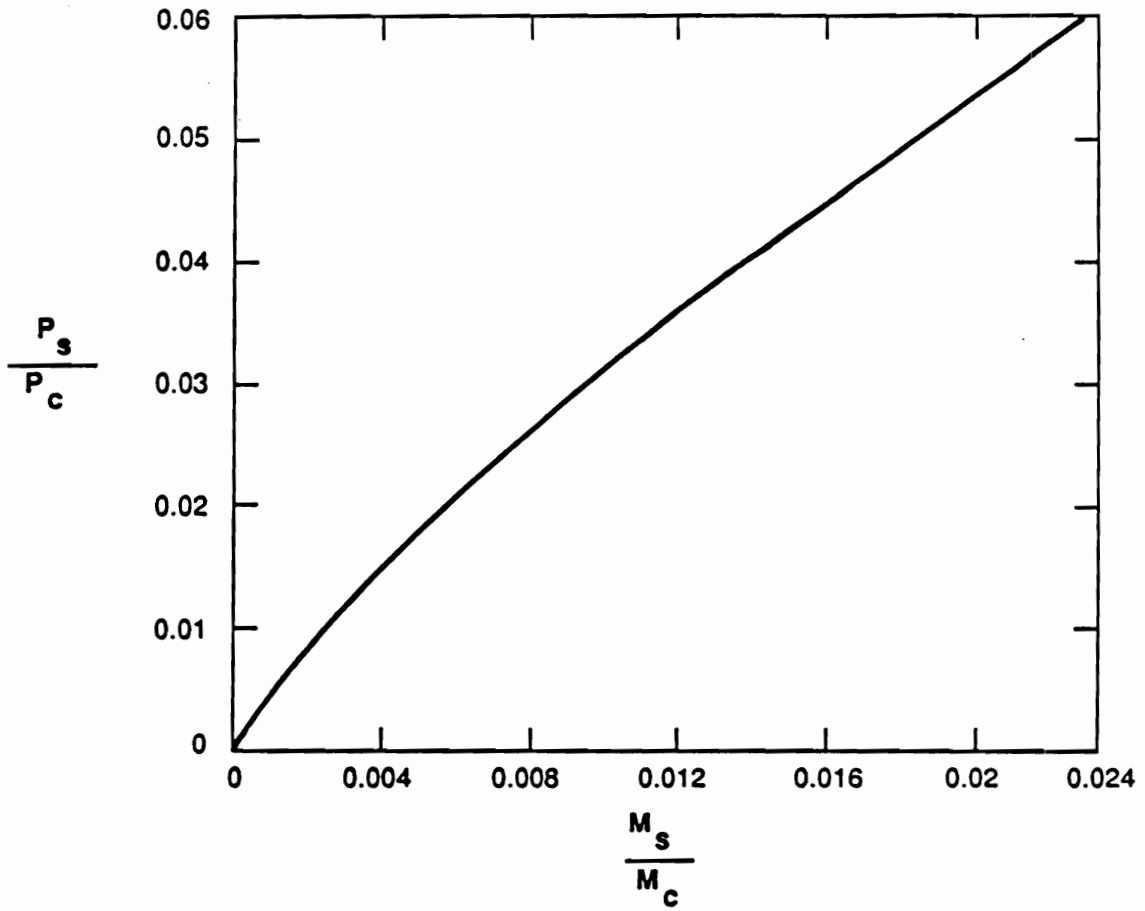


Figure 3.11 Lateral Load Versus Moment for Fixed-Head Piles and Drilled Shafts in Clay (After Evans and Duncan, 1982)

drilled shafts in sand and clay. These charts show the variation of M_S/M_C with P_S/P_C , where M_S = maximum moment in a single pile or drilled shaft and M_C = characteristic moment.

Using these charts, the bending moment in a laterally loaded pile or drilled shaft can be estimated as follows:

- 1) Refer to step (1) in Section 3.2.1.1.
- 2) Refer to step (2) in Section 3.2.1.1.
- 3) Determine the characteristic load (P_C) using Equation 3-1 for clay or 3-2 for sand.
- 4) Calculate the lateral load, P_S and the value of the load ratio, P_S/P_C .
- 5) Use Fig. 3.10 for fixed-head piles or drilled shafts in sand and Fig. 3.11 for fixed-head piles or drilled shafts in clay to determine the value of M_S/M_C .
- 6) Determine the characteristic moment (M_C) which is defined by Equations 3-3 and 3-4.
- 7) Calculate $M_S = M_C(M_S/M_C)$.

3.2.1.4 Bending Moments in Free-Head Piles or Drilled Shafts

The maximum bending moment in a free-head pile (or drilled shaft) occurs in the portion of the pile that extends below ground or the portion above ground. The magnitude of the maximum moment is needed for design, and, in some cases, it may be necessary also to know the depth below ground at which the maximum moment occurs. These quantities cannot be determined directly using the procedure developed by Evans and Duncan, but they can be calculated using the theory described by Matlock and Reese (1961), together with the value of groundline deflection calculated using the Evans and Duncan (1982) procedure. The technique for estimating groundline deflections of free-head piles and drilled shafts was explained in Section 3.2.1.2. When the groundline deflection (Y_S) has been determined, the magnitude of the maximum moment and its depth below ground can be estimated as follows:

1) Calculate the characteristic length (T) of the drilled shaft by solving the following equation for T (Matlock and Reese, 1961):

$$Y_S = \frac{2.435P_S}{E_p I_p} T^3 + \frac{1.623M_e}{E_p I_p} T^2 \quad (3-5)$$

where Y_s , E_p , I_p and P_s are as defined previously and T is the characteristic length. The value of T can be determined using repeated trials.

3) Calculate the maximum bending moment using the following expression:

$$M_{\max} = k_M M_e \quad (3-6)$$

where M_e is the bending moment at the groundline ($M_e = P_s e$), P_s is the lateral load, e is the eccentricity of the lateral load above the groundline, and k_M is a moment multiplier which is a function of T/e . The value of k_M can be calculated as follows:

$$k_M = 1 + 0.756(T/e) \quad (3-7)$$

where T is the characteristic length calculated from Equation 3-5. The location of the maximum bending moment can be estimated using Table 3.2.

3.2.1.5 Deflections and Bending Moments in Piles or Drilled Shafts With Caps Above Ground

When piles or piers are attached to a cap above ground, with an air gap between the bottom of the cap and the ground, the maximum bending moment can occur below ground

Table 3.2 Approximate location of the maximum bending moment in free-head piles or drilled shafts

T/e	z/T
0.0	0.0
0.1	0.4
0.2	0.5
0.3	0.6
0.4	0.7
0.5	0.8
0.8	0.9
1.6	1.0
3.0	1.2
14.0	1.4

(as discussed in the previous section) or at the top of the pile (the bottom of the cap). For piles connected to a cap above ground, expressions for the deflection of the cap and the magnitudes of the maximum bending moment in the pile can be derived using beam theory and the Evans and Duncan nonlinear superposition procedure. The magnitude of the maximum bending moment at the top of the pile (the bottom of the cap) can be estimated using the following equation:

$$M_T = \frac{\frac{M_e}{6} \left[3 + \left(\frac{z_{\max}}{L_u} \right)^2 \right] + M_{\max} \left(\frac{z_{\max}}{L_u} \right)}{1 + \left(\frac{z_{\max}}{L_u} \right)} \quad (3-8)$$

where M_{\max} = maximum bending moment for a free-head pile that occurs below ground, estimated using the nonlinear superposition procedure described in Section 3.2.1.4

z_{\max} = depth below ground where M_{\max} occurs

L_u = unsupported length of free-head pile or drilled shaft (L_u = eccentricity, e), and

M_e = moment at the groundline for a free-head pile
(= $P_s e$ or $P_s L_u$)

Equation 3-8 was derived with the aid of Fig. 3.12 and the following assumptions:

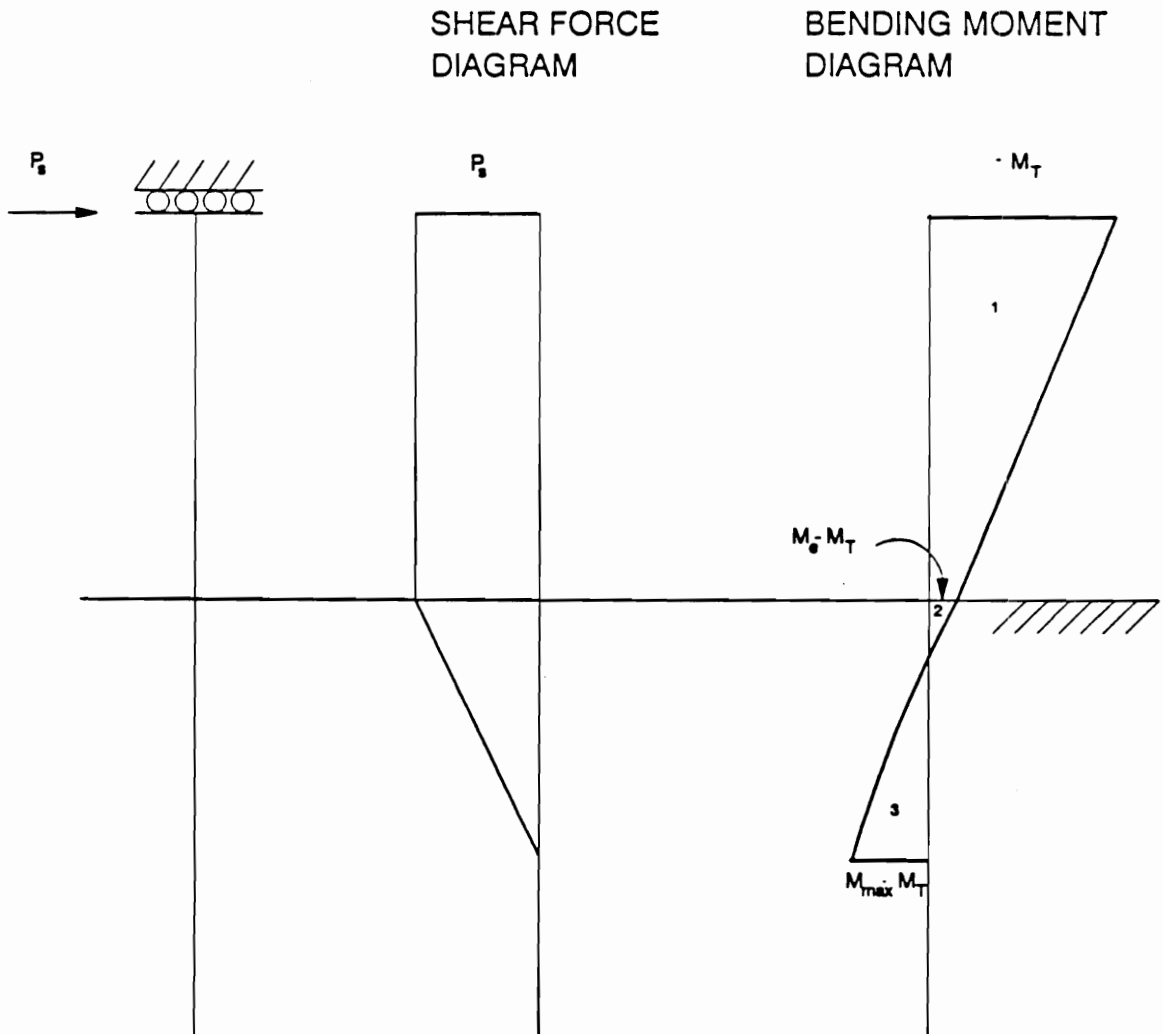


Figure 3.12 Idealized Shear Force and Bending Moment Diagram In a Pile That Can Translate But Not Rotate At The Top

- 1) The shear force diagram decreases linearly from P_S at the ground surface to zero at the location of the maximum bending moment.
- 2) The slope at the location of the maximum bending moment is zero.
- 3) The cap provides complete rotational restraint at the top of the pile. For this condition, the area underneath the bending moment diagram on the side for positive moments is equal to the area underneath the bending moment diagram on the side for negative moments, i.e. in Fig. 3.12, Area 1 + Area 2 = Area 3.

The magnitude of the maximum bending moment below ground for this boundary condition is equal to $(M_{\max} - M_T)$.

The deflection of the cap above ground may be divided into two components. The first is the deflection of the free-head pile at the groundline (Y_{ground}), which can be estimated using nonlinear superposition of the deflection caused by a groundline lateral load (P_S), and the deflection caused by the moment at the groundline which is equal to $(M_e - M_T)$. Note that since M_e is always less than M_T , $(M_e - M_T)$ is always negative, and the deflection components caused by P_S and $(M_e - M_T)$ are in opposite directions.

The second component of the deflection is the displacement of the cap relative to the pile at the groundline ($Y_T - Y_{\text{ground}}$). This can be evaluated by

integrating the expression for the bending moment above the groundline twice, and by dividing by the flexural stiffness ($E_p I_p$) of the pile or drilled shaft. The resulting expression for this deflection component is:

$$Y_T - Y_{\text{ground}} = \frac{L_u^2}{6E_p I_p} [M_e - 3M_T] \quad (3-9)$$

where L_u , M_e and M_T are as defined previously. To calculate the deflection of the cap Y_T , Y_{ground} and $(Y_T - Y_{\text{ground}})$ are added together.

3.2.2 Simplified Procedure for Design of Single Fixed-Head Piles and Drilled Shafts to Resist Lateral Loads

Driven Piles

The Evans and Duncan procedure for estimating lateral deflections and bending moments in laterally loaded fixed-head piles has been used to develop lateral load-deflection curves and lateral load-moment curves for some commonly-used pile sections. Charts for prestressed concrete piles (10 in., 12 in., 14 in., 16 in., and 18 in. square) and steel-H piles (HP 10 X 42, HP 10 X 57, HP 12 X 53, HP 12 X 74, HP 14 X 73, and HP 14 X 89) in sand and clay are shown in Figs. 3.13 through 3.16. For these piles and soil conditions, deflections can be estimated directly using the charts. For

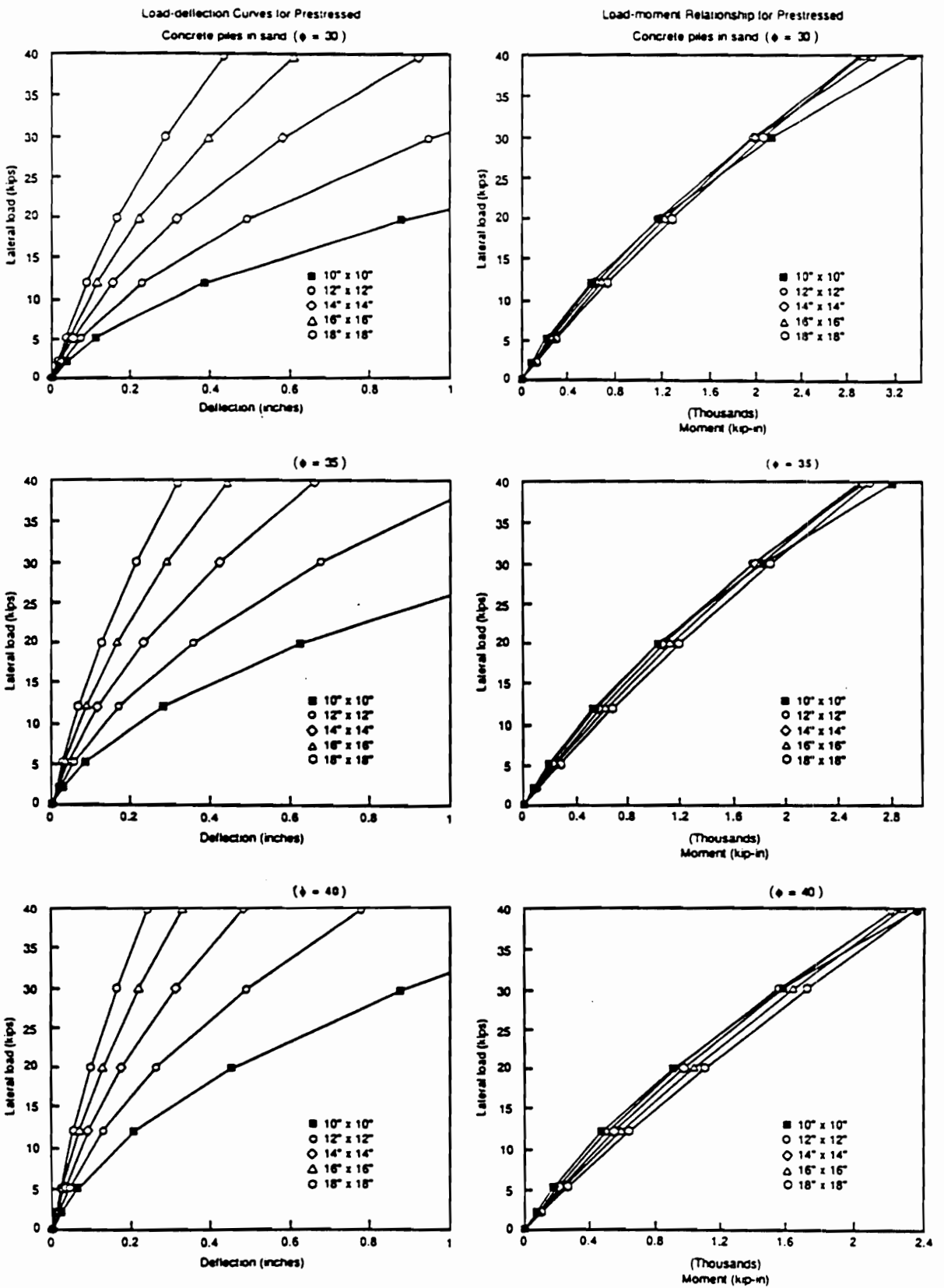


Figure 3.13 Load Versus Deflection and Load Versus Moment for Prestressed Concrete Piles in Sand

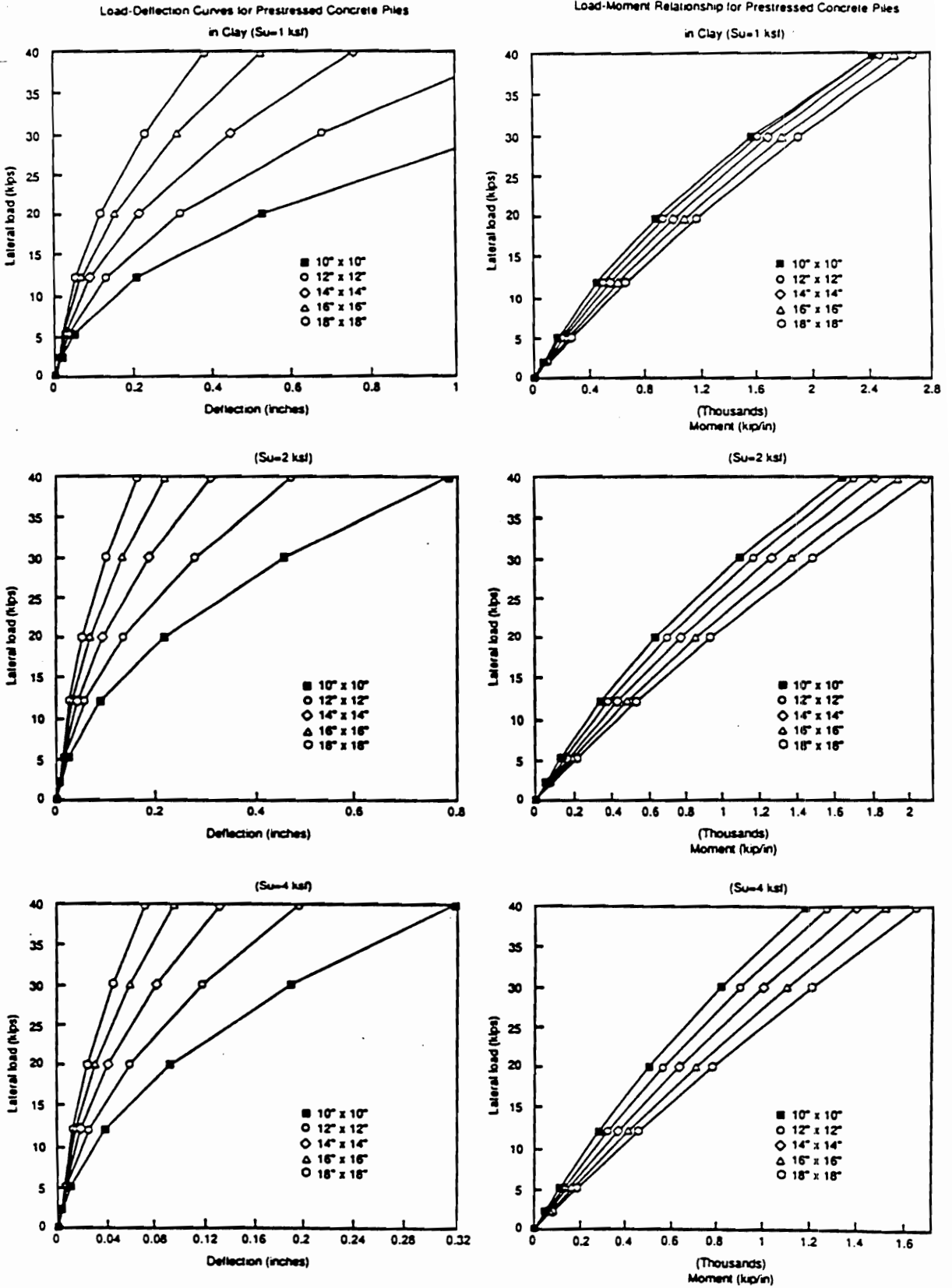


Figure 3.14 Load Versus Deflection and Load Versus Moment for Prestressed Concrete Piles in Clay

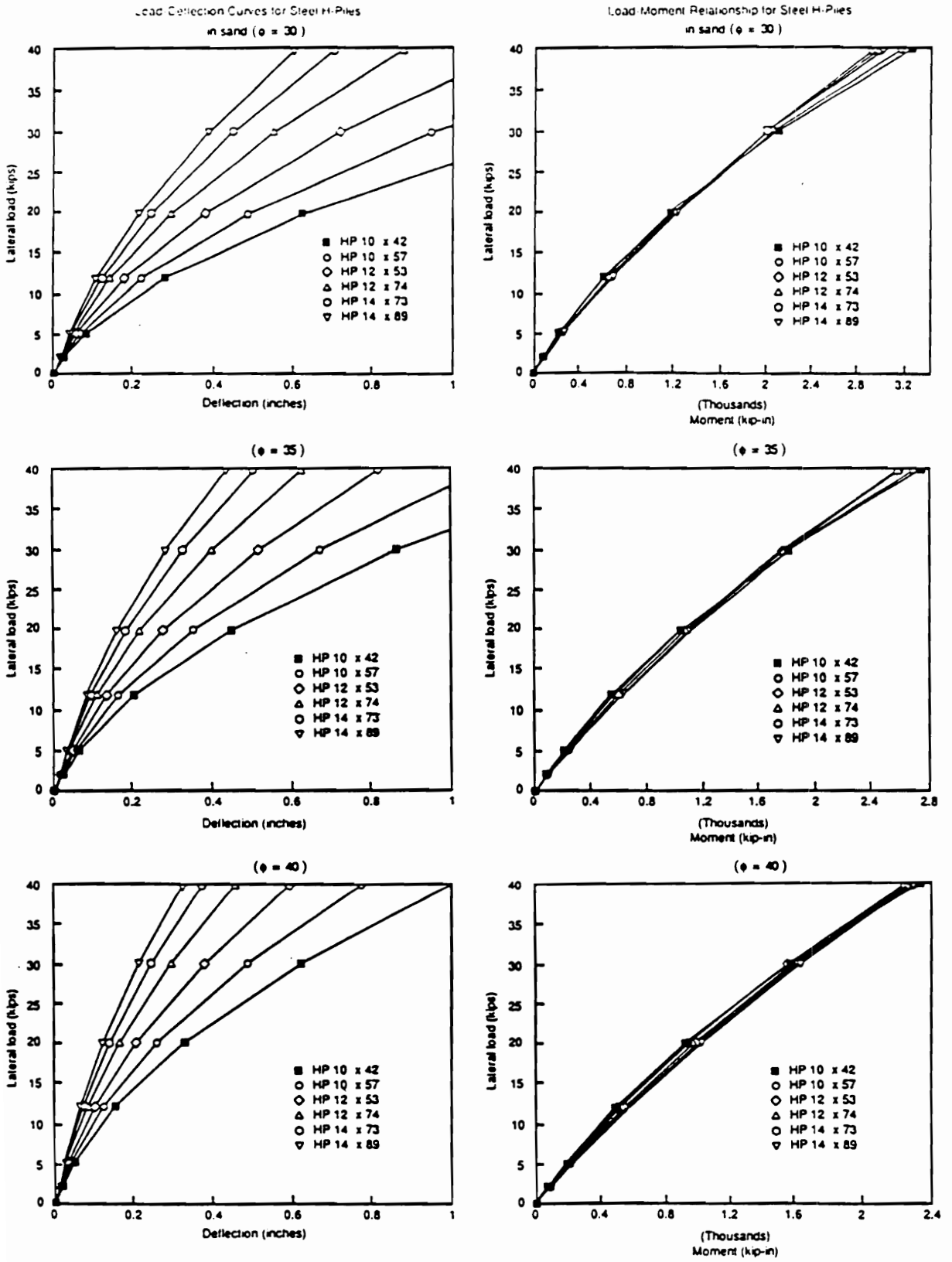


Figure 3.15 Load Versus Deflection and Load Versus Moment for Steel-H Piles in Sand

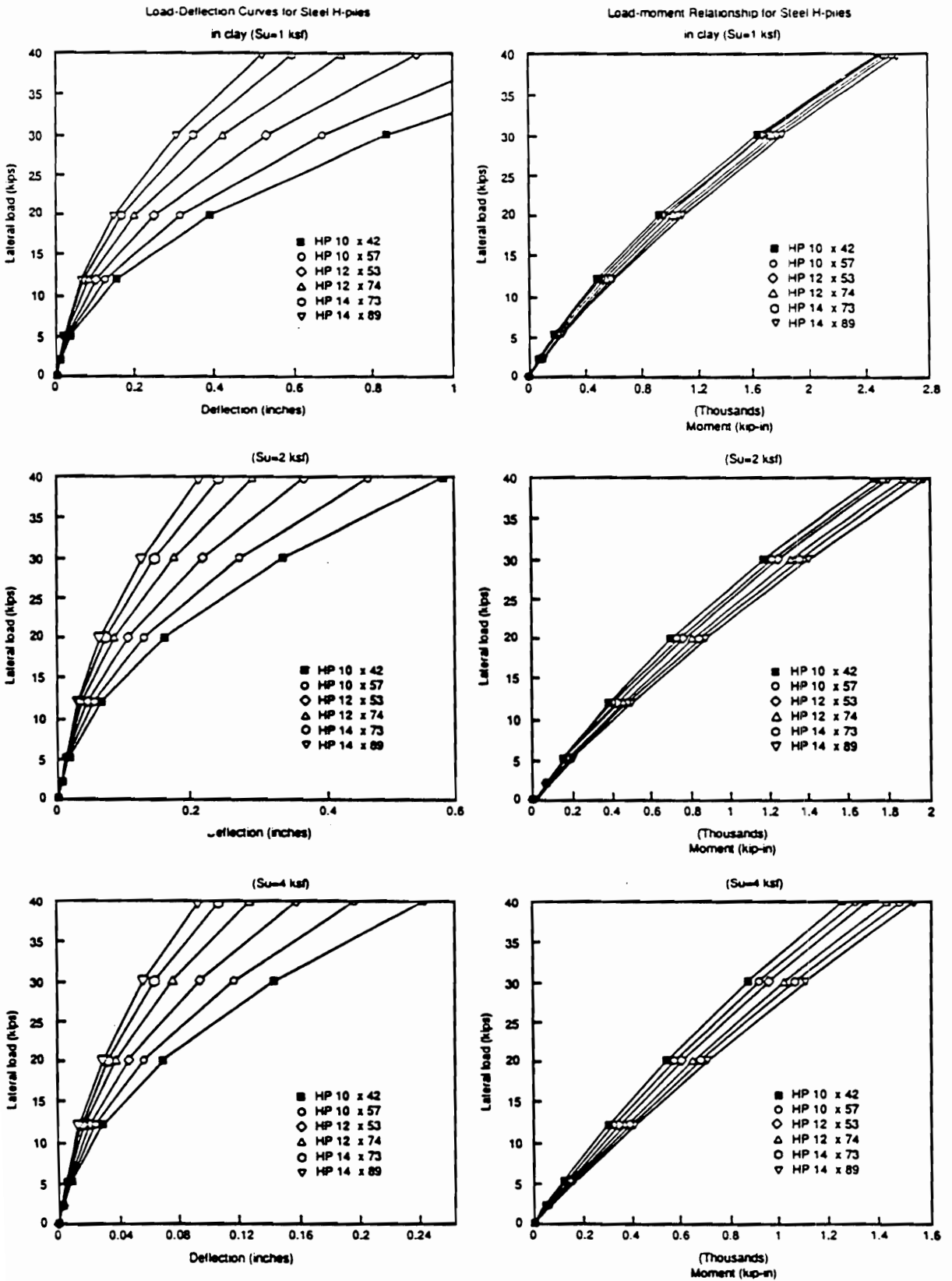


Figure 3.16 Load Versus Deflection and Load Versus Moment for Steel-H Piles in Clay

example, a lateral load of 10 kips acting on a 12 in. X 12 in. prestressed concrete pile driven in clay with $S_u = 1$ ksf will result in a lateral deflection of about 0.1 in. (Fig. 3.14) and a bending moment of 400 kip-in.

For sands, charts were developed for friction angles of 30° , 35° and 40° . The water table was assumed to be at or above the ground surface. For intermediate values of friction angle between those shown in the charts, deflections may be estimated by interpolation.

For clays, the load-deflection curves were developed for undrained shear strengths of 1, 2 and 4 ksf. Deflections for intermediate values of undrained shear strengths can be estimated by interpolation.

Drilled Shafts

The Evans and Duncan procedure for estimating lateral deflections and bending moments in laterally loaded fixed-head drilled shafts has been used to develop lateral load-deflection curves and lateral load-moment curves for some commonly-used drilled shaft sections. Charts for drilled shafts of 18 in., 24 in., 30 in. and 36 in. diameters, with percentages of reinforcement equal to 1%, 2%, 4% and 8%, constructed in sand and clay, are shown in Figs. 3.17 through 3.24. For these drilled shafts and soil conditions, deflections can be estimated directly using the charts. For

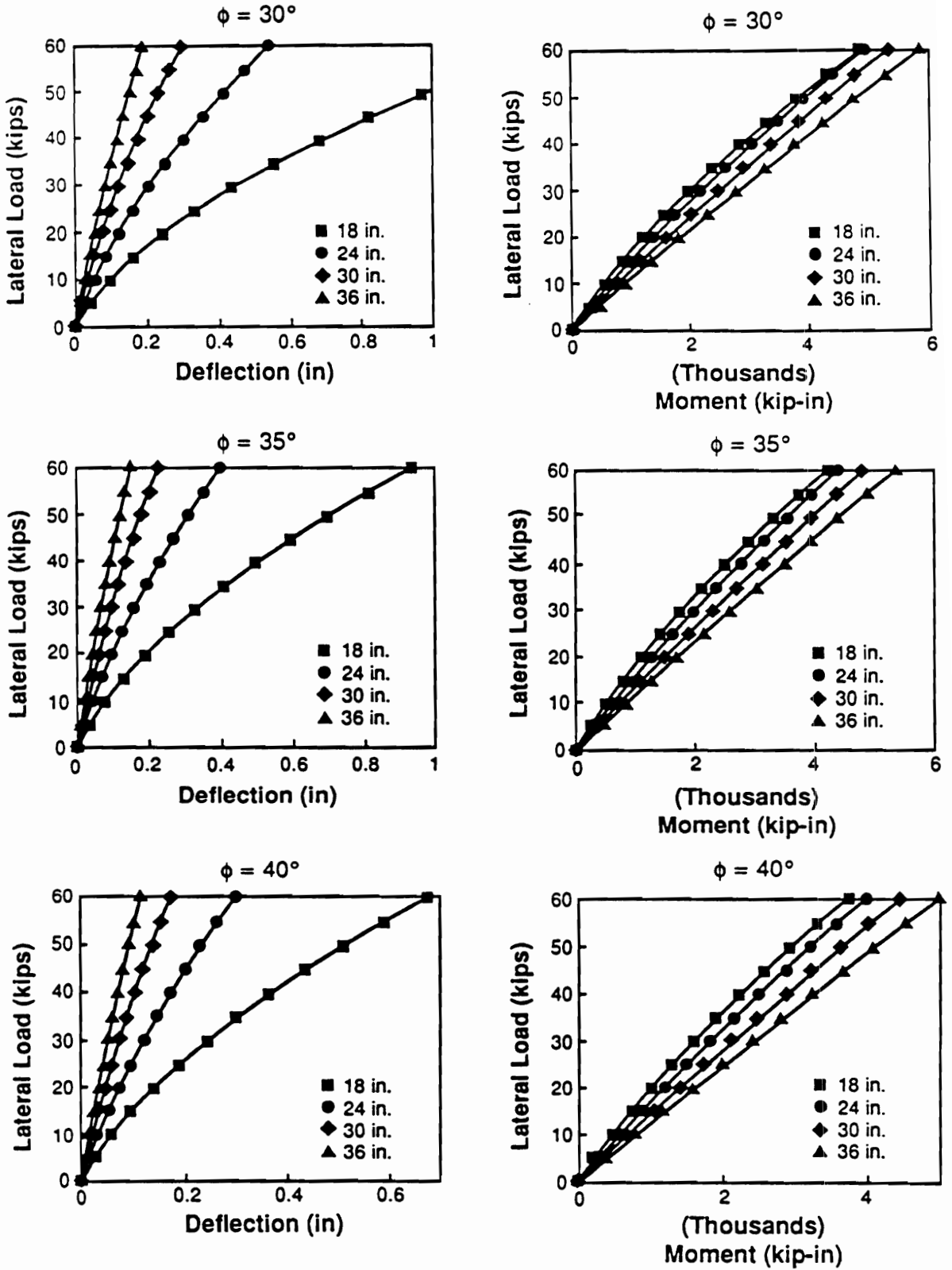


Figure 3.17 Load Versus Deflection and Load Versus Moment for Drilled Shafts ($A_y/A_g = 1\%$) in Sand

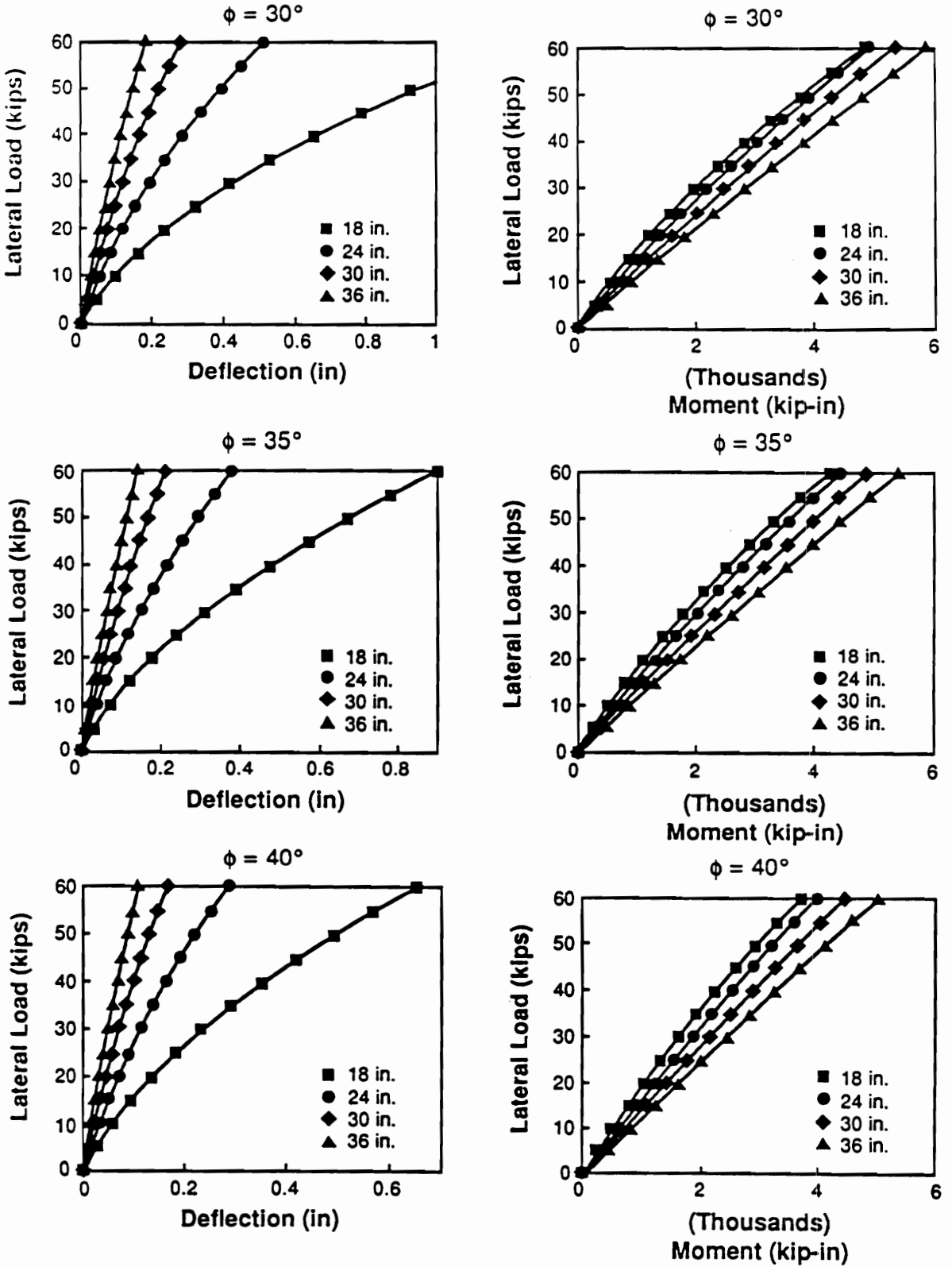


Figure 3.18 Load Versus Deflection and Load Versus Moment for Drilled Shafts ($A_y/A_g = 2\%$) in Sand

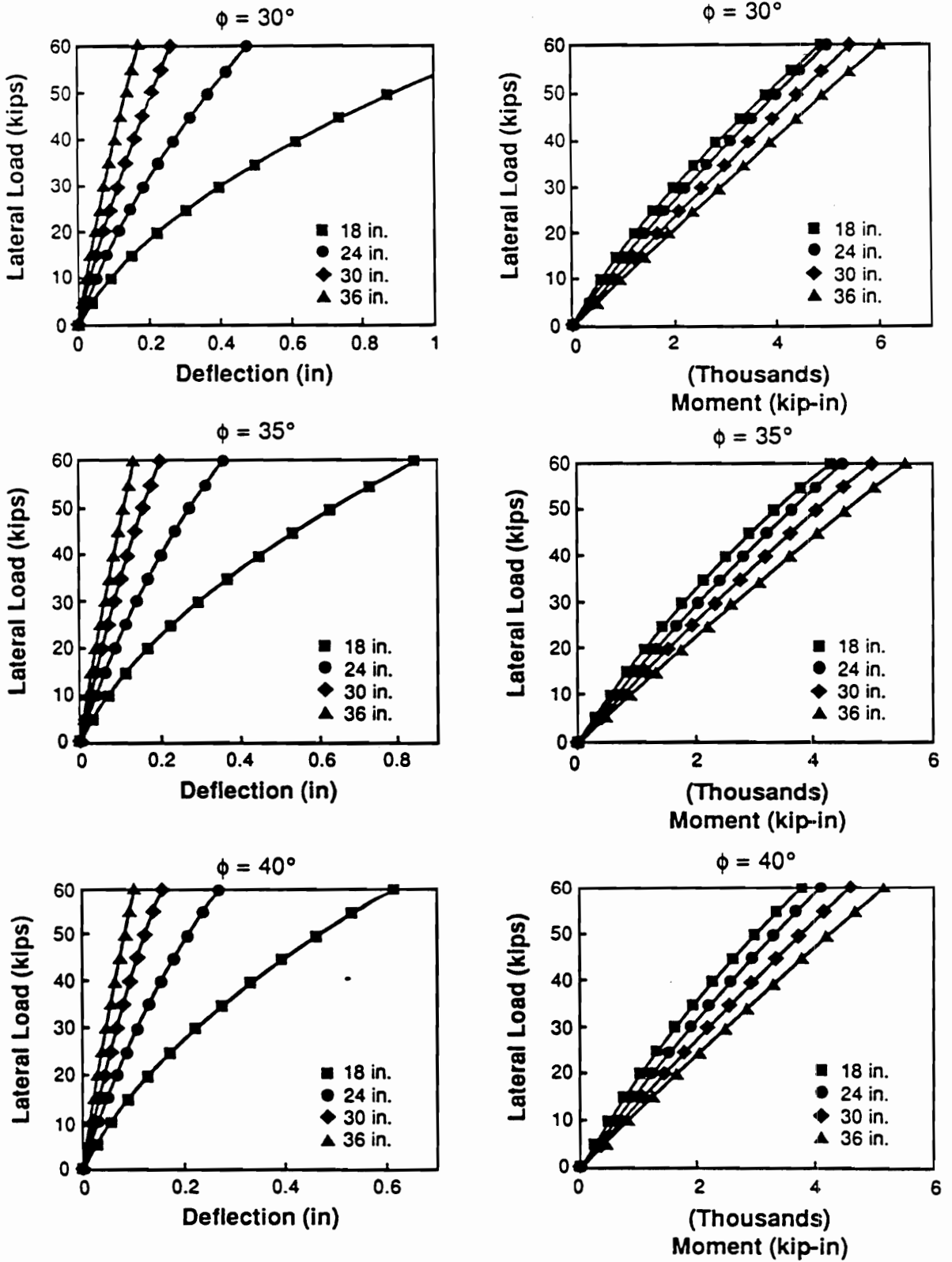


Figure 3.19 Load Versus Deflection and Load Versus Moment for Drilled Shafts ($A_y/A_g = 4\%$) in Sand

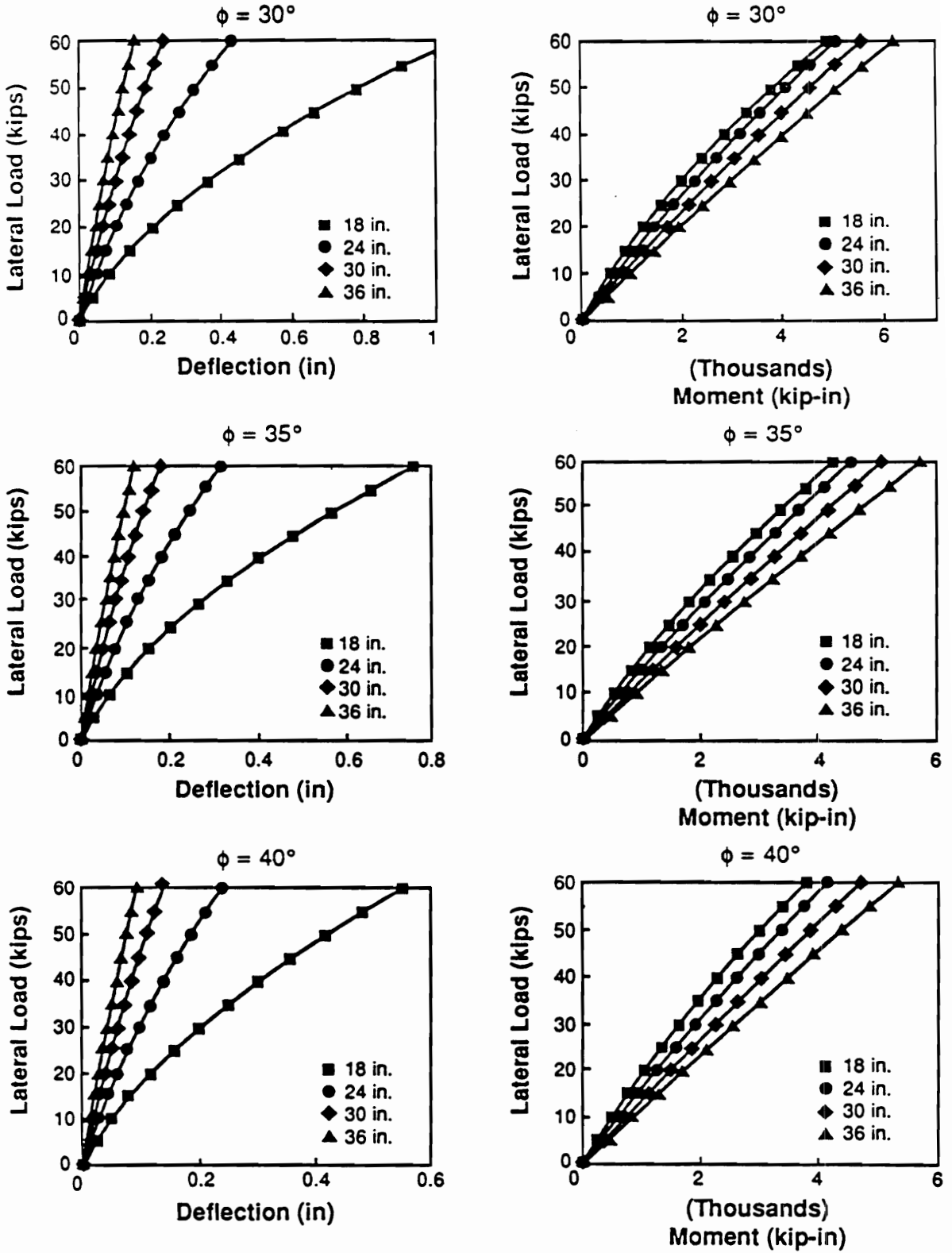


Figure 3.20 Load Versus Deflection and Load Versus Moment for Drilled Shafts ($A_y/A_g = 8\%$) in Sand

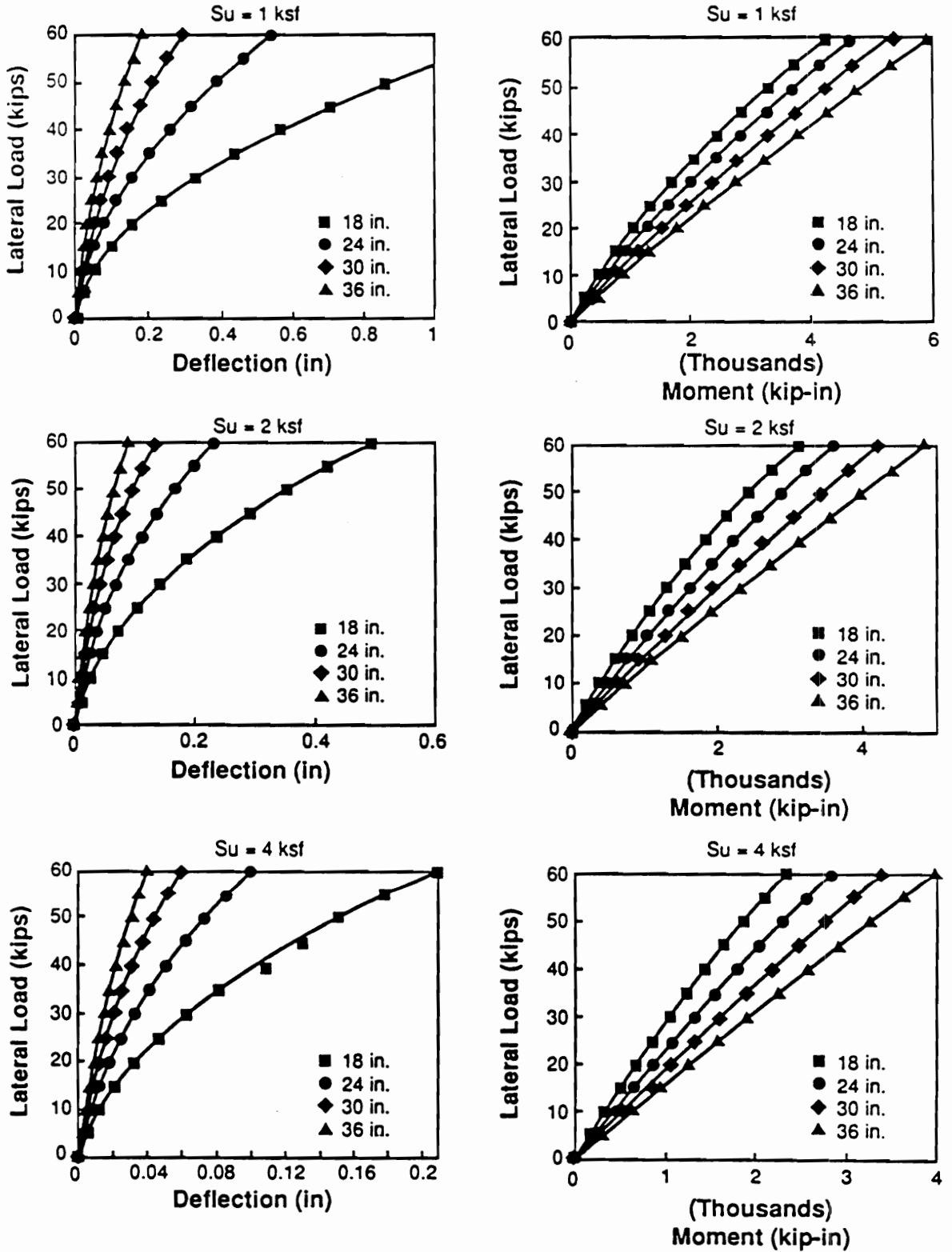


Figure 3.21 Load Versus Deflection and Load Versus Moment for Drilled Shafts ($A_y/A_g = 1\%$) in Clay

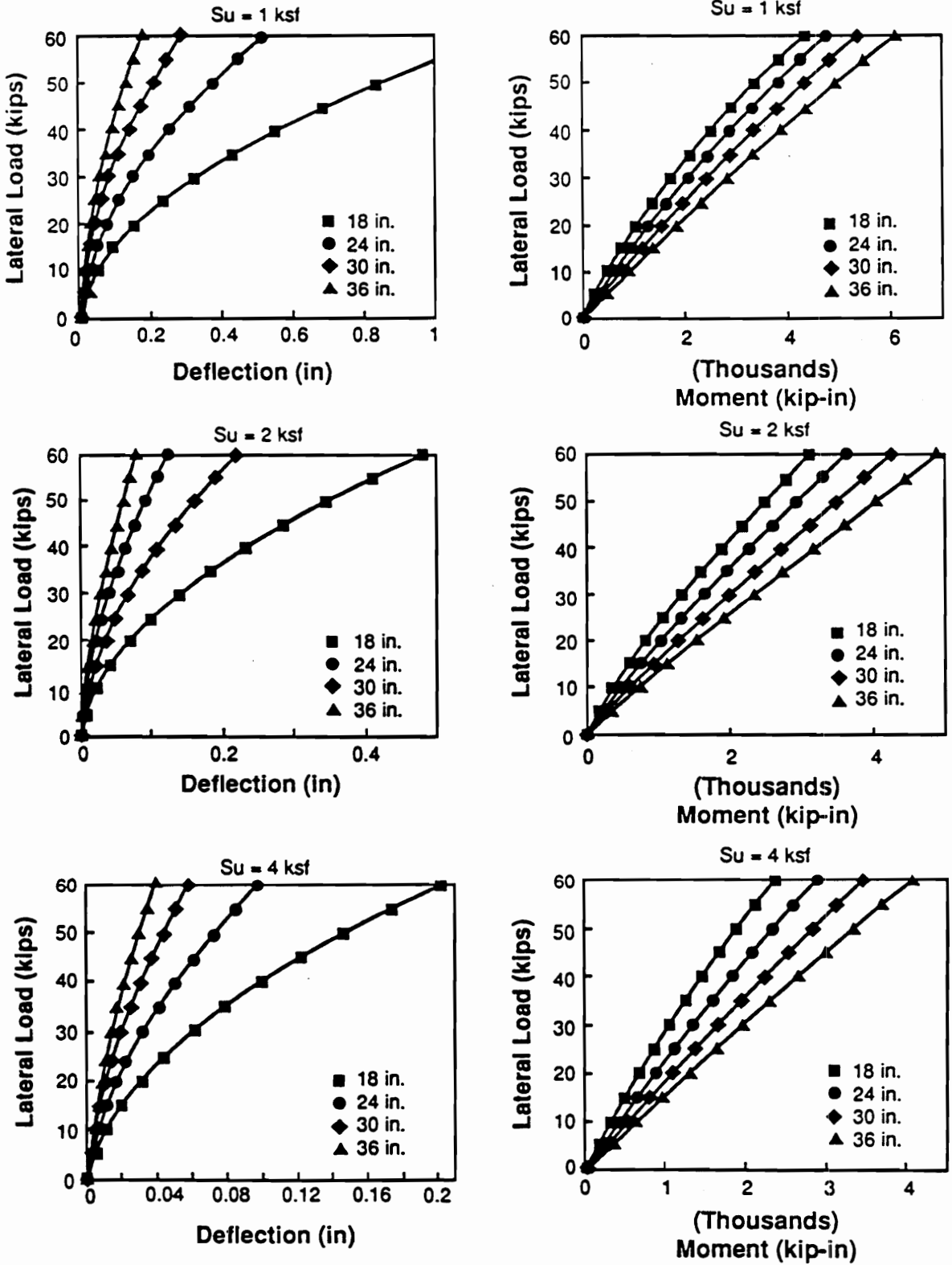


Figure 3.22 Load Versus Deflection and Load Versus Moment for Drilled Shafts ($A_y/A_g = 2\%$) in Clay

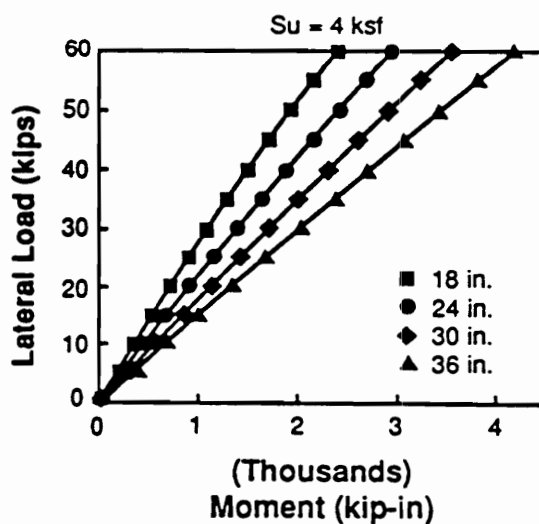
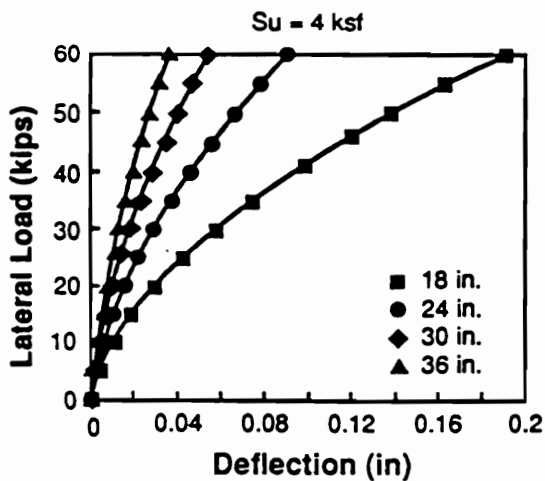
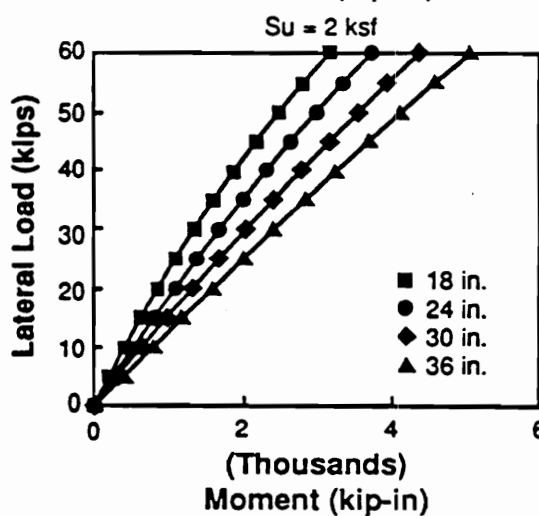
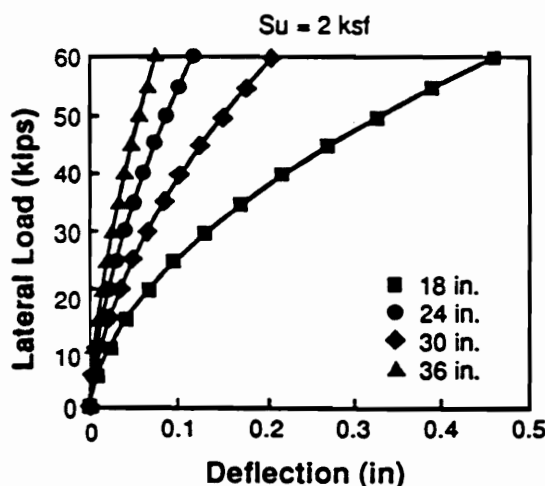
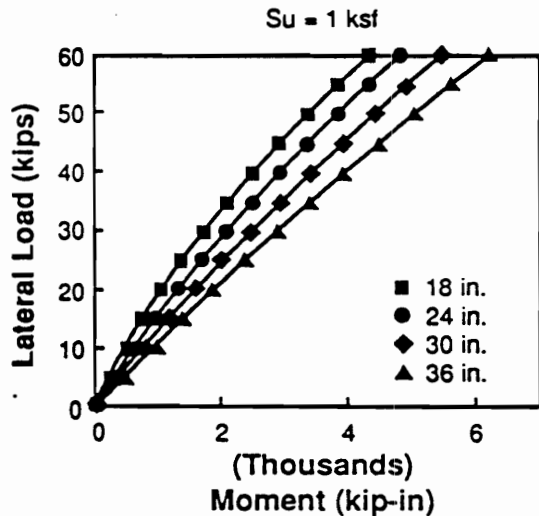
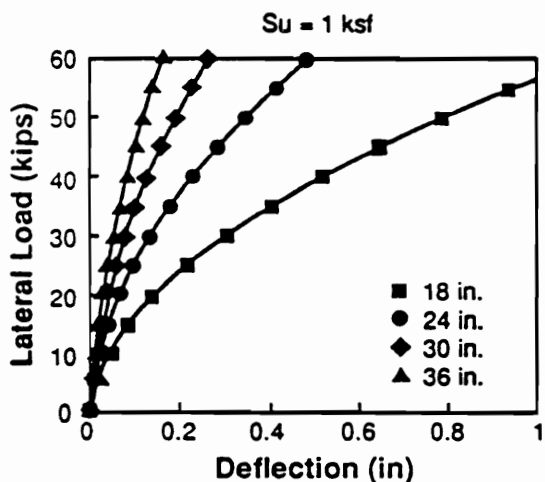


Figure 3.23 Load Versus Deflection and Load Versus Moment for Drilled Shafts ($A_y/A_g = 4\%$) in Clay

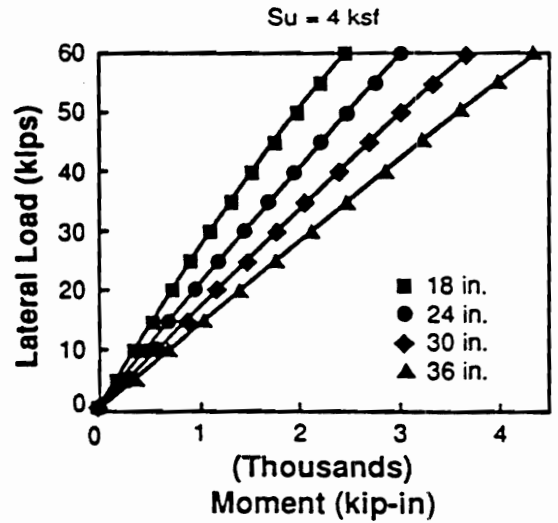
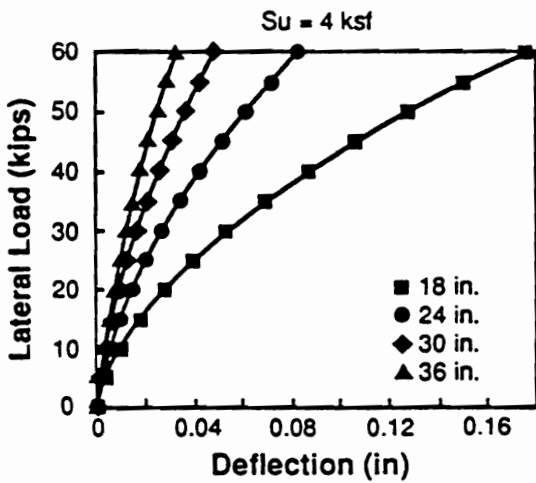
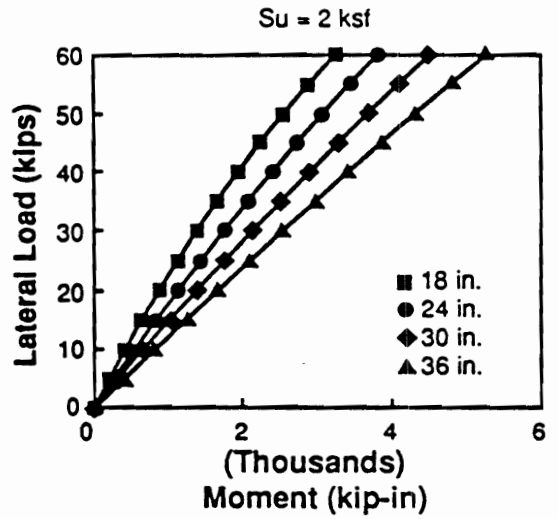
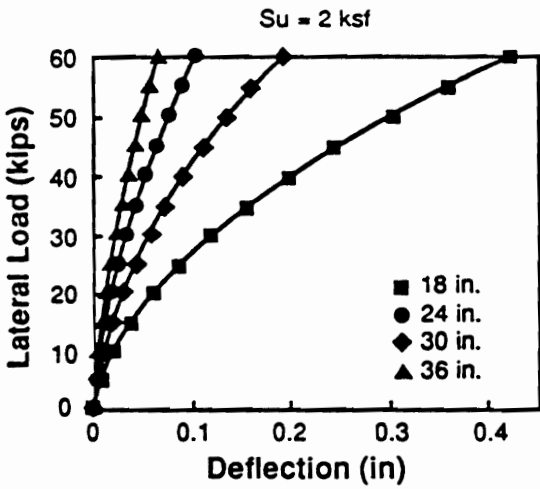
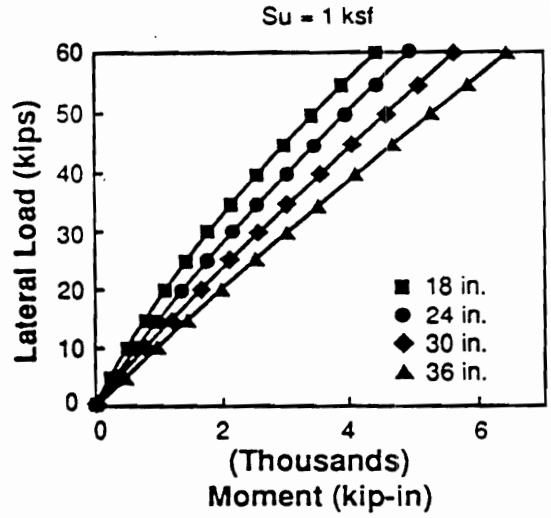
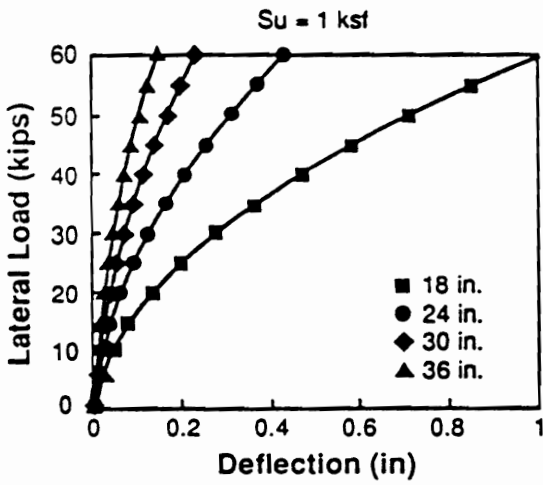


Figure 3.24 Load Versus Deflection and Load Versus Moment for Drilled Shafts ($A_y/A_g = 8\%$) in Clay

example, a lateral load of 25 kips acting on an 18 in. drilled shaft with 4% steel reinforcement, constructed in clay with an undrained shear strength of 2 ksf, will result in a lateral deflection of about 0.1 in. and a moment of 1300 kip-in (Fig. 3.23).

For sands, charts were developed for friction angles of 30°, 35° and 40°. The water table was assumed to be at or above the ground surface. For intermediate values of friction angle between those shown in the charts, deflections may be estimated by interpolation.

For clays, load-deflection curves were developed for undrained shear strengths of 1, 2 and 4 ksf. Deflections for intermediate values of undrained shear strengths can be estimated by interpolation.

3.3 Groups of Piles and Drilled Shafts

A simplified procedure for analyzing laterally loaded groups of piles and drilled shafts has been developed based on Focht and Koch's (1973) procedure for group behavior, and Evans and Duncan (1982) procedure for the behavior of single piles and drilled shafts. The Evans and Duncan procedure is used to obtain single pile deflections and maximum bending moments instead of the p-y analysis because, unlike p-y analysis, the Evans and Duncan procedure is non-iterative,

and lends itself well to a parametric study of a large number of pile sizes, pile stiffnesses, soil strengths and soil stiffnesses. No distinction need be made between groups of piles and groups of drilled shafts.

3.3.1 Focht and Koch's Procedure

As mentioned in Section 2.2.2.2, Focht and Koch's procedure assumes that group deflection consists of two components: a component due to non-linear soil behavior occurring close to the individual piles, and another due to pile-soil-pile interaction. The deflection component due to non-linear soil behavior can be predicted through the use of the Evans and Duncan procedure, while the deflection component due to pile-soil-pile interaction is estimated using Poulos' (1971) elastic interaction coefficients.

Focht and Koch (1973) modified Poulos's (1971) elastic procedure for estimating pile group deflection (Equation 2-29). The procedure for predicting the lateral deflection of a pile within a group is as follows:

$$\rho_k = \bar{\rho}_F \left[\sum_{\substack{j=1 \\ j \neq k}}^{N_{\text{pile}}} (P_j \alpha_{\rho} F_{kj}) + R P_k \right] \quad (3-10)$$

where ρ_k = lateral deflection of pile k (L)

$\bar{\rho}_F$ = unit elastic displacement of a single pile under

unit horizontal load (LF^{-1})

$$= I_{\rho F} / E_S Z \quad (3-11)$$

$I_{\rho F}$ = influence factor (Fig. 2.14). $I_{\rho F}$ is a function of K_R defined in Equation 3-13 below.

E_S = Young's modulus of soil (FL^{-2})

Z = length of the pile (L).

N_{pile} = number of piles in the group

P_j = lateral load on pile j (F)

$\alpha_{\rho F k j}$ = elastic interaction factor for determining the influence of pile j on pile k, based on the spacing between piles j and k and the angle θ

θ = angle between direction of loading and the line joining the centers of piles j and k

P_k = lateral load on pile k (F)

R = relative stiffness factor

$$R = Y_S / \rho \quad (3-12)$$

Y_S = non-linear p-y deflection of a single pile at the mudline (calculated using the Evans and Duncan procedure)

ρ = elastic deflection of a single pile at the mudline

$$= \bar{\rho}_F P_S$$

P_S = average lateral load per pile = P_g / N_{pile}

P_g = lateral load acting on the group

In computing Y_S and ρ , the lateral load on the single pile is computed as the total lateral load on the group divided by the number of piles or drilled shafts ($P_S = P_G/N_{\text{pile}}$).

The interaction factor, $\alpha_{\rho Fk_j}$, can be obtained from Fig. 2.15 for fixed-head piles. $\alpha_{\rho Fk_j}$ is a function of the spacing to diameter ratio (s/D), θ and K_R , where s = center-to-center pile spacing, D = pile width or diameter and K_R is the pile flexibility factor defined as follows:

$$K_R = \frac{E_p I_p}{E_S Z^4} \quad (3-13)$$

where E_p = Young's modulus of pile (FL^{-2}) and I_p = moment of inertia of pile (L^4).

If the piles are connected by a cap, then the piles will all deflect equally. Equation 3-10 yields a set of N_{pile} equations but there are a total of $(N_{\text{pile}} + 1)$ unknowns; N_{pile} unknown values of reaction in each pile, and one unknown value of group deflection, $Y_g = \rho_1 = \rho_2 = \dots = \rho_{N_{\text{pile}}}$. The remaining equation needed in order to solve for the set of $(N_{\text{pile}} + 1)$ unknowns is the requirement that the sum of the individual pile loads must equal the load on the group, P_g , i.e.

$$\sum_{j=1}^{N_{\text{pile}}} P_j = P_g \quad (3-14)$$

Although Figs. 2.14 (for determining $I_{\rho F}$) and 2.15 (for determining $\alpha_{\rho F k j}$) was developed for a Poisson's ratio of 0.5, they can be used for both cohesive and cohesionless soils because the sensitivity of the value of Poisson's ratio to the solution for ρ_k is small. The solution for ρ_k is, however, sensitive to the value of R , which is related to the elastic deflection of the single pile, ρ , through Equation 3-12. The value of ρ is very sensitive to the value of soil modulus, E_s (Reese et al., 1984). Therefore, a reliable estimate of the soil modulus is necessary; the procedure used to evaluate E_s is given below.

Estimation of Soil Modulus

The estimation of $\bar{\rho}_F$ and $I_{\rho F}$, which is a function of K_R , requires an estimation of the value of the elastic soil modulus, E_s . The modulus of real soils changes with stress level due to the non-linear behavior of the soil. However, the soil behavior can be approximated as linearly elastic at low stress (strain) levels. The value of E_s can be estimated as follows:

1) For the group, select a pile or drilled shaft section of diameter, D , length, Z , Young's modulus, E_p , moment of

inertia, I_p , and number of piles or drilled shafts, N_{pile} , and determine the design lateral load on the group, P_g .

2) Calculate a reduced lateral load $0.1P_S = 0.1P_g/N_{pile}$ and use non-linear elastic analysis to estimate the lateral deflection, Y_S corresponding to a lateral load $0.1P_S$.

3) Calculate $\bar{\rho}_F = Y_S/0.1P_S$.

4) Guess a value of E_S .

5) Calculate K_R using Equation 3-13.

6) Determine the value of $I_{\rho F}$ from Fig. 2.14.

7) Calculate a new value of soil modulus, $E_S^* = I_{\rho F}/\bar{\rho}_F Z$, where $\bar{\rho}_F$ is obtained from step 3.

8) Compare E_S with E_S^* . If they are not similar, calculate the soil modulus as the average of E_S and E_S^* , and repeat steps (5) through (7) until they match.

These procedures have been coded in a computer program to facilitate parametric studies of a large number of groups

of deep foundations (See Appendix A for documentation of the computer program).

3.3.2 Parametric Studies for Deflection of Groups of Piles and Drilled Shafts

A group of piles will deflect more than a single pile subjected to the same lateral load per pile. This is due to interaction effects whereby deflection of each pile in a group causes deflection of the surrounding soil and thereby increases the deflections of neighboring piles. However, where a single row of piles are constructed side by side and loading is normal to a line containing the pile heads, group action need not be considered unless the piles are closer than three pile diameters center-to-center. Group action must be considered when the lateral loads act in line with the single row of piles. It will be useful therefore, to establish a group deflection amplification factor (C_y), that when multiplied with the deflection of a single pile (Y_s), yields the group deflection (Y_g) i.e.

$$Y_g = C_y Y_s \quad (3-15)$$

where C_y is a group deflection amplification factor (greater than 1) that accounts for pile-soil-pile interaction effects in groups of piles and drilled shafts.

A computer program was developed to calculate single pile deflection using the Evans and Duncan procedure, and group deflection using the procedure of Focht and Koch. Parametric studies were performed only for the case where the piles and drilled shafts are connected by a cap that provides rotational restraint at the top. Groups of free-head piles or drilled shafts are less common, and the free-head condition was not analyzed. The following parameters were varied:

- 1) diameter of pile or drilled shaft ($D = 10$ in. to 30 in.)
- 2) stiffness of pile or drilled shaft ($E_p = 1500$ ksi [for timber] to 29 000 ksi [for steel])
- 3) type of soil (cohesive or cohesionless)
- 4) shear strength of soil ($\phi' = 30^\circ$ to 40° for sands and $S_u = 1$ ksf to 4 ksf for clays)
- 5) number of piles or drilled shafts ($N_{pile} = 2$ to 25)
- 6) spacing of piles or drilled shafts ($s/D = 2$ to 5)
- 7) magnitude of lateral load ($P_s = 5$ kips/pile to 20 kips/pile), and
- 8) density of soil in the case of cohesionless material (buoyant unit weights only).

The parametric studies yielded a large number of data from which a simple expression for C_y was developed. The expression is as follows:

$$C_y = \frac{A + N_{\text{pile}}}{B \sqrt{\frac{s}{D} + \frac{P_s}{C P_N}}} \quad (3-16)$$

where N_{pile} = number of piles in group

s = average spacing of piles

D = diameter of pile

P_s = average lateral load per pile

= P_g/N_{pile}

P_g = lateral load on the group of piles

$P_N = K_p \gamma D^3$ for sand (3-17)

$P_N = S_u D^2$ for clay (3-18)

γ = total unit weight of sand

K_p = passive earth pressure coefficient

= $\tan^2(45^\circ + \phi'/2)$

ϕ' = average angle of internal friction of sand
within the upper 8 pile diameters

S_u = average undrained shear strength of clay
within the upper 8 pile diameters

$A = 16$ for clay

$A = 9$ for sand

$B = 5.5$ for clay

$B = 3$ for sand

$C = 3$ for clay

$C = 16$ for sand

This equation was developed for uniformly spaced piles and drilled shafts, but can be used for groups with non-

uniform spacing if the average pile or shaft spacing is used in the calculations. A comparison of values of Y_g/Y_s calculated using the computer program with values of Y_g/Y_s computed using Equation 3-16 is shown in Fig. 3.25 for groups of 14 in. prestressed concrete piles, and Fig. 3.26 for groups of 30 in. drilled shafts in sands. Figs. 3.27 and 3.28 show similar results for groups of piles and shafts in clays. The vertical axes represent values from the computer solutions while the horizontal axes represent the values predicted by Equation 3-16. The following observations can be made from these four figures:

- 1) The scatter for group deflections is greater for groups of piles and shafts in cohesive material than in cohesionless material. The coefficient of variation for the group deflection in cohesionless material is 5.5% compared to 8% in cohesive soils.
- 2) The simplified method of predicting group deflections tend to err on the safe side, i.e. the method overpredicts more often than it underpredicts. In cohesionless material, Equation 3-16 overpredicts the group deflection by at most, 30% and underpredicts by 5%. In cohesive soils, the overprediction can be as high as 35%, and the underprediction as low as 20%.

If the lateral displacement of a group of piles (Y_g) is greater than the tolerable value, the diameter of the piles,

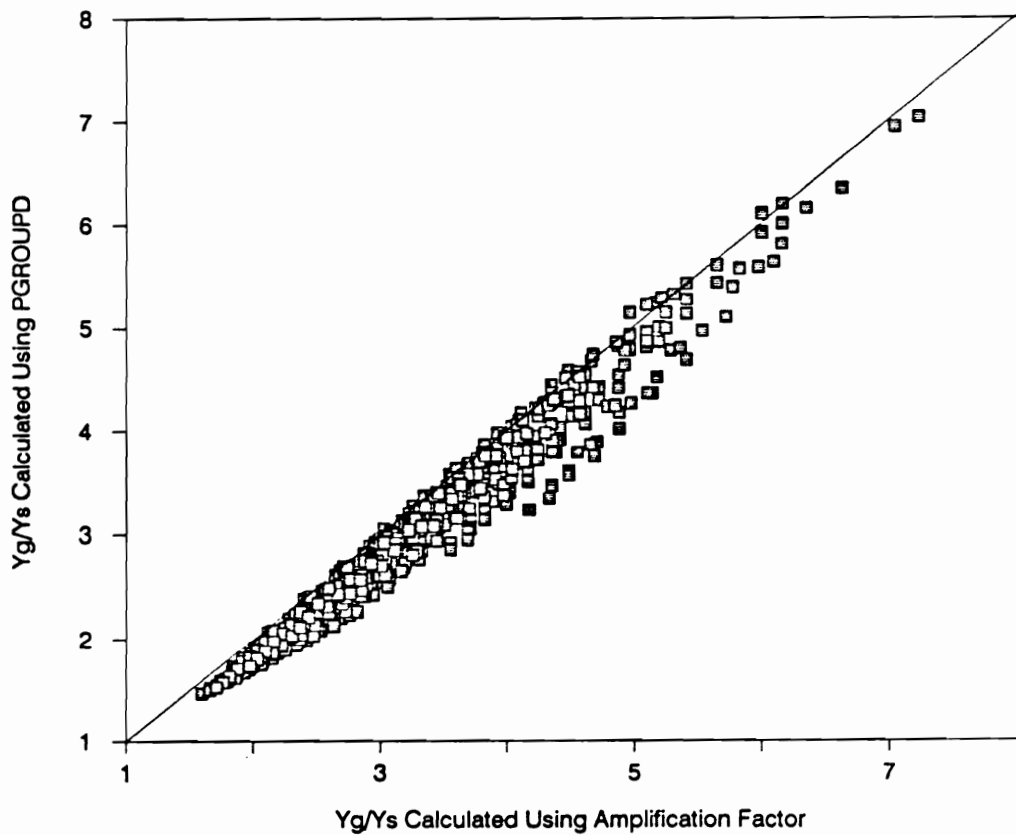


Figure 3.25 Comparison of Values of Y_g/Y_s Calculated Using the Deflection Amplification Factor With Those Using PGROUPD for Groups of 14 in. Prestressed Concrete Piles in Sand

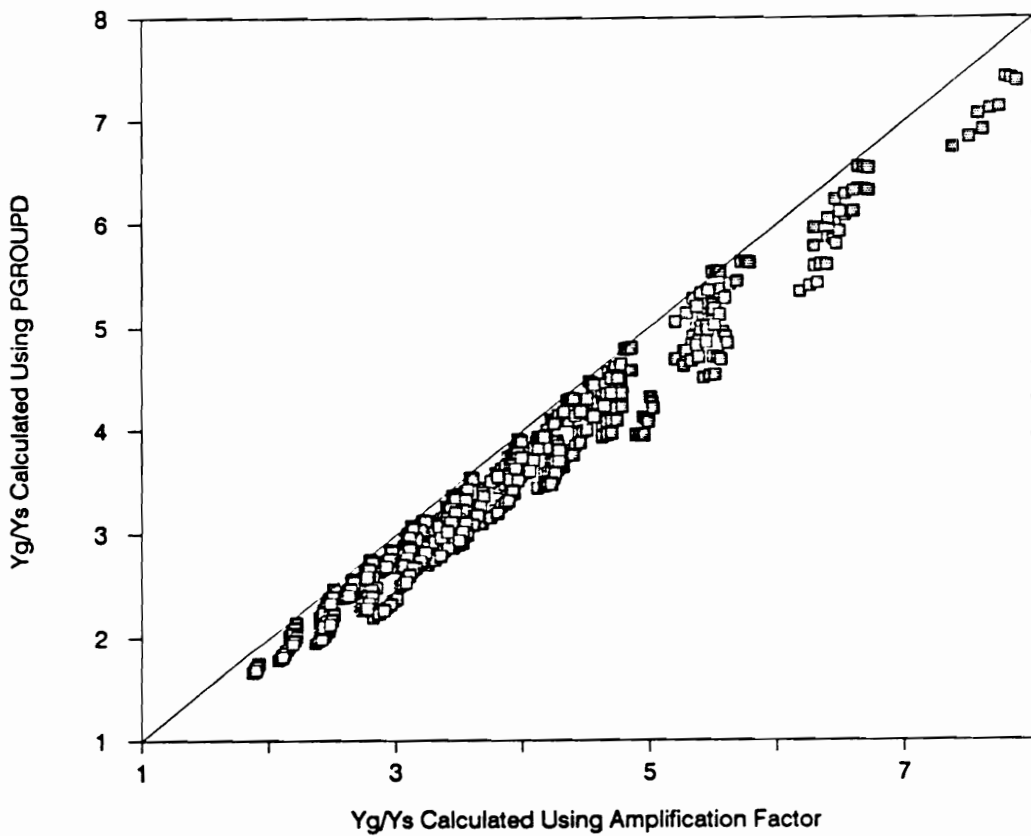


Figure 3.26 Comparison of Values of Y_g/Y_s Calculated Using the Deflection Amplification Factor With Those Using PGROUPD for Groups of 30 in. Drilled Shafts in Sand

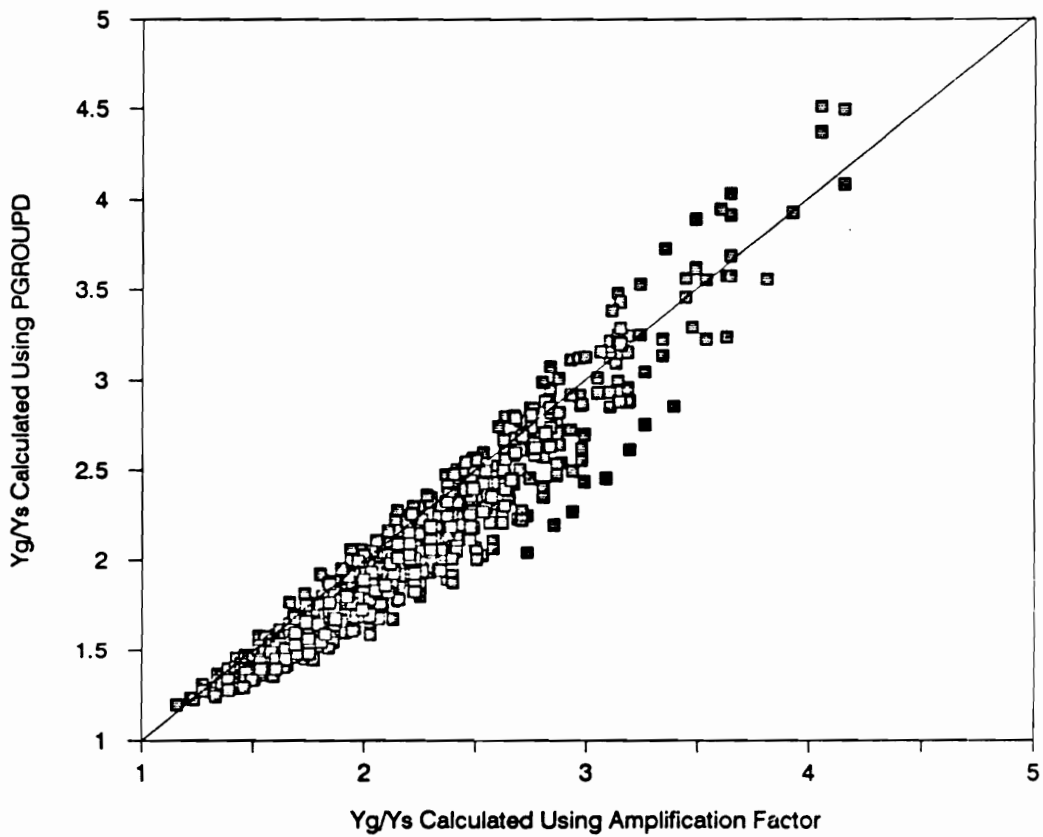


Figure 3.27 Comparison of Values of Y_g/Y_s Calculated Using the Deflection Amplification Factor With Those Using PGROUPD for Groups of 14 in. Prestressed Concrete Piles in Clay

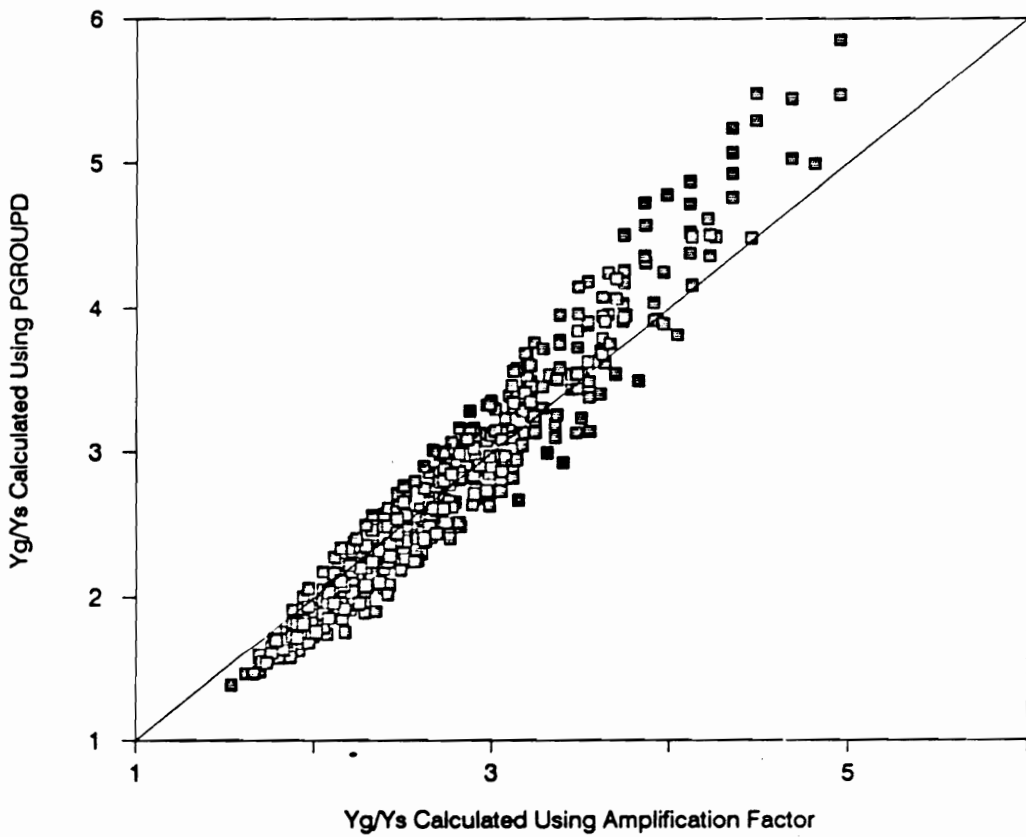


Figure 3.28 Comparison of Values of Y_G/Y_S Calculated Using the Deflection Amplification Factor With Those Using PGROUPD for Groups of 30 in. Drilled Shafts in Clay

the number of piles, or the pile spacing should be increased until Y_G is less than the tolerable value. Equation 3-16 provides a convenient and simple means for performing this otherwise tedious task.

3.3.3 Bending Moments in Groups of Piles and Drilled Shafts

As discussed previously, the deflection of any pile in a group causes deflection of the surrounding soil and piles, thus leading to larger deflection for the group than for single piles subjected to the same load per pile. The bending moment in a pile within a group is also larger than that in a single pile subjected to the same loading. This is because the interaction effects, by causing more deflection, also increase the bending moment in the piles.

Brown et al. (1987 and 1988) found that the maximum bending moment in a group of free-head piles occur in the leading row (or front row) of piles. However, current theories on lateral loading of groups of piles (including the Focht and Koch procedure) are not able to predict this behavior. Methods based on the theory of elasticity always predict that the largest loads are carried by the corner piles.

A semi-empirical procedure that provides a reasonable approximation of the maximum bending moment in the leading

row of a group of piles has been developed by modifying the theory described by Focht and Koch (1973). The increase in moment due to group interaction was studied for a large number of cases by first estimating the group deflection using the theory of Focht and Koch (1973), and then "softening" the soil (reducing S_u for clays or ϕ' for sands) until the single pile deflection (calculated using the Evans and Duncan approach) matched the lateral deflection of the group (Duncan, 1988). The real problem, however, is more complex, requiring knowledge of the distribution of loads to the piles in relation to their location, spacing, soil and pile stiffnesses, and the nature of the loading (cyclic versus static). While the theories on which the method is based do not reflect the unique conditions in the front row of piles, it is believed that the method is an improvement over the current absence of guidance available for engineers.

This routine is also incorporated in the computer program mentioned in Section 3.3.1 and Appendix A for groups of fixed-head piles and drilled shafts. Parametric studies were performed using this program, and the results are presented in the following section.

3.3.4 Parametric Studies for Maximum Bending Moments in Groups of Piles and Drilled Shafts

Through a similar parametric study as with group deflections, a moment amplification factor (C_M) that relates the maximum bending moment of the most severely loaded pile in the group to the maximum bending moment in a single pile can be written as follows:

$$M_g = C_M M_s \quad (3-19)$$

where M_g = maximum bending moment of the most severely loaded pile within a group, C_M = moment amplification factor that accounts for pile-soil-pile interaction effects in a group of piles, and M_s = maximum bending moment in a single fixed-head pile subjected to a lateral load, $P_s = P_g/N_{\text{pile}}$. M_s can be calculated using the procedure of Evans and Duncan (Section 3.2.1.3) or the charts in Section 3.2.2. The parametric studies yielded the following expression for C_M :

$$C_M = C_Y^n \quad (3-20)$$

where C_Y = group deflection amplification factor
(Equation 3-16)

$$n = \frac{P_s}{150P_N} + 0.25 \text{ for clay} \quad (3-21)$$

$$n = \frac{P_s}{300P_N} + 0.3 \text{ for sand} \quad (3-22)$$

P_N is as defined previously in Equations 3-17 and 3-18.

The maximum bending moment in a group of piles or drilled shafts can be estimated very quickly using this method. The use of Equations 3-19 and 3-20 enables the engineer to avoid the tedious process of softening the soil to match single pile deflections calculated using non-linear (Evans and Duncan) analysis, with the group deflection. A comparison of values of M_g/M_s calculated using the computer program with values of M_g/M_s computed using Equation 3-20 are shown in Fig. 3.29 for groups of 14 in. prestressed concrete piles and Fig. 3.30 for groups of 30 in. drilled shafts in sands. Figs. 3.31 and 3.32 are similar graphs for groups of piles and drilled shafts in clays. The following observations can be made from these four figures:

- 1). Regardless of whether the soil is cohesive or cohesionless, the scatter in the values of maximum bending moments is approximately the same (coefficient of variation is approximately 20% to 25%).
- 2) The simplified method tends to overpredict maximum bending moments in groups of piles and drilled shafts more than it underpredicts. In cohesionless material, Equation 3-20 overpredicts the maximum bending moment by at most, 11% and underpredicts by 3%, while in cohesive soils, the

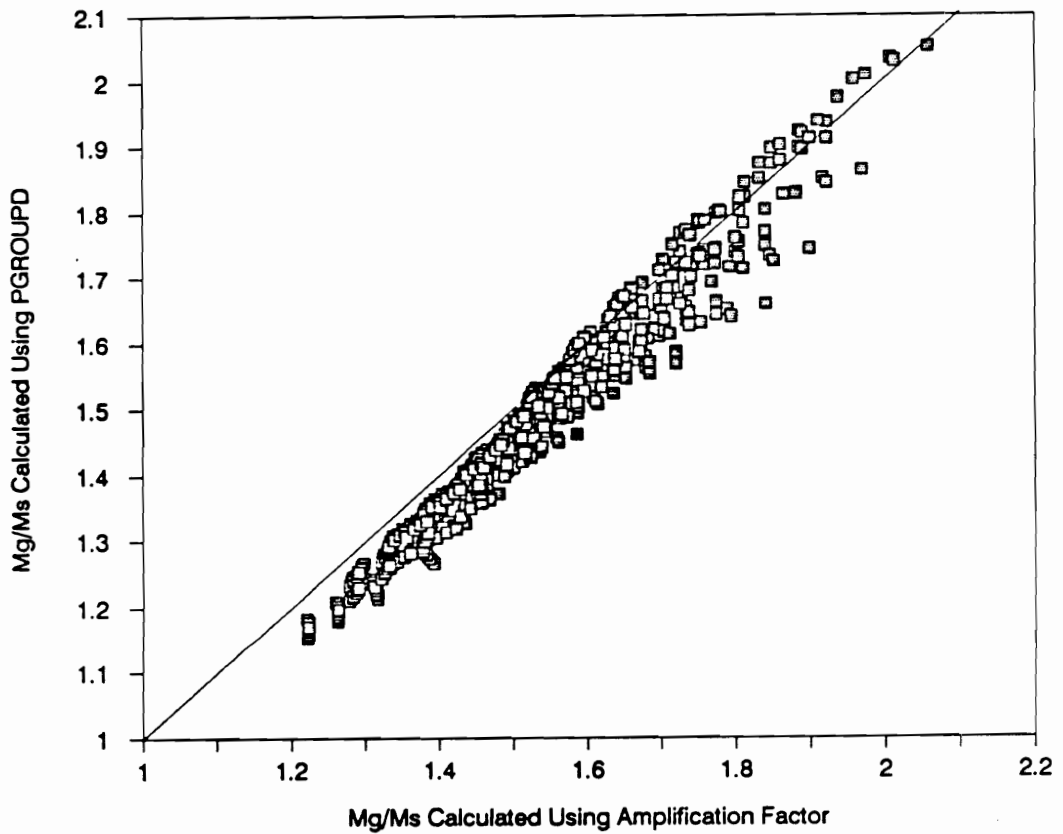


Figure 3.29 Comparison of Values of M_g/M_s Calculated Using the Moment Amplification Factor With Those Using PGROUPD for Groups of 14 in. Prestressed Concrete Piles in Sand

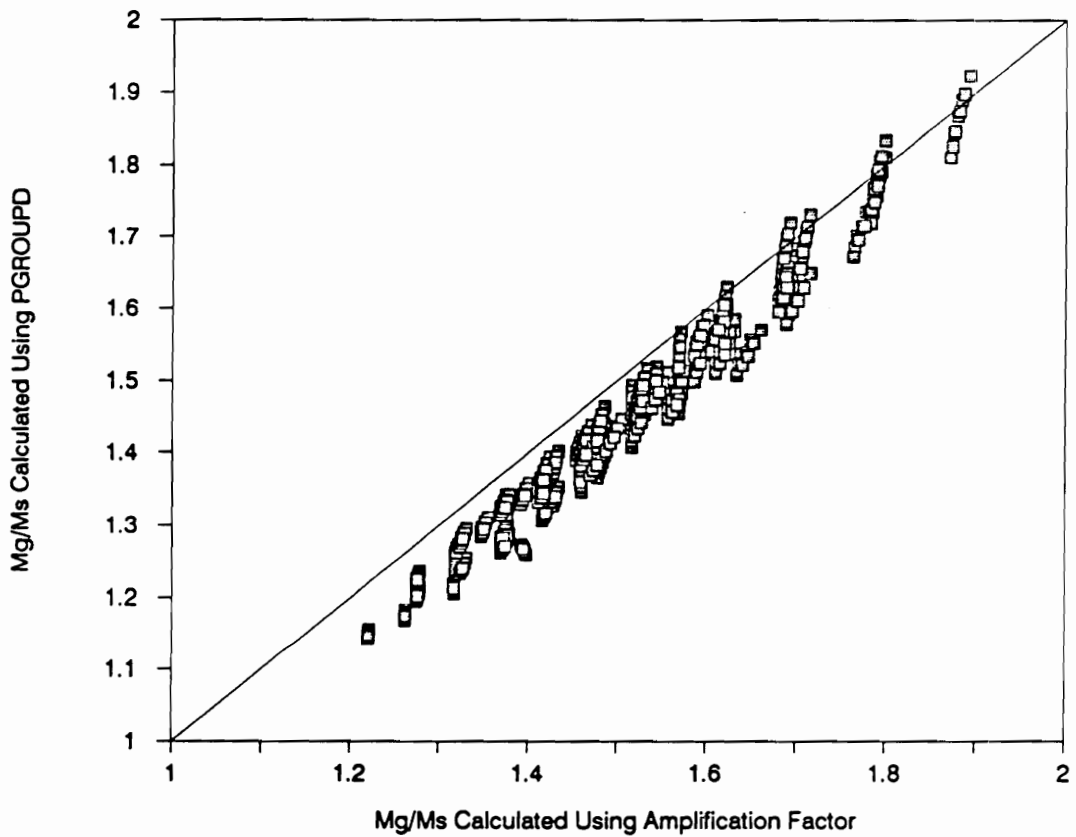


Figure 3.30 Comparison of Values of M_G/M_S Calculated Using the Moment Amplification Factor With Those Using PGROUPD for Groups of 30 in. Drilled Shafts in Sand

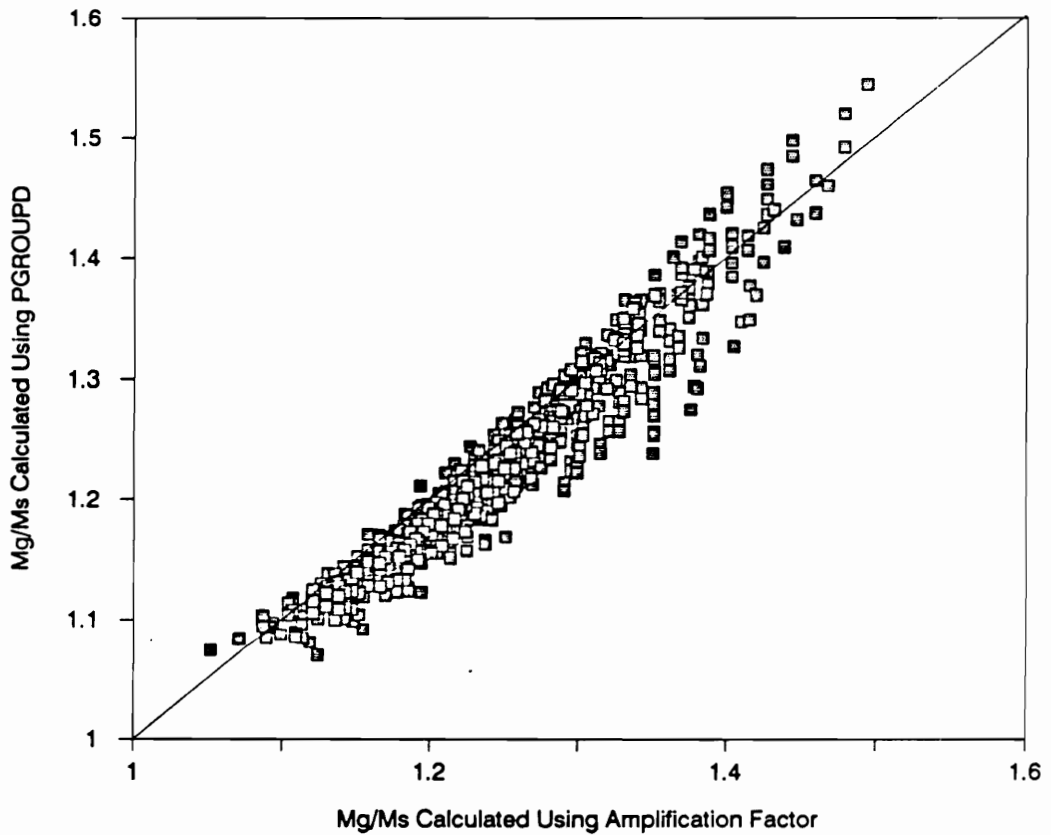


Figure 3.31 Comparison of Values of M_g/M_s Calculated Using the Moment Amplification Factor With Those Using PGROUPD for Groups of 14 in. Prestressed Concrete Piles in Clay

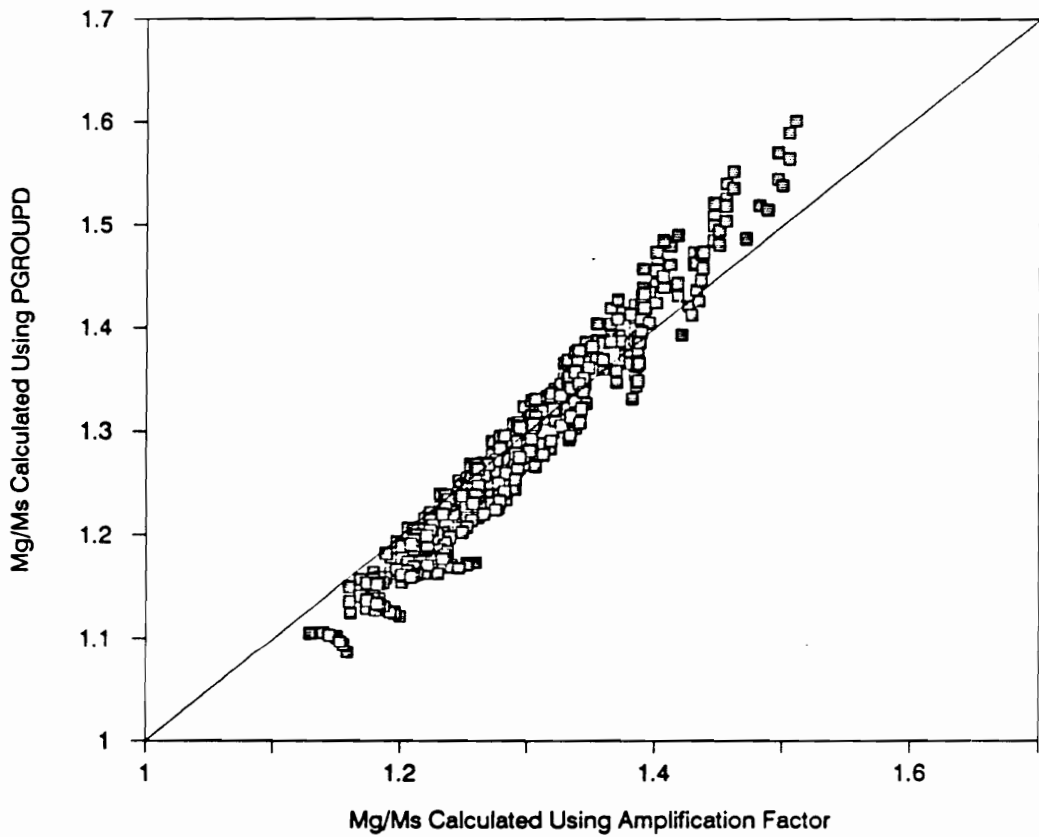


Figure 3.32 Comparison of Values of M_G/M_S Calculated Using the Moment Amplification Factor With Those Using PGROUPD for Groups of 30 in. Drilled Shafts in Clay

overprediction can be as high as 9% and the underprediction as low as 6%.

3.4 Field Experiments

Carefully performed and well-instrumented full scale experiments provide the best means of verifying newly developed analytical procedures. Lateral load tests on pile groups have been performed and reported by Feagin (1937 & 1953), Evans (1953), O'Halloran (1953), Gleser (1953), Beatty (1970), Kim and Brungraber (1976), Jamiolkowski (1976), Manoliu et al. (1977), Matlock et al. (1980), Holloway et al. (1981), Schmidt (1981), and Brown et al. (1987 & 1988). Among these tests, only a few were accompanied by high quality soil investigation programs, and were well instrumented to measure group deflections, lateral load distribution among piles within the group, and bending moments in the individual piles.

The following full scale lateral load tests were used to compare the results from the simplified method and the experimental results:

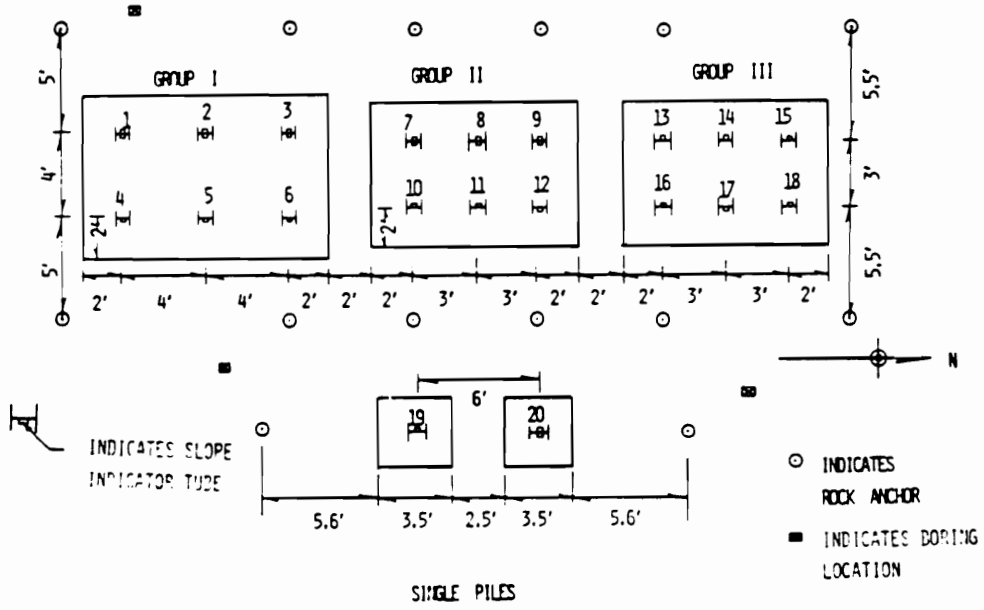
- 1) Kim and Brungraber (1976)
- 2) Holloway et al. (1981)
- 3) Brown et al. (1987) and
- 4) Brown et al. (1988).

Only Kim and Brungraber's (1976) experiment was carried out on fixed-head pile groups. The load test performed by Holloway et al. (1981) was on a group of timber piles that were connected by a cap suspended 3 ft above the ground. Both experiments conducted by Brown et al. (1987 & 1988) were performed using a moment-free loading frame, through which the lateral load on the pile group was applied 1 ft above the groundline.

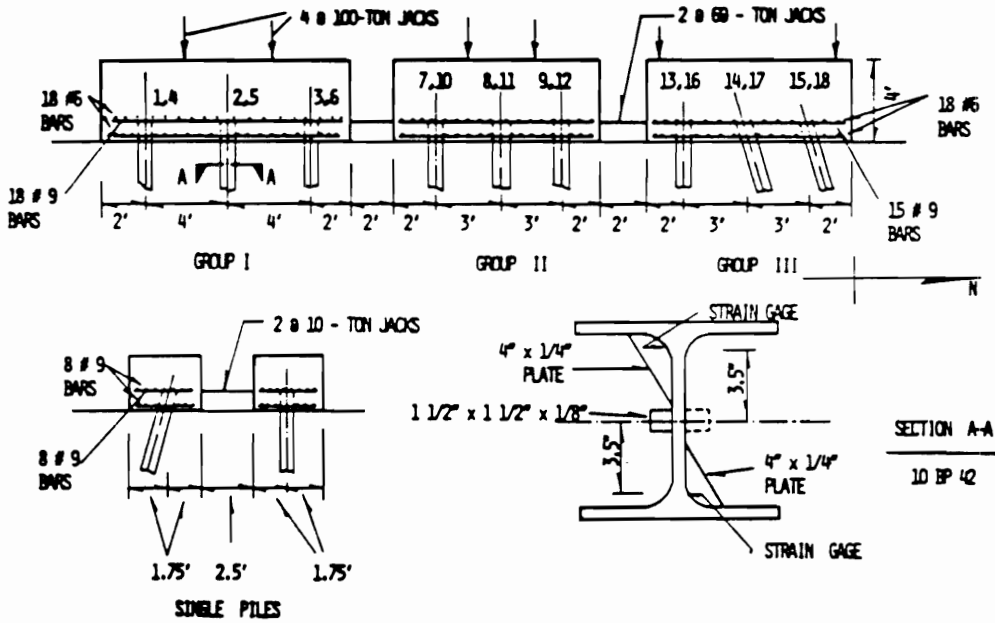
1. Kim and Brungraber (1976)

Kim and Brungraber (1976) performed three series of lateral load tests on pile groups at the Bucknell University campus farm. Their intent was to simulate loads occurring on bridge abutment foundations. Series B was conducted 9 months after series A, and series C, 4 months after series B. Results from the tests of series B and C were well documented and the differences between the two were not significant. Kim and Brungraber reported that lateral deflections from series A differed from those for series B by as much as 100%. The discussion will include test results from only series B and C.

Two of the pile groups, groups I and II, contained vertical piles spaced 4 ft and 3 ft apart center-to-center, respectively (Fig. 3.33). The third group (group III)



Pile Layout—Plan View



Pile Layout—Elevation View

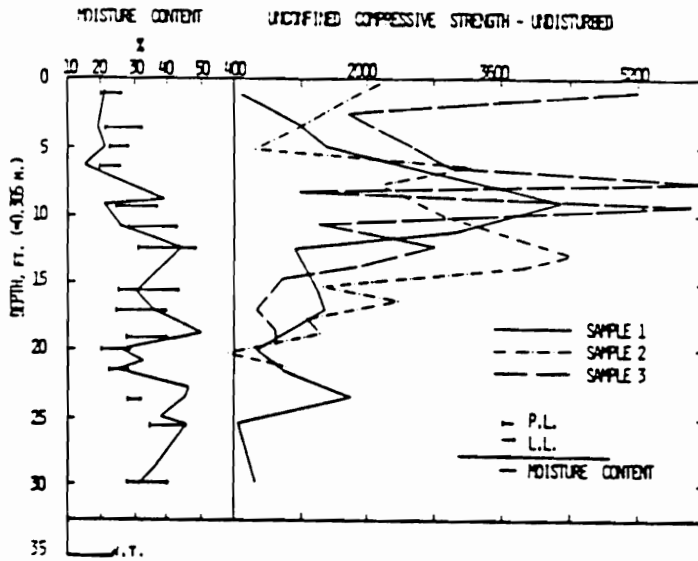
Figure 3.33 Pile Layout - Bucknell University Test Site (After Kim and Brungraber, 1976)

contained piles driven at a batter. The piles were all embedded 12 in. into 4 ft thick reinforced concrete caps. The caps were all in contact with the ground.

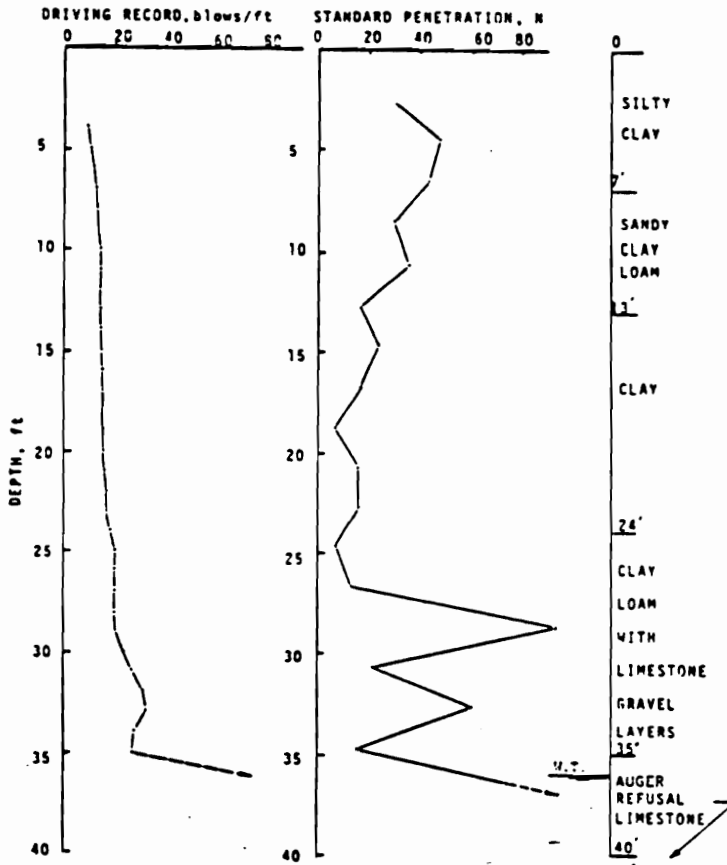
The pile section consisted of a 10BP42 steel-H pile ($D = 9.7$ in., $E_p = 29\,000$ ksi, $I_p = 224.2$ in⁴). Six piles were driven in each group in a 3 X 2 arrangement. The piles were driven to refusal on top of a limestone layer at a depth of approximately 40 ft.

The portion of the ground that is of importance to lateral load is the top 8 pile widths (6.5 ft). The soil profile, SPT blow counts and results of unconfined compression tests are shown in Fig. 3.34. The SPT blow counts in the top 6.5 ft are all greater than or equal to 30, indicating that the silty clay layer is hard ($S_u > 8$ ksf [Terzaghi and Peck, 1967]). However, unconfined compression strengths average only 2000 psf implying that $S_u = 1000$ psf. Because unconfined compression tests usually provide shear strengths that are too low, and because the SPT blow counts are so high, it was decided to use a value of S_u of 2000 psf in the analysis.

The deflection and maximum bending moments in a single fixed-head 10BP42 pile were estimated using the Evans and Duncan procedure. These values of deflection and moment were then amplified to those for the group using Equations 3-16 and 3-20 respectively. A vertical single pile was



Laboratory Soil Data



Boring and Pile Driving Record

Figure 3.34 Soil Profile, Standard Penetration Test Data, Laboratory Test Results and Pile Driving Record for the Bucknell University Test Site (After Kim and Brungraber, 1976)

tested by Kim and Brungraber but the moment at the pile head was zero, indicating a free-head condition. The different end conditions of the single pile and pile groups do not allow a direct comparison of the results.

The experimental results and results from the analysis using the simplified procedure are shown in Tables 3.3 and 3.4. The following observations can be made:

- 1) The predicted and measured values of deflections and moments for the group with the smaller spacing (group II) agree reasonably well.
- 2) The predicted and measured values of deflection and moment for the pile group with the larger spacing (group I) agree reasonably well when the lateral load was 16.67 kips/pile. However, the predicted values exceed the measured values by 100% for the load of 33.33 kips/pile.

2. Holloway (1981)

Holloway, Moriwaki, Finno and Green (1981) reported a lateral load test on a group of eight timber piles in sand at the site of Lock and Dam 26 on the Mississippi River near Alton, Illinois. The test set up is shown in Fig. 3.35. The pile group was constructed in a trench where 24 ft of overburden consisting of cohesive flood plain deposits were excavated. This exposed a 20 ft layer of recent alluvium

Table 3.3 Comparison of predicted versus measured values of lateral deflection of pile groups in the Bucknell University test (Kim and Brungraber, 1976).

GROUP I ($s/D = 5.0$)

Lateral Load/Pile (kips)	Y_s Calculated (in.)	Y_s Measured (in.)	Y_g Calculated (in.)	Y_g Measured (in.)	
				Series B	Series C
16.67	0.11	-	0.15	0.12	0.09
33.33	0.40	-	0.45	0.21	0.15

GROUP II ($s/D = 3.7$)

Lateral Load/Pile (kips)	Y_s Calculated (in)	Y_s Measured (in.)	Y_g Calculated (in.)	Y_g Measured (in.)	
				Series B	Series C
16.67	0.11	-	0.16	0.23	0.28
33.33	0.40	-	0.47	0.37	0.36

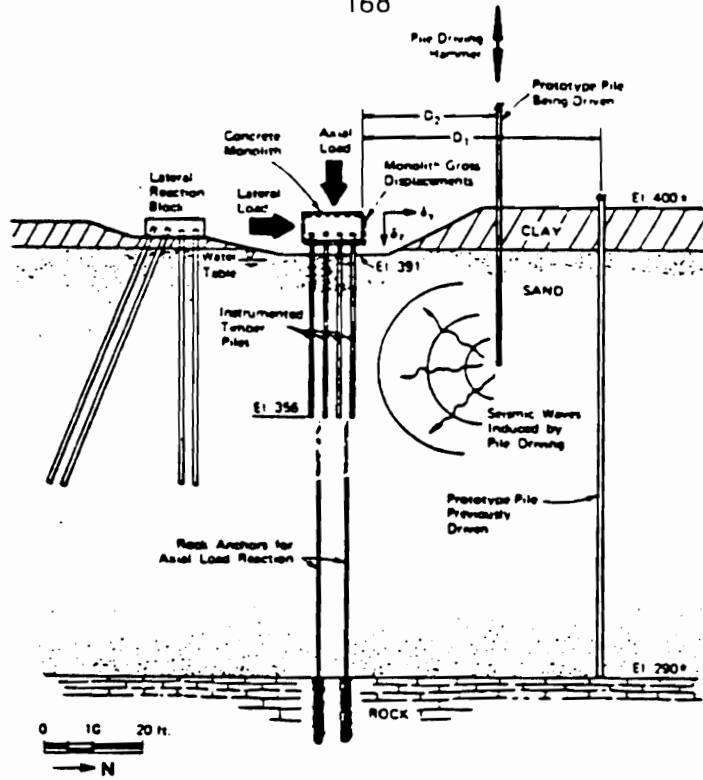
Table 3.4 Comparison of predicted versus measured values of bending moments of piles in pile groups in the Bucknell University test (Kim and Brungraber, 1976).

GROUP I ($s/D = 5.0$)

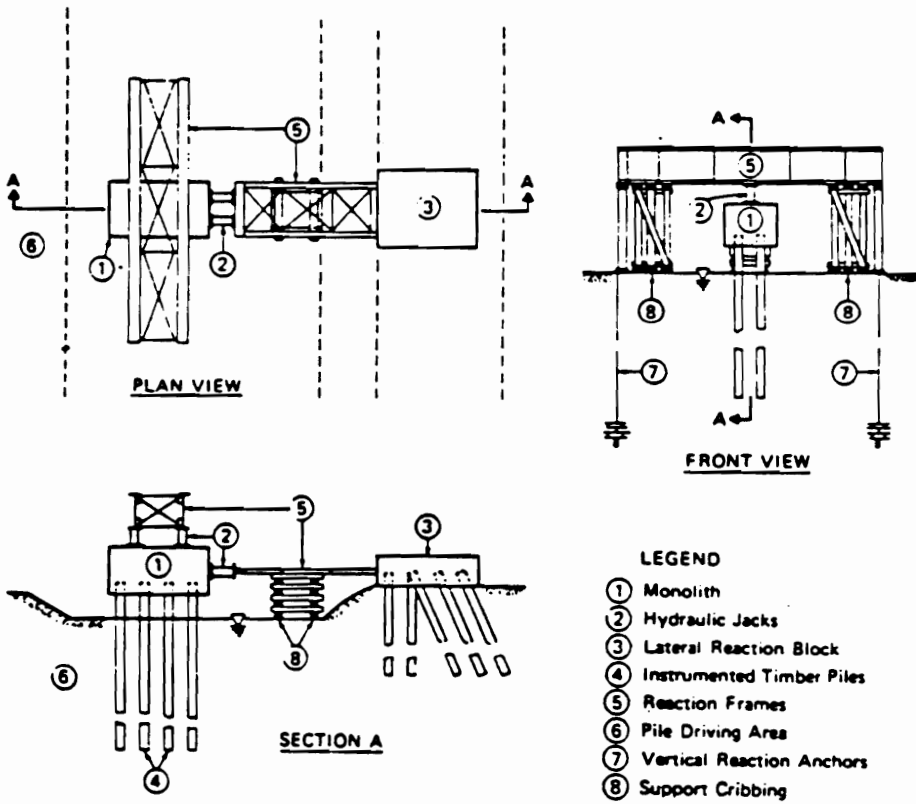
Lateral Load/Pile (kips)	M_s Calculated (kip-in)	M_s Measured (kip-in)	M_g Calculated (kip-in)	M_g Measured (kip-in)	
				Series B	Series C
16.67	560	-	620	479	457
33.33	1350	-	1420	742	707

GROUP II ($s/D = 3.7$)

Lateral Load/Pile (kips)	M_s Calculated (kip-in)	M_s Measured (kip-in)	M_g Calculated (kip-in)	M_g Measured (kip-in)	
				Series B	Series C
16.67	560	-	631	936	497
33.33	1350	-	1445	1470	672



Concept of Pile Testing Program



Typical Test Setup

Figure 3.35 Load Test Setup at the Site of Lock and Dam 26 (After Holloway et al., 1981)

(sand) that was the layer of greatest importance with regard to lateral loading. The piles penetrated through the recent alluvium and 15 ft into a layer of dense to very dense outwash, making a total embedment depth of 35 ft.

The piles were 14 inch butt diameter timber piles ($E_p = 1500$ ksi, $I_p = 1886$ in⁴) instrumented with strain gages and telltales as shown in Fig. 3.36. The piles were jetted into place for the first 30 ft of penetration, and the final 5 ft of penetration was accomplished by driving. The piles were all installed vertically in a 2 X 4 arrangement at a spacing of 3 ft center-to-center, and embedded 2 ft into the cap.

Removal of 24 ft of the flood plain deposit resulted in an overconsolidated condition in the underlying sand. The variation of the overconsolidation ratio with depth is shown in Fig. 3.37. Using the cone penetration test results of Fig. 3.38 (conducted before pile installation but after excavation by Woodward-Clyde Consultants, 1979) and Lunne and Christoffersen's (1985) procedure of interpreting friction angles for overconsolidated sands, the angle of internal friction of the top 9 ft (eight pile diameters) of the recent alluvium was estimated to be 43°.

Deflections and maximum bending moments in single fixed-head and free-head piles were analyzed using p-y analysis (with the aid of the computer program COM622), and also using the Evans and Duncan (1982) procedure. The

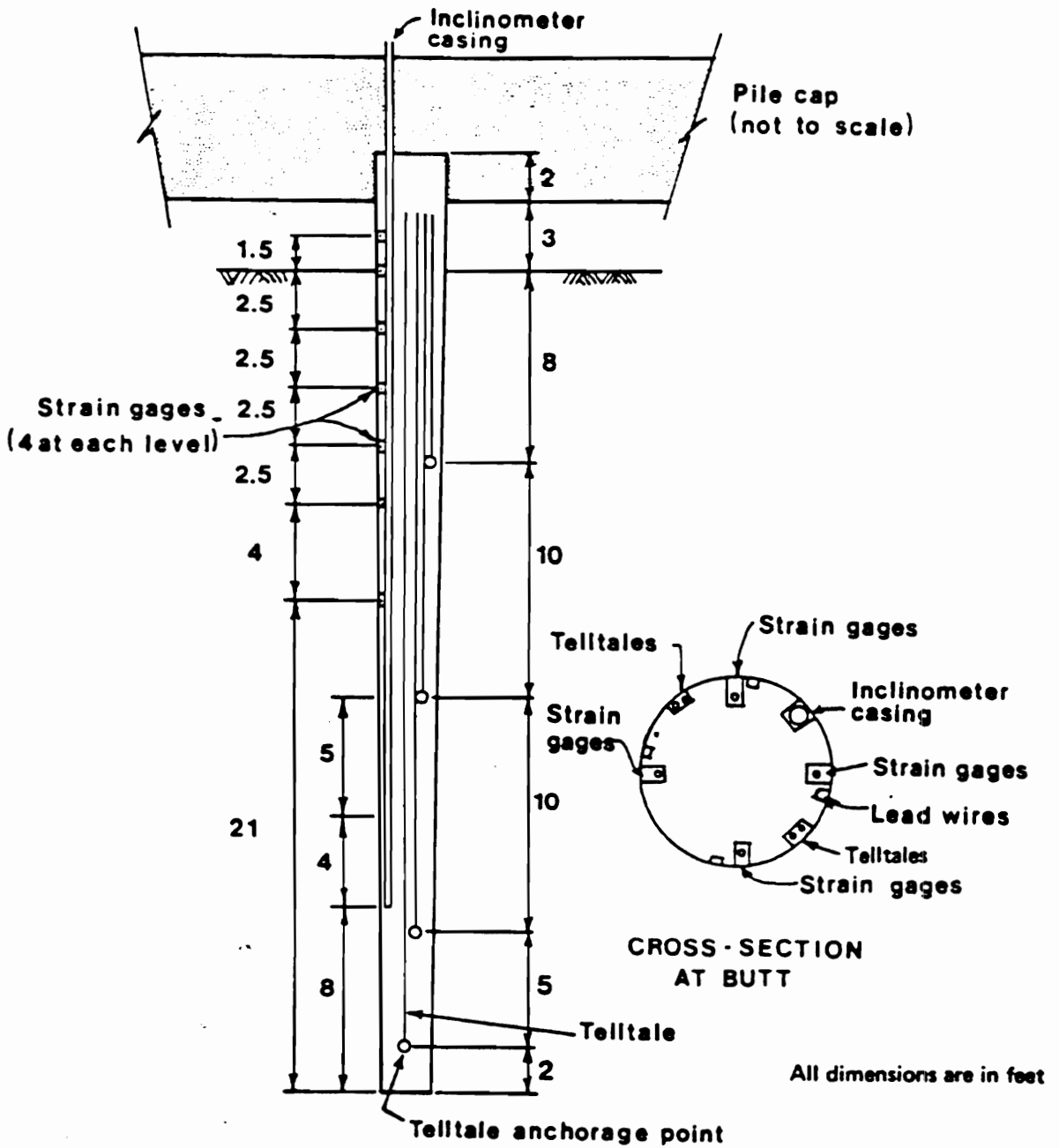


Figure 3.36 Timber Pile Instrumentation at the Site of Lock and Dam 26 (After Holloway et al., 1981)

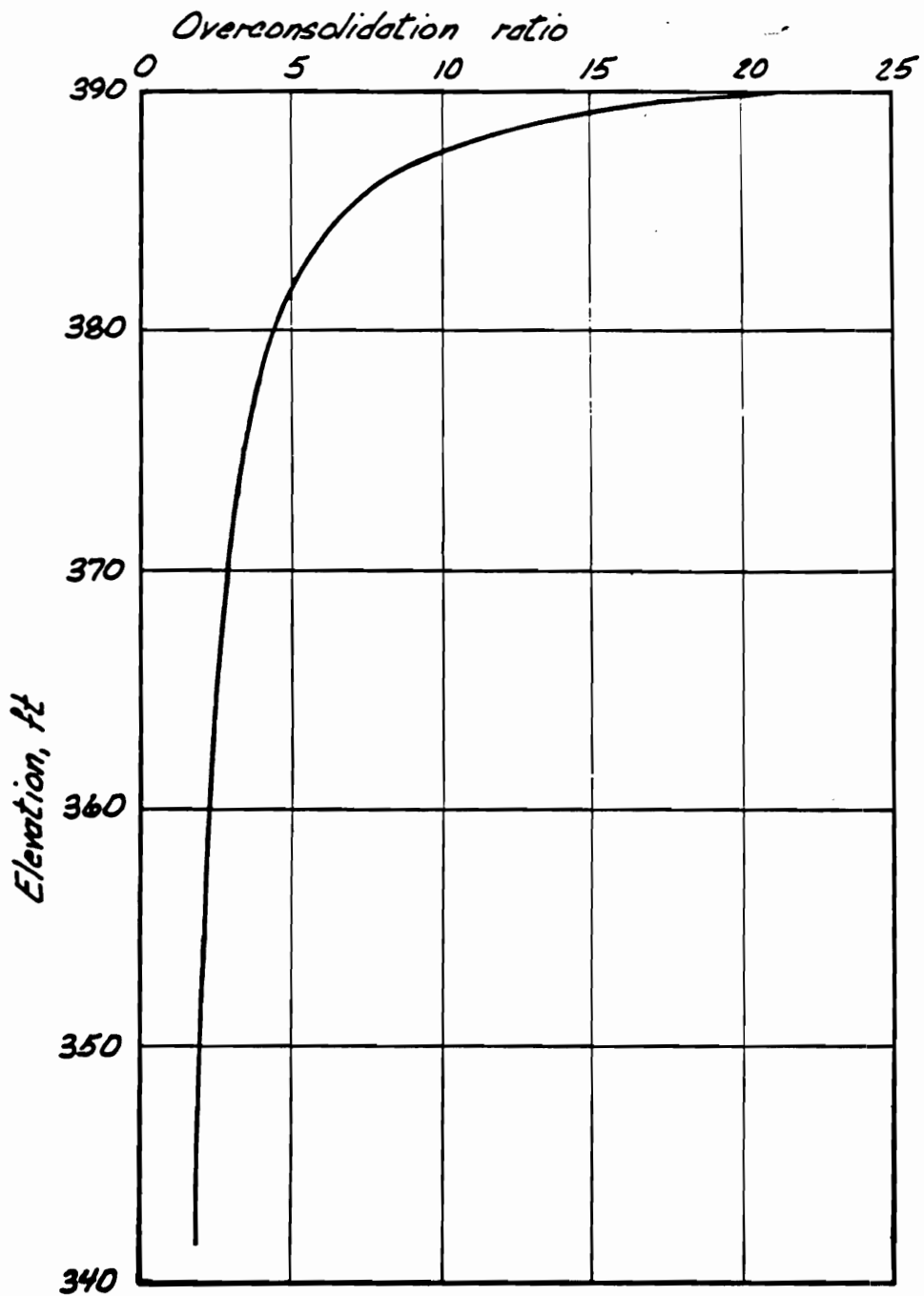


Figure 3.37 Variation of Overconsolidation Ratio with Depth at the Site of Lock and Dam 26 (After Woodward-Clyde Consultants, 1979)

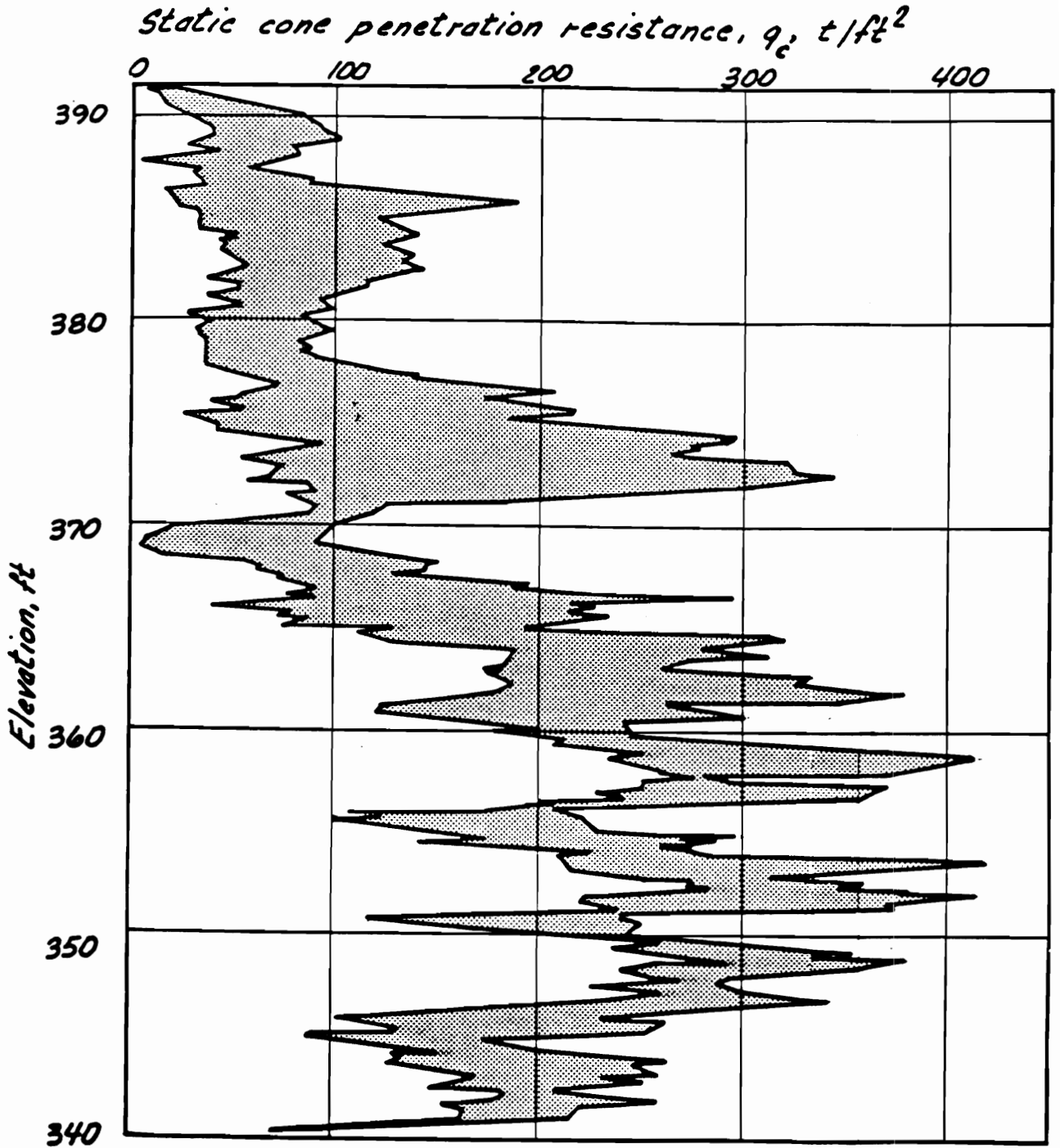


Figure 3.38 Results of Cone Penetration Tests Before Pile Installation at the Site of Lock and Dam 26 (After Woodward-Clyde Consultants, 1979)

results are shown in Table 3.5 for deflections and Table 3.6 for maximum bending moments. There is very good agreement between the two methods of analysis, with the majority of the values calculated using the two procedures being within 10% of each other.

When the cap is 3 ft above ground, the behavior is different from that of a fixed-head pile or a free-head pile. This condition can be analyzed using the approximate procedure described in Section 3.2.1.5. To provide results for comparison, the computer program COM622 was used to analyze a laterally loaded single timber pile fixed 3 ft above ground, the results of which are shown in Fig. 3.39 for deflection and Table 3.7 for maximum bending moment. Comparisons between this case with the fixed-head and free-head cases are also shown in Fig. 3.39 for deflections, and Table 3.7 for maximum bending moments. From Fig. 3.39, it can be seen that values of deflection calculated using the approximate procedure outlined in Section 3.2.1.5 and COM622 agree very well. It can also be seen that the deflection of the pile fixed 3 ft above ground is intermediate between those of a fixed-head pile and a free-head pile. From Table 3.7, the values of maximum bending moments occurring in the pile fixed above ground calculated using the approximate procedure are within about 10% of those calculated using COM622. It can also be seen that the moments in the pile

Table 3.5 Comparison of single pile deflections predicted using p-y analysis with those using the Evans and Duncan procedure for the load test conditions in Lock and Dam 26, Alton, Illinois

Lateral Load per pile P_s (kips)	Y_s obtained from p-y analysis (in.)		Y_s obtained from Evans and Duncan procedure (in.)	
	Fixed-Head	Free-Head	Fixed-Head	Free-Head
12	0.17	0.64	0.19	0.68
24	0.48	2.37	0.53	2.04
30	0.70	3.86	0.76	2.98

Table 3.6 Comparison of maximum moments in single piles predicted using p-y analysis with those using the Evans and Duncan procedure for the load test conditions in Lock and Dam 26, Alton, Illinois

Lateral Load per pile P_s (kips)	M_s obtained from p-y analysis (kip-in)		M_s obtained from Evans and Duncan procedure (kip-in)	
	Fixed-Head	Free-Head	Fixed-Head	Free-Head
12	399	425	427	463
24	917	1120	1010	1140
30	1215	1550	1350	1550

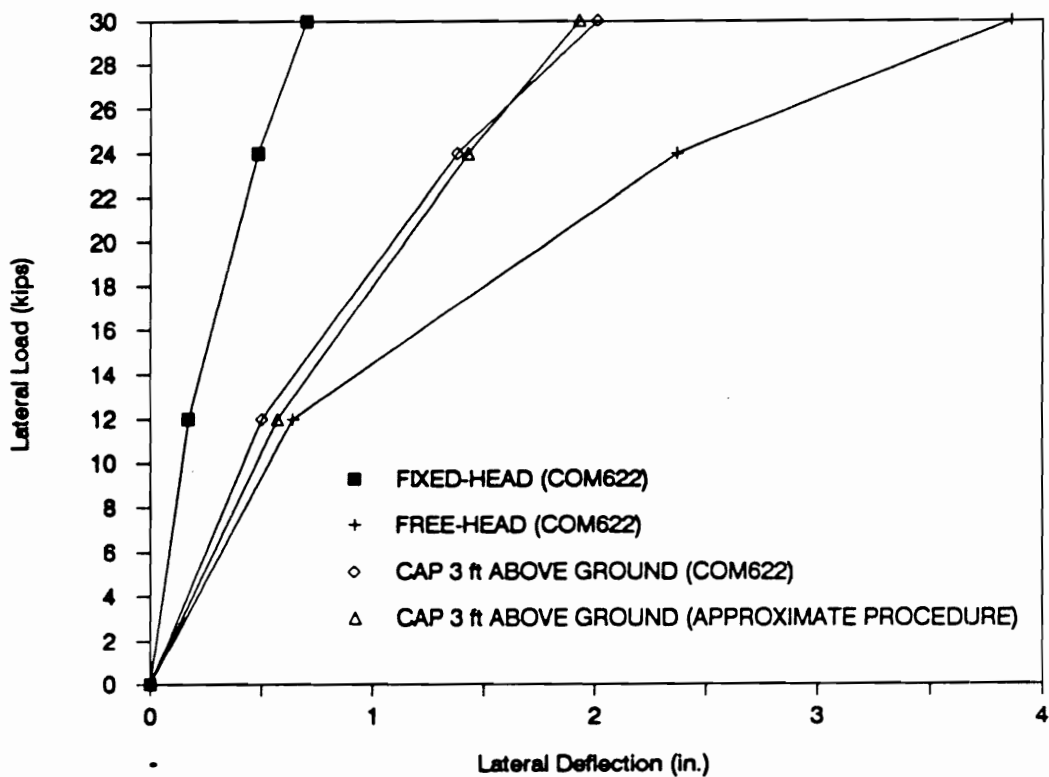


Figure 3.39 Lateral Load-Deflection Response of a Single Timber Pile at the Site of Lock and Dam 26

Table 3.7 Comparison of values of maximum bending moment calculated from p-y analyses of (1) a free-head pile, (2) a fixed-head pile and (3) a pile fixed to a cap 3 ft above ground

Lateral load per pile P_s (kips)	COM622 Analyses			Approximate Procedure
	Moment in a free-head pile (kip-in)	Moment in a fixed-head pile (kip-in)	Moment in a pile fixed to a cap 3 ft above ground (kip-in)	Moment in a pile fixed to a cap 3 ft above ground (kip-in)
12	425	399	636	589
24	1120	917	1420	1340
30	1550	1220	1860	1750

fixed above ground are higher than those for the fixed-head pile or free-head pile loaded at the groundline. The maximum moment was found to occur at the top of the pile (3 ft above ground).

The simplified procedure for amplifying single pile deflections and moments to estimate deflections and moments for the group was applied to the results of both the COM622 analysis and the approximate procedure. A comparison of the calculated and measured values of group deflection is shown in Fig. 3.40. The simplified procedure overpredicts the group deflections by about 100% at loads of 12 and 24 kips per pile. At $P_s = 30$ kips/pile, the agreement is very good. The measured deflections increased very rapidly at loads in excess of 24 kips, indicating that the behavior of these piles at very high loads may be governed by the structural strength of the piles. This comparison indicates that the simplified method provides estimates of group deflection that tend to be conservative.

The simplified procedure was also used to amplify values of single pile moments calculated using the approximate procedure and COM622 to estimate the group moments. A comparison of these values with the maximum moments measured in the leading row of piles is shown in Table 3.8. The estimated values of maximum moment exceed the measured values by about 30%. These results seem

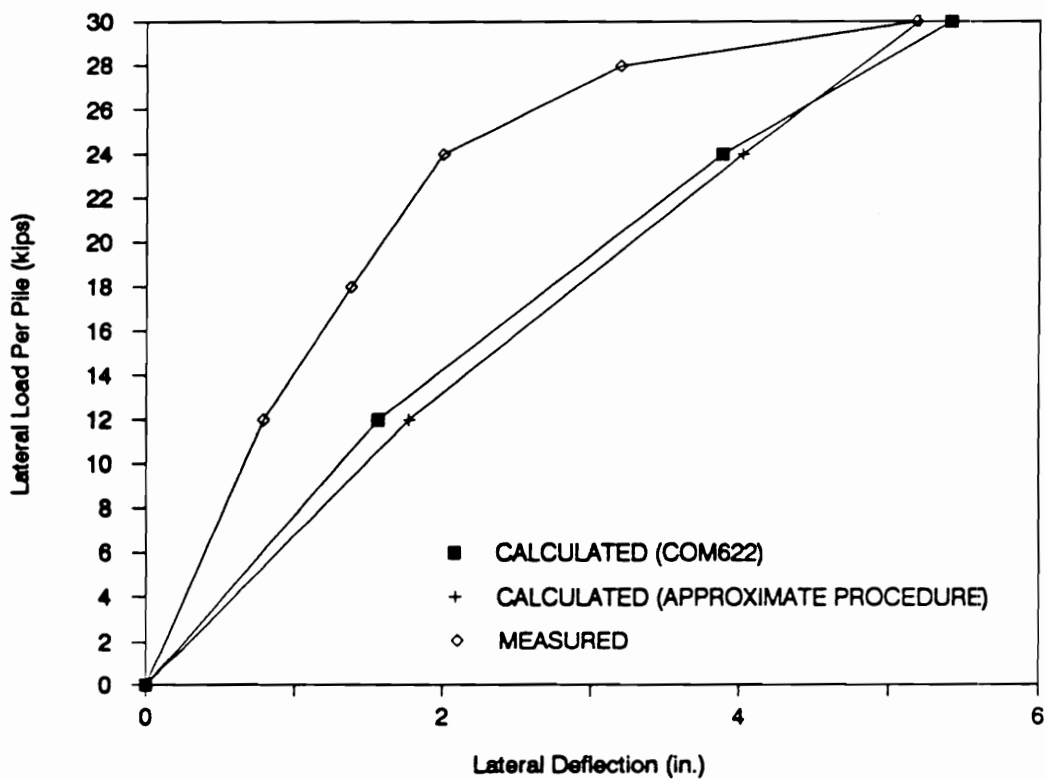


Figure 3.40 Comparison of Measured and Predicted Values of Deflection of the Pile Group at the Site of Lock and Dam 26

Table 3.8 Comparison of measured and predicted values of maximum bending moment in the pile group at Lock and Dam 26, Alton, Illinois

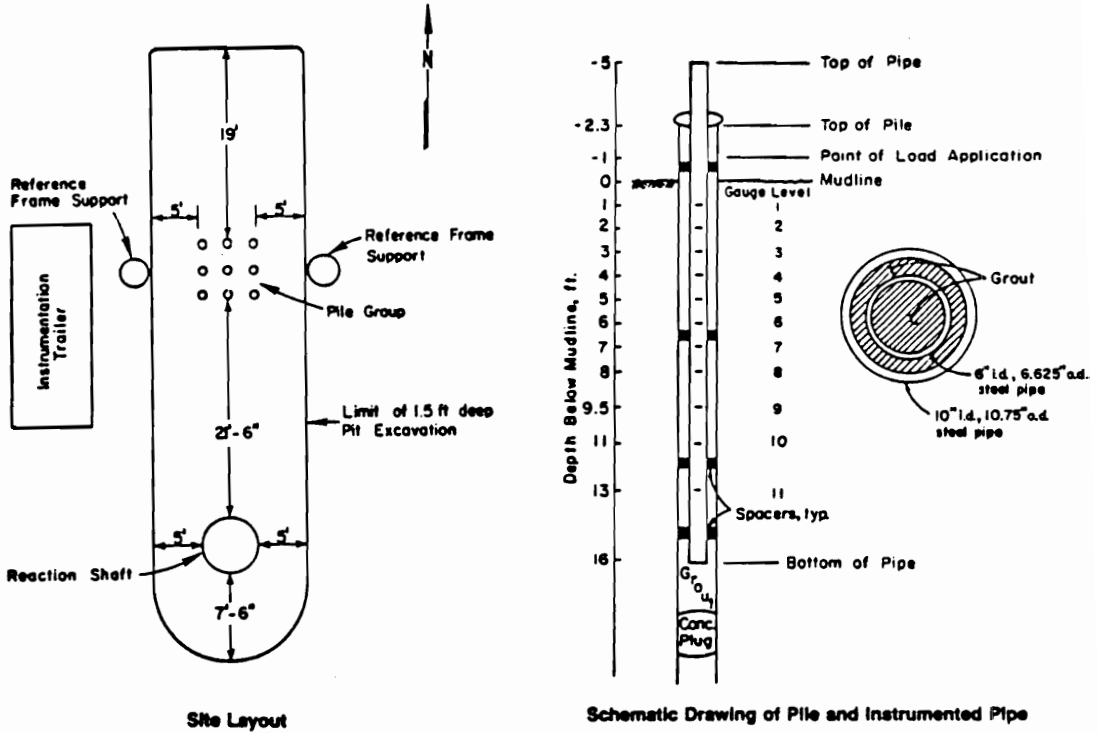
Lateral load per pile P_s	Calculated					Measured M_g
	M_s from COM622	M_s from approx. proc.	M_g/M_s from simplified proc.	M_g (M_s from COM622)	M_g (M_s from approx. proc.)	
kips	kip-in	kip-in	kip-in	kip-in	kip-in	kip-in
12	636	589	1.47	935	866	700
30	1860	1750	1.49	2770	2600	2200

reasonable considering the fact that the amplification factors were developed for fixed-head pile groups. Simplified methods of predicting pile group behavior should ideally yield results that are, if not accurate, then conservative. In this load test, this is the case.

3. Brown et al. (1987)

Brown, Reese and O'Neill (1987) conducted lateral load tests on a group of nine steel-pipe piles at the University of Houston campus. The site layout, the schematic drawing of the instrumented pipe, and the variation of shear strength with depth are shown in Fig. 3.41. Lateral load tests on a single instrumented pipe pile was also conducted so that a comparison between group response and single pile response could be made.

The piles were steel pipes with 10.75 in. outer diameter and an inner diameter of 10 in. Inserted in these pipes were smaller steel pipes (outer diameter = 6.625 in., inner diameter = 6 in.) that housed strain gages. The void space between the pipes was grouted with concrete. The flexural stiffness ($E_p I_p$) of the pile was calculated using a transformed section that accounts for the presence of the inner pipe and concrete grout. If the Young's modulus of the pile was taken to be that of steel ($E_p = 29\ 000$ ksi),



Site Layout

Schematic Drawing of Pile and Instrumented Pipe

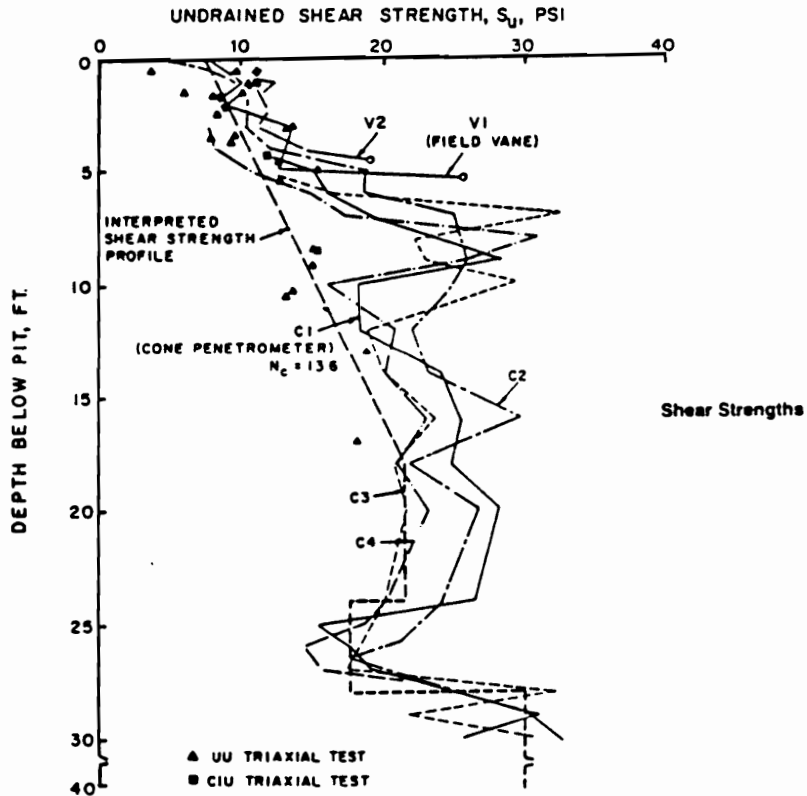


Figure 3.41 Site Layout and Soil Strength Profile for the University of Houston Test Site of a Laterally Loaded Pile Group in Beaumont Clay (After Brown et al., 1987)

then the value of moment of inertia of the pile that has the same flexural stiffness as the composite pipe was calculated to be 243 in^4 . The nine piles were driven close-ended in a 3 X 3 arrangement, with a spacing of 3 diameters center-to-center. The piles penetrated to a depth of 43 ft.

The portion of the ground that is of greatest importance to lateral load behavior is the top 8 pile diameters (7 ft). It consists of stiff, preconsolidated Beaumont clay with very closely spaced joints or fissures (spacing on the order of 0.25 in.). From Fig. 3.41, it may be seen that the average undrained shear strength for the top 7 ft is approximately 10 psi.

The loads were applied 1 ft above ground, through a loading frame that provided moment-free connections to the piles. The deflections and bending moments that were measured during the tests for the single pile and pile group are shown in Figs. 3.42 and 3.43.

In order to study the load tests of Brown et al. (1987), values of deflections and maximum bending moments in a single free-head pile were estimated using the nonlinear superposition procedure of Evans and Duncan (1982) to account for the 1 ft eccentricity of the load. These values of deflections and bending moments were then amplified to estimate values of deflection and moment for the group using Equations 3-16 and 3-20. Although Equations 3-16 and 3-20

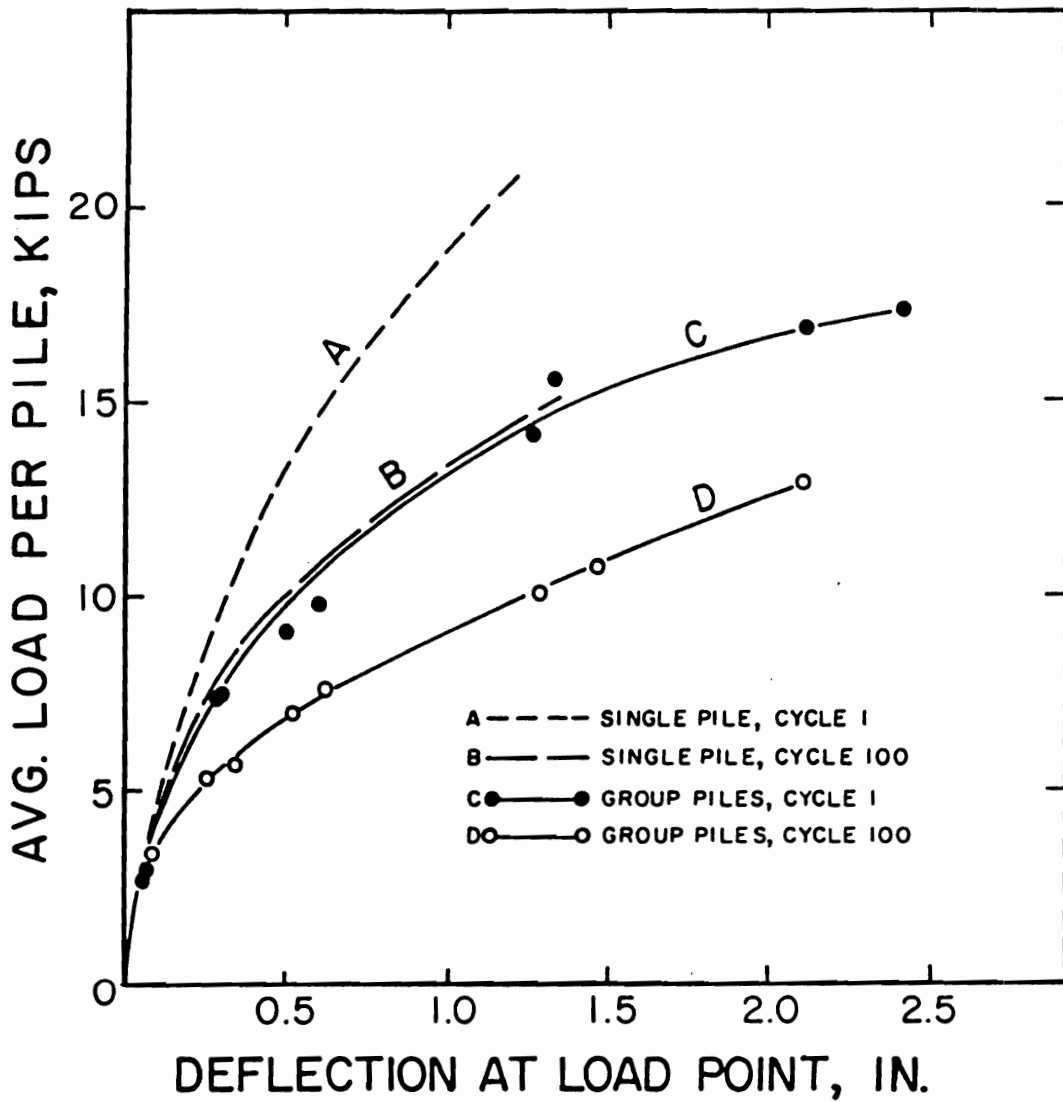


Figure 3.42 Lateral Load Deflection Response of Piles in Beaumont Clay - University of Houston (After Brown et al., 1987)

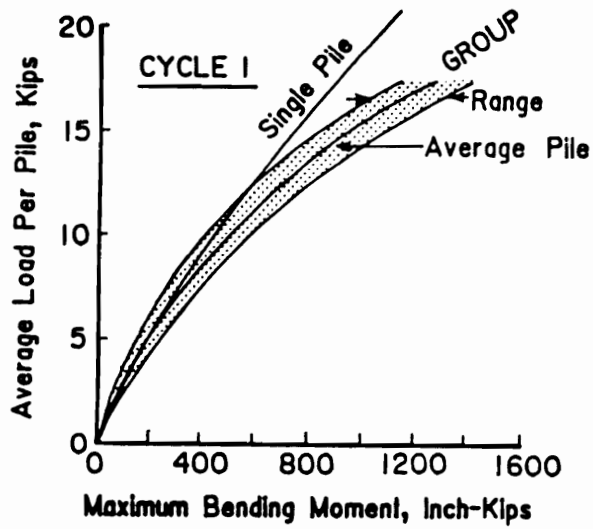


Figure 3.43 Bending Moments in Piles in Beaumont Clay - University of Houston (After Brown et al., 1987)

strictly apply only to groups of fixed-head piles, they can be applied with some approximation to free-head piles. A comparison of the calculated and measured values of deflection are shown in Table 3.9, and the moments are shown in Table 3.10.

The calculated values of single pile deflections and maximum bending moments are in excellent agreement with the measured values. At loads of 5 and 10 kips per pile, the calculated values of group deflections and maximum moments in the most heavily loaded pile in the group are also in excellent agreement with the measured values. However, at a load of 15 kips per pile, the group deflection was underestimated by 36%, while the group moment was underestimated by 15%. Overall, the accuracy of the calculations is reasonable considering the fact that the free-head group was analyzed using the simplified method developed for fixed-head pile groups.

4. Brown et al. (1988)

After performing the lateral load tests on the nine pile group in Beaumont clay at the University of Houston test site, Brown, Morrison and Reese (1987) conducted a similar research program at the same site using the same nine pile group. The natural Beaumont clay was excavated

Table 3.9 Comparison of predicted versus measured values of lateral deflection of pile groups in Beaumont clay at the University of Houston test site (Brown et al., 1987)

Lateral Load/Pile (kips)	Y_s Calculated (in.)	Y_s Measured (in.)	Y_g Calculated (in.)	Y_g Measured (in.)
5	0.11	0.11	0.20	0.19
10	0.34	0.32	0.52	0.53
15	0.68	0.63	0.91	1.43
20	1.14	1.13	1.36	-

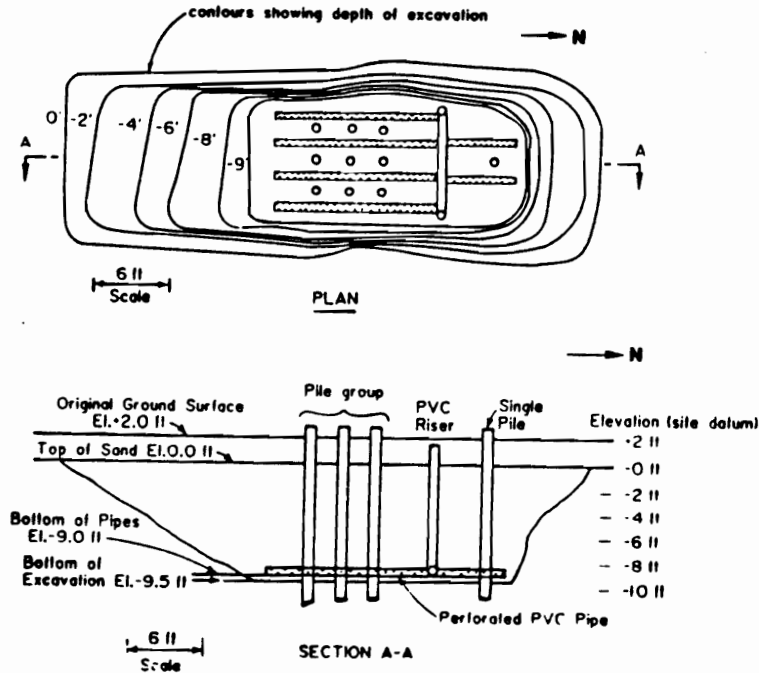
Table 3.10 Comparison of predicted versus measured values of bending moments in piles in pile groups in Beaumont clay at the University of Houston test site (Brown et al., 1987)

Lateral Load/Pile (kips)	M_s Calculated (kip-in)	M_s Measured (kip-in)	M_g Calculated (kip-in)	M_g Measured (kip-in)
5	201	200	243	200
10	449	430	525	510
15	728	750	823	970
20	1030	1100	1124	-

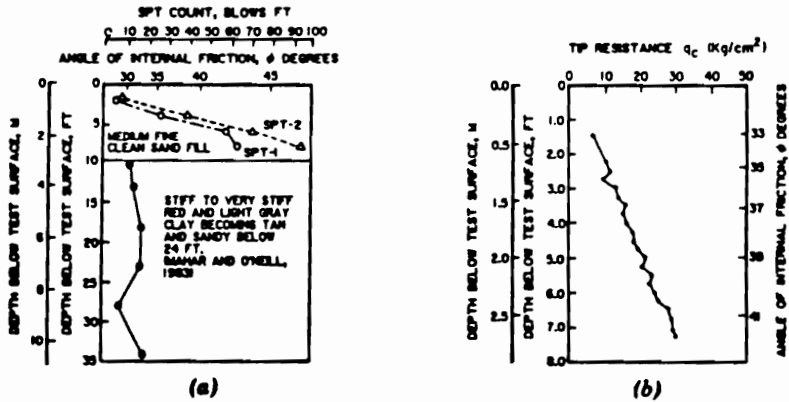
and sand backfill was compacted around the piles (Fig. 3.44). The sand layer extends to a depth of approximately 10 pile diameters. Therefore, the response of the pile group to lateral loading in these tests would be expected to be governed by the strength and stiffness of the sand.

The sand was kept saturated during the test through the use of a perforated pipe system at the bottom of the excavation. The pipe system and penetration test results (SPT and CPT) on the sand are shown in Fig. 3.44. By applying Robertson and Campanella's (1983) procedure for estimating friction angle of sands from CPT data, the compacted sand was estimated to have a friction angle of 42° . The buoyant unit weight was calculated to be 61.6 pcf.

Similar to the analysis on the pile group in Beaumont clay, the deflection and maximum bending moments in a single free-head pile were estimated using nonlinear superposition to account for the eccentricity of the load, and amplified to estimate the deflections and moments for the group. The deflections and bending moments that were measured during the tests for the single pile and pile group are shown in Figs. 3.45 and 3.46. A comparison of the calculated and measured results are shown in Table 3.11 for deflections and Table 3.12 for bending moments. Based on these comparisons, the following observations can be made:



Excavation and Pipe System for Saturating Sand



Site Conditions and Results from Penetration Tests

Figure 3.44 Site Layout and Soil Strength Profile for the University of Houston Test Site of a Laterally Loaded Pile Group in Compacted Sand (After Brown et al., 1988)

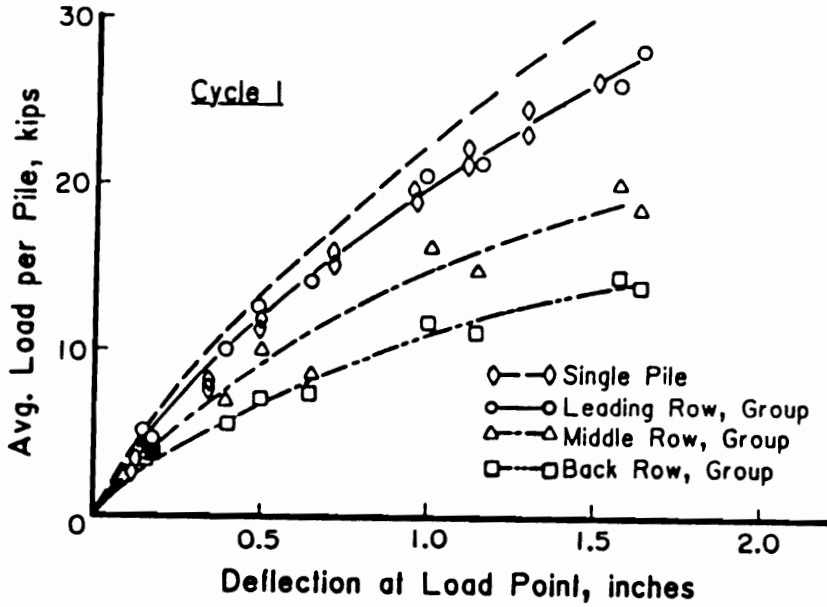


Figure 3.45 Lateral Load Deflection Response of Piles in Compacted Sand - University of Houston (After Brown et al., 1988)

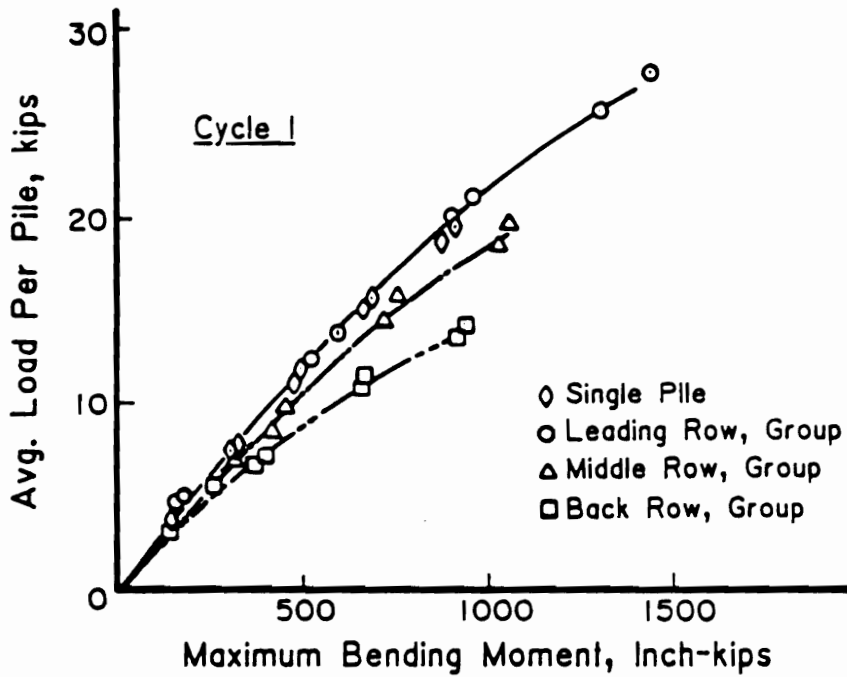


Figure 3.46 Bending Moments in Piles in Compacted Sand
 - University of Houston (After Brown et al.,
 1988)

Table 3.11 Comparison of predicted versus measured values of lateral deflection of pile groups in compacted sand at the University of Houston test site (Brown et al., 1988)

Lateral Load/Pile (kips)	Y_s Calculated (in.)	Y_s Measured (in.)	Y_g Calculated (in.)	Y_g Measured (in.)
5	0.16	0.15	0.50	0.23
10	0.40	0.33	1.16	0.54
15	0.73	0.58	1.95	1.00
20	1.15	0.87	2.88	1.60

Table 3.12 Comparison of predicted versus measured values of bending moments in piles in pile groups in compacted sand at the University of Houston test site (Brown et al., 1988)

Lateral Load/Pile (kips)	M _s Calculated (kip-in)	M _s Measured (kip-in)	M _g Calculated (kip-in)	M _g Measured (kip-in)
5	221	200	325	200
10	471	410	697	410
15	742	740	1110	740
20	1030	910	1560	910

1) The calculated values of group deflection are compared to the deflection of piles in the middle row since they best represent the deflection of the group for a given value of an average load per pile. As can be seen in Table 3.11, the calculated values of group deflection are about twice as large as the measured values.

2) Since little difference is noted in the measured values of maximum moment in the single pile and in the group, and since the moment amplification factor C_M is always greater than 1, the simplified method overestimates the maximum moment in this pile group; the difference is about 60%.

3) In this load test, the simplified method tends to be conservative when values of deflections and maximum moments from a single free-head pile are used to estimate group deflections and moments. One possible explanation may be as follows: the loads were applied in several increments, and at each load increment, the loads were cycled. This could possibly have led to densification of the sand, resulting in lower values of group deflections and moments when the loads were increased.

CHAPTER FOUR

DEVELOPMENT OF PERFORMANCE FACTORS FOR LOAD FACTOR DESIGN OF DEEP FOUNDATIONS

In the United States, load factor design (LFD) concepts are used in the ACI design code (1989), in the AASHTO specifications for both concrete and steel bridge superstructures (AASHTO, 1989), and in the AISC (1986) specifications for the design of steel buildings. However, there are no provisions for foundation design using LFD procedures. Foundations are usually designed using working stress design. Hence engineers who use LFD for structural design must develop two sets of loads - one set of loads for the design of the superstructure, and another set of loads for the design of foundations. Development of load factor design for foundations will make this duplication of effort unnecessary. Other advantages of developing LFD for foundations include: (1) consistent safety margins are attained in both structure and foundation, and (2) LFD results in more economical use of materials.

In load factor design, safety against failure for a given limit state requires that the factored ultimate resistance exceeds the factored loads. There are at least two ways in which the factored resistance can be specified:

1) In the first format, an overall performance factor is applied to the resistance side of the equation for each applicable limit state. With this approach, the factored resistance for a given limit state is given by ϕR_n , where ϕ = performance factor, with a value less than unity and R_n = nominal resistance. This is the format followed by ACI for concrete design, and AISC for LRFD of steel structures. The advantages of this approach are its simplicity and its familiarity to many designers.

2) The second approach employs partial resistance factors which are applied directly to the individual variables in the resistance equation. In this approach, partial factors are applied to the individual soil strength properties such as cohesion and angle of internal friction. These partial resistance factors are typically specified only once in the design code, and the same factors are used for all ultimate limit states.

The second approach is more sophisticated, since the partial factors are related directly to the parameters that are the sources of variability in strength. This format was adopted by the Danish Foundation Code (1985) and the Ontario Highway Bridge Design Code (1983). However, in the Ontario Highway Bridge Design Code, different partial factors were used for the same soil parameters for different limit

states. A disadvantage of the partial factor approach is that it is not consistent with resistance factors on structural elements which consider overall measures of performance, such as bending strength. The second approach was considered by ACI but was not acceptable to many engineers, and was rejected by the ACI membership. The "overall performance factor" format is the preferred approach to LFD of deep foundations, and will be the format adopted.

In the sections that follow, the determination of performance factors for axial capacities of driven piles and drilled shafts for the AASHTO code (for bridges) and the ASCE Standard 7-88 (for buildings and other structures) is described. A procedure for extending the results of this calibration exercise to any other design code will also be presented.

4.1 Single Piles

4.1.1 Introduction

In this section, results of the code calibration are presented for several methods of predicting pile capacity described in Chapter 2. The methods considered include both rational methods and empirical methods based on in situ tests. Resistance statistics for driven piles and the

results of the reliability analyses are presented. Performance factors obtained by reliability based calibration are summarized and the rationale for the selection of the performance factors is discussed.

4.1.2 Resistance Statistics

The calculated ultimate bearing capacity, Q_{ult} , of a deep foundation in reality can differ from the measured or actual bearing capacity, Q_m . To account for the discrepancy between Q_{ult} and Q_m , correction factors that represent the different sources of uncertainties are introduced as follows:

$$Q_m = \prod_{i=1}^n N_i Q_{ult} \quad (4-1)$$

where N_i is the correction factor for the error source i and n is the number of sources of error.

The uncertainty associated with a correction factor N_i , may be represented by the mean value, \bar{N}_i and the c.o.v., V_i . The mean value of N_i is a measure of the bias caused by the error source i , on the ultimate bearing capacity. The c.o.v., V_i , is a measure of the scatter of the correction factor, which in turn affects the variability of the ultimate bearing capacity. Assuming that the correction

factors are statistically independent, first order analysis of the uncertainties affecting the ultimate bearing capacity yield the mean and c.o.v. of Q_m as follows:

$$\bar{Q}_m = \prod_{i=1}^n \bar{N}_i \bar{Q}_{ult} \quad (4-2)$$

and

$$V_{Q_m} = \sqrt{\sum_{i=1}^n V_i^2} \quad (4-3)$$

The following sources of error are considered in the reliability analysis:

(1) model error where there may be an overall bias in the prediction method.

(2) time and reconsolidation in the case of clays. Because of the time dependent properties of clay, the capacity will change with time. Pile load tests are generally performed shortly after installation, but the maximum load on the structure may occur years after installation. Therefore, in clays which consolidate and gain strength after pile installation, load tests may underestimate the pile capacity.

(3) inherent spatial variability. Soil properties are known to be correlated between any two points. The uncertainty associated with a soil property at a point is

larger than if it were measured over a certain distance or volume because of the averaging effect.

(4) systematic error in the soil strength which accounts for the bias and repeatability of the tests used for measuring soil parameters. This may be due to equipment, procedural and rate of testing effects.

Other possible sources of error include the following (Tang, 1989):

(1) Statistical uncertainty due to insufficient soil samples at the site - The uncertainty in the predicted value of a soil parameter is inversely proportional to the square root of the number of samples tested, i.e. the c.o.v. due to statistical uncertainty is equal to $V_c/\sqrt{N_{\text{samples}}}$, where V_c is the c.o.v. of the measured strength and N_{samples} is the number of samples tested. The reliability analysis performed for deep foundations is not site specific, and this quantity is assumed to be negligible. The bias factor due to statistical uncertainty is assumed to be unity.

(2) Error in determining the value of the ultimate load - Equipment used in load testing piles could take some of the load applied to the piles via friction in the jack (Tang, 1989). Also, even if a certain failure criteria (eg. Davisson's, 1973) was used to define the ultimate load in piles, different engineers using the same method could give

different estimates of pile capacity. Such sources of error are not easily quantified.

The resistance statistics for three rational (α , β , and λ methods) and two in situ methods (SPT and CPT methods) are presented below.

a) Rational Methods For Driven Piles

Sidi (1986) analyzed numerous pile load tests in cohesive soils and compared them to the predicted capacities using rational methods. Three of the rational methods he considered include the α , β and λ methods. The α method (Tomlinson, 1987), which is a total stress method, and the λ method (Vijayvergiya and Focht, 1973), which is a mixed method, both require the knowledge of the undrained shear strength of the clay. The β method (Esrig and Kirby, 1979), which is an effective stress method, requires an estimation of the stress history of the clay.

Sidi separated the resistance statistics for the α and λ methods into two distinct groups: the first group called Type I clay is for clays with undrained shear strengths, S_u , less than 1000 psf, while the second group (Type II) is for clays with S_u greater than 1000 psf.

Sidi (1986) accounted for the effect of inherent spatial variability of soil parameters through the use of

random field theory. Using a variance function (Vanmarcke, 1983), the c.o.v. of a soil property at a point can be reduced to the c.o.v. of the soil property over a spatial length. With an appropriate variance function, he found that the coefficient of variation for inherent spatial variability for the α and λ methods is equal to $1/\sqrt{Z}$, where Z is the pile length in ft. The bias factor for inherent spatial variability can be taken as unity. The uncertainty in the unit weight (used for calculating the effective overburden pressure in the λ method) is disregarded because it is small compared to the uncertainty in the shear strength. The bias factor for inherent spatial variability of OCR used in the β method is assumed to be unity while the c.o.v is small and therefore, assigned a value of 0.05. Statistics (bias factors and c.o.v.'s) for the various sources of error considered by Sidi are summarized in Table 4.1.

b) In Situ Methods For Driven Piles

In situ tests are useful for estimating shear strengths especially of sandy soils. The uncertainties associated with the SPT and CPT tests are discussed below.

Table 4.1 Summary of statistics for axial capacity of friction piles (After Sidi, 1986)

Correction	Type I Clay		Type II Clay		Effective Stress Analysis	
	Mean	COV	Bias	COV	Bias	COV
Model Error						
α method	1.104	0.208	2.34	0.568	-	-
λ method	1.02	0.414	0.84	0.174	-	-
β method	-	-	-	-	1.032	0.213
Time and Reconsolidation	1.113	0.04	1.0	0.0	-	-
Inherent Spatial Variability	1.0	$\frac{1}{\sqrt{2}}$	1.0	$\frac{1}{\sqrt{2}}$	1.0	0.05 ¹
Systematic Error						
UU Triaxial						
$\frac{S_u}{\sigma_v'}$	0.945	0.179	1.02	0.098	-	-
$\frac{S_u}{\sigma_v'}$	0.945	0.179	1.03	0.136	-	-
$\frac{S_u}{\sigma_v'}$	0.945	0.179	1.03	0.153	-	-
Consolidation Test						
OCR					1.0	0.15 ¹

¹ Estimated value

SPT

The standard penetration test is the most common in situ test for soils. However, many variations of the test equipment give rise to different energy levels imparted into the soil. Such factors include the type of hammer (which affects the amount of energy delivered to the system), length of drill rods, diameter of borehole, nature of drilling fluid, type of drill bit, type of sampling spoon, rate of blow count and type of drill rods (Seed and DeAlba, 1986). Most of these effects may be minimized by standardizing the test. Nevertheless, variability in the equipment and procedure cannot be eliminated. Orchant et al. (1988) found that systematic error due to equipment, procedure and random effects cause a certain degree of variation. They proposed the c.o.v. values shown in Table 4.2 for these effects. It is assumed that the bias factors approach unity due to an averaging effect.

Other sources of error considered are also shown in Table 4.2. Meyerhof (1976) suggests that correcting the SPT-N value against a standard overburden pressure of 1 tsf when estimating the end bearing would lead to improved results of pile capacity prediction in sands. Studies have shown that 5 models for overburden correction of SPT-N values [Bazaraa (1967), Peck et al. (1974), Seed (1979), Skempton (1986) and Liao and Whitman (1986)] give very

Table 4.2 Summary of statistics for axial capacity of piles using in situ test results

Correction	SPT		Mechanical Cone		Electric Cone	
	Mean	COV	Mean	COV	Mean	COV
Model Error	1.3	0.5	1.03	0.357	1.03	0.357
Equipment, Procedure and Random	1.0	0.15-0.45	1.0	0.15-0.25	1.0	0.05-0.15
Inherent Spatial Variability	1.0	$\frac{1.42}{\sqrt{Z}}$	1.0	$\frac{0.903}{\sqrt{Z}}$	1.0	$\frac{0.903}{\sqrt{Z}}$
Overburden Correction	1.0	0.07	-	-	-	-

similar results. Meyerhof's SPT method for predicting pile capacity in sands was estimated to have a bias of 1.3 and a c.o.v. of 0.5.

Vanmarcke showed that the c.o.v. of a soil property is reduced when the property is averaged over a length or volume. The amount of reduction depends on the variance function, $\Gamma(\Delta z)$, which is defined as the ratio of the c.o.v. of a random variable averaged over a length Δz $[(V_i)_{\Delta z}]$, to the point c.o.v. of that random variable $[V_i]$:

$$\Gamma(\Delta z) = \frac{(V_i)_{\Delta z}}{V_i} \quad (4-4)$$

Vanmarcke (1977) defined the scale of fluctuation, θ_s , as "the distance within which the soil property shows relatively strong correlation or persistence from point to point." He further showed that the variance function is related to the scale of fluctuation as follows:

$$\Gamma(\Delta z) = \left[\frac{\theta_s}{\Delta z} \right]^{1/2} \quad (4-5)$$

Equating the expressions for $\Gamma(\Delta z)$ given by Equations 4-4 and 4-5, the c.o.v. of a soil property over a depth Δz can be written as:

$$(V_i)_{\Delta z} = \left[\frac{\theta_s}{\Delta z} \right]^{1/2} V_i \quad (4-6)$$

where θ_s is the scale of fluctuation of the soil property and V_i is the c.o.v. of the soil property at a point.

Table 4.3 shows the scale of fluctuation and the point c.o.v. for the SPT blow count.

CPT

Orchant et al. (1988) surveyed CPT data for both mechanical and electric cones. The equipment, procedural and random effects give rise to uncertainty in the cone resistance indicated by the values of c.o.v. in Table 4.2. It is however, not customary to correct CPT data for overburden pressure. Using the load test data of Robertson and Campanella (1988) and Horvitz et al. (1981), the model error and c.o.v. for Schmertmann's CPT method for predicting pile capacities are shown in Table 4.2. The bias factor and c.o.v. for inherent spatial variability in the sleeve friction resistance and cone resistance from the CPT are also shown in Table 4.2. They were calculated using the values of scale of fluctuation and point c.o.v. given in Table 4.3.

4.1.3 Load Statistics

Load statistics for buildings and bridges are summarized in Table 4.4.

Table 4.3 Scale of fluctuation and point coefficients of variation for in situ soil parameters

	SCALE OF FLUCTUATION	C.O.V.point
SPT	8 ft (After Vanmarcke, 1977)	0.42 (After Briaud & Tucker, 1984)
CPT	2 m (6.56 ft) (After Baecher et al., 1983)	0.35-0.71 (After O'Neill, 1986) 0.33 (After Grigoriu et al., 1987) Value used = 0.37

Table 4.4 Statistics for dead and live loads

Bridges

	Span = 60 ft ($S_D/S_L = 1.0$)		Span = 250 ft ($S_D/S_L = 3.7$)	
	Bias	COV	Bias	COV
Dead Load	1.05	0.09	1.05	0.09
Live Load	1.22	0.11	1.05	0.11

Buildings

	Influence Area, A_I (ft ²)							
	1000		2000		5000		10000	
	Bias	COV	Bias	COV	Bias	COV	Bias	COV
Dead Load	1.05	0.10	1.05	0.10	1.05	0.10	1.05	0.10
Live Load	1.08	0.25	1.09	0.25	1.11	0.25	1.13	0.25

Bridges

Grouni and Nowak (1984) attributed the dead load acting on bridges to the weight of factory-made members and the structural components produced in the field, which include the weight of concrete and the weight of the wearing surface. Dead load acting on bridges can be assumed to be normally distributed. Grouni and Nowak found that the bias factor for dead load is approximately 1.05 for Canadian bridges. Because the dead load can usually be calculated quite accurately, the same value of bias factor will be applicable to bridges in the U.S. Moses and Ghosn (1985) found that the c.o.v. for dead load on bridges is approximately 9%.

The bias factor for the maximum live load (truck loading) acting on bridges vary with span length. The values of the bias factor for live load on bridges with span lengths ranging from 60 ft ($S_D/S_L = 1.0$) to 250 ft ($S_D/S_L = 3.7$) are shown in Table 4.4. According to Grouni and Nowak (1984), the c.o.v. for live load is approximately 11%.

Buildings

Dead load in buildings may be attributed to the weight of the structural elements, permanent equipment, partitions and installations, roofing, floor coverings, etc. (Ellingwood et al., 1982). As with bridges, the probability

distribution for dead load can be assumed to be normal. Ellingwood et al. (1982) proposed that values of the bias factor and c.o.v. for dead load can be taken as 1.05 and 0.1 respectively.

Models for predicting the nominal value of the lifetime maximum total live load for buildings have been published by several authors (see reference by Ellingwood et al., 1982). For office buildings, the nominal value of maximum total live load (S_L) is given by the ASCE Standard 7-88 (1990) as follows:

$$S_L \text{ (lb/ft}^2\text{)} = 50(0.25 + 15/\sqrt{A_I}) \quad (4-7)$$

where A_I is the influence area. The mean value of maximum live load (\bar{S}_L) can be calculated using the following model for live load (Ellingwood et al., 1982):

$$\bar{S}_L \text{ (lb/ft}^2\text{)} = 14.9 + 763/\sqrt{A_I} \quad (4-8)$$

The bias factor for live load (λ_L) is obtained by dividing Equation 4-8 by Equation 4-7 as follows:

$$\lambda_L = \bar{S}_L/S_L = \frac{14.9 + 763/\sqrt{A_I}}{50(0.25 + 15/\sqrt{A_I})} \quad (4-9)$$

It can be seen from Equation 4-9 that the bias factor for live load varies with the influence area. According to Ellingwood et al. (1982), the variation of c.o.v. with the

influence area is small, and they suggested that a c.o.v. of 0.25 for maximum live load is sufficiently accurate.

Comparison of the load statistics and resistance statistics show that the values of c.o.v. for resistance are much larger than those for loads. Also, the magnitude of the resistance should be larger than the magnitude of the loads by a factor equal to the factor of safety. Therefore, the uncertainty in the resistance will constitute a larger percentage of the total uncertainty, implying that the calibration results will not be highly sensitive to the load statistics.

4.1.4 Results of Calibration

4.1.4.1 Reliability Indices

Reliability indices for the five methods selected for calibration are shown in Figs. 4.1 and 4.2. Those in Fig. 4.1 were calculated using the lognormal method, and those in Fig. 4.2 were calculated using the advanced procedure. Values of reliability indices were calculated for two dead to live load ratios ($S_D/S_L = 1$ and 3.7). It was found that the reliability indices for bridges and buildings are similar, because the uncertainty in the resistance constitutes a larger percentage of the total uncertainty,

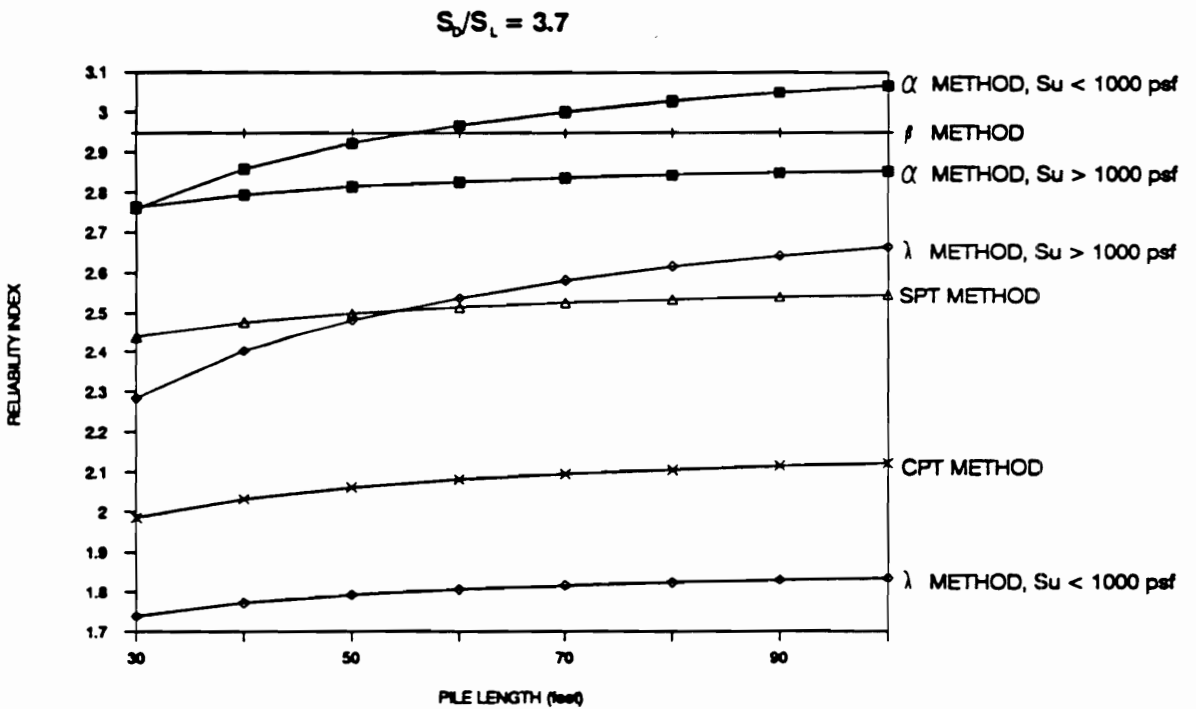
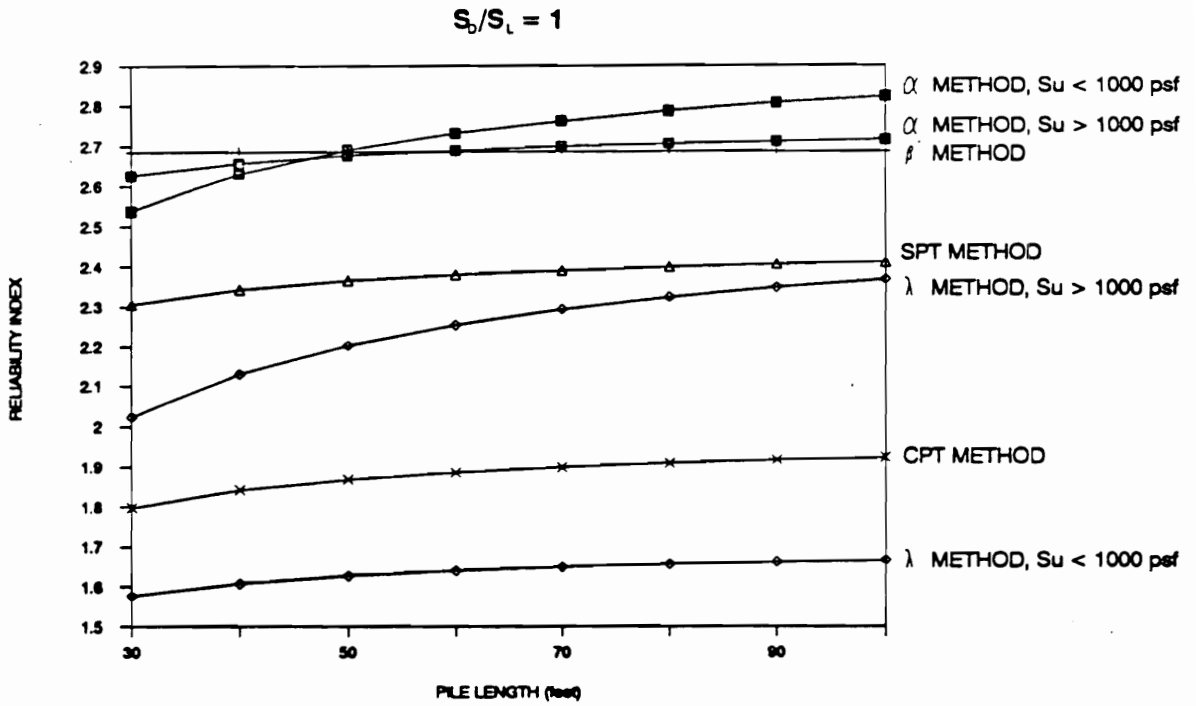


Figure 4.1 Reliability Index Versus Pile Length for Lognormally Distributed Load and Resistance

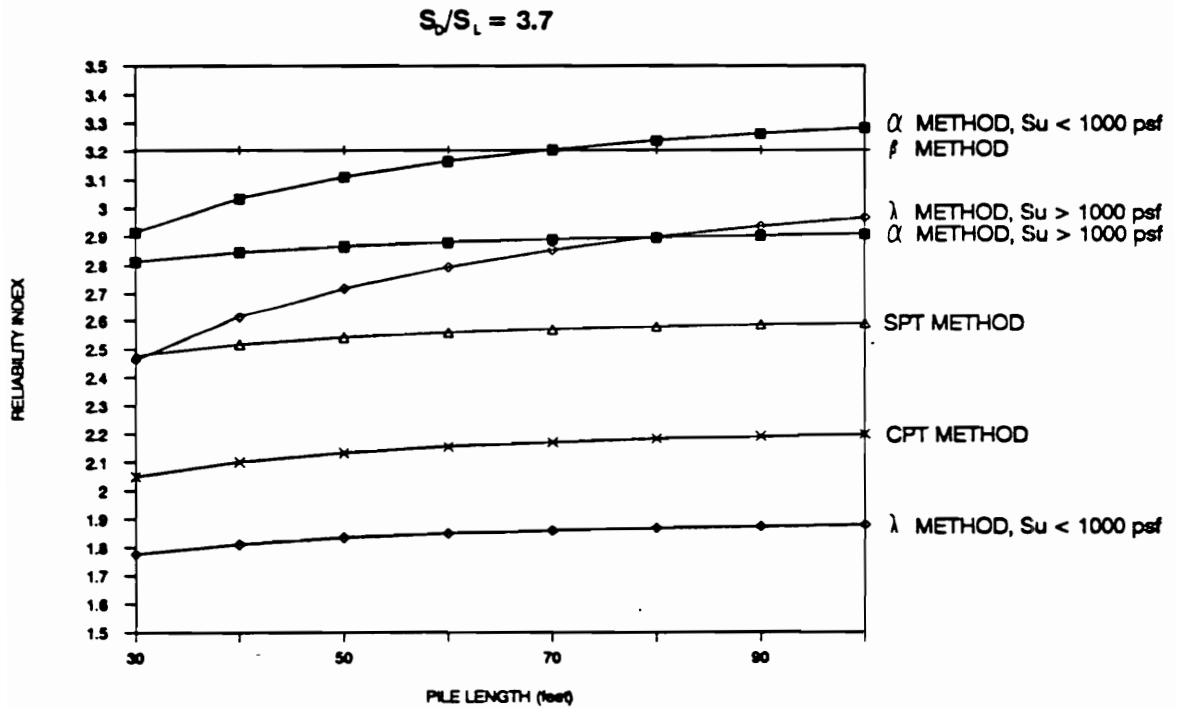
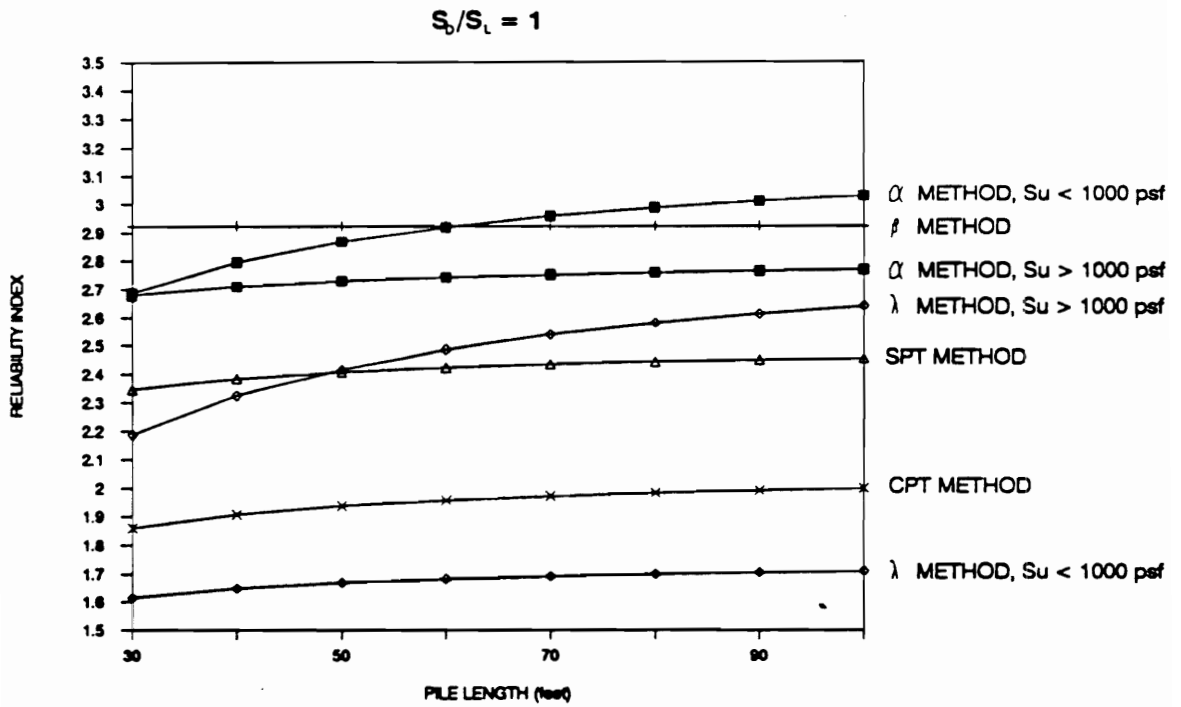


Figure 4.2 Reliability Index Versus Pile Length Using the Advanced Method

and the values of reliability indices are thus relatively insensitive to the load statistics.

Based on the results of the reliability analysis, the following observations can be made:

- 1) The values of reliability index increase with increasing span length for bridges. This is due to the fact that the ratio of dead to live load increases with span length. Since the uncertainty in the dead load is lower than the uncertainty in the live load, this has the effect of reducing the total uncertainty in the load, thus resulting in higher values of reliability index.
- 2) The reliability indices for driven piles vary between 1.6 and 3.1 using the lognormal method while the advanced method yielded values between 1.6 and 3.3.

The α , β and λ methods for predicting pile capacities in clay and the CPT method for predicting pile capacities in sand all employ a factor of safety of 2.5. The factor of safety associated with the SPT method is typically 4.

4.1.4.2 Target Reliability Indices

Meyerhof (1970) suggested that the probability of failure of foundations should be between 10^{-3} and 10^{-4} , which corresponds to values of reliability indices between 3 and 3.6 (Table 2.9).

Reliability indices for offshore piles reported by Wu et al. (1989) are between 2 and 3. They calculated that the reliability index for pile systems is approximately 4.0, corresponding to a lifetime probability of failure of 0.00005. Tang et al. (1990) reported that offshore piles have reliability indices ranging from 1.4 to 3.0.

Reliability indices for driven piles are summarized in Table 4.5. Values of reliability indices between 1.6 and 3.1 were obtained for the lognormal procedure, and the values are relatively insensitive to the ratio of dead to live load. Thus a target reliability index between 2.5 to 3.0 may be appropriate. However, piles are usually used in groups. Failure of one pile does not necessarily imply that the pile group will fail. Because of this redundancy in pile groups, it is felt that the target reliability index for driven piles can be reduced from 2.5 to 3.0 to a value between 2.0 and 2.5.

4.1.4.3 Performance Factors

Performance factors obtained by fitting with the existing working stress design specifications are shown in Table 2.8 for dead to live load ratios ranging from 1 to 4. As mentioned earlier, the safety factor for the three rational methods and the CPT method is usually taken as 2.5,

Table 4.5 Summary of reliability indices for driven piles

Ratio of Dead to Live Load	Lognormal	Advanced
1.0	1.6-2.8	1.6-3.0
3.7	1.7-3.1	1.8-3.3

while the safety factor for the SPT method is usually about 4. Calibration by fitting with working stress design at low dead to live load ratios yields performance factors that are unconservative. Since live load factors are usually greater than dead load factors, low values of dead to live load ratios result in lower total factored loads for the same working load.

Bridges

Performance factors obtained from the reliability based calibration procedure are shown in the top half of Table 4.6. The values shown are based on target reliability indices of 2.0 and 2.5 and a dead to live load ratio of 3.7, which corresponds to a bridge span length of 250 ft. The values of performance factor varies from 0.38 to 0.96 depending on the method used for predicting pile capacity, the type of soil, the length of the pile and the target reliability index. Results of the calibration indicate that performance factors are not sensitive to pile length. Also, the performance factors are relatively insensitive to the ratio of dead load to live load. This is due to the fact that uncertainties in soil parameters and uncertainties in the prediction equation are considerably higher than the uncertainties associated with the loads.

Table 4.6 Performance factors for driven piles

Bridges

Pile Length	α -method		β -method	λ -method		CPT	SPT
	Type I	Type II		Type I	Type II		
$\beta_T = 2.0$							
30 ft	0.78	0.92	0.79	0.53	0.65	0.59	0.48
100 ft	0.84	0.96	0.79	0.55	0.71	0.62	0.51
$\beta_T = 2.5$							
30 ft	0.65	0.69	0.68	0.41	0.56	0.48	0.36
100 ft	0.71	0.73	0.68	0.44	0.62	0.51	0.38
Selected	0.70		0.50	0.55		0.55	0.45

Buildings

Pile Length	α -method		β -method	λ -method		CPT	SPT
	Type I	Type II		Type I	Type II		
$\beta_T = 2.0$							
30 ft	0.74	0.92	0.73	0.52	0.60	0.57	0.48
100 ft	0.79	0.95	0.73	0.54	0.65	0.60	0.50
$\beta_T = 2.5$							
30 ft	0.60	0.67	0.61	0.39	0.50	0.45	0.35
100 ft	0.65	0.70	0.61	0.42	0.55	0.48	0.37
Selected	0.65		0.45	0.50		0.50	0.40

Recommended values of performance factors for each of the method are also summarized in the last row of Table 4.6. Studies have shown that among the 3 rational methods for predicting pile capacities in clays, the following is judged to be the order of reliability of the methods in descending order: (1) α method, (2) λ method (3) β method. The recommended values in Table 4.6 reflect this trend. Calibration results indicate that the performance factor for the β method is high (0.68 to 0.79). However, the β method when applied by different engineers, can give widely divergent estimates of pile capacity and therefore a lower value of ϕ (0.5) is assigned to the method. The recommended performance factor for the CPT method is 0.55 while for the SPT method, a value of 0.45 is recommended. The CPT method is more reliable than the SPT method because of the continuous nature of measurements afforded in a CPT test, even though the factor of safety associated with the SPT is higher. Thus a higher value of performance factor is recommended for the CPT method than the SPT method.

Buildings

Performance factors obtained from the reliability based calibration procedure are shown in the bottom half of Table 4.6. The values shown in the table are based on target reliability indices of between 2.0 and 2.5 and a dead to

live load ratio of 2.0. The value of dead to live load ratio of 2.0 was chosen to reflect more closely the ratios of dead to live load in buildings. It can be seen that values of performance factors are lower than those for bridges, ranging from 0.37 to 0.95. These values are lower primarily because the load factors for buildings are less than those for bridges, and thus lower ϕ factors are needed to achieve the same level of reliability.

Performance factors derived from the reliability based calibration for buildings are plotted against the performance factors for bridges in Fig. 4.3. The figure shows that an approximately linear relationship exists between performance factors for buildings and those for bridges. This approximate relationship can be established as follows: the load factor design criteria for two different codes, Code A and Code B, are given by the following equations:

$$\text{For Code A: } \phi_{AR_n} \geq \frac{\gamma_{DA} S_{DA} / S_{LA} + \gamma_{LA}}{FS(S_{DA} / S_{LA} + 1)} \quad (4-10)$$

$$\text{For Code B: } \phi_{BR_n} \geq \frac{\gamma_{DB} S_{DB} / S_{LB} + \gamma_{LB}}{FS(S_{DB} / S_{LB} + 1)} \quad (4-11)$$

Dividing Equation 4-10 by 4-11 gives the ratio ϕ_A / ϕ_B as follows:

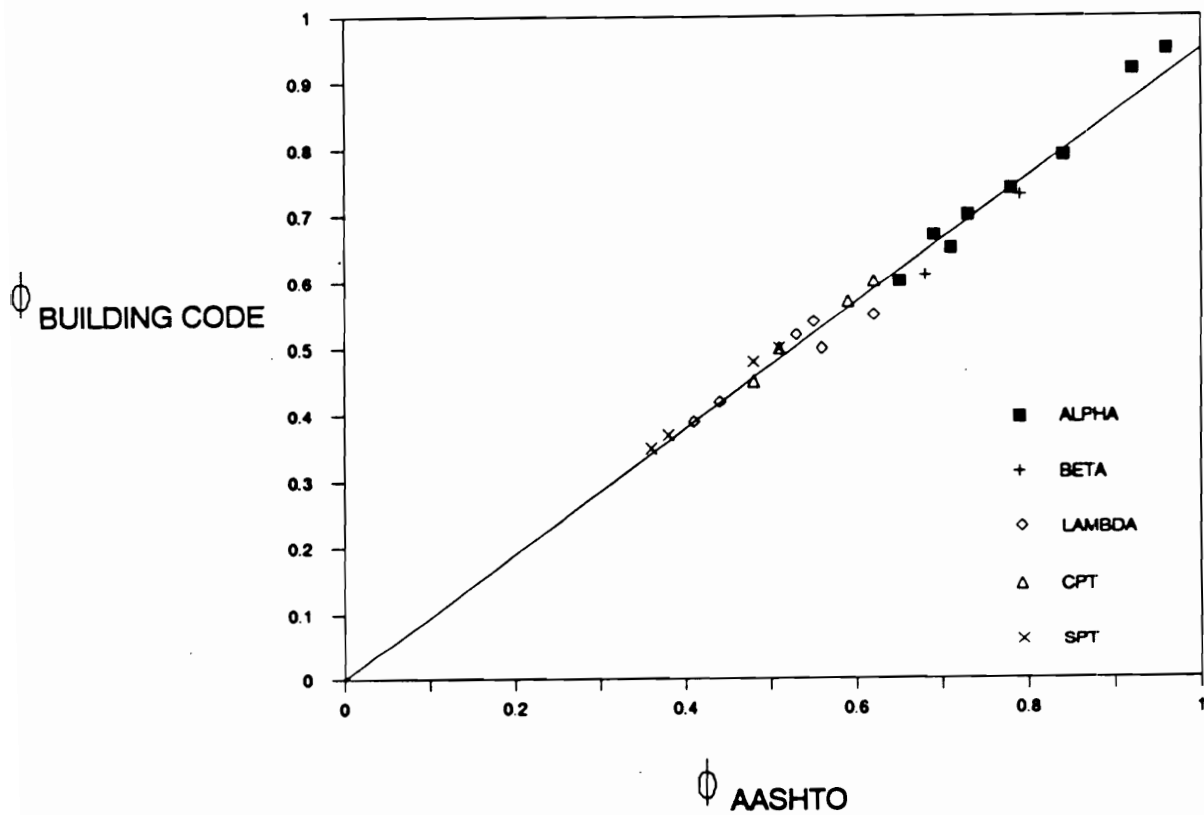


Figure 4.3 Comparison of Performance Factors for Building Code with Performance Factors for AASHTO - Driven Piles

$$\frac{\phi_A}{\phi_B} = \frac{\gamma_{DA} S_{DA}/S_{LA} + \gamma_{LA}}{\gamma_{DB} S_{DB}/S_{LB} + \gamma_{LB}} \frac{S_{DB}/S_{LB} + 1}{S_{DA}/S_{LA} + 1} \quad (4-12)$$

If Code A refers to AASHTO and Code B refers to the building code (ASCE Standard 7-88, 1990), then Equation 4-12 becomes:

$$\frac{\phi_A}{\phi_B} = \frac{1.3 S_{DA}/S_{LA} + 2.17}{1.2 S_{DB}/S_{LB} + 1.6} \frac{S_{DB}/S_{LB} + 1}{S_{DA}/S_{LA} + 1} \quad (4-13)$$

If $S_{DA}/S_{LA} = 3.7$ and $S_{DB}/S_{LB} = 2.0$, Equation 4-13 yields $\phi_B = 0.9\phi_A$. Using linear regression, the equation of the straight line in Fig. 4.3 is $\phi_{\text{Building Code}} = 0.95\phi_{\text{AASHTO}}$.

The above exercise demonstrates that once the calibration procedure has been carried out for one code, it is easy to use the results and extend it to any other code provided that the statistics for the loads are not significantly different.

4.1.4.4 Other Performance Factors

Performance factors for driven piles including those that have not been calibrated using reliability theory are summarized in this section for the AASHTO code. The corresponding performance factors for the building code are between 0.9 and 0.95 times the values of performance factors for bridges.

Table 4.7 summarizes the performance factors for driven piles including those for ultimate limit states that were not calibrated using reliability theory. The bases for the selection of the performance factors that were derived from the reliability-based calibration procedure are presented below.

End Bearing of Piles in Clay. The factor of safety for the end bearing capacity of piles in clay typically varies between 2 and 3. Skempton's (1951) equation for end bearing has been tried and tested and found to work well in practice. Moreover, the end bearing of piles in saturated clay is usually only a small percentage of the total pile capacity. Thus it would be appropriate to use the smaller factor of safety of 2 when determining the performance factor by fitting with working stress design. The corresponding value of ϕ using Equation 2-41, $S_D/S_L = 3.7$, $\gamma_D = 1.3$, and $\gamma_L = 2.17$, is approximately 0.7.

End Bearing of Piles in Sand. This method refers to the effective stress method of estimating end bearing capacity of piles in sand (Kulhawy et al., 1983) that requires an estimation of the friction angle (usually from in situ tests). The performance factors for the CPT and SPT methods are 0.55 and 0.45 respectively. Additional uncertainties

Table 4.7 Summary of Performance Factors for Driven Piles Under Axial Load

	METHOD/SOIL/CONDITION		PERFORMANCE FACTOR
ULTIMATE BEARING CAPACITY OF SINGLE PILES	SKIN	α -method	$\phi_{qs} = 0.70$
	FRICTION	β -method	$\phi_{qs} = 0.50$
		λ -method	$\phi_{qs} = 0.55$
		Clay (Skempton, 1951)	$\phi_{qp} = 0.70$
	END BEARING	Sand (Kulhawy, 1983) ϕ from CPT	$\phi_{qp} = 0.45$
		ϕ from SPT	$\phi_{qp} = 0.35$
		Rock (Canadian Geotech. Society, 1985)	$\phi_{qp} = 0.50$
	SKIN FRICTION	SPT-method	$\phi_q = 0.45$
	AND	CPT-method	$\phi_q = 0.55$
	END BEARING	Load Test	$\phi_q = 0.80$
Pile Driving Analyzer		$\phi_q = 0.70$	
BLOCK FAILURE	Clay	$\phi_g = 0.65$	
UPLIFT CAPACITY OF SINGLE PILES	α -method	$\phi_u = 0.60$	
	β -method	$\phi_u = 0.40$	
	λ -method	$\phi_u = 0.45$	
	SPT-method	$\phi_u = 0.35$	
	CPT-method	$\phi_u = 0.45$	
	Load Test	$\phi_u = 0.80$	
GROUP UPLIFT CAPACITY	Sand	$\phi_{ug} = 0.55$	
	Clay	$\phi_{ug} = 0.55$	

are involved when estimating the friction angle from cone resistance and SPT blow counts. Therefore, the performance factors must be reduced as follows: if the friction angle is estimated from CPT data, then $\phi = 0.45$, and if the friction angle is estimated from SPT data, then $\phi = 0.35$, i.e. the performance factor is equal to that for the in situ method of predicting pile capacity, less 0.1.

End Bearing of Piles in Rock. (See Equations 2-25 and 2-26). The Canadian Geotechnical Society (1985) recommends a factor of safety of 3 for their method. The corresponding performance factor calculated using Equation 2-41, $S_D/S_L = 3.7$, $\gamma_D = 1.3$, and $\gamma_L = 2.17$, is approximately 0.5.

Capacity of Piles from Load Test. Pile load tests provide one of the most reliable estimates of pile capacity. A high value of performance factor is thus warranted. The value selected is 0.8 which corresponds to a factor of safety of approximately 1.9.

Pile Driving Analyzer. Careful monitoring of pile installation with the pile driving analyzer allows the use of a higher value of performance factor than those for the static methods, but a lower value than that for the load test. Thus, a performance factor of 0.7 is recommended if

the pile driving analyzer is used by competent personnel to monitor the pile driving.

Block Failure of Pile Groups in Clay. If the pile spacing is small enough, pile groups can fail as a unit consisting of the piles and the block of soil contained within the piles. Piles are usually spaced at 2.5 to 4 pile diameters apart (center-to-center). Block failure is seldom critical at large spacings, and a performance factor of 0.65 corresponding to a factor of safety of 2.3 appears to be appropriate.

Uplift Capacity of Piles and Pile Groups. Performance factors for uplift capacity of piles and pile groups should be lower than those for axial compression because (a) the diameter and thus, the area of the pile shaft decreases in tension due to the Poisson effect, thereby making uplift capacity smaller than compressive load capacity, and (b) piles in tension unload the soil, which reduces the overburden effective stress and hence the uplift skin friction resistance of the pile. Therefore, performance factors for uplift capacity are lower than those for axial compression by 0.1.

4.2 Single Drilled Shafts

4.2.1 Introduction

In this section, the results of the code calibration for drilled shafts is discussed. The load statistics are described in Section 4.1.3. Statistics for the capacity of drilled shafts are presented, and the results of the reliability analysis are summarized. Finally, the selection of target reliability indices and performance factors is discussed for both bridges and buildings.

4.2.2 Resistance Statistics

Methods for designing drilled shaft foundations that were considered include Reese and O'Neill's (1988) total stress method for drilled shafts in clays, and two methods of predicting side resistance of drilled shafts socketed in rock (Section 2.1.3).

Resistance statistics for these methods are summarized in Table 4.8. Statistics for the model error shown in Table 4.8 have been compiled from data of load tests on drilled shafts in clays (Reese and O'Neill, 1988), while those for drilled shafts socketed in rock are based on load test data reported by Horvath and Kenney (1979). The values of bias

Table 4.8 Summary of statistics for axial capacity of drilled shafts

Correction	Reese & O'Neill		Horvath & Kenney		Carter & Kulhawy	
	Mean	COV	Mean	COV	Mean	COV
Model Error	1.04	0.147	1.65	0.369	1.62	0.459
Systematic Error	1.02	0.098	1.00	0.200	1.00	0.200*
Inherent Spatial Variability	1.00	$\frac{1}{\sqrt{Z}}$	1.00	$\frac{0.490}{\sqrt{Z}}$	1.00	$\frac{0.984^{**}}{\sqrt{Z}}$

* Estimated value

** Based on a point c.o.v. of the uniaxial compressive strength of 0.44 (After Savely, 1987) and a scale of fluctuation of 5 ft.

factor and c.o.v. for inherent spatial variability and systematic error are also listed in Table 4.8.

As discussed previously in Section 2.1.3.2, five methods [Touma and Reese (1974), Meyerhof (1976), Quiros and Reese (1977), Reese and Wright (1977), and Reese and O'Neill (1988)] have been used for estimating the side resistance and end bearing capacities of drilled shafts in sands and gravels. Comparison of these methods shows that they may result in widely divergent estimates of capacity for the same conditions. Unfortunately, the information available from field load tests at present is insufficient to enable determination of resistance statistics for drilled shafts in sands and gravels. Thus, these methods have not been calibrated using reliability theory.

4.2.3 Results of Calibration

4.2.3.1 Reliability Indices

Values of reliability indices versus length of drilled shaft for the three methods (Reese and O'Neill's method, Horvath and Kenney's method, and Carter and Kulhawy's method) are shown in Fig. 4.4 (lognormal method) and Fig. 4.5 (advanced method). The graph at the top is for a dead to live load ratio of 1, while the dead to live load ratio is 3.7 for the bottom graph. Once again, reliability

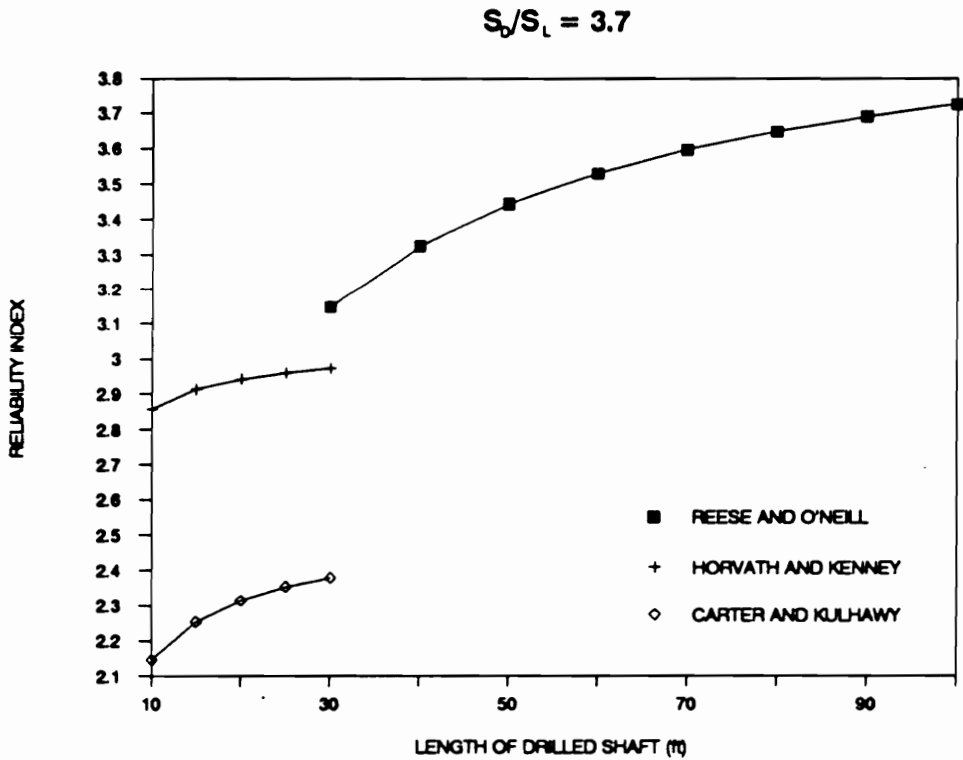
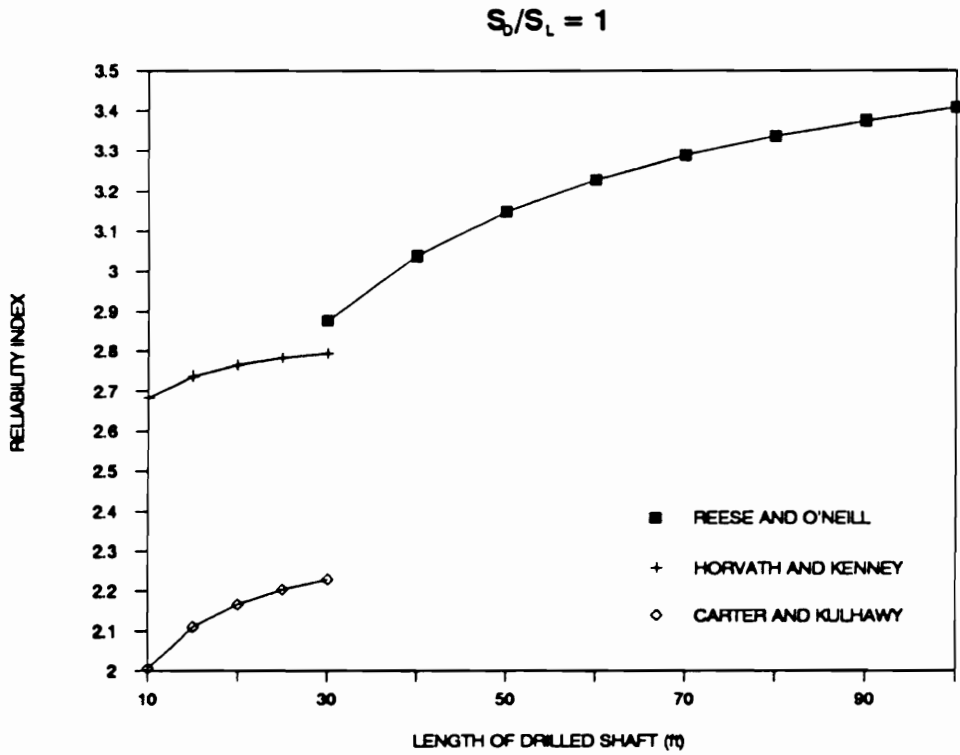


Figure 4.4 Reliability Index Versus Length of Drilled Shaft for Lognormally Distributed Load and Resistance

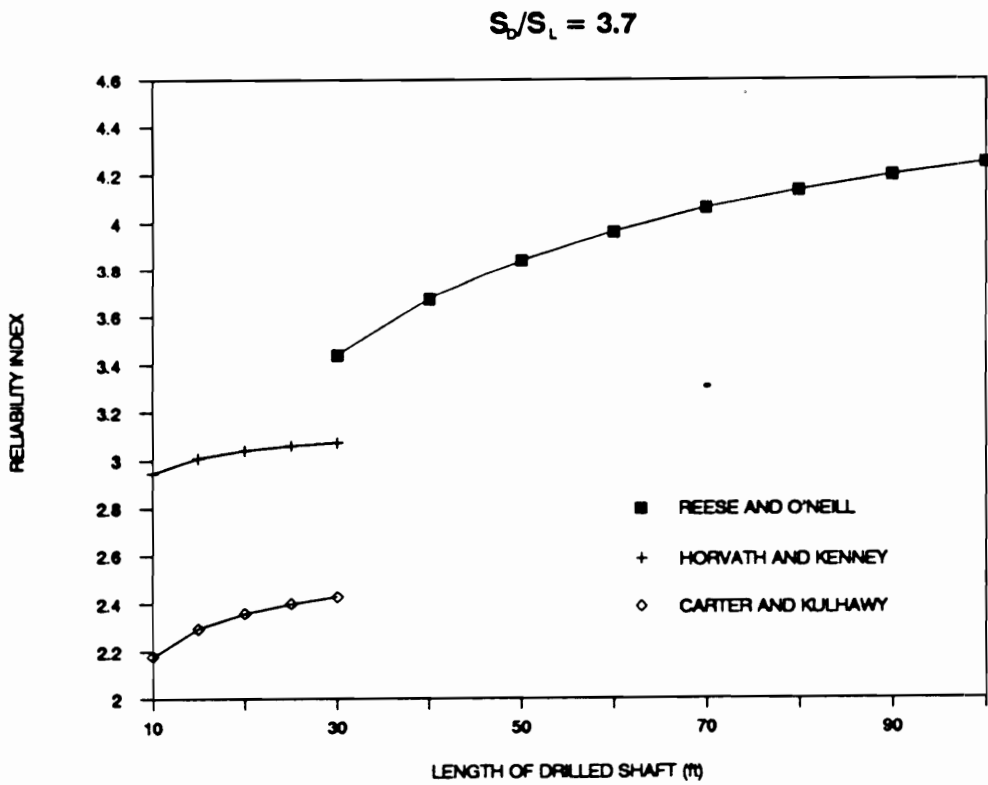
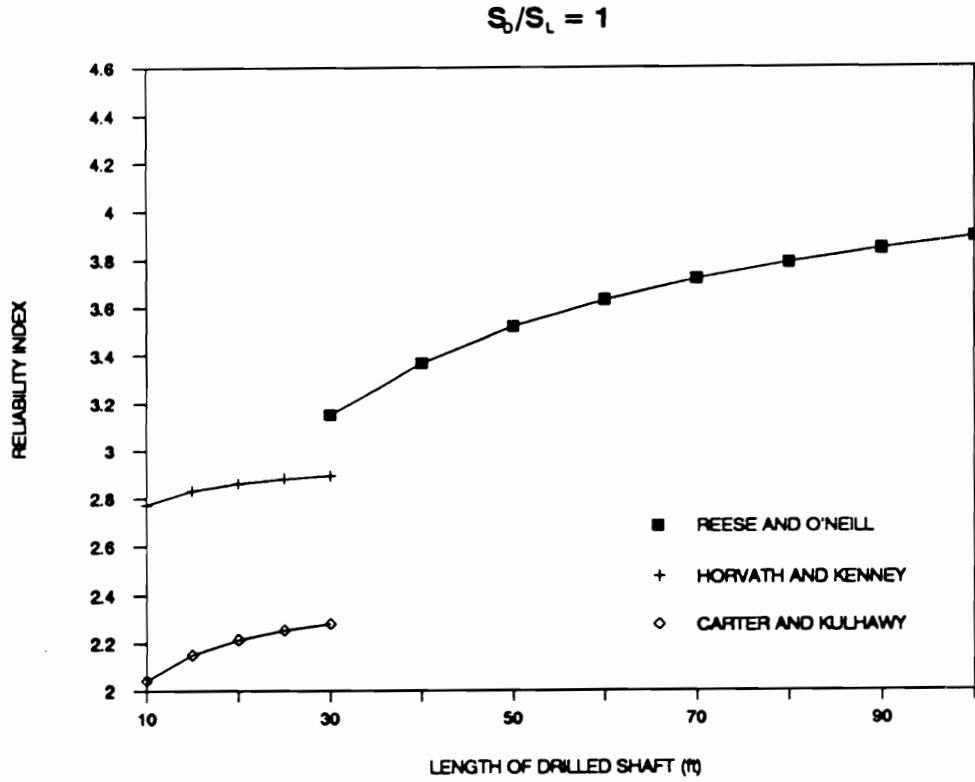


Figure 4.5 Reliability Index Versus Length of Drilled Shaft Using the Advanced Method

indices for drilled shafts in bridges are similar to those for buildings because the uncertainty in the resistances constitutes a larger percentage of the total uncertainty, i.e. the reliability indices are fairly insensitive to the load statistics.

Based on the results of the reliability analysis, the following observations are made:

- 1) Reliability indices for Reese and O'Neill's total stress method vary between 2.9 and 3.7 for the lognormal method, and between 3.1 and 4.3 for the advanced method.
- 2) Reliability indices for Horvath and Kenney's method are higher than those for Carter and Kulhawy's method. This is due to the higher c.o.v. for inherent spatial variability in Carter and Kulhawy's method. In Horvath and Kenney's method, the shaft resistance varies with the square root of the uniaxial compressive strength of the rock (Equation 2-24), while in Carter and Kulhawy's method, the shaft resistance varies linearly with the uniaxial compressive strength of the rock (Equation 2-23). Evaluating the c.o.v. of the side resistance using first-order-second-moment theory indicates that the c.o.v. of the square root of a random variable is half the c.o.v. of that random variable.

4.2.3.2 Target Reliability Indices

Reliability indices for drilled shafts are summarized in Table 4.9. For the lognormal format, the values of reliability index range from 2.0 to 3.7. For the advanced method, the reliability indices vary from 2.0 to 4.3. Thus, a target reliability index between 2.5 and 3.0 may be appropriate for the design of drilled shafts. It should be noted that a slightly higher value was selected for the target reliability index for individual drilled shafts as compared to driven piles since drilled shafts are frequently used individually, as well as in groups.

4.2.3.3 Performance Factors

Performance factors for the three methods obtained from the reliability based calibration using a target reliability index of 2.5 are shown in Table 4.10.

Bridges

The performance factors recommended for design are based on a dead to live load ratio of 3.7, and are given as follows:

Table 4.9 Summary of reliability indices for drilled shafts

Ratio of Dead to Live Load	Lognormal	Advanced
1.0	2.0-3.4	2.0-3.9
3.7	2.1-3.7	2.2-4.3

Table 4.10 Performance factors for drilled shafts obtained from reliability-based calibration with a target reliability index of 2.5

Bridges

Pile Length	Reese & O'Neill	Horvath & Kenney	Carter & Kulhawy
$\beta_T = 2.5$			
10 ft	-	0.70	0.49
30 ft	0.72	0.73	0.56
100 ft	0.80	-	-
$\beta_T = 3.0$			
10 ft	-	0.56	0.37
30 ft	0.62	0.59	0.43
100 ft	0.71	-	-
Selected	0.65	0.65	0.55

Buildings

Pile Length	Reese & O'Neill	Horvath & Kenney	Carter & Kulhawy
$\beta_T = 2.5$			
10 ft	-	0.66	0.47
30 ft	0.64	0.69	0.54
100 ft	0.70	-	-
$\beta_T = 3.0$			
10 ft	-	0.51	0.35
30 ft	0.53	0.54	0.41
100 ft	0.59	-	-
Selected	0.60	0.60	0.50

1) For estimating drilled shaft capacities in clays using Reese and O'Neill's method, the performance factor is recommended to be 0.65.

2) Horvath and Kenney's method should have a higher performance factor (0.65) than Carter and Kulhawy's method (0.55) for reasons explained in Section 4.2.3.1.

Buildings

The performance factors recommended for design are based on a dead to live load ratio of 2. It has been shown in Section 4.1.4.3 that the performance factors for buildings are approximately 0.9 times the values for bridges. The values of performance factor in the bottom half of Table 4.10 reflect this fact. A comparison of the performance factors for buildings with those for bridges is shown in Fig. 4.6. Using linear regression, the equation of the line was found to be $\phi_{\text{Building Code}} = 0.91\phi_{\text{AASHTO}}$.

Due to the lack of field data, it is not possible at present to determine which of the methods of predicting drilled shaft capacities in sands and gravels is most reliable and most generally applicable. It is therefore, not also possible to determine with precision, what values of performance factors should be used for drilled shafts in sands and gravels. Accordingly, the best procedure appears

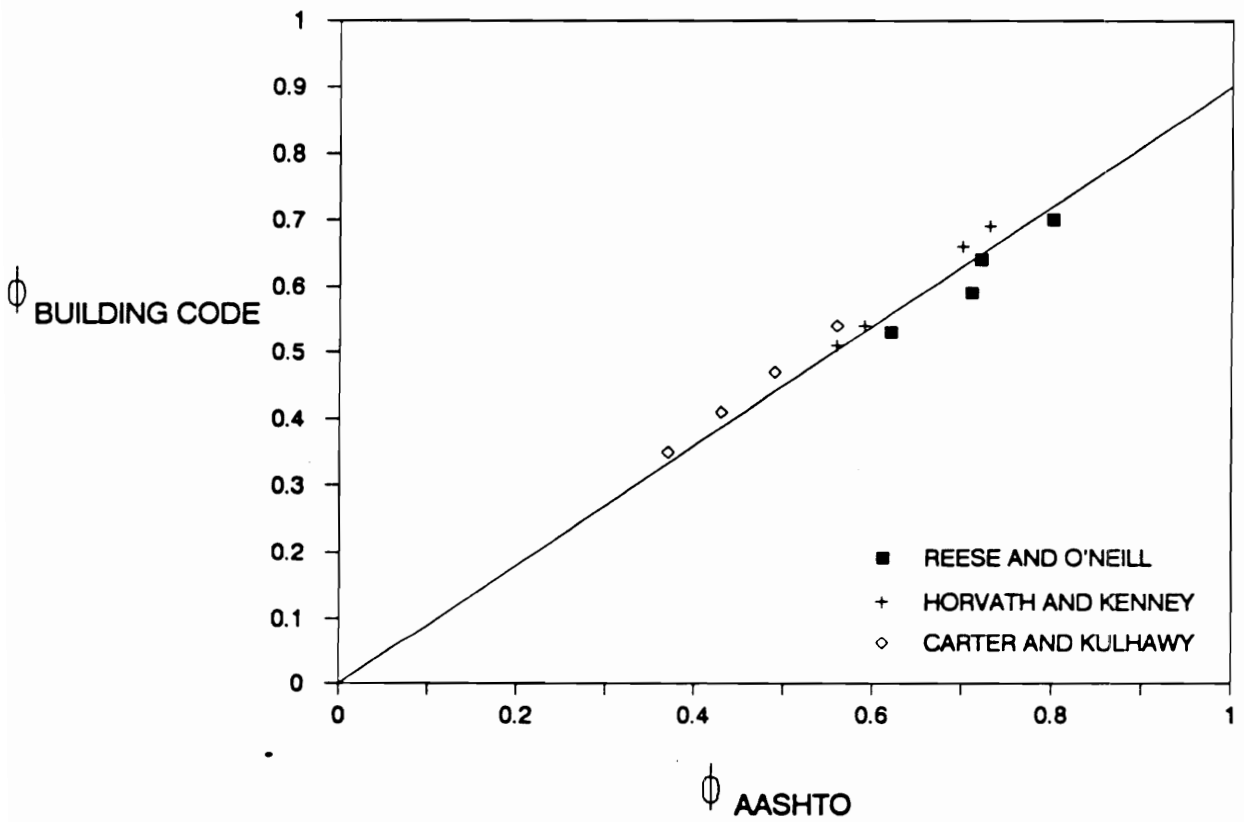


Figure 4.6 Comparison of Performance Factors for Building Code with Performance Factors for AASHTO - Drilled Shafts

to be to estimate the capacity using judgment, and any available experience with similar conditions. The large variability of the capacities of drilled shafts in sand logically suggests that values of performance factors for shafts in sands should be smaller than for shafts in clay.

4.2.3.4 Other Performance Factors

Performance factors for drilled shafts are summarized in Table 4.11 for the AASHTO code only. As discussed previously, corresponding values of performance factors for the building code are approximately 0.9 times the values in Table 4.11.

Table 4.11 also shows values of performance factors for ultimate limit states other than those for which performance factors were obtained by the reliability based calibration procedure. The bases for the selection of these performance factors are given below.

Side Resistance of Drilled Shafts in Clay. This method refers to the effective stress or β method for drilled shafts in clay proposed by Stas and Kulhawy (1984). There is considerable uncertainty in the estimation of the coefficient of lateral earth pressure and therefore, a

Table 4.11 Summary of performance factors for drilled shafts under axial loads

	METHOD/SOIL/CONDITION	PERFORMANCE FACTOR	
ULTIMATE BEARING CAPACITY OF SINGLE DRILLED SHAFTS	SIDE RESISTANCE IN CLAY	α -method (Reese & O'Neill) β -method (Stas & Kulhawy)	0.65 0.50
	BASE RESISTANCE IN CLAY	Total Stress (Reese & O'Neill) Effective Stress (Stas & Kulhawy)	0.55 0.45
	SIDE RESISTANCE IN SAND	1) Touma & Reese 2) Meyerhof 3) Quiros & Reese 4) Reese & Wright 5) Reese & O'Neill	See Discussion in Section 4.2.3.3
	BASE RESISTANCE IN SAND	1) Touma & Reese 2) Meyerhof 3) Quiros & Reese 4) Reese & Wright 5) Reese & O'Neill	See Discussion in Section 4.2.3.3
	SIDE RESISTANCE IN ROCK	Carter & Kulhawy Horvath and Kenney	0.55 0.65
	BASE RESISTANCE IN ROCK	Canadian Geotechnical Society Pressuremeter Method (Canadian Geotech. Society, 1985)	0.50 0.50
	SIDE RESISTANCE & END BEARING	Load Test	0.80
	BLOCK FAILURE	Clay	0.65

Table 4.11 Continued

	METHOD/SOIL/CONDITION	PERFORMANCE FACTOR
UPLIFT CAPACITY OF SINGLE DRILLED SHAFTS	CLAY α -method (Reese & O'Neill)	0.55
	β -method (Stas & Kulhawy)	0.40
	Belled Shafts	0.50
	SAND 1) Touma & Reese 2) Meyerhof 3) Quiros & Reese 4) Reese & Wright 5) Reese & O'Neill	See Discussion in Section 4.2.3.3
ROCK	Carter & Kulhawy	0.45
	Horvath & Kenney	0.55
	Load Test	0.80
GROUP UPLIFT CAPACITY	Sand	0.55
	Clay	0.55

performance factor of 0.5 (similar to the β method for piles) is appropriate.

Base Resistance of Drilled Shafts in Clay. This method refers to the effective stress method for estimating base resistance of drilled shafts in clay by Stas and Kulhawy (1984). The settlement required to mobilize base resistance is larger than that required to mobilize side resistance. Moreover, the movement required to mobilize the base resistance is proportional to the diameter of the base, and the diameter of the base of a drilled shaft can be relatively large. Thus, a lower value of performance factor (0.45) for base resistance of drilled shafts in clay using the effective stress method is recommended.

Base Resistance of Drilled Shafts in Rock. Refer to Equations 2-25 and 2-26 (Canadian Foundation Engineering manual, 1985). The value of performance factor recommended is 0.5, which is the same value that is recommended for driven piles corresponding to a safety factor of 3. The Canadian Foundation Engineering Manual also recommends a safety factor of 3 for the pressuremeter method of estimating base resistance of drilled shafts in rock. Therefore, the performance factor for the pressuremeter method is also recommended to be 0.50.

Uplift Resistance of Belled Shafts in Clay. This refers to the method of predicting the uplift capacity of drilled shafts with an enlarged base assuming that the bell behaves as an anchor (Yazdanbod et al., 1987). A safety factor of 3 is warranted for this method, and the corresponding value of performance factor is recommended to be 0.5.

Performance factors for the bearing capacity of drilled shafts obtained from load tests, block failure of groups of drilled shafts in clays and uplift capacity of groups of drilled shafts are the same as those for driven piles. The performance factors for the static methods of estimating uplift capacity of single drilled shafts from soil parameters are the same as those for axial compression in Table 4.11, less 0.1. The rationale for this is the same as for piles, i.e. because:

- (a) the diameter, and thus the area of the shaft decreases in tension due to the Poisson effect, thereby making uplift capacity smaller than compressive load capacity, and
- (b) shafts in tension unload the soil, which reduces the overburden effective stress and hence the uplift skin friction resistance of the drilled shaft.

It has been shown that reliability analysis can be used for calibrating methods of predicting capacities of deep

foundations with existing codes. However, the calibration results should also be coupled with engineering judgment and experience so as not to compromise on actual trends in practice.

4.3 Groups of Piles or Drilled Shafts

The choice of a global factor of safety in WSD involves a fairly large degree of empiricism. Often values of safety factor are selected based on experience. Calibration of codes in LFD format relies on this choice of safety factor, and on the load and resistance statistics, which may sometimes be difficult to evaluate because of a lack of data.

The procedure for evaluating the probability of failure of a group of piles or drilled shafts is even more involved in that many other factors have to be considered. Some of these factors can be illustrated by means of the following example (Rojiani, 1989).

A group of four piles (Fig. 4.7) is acted on by a normally distributed load with a mean value of 320 kips and a standard deviation of 20 kips. The mean bearing capacity of each pile is 140 kips with a standard deviation of 20 kips.

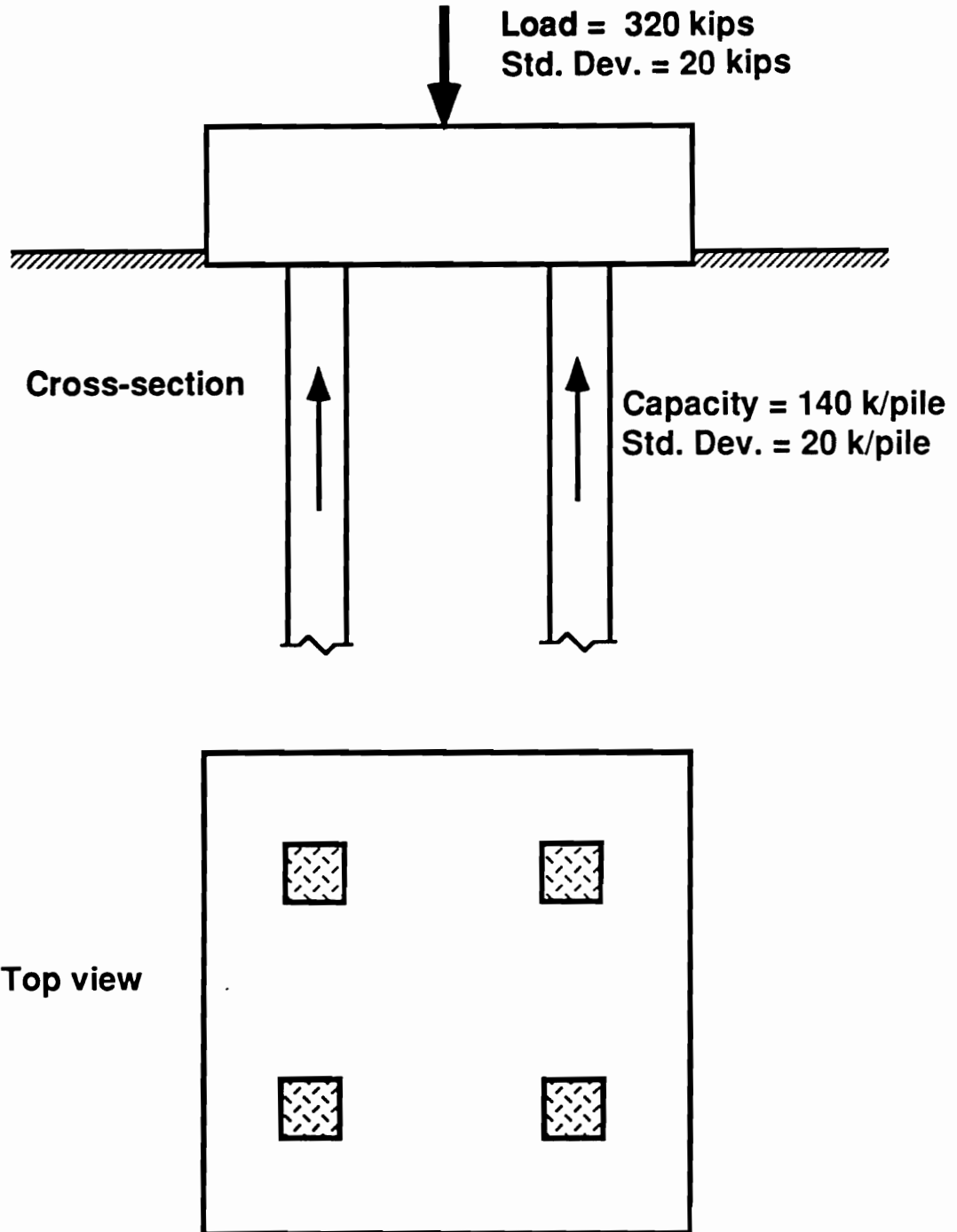


Figure 4.7 Example Problem for Probability of Failure of Pile Groups

The probability of failure of one pile can be calculated as follows:

Mean load on each pile = $320/4 = 80$ kips

Standard deviation of the load on each pile = $20/4 = 5$ kips

Using Equation 2-49, the probability of failure of one pile is

$$\begin{aligned}
 P_f &= 1 - \phi \left[\frac{140 - 80}{\sqrt{20^2 + 5^2}} \right] \\
 &= 1 - \phi[2.91] \\
 &= 1 - 0.998193 \\
 &= 0.001807
 \end{aligned}$$

A group of piles can be modeled either as a series system or as a parallel system. A series system is only as strong as its weakest link, i.e. failure of any one pile constitutes failure of the group. Failure of a parallel system, however, requires failure of all the piles. Another assumption that must be made pertains to the correlation between individual piles. If F_i denotes failure of pile i , and S_j denotes survival of pile j , then the probability of failure of a group of piles with uncorrelated capacities that behaves as a series system can be calculated as follows:

$$\begin{aligned}
 P_f &= P[F_1S_2S_3S_4] + P[S_1F_2S_3S_4] + P[S_1S_2F_3S_4] + P[S_1S_2S_3F_4] \\
 &= 4(0.001807)(0.998193)^3 \\
 &= 0.00719
 \end{aligned}$$

If the capacities are perfectly correlated and the four pile group is modeled as a series system, then if one pile fails, the whole group will fail. The probability of failure of such a pile group is evaluated as follows:

$$\begin{aligned}
 P_f &= P[F_1F_2F_3F_4] \\
 &= P[F_1/F_2F_3F_4]P[F_2/F_3F_4]P[F_3/F_4]P[F_4] \\
 &= (1)(1)(1)(0.001807) \\
 &= 0.001807
 \end{aligned}$$

In order to evaluate the probability of failure of a parallel system of piles, expressions for the mean and variance of the resistance must first be evaluated. The expressions are as follows:

$$\text{Total capacity of 4 piles } R = R_1 + R_2 + R_3 + R_4$$

Mean value of R,

$$\begin{aligned}
 \bar{R} &= \bar{R}_1 + \bar{R}_2 + \bar{R}_3 + \bar{R}_4 \\
 &= 4(140) \\
 &= 560 \text{ kips}
 \end{aligned}$$

Variance of R

$$\begin{aligned}
 \sigma_R^2 &= \sigma_{R1}^2 + \sigma_{R2}^2 + \sigma_{R3}^2 + \sigma_{R4}^2 + 2\text{COV}[R_1R_2] + 2\text{COV}[R_1R_3] + \\
 &\quad 2\text{COV}[R_1R_4] + 2\text{COV}[R_2R_3] + 2\text{COV}[R_2R_4] + 2\text{COV}[R_3R_4]
 \end{aligned}$$

$$\begin{aligned}
&= \sigma_{R1}^2 + \sigma_{R2}^2 + \sigma_{R3}^2 + \sigma_{R4}^2 + 2\rho_{R1R2}\sigma_{R1}\sigma_{R2} + \\
&\quad 2\rho_{R1R3}\sigma_{R1}\sigma_{R3} + 2\rho_{R1R4}\sigma_{R1}\sigma_{R4} + 2\rho_{R2R3}\sigma_{R2}\sigma_{R3} + \\
&\quad 2\rho_{R2R4}\sigma_{R2}\sigma_{R4} + 2\rho_{R3R4}\sigma_{R3}\sigma_{R4}
\end{aligned}$$

where $\text{COV}[X,Y]$ is the covariance of X and Y, defined as the expected value of the products of $(X - \bar{X})$ and $(Y - \bar{Y})$, and ρ_{XY} is the coefficient of correlation between X and Y, defined as:

$$\rho_{XY} = \frac{\text{COV}[X,Y]}{\sigma_X\sigma_Y} \quad (4-14)$$

where σ_X and σ_Y are the standard deviations of X and Y respectively. If the pile capacities are uncorrelated, $\rho_{RiRj} = 0$.

$$\bar{R} = 560 \text{ kips}$$

$$\begin{aligned}
\sigma_R^2 &= \sigma_{R1}^2 + \sigma_{R2}^2 + \sigma_{R3}^2 + \sigma_{R4}^2 \\
&= 4(20)^2 \\
&= 1600
\end{aligned}$$

$$\sigma_R = 40 \text{ kips}$$

The probability of failure of the same group of four piles assuming that the capacities are statistically independent, and that the pile group behaves as a parallel system can be evaluated as follows:

$$\begin{aligned}
 P_f &= 1 - \phi \left[\frac{\bar{R} - \bar{S}}{\sqrt{\sigma_R^2 + \sigma_S^2}} \right] \\
 &= 1 - \phi \left[\frac{560 - 320}{\sqrt{40^2 + 20^2}} \right] \\
 &= 1 - \phi[5.37]
 \end{aligned}$$

$$P_f = 0.0000000415$$

If the pile capacities are perfectly correlated, $\rho_{R_i R_j} = 1$.

$$\begin{aligned}
 \sigma_R^2 &= 4(20)^2 + 2(1)(20)(20)6 \\
 &= 6400 \\
 \sigma_R &= 80 \text{ kips}
 \end{aligned}$$

The probability of failure, assuming a parallel system of piles and perfect correlation in the pile capacities, can be calculated as follows:

$$\begin{aligned}
 P_f &= 1 - \phi \left[\frac{560 - 320}{\sqrt{80^2 + 20^2}} \right] \\
 &= 1 - \phi[2.91]
 \end{aligned}$$

$$P_f = 0.001807$$

The results of these calculations are summarized below:

	CORRELATED	INDEPENDENT
SERIES	0.00181	0.00719
PARALLEL	0.00181	0.0000000415

It is clear from the results of these calculations that one of the important issues that must be considered when evaluating the probability of failure of a group of piles is the degree to which the capacities are correlated. Perfect correlation between piles in both series and parallel systems implies that if one pile fails, then all the other piles will fail too. The group failure probability in the case of perfect correlation between piles thus reduces to the probability of failure of a single pile. In reality, the occurrence of perfect correlation is highly unlikely.

The opposite of perfect correlation is complete statistical independence. In this case, the assumption of whether the pile group behaves as a parallel (ductile) or a series (brittle) system is important. Failure of one pile in a ductile system will mean that the additional load is redistributed to the other piles, and if a second pile fails, the load will be further redistributed to the remaining piles, and so on. Failure of the group will only occur if the last surviving pile fails. The other extreme is the brittle system where some feature in the pile group exists that has the effect that as soon as the first pile fails, all of the other piles will fail immediately.

In the example above, the assumption of statistical independence in the piles yields a probability of failure of a brittle system that is 5 orders of magnitude higher than a

ductile system. The question of whether piles are perfectly correlated versus statistically independent, or whether the group is ductile as opposed to brittle, is thus extremely important with regard to evaluating the group failure probability. Such large differences in the probability of failure are clearly significant.

The problem of pile group failure is further complicated by the nature of failure itself. Failure of groups of piles can take one of several forms:

(1) Plunging failure may be preceded by settlement, which can constitute an unacceptable mode of behavior. Therefore safety and failure is not a "black or white" issue. What constitutes failure depends also on the amount of settlement that can be tolerated by the structure.

(2) Piles bearing on sound rock can fail structurally, which brings into consideration other reliability issues and other statistical data.

(3) Groups of piles that are closely spaced can fail as a block containing the piles and the soil between the piles. This mode of failure is not governed by the statistics relating to the individual pile capacities.

(4) Pile groups that are founded in a strong stratum overlying a weaker layer can fail by punching into the weaker layer.

Therefore, the example problem above is a simplified view of actual behavior.

Factors that would make a pile group tend to a series system as opposed to a parallel system, and factors that would make the piles tend to be correlated as opposed to be statistically independent are examined. Some of these factors include the following:

- 1) properties of the structural elements (eg. rigidity of the pile cap)
- 2) properties of the soil which can influence the rate of pore pressure dissipation
- 3) magnitude and eccentricity of the load
- 4) geometric positions of the piles in the group
- 5) installation effects such as driving order and vertical alignment of the piles, and
- 6) interaction of cap and soil.

SERIES VERSUS PARALLEL

An example of a series system of piles would be one in which failure of one pile causes failure of the surrounding soil, then failure of neighboring piles, and ultimately the failure propagates until the whole group fails (i.e. progressive type of failure). A pile group that was load tested by O'Neill et al. (1982) behaved in this way. The

soil was an overconsolidated slickensided clay. It would therefore be reasonable to assume that pile groups in overconsolidated clays with inherent planes of weaknesses such as slickensides, or heavily jointed clays that undergo strain softening, or highly sensitive or structured clays are more likely to behave as series systems.

CORRELATED VERSUS UNCORRELATED

Factors that influence the correlation between piles include:

1) Variability of Soil Properties - The variability of soil is influenced by its mode of formation. Calm-water sedimentary deposits for instance, will very likely exhibit fairly uniform properties. On the other hand, residual soils will more likely have random and erratic properties, typified by pockets of weak and strong materials. It seems reasonable to expect a higher correlation between the capacities of piles if the group is in a uniform soil than if it is in a nonuniform soil deposit.

2) Rate of Pore Pressure Dissipation - The rate of pore pressure dissipation is a function of the soil properties such as permeability and compressibility, and the geometry and boundary conditions of the flow regime.

O'Neill (1983) argued that pore pressures dissipate at a much slower rate around pile groups than around single piles. The more piles there are in the group, the slower the rate of dissipation. Flaate (1972) found that pore pressures dissipate at a much slower rate around interior piles than around exterior piles. Since pile capacities are related to the effective stresses, the capacities of the corner piles would be expected to be highest soon after driving, followed by the edge and interior piles. A pile group constructed in cohesive soils would therefore exhibit low correlation between the capacities of its piles if it were loaded prior to complete dissipation of pore pressures.

3) Eccentricity of the Loads - Most piles in an axially loaded pile group carry compressive loads. However, some piles, especially those furthest away from the point of application of the load, may carry uplift forces if the eccentricity is large. While piles in compression derive their resistances from downward skin friction and end bearing, piles in tension derive their resistances from upward skin friction, soil suction and the weight of the pile. It is therefore reasonable to assume that there might be little correlation between piles in tension and piles in compression, because the sources of contribution to the resistances are different.

4) Pile Alignment - Piles in a group that are all vertical will be expected to have a higher correlation than those in which the piles are driven out of plumb. Thus it is also reasonable to assume that there will be a higher correlation in a group of vertical piles than a group of batter piles.

5) Driving Order - Model and full scale tests on pile groups in cohesive soils [Whitaker (1957) and O'Neill et al. (1982)] indicate that the order of driving affects the distribution of loads to the piles. This effect in pile groups in cohesive soils can be seen in Fig. 4.8, where driving orders A and B are those for the model tests conducted by Whitaker (1957), while driving order C is that of a full scale load test conducted by O'Neill et al., (1982).

The effects of driving order of piles in cohesive soils are also related to the magnitude of the loads, as indicated in Table 4.12. At low loads, a correlation exists between the loads in the piles since the gradients of the curves in Fig. 4.8 are all fairly constant. At higher loads, the curves cross over each other in groups A and C, thereby obscuring the correlation between piles. However, pile group B exhibited a constant correlation in loads carried by piles, even when the load was approaching the failure load.

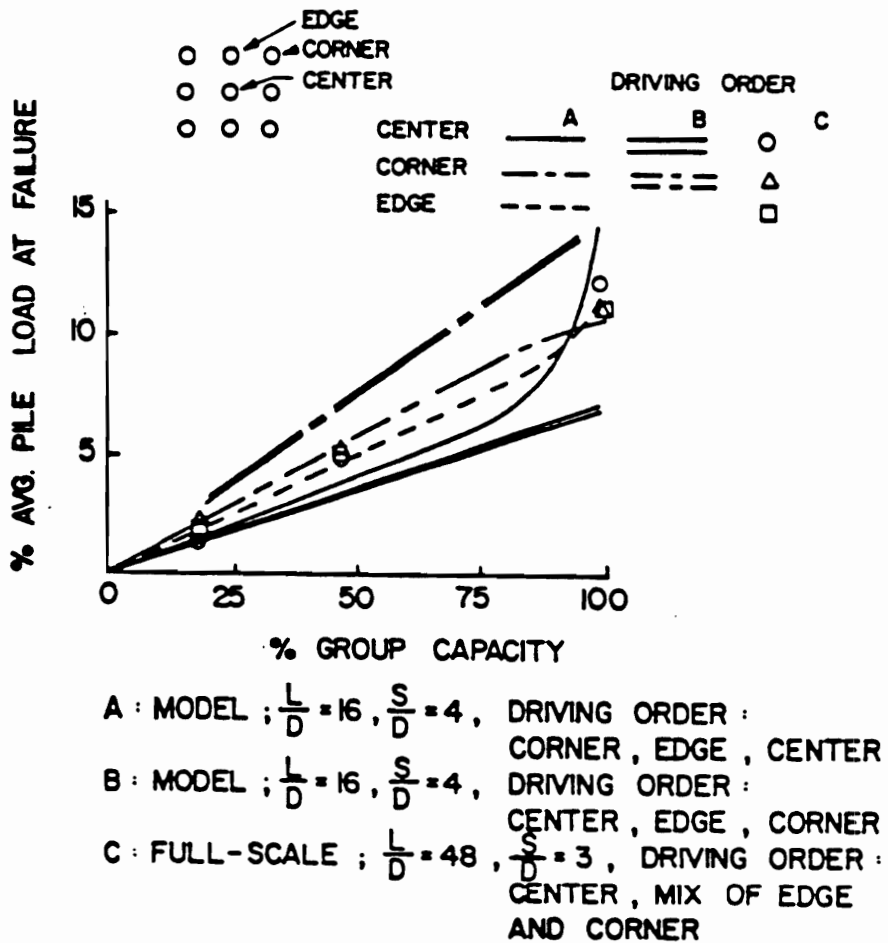


Figure 4.8 Clay: Driving Order and Load Level Effects on Load Distribution in Piles in Pile Groups (From O'Neill, 1983)

Table 4.12 Degree of correlation between piles as related to pile driving order and magnitude of loads

		DRIVING ORDER	
		"Outside-In" Group A	"Inside-Out" Group B
MAGNITUDE OF LOADS	Small	High	High
	Large	Low	High*

* Except for pile groups in overconsolidated slickensided soils (such as Group C) that have a tendency to behave as a series system.

Pile group C was driven in an overconsolidated slickensided clay. Although driving order C was similar to driving order B, the excess pore pressures dissipated so quickly during and immediately after installation that the load distribution in group C resembled that of group A, i.e. the center piles carried the most load when failure was imminent. O'Neill and Hawkins (1983) explained that this effect was brought about by progressive failure in group C, where the corner piles failed first. The failure then propagated to the other piles. As discussed earlier, a progressive type of failure implies that the pile group behaves as a series system.

Load tests on pile groups in sands indicate that the load on the center piles are always the highest, irrespective of whether the piles are driven "outside-in" [See Fig. 4.9, Kishida (1967)], "inside-out" [See Fig. 4.9, Beredugo (1966)] or whether the piles are installed simultaneously [Vesic (1969)].

6) Interaction of Cap and Soil - Contact of the cap with the soil can increase the load carrying capacity of the group. The implication of cap-soil contribution to group capacity is that any correlation that exists between resistances of individual piles is inaccurate if the contribution of the cap is not considered. In fact, the

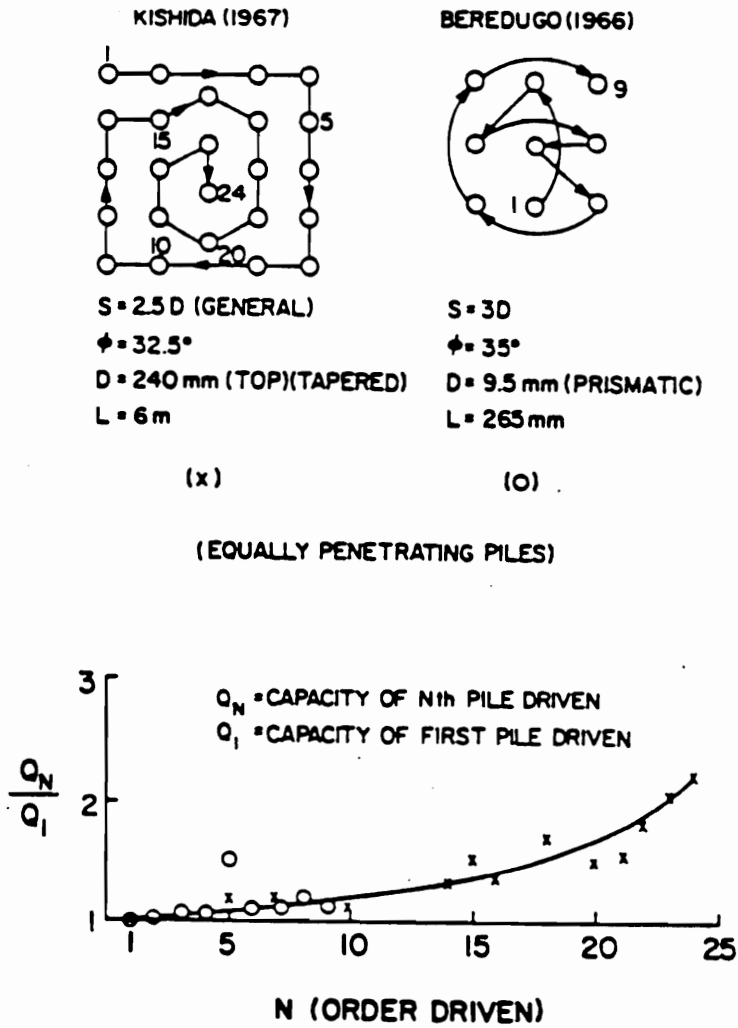


Figure 4.9 Sand: Driving Order Effects on Load Distribution in Piles in Pile Groups (From O'Neill, 1983)

contribution of the cap-soil interaction is usually ignored in conventional practice.

There currently exist no rational guidelines for determining whether a pile group tends to behave as a series system or a parallel system of piles, and for determining the degree of correlation between piles in pile groups. Even though these concepts cannot be quantified accurately, an attempt has been made above to present them in a qualitative manner.

CHAPTER FIVE

SUMMARY AND CONCLUSIONS

The studies described herein have been concerned with the development of simplified procedures for analyzing laterally loaded deep foundations, and the development of performance factors that can be used in load factor design of axially loaded deep foundations.

The simplified procedure for analyzing laterally loaded deep foundations began with development of a computer program, PGROUPD. This program uses the Evans and Duncan (1982) procedure, which simulates p-y analyses, to estimate deflections and maximum bending moments in single fixed-head piles and drilled shafts. Group deflections are estimated through the Focht and Koch (1973) procedure in the program, while bending moments in the group are obtained by softening the soil until the single pile deflection matches the group deflection (Duncan, 1988). The bending moment in the group is then approximated as the value of the single pile moment in the softened soil.

The computer program PGROUPD was used to develop charts for estimating deflections and maximum bending moments in some of the more common types of single fixed-head piles and drilled shafts. It was also used to perform parametric studies of a large number of groups of piles and drilled

shafts. Based on the results of these analyses, simple formulae for estimating group deflections and moments were derived. These simple formulae will enable engineers to analyze and design groups of deep foundations more quickly.

The simplified procedure was then used to analyze four well-documented and well-instrumented pile group load tests. Two of the groups were in cohesive soils, and two were in cohesionless soils.

The results of the lateral load tests on fixed-head pile groups conducted by Kim et al. (1976) were compared to those calculated using the simplified procedure. Studies were made on two groups with pile spacings of 3.7 and 5 diameters. Comparison of the results showed that measured values of deflections and moments in the group with the smaller pile spacing agreed well with the calculated values. The results of the calculations were also reasonable for the group with the larger pile spacing at low magnitude of loads. However, the moments and deflections were overestimated by 100% at high loads.

Studies were also made on a load test conducted by Holloway et al. (1981) on a group of timber piles connected by a cap 3 ft above ground. In terms of calculated single pile deflections, the behavior of a pile fixed 3 ft above ground was found to be intermediate between a fixed-head pile and a free-head pile. The single pile deflections and

moments for this boundary condition were estimated using p-y analyses as well as an approximate procedure that was developed from beam theory and the Evans and Duncan nonlinear superposition procedure. They were then amplified to those for the group using the simplified procedure. Comparison of the measured and calculated values of group deflection showed that the simplified procedure overestimated the group deflections by 95% at low loads, but the calculated and measured group deflections agreed very well at high values of load. The bending moments were overestimated by as much as 35%. These results are satisfactory considering that the simplified procedure was developed for fixed-head pile groups, and that the load deflection response indicated that the piles may be yielding structurally.

A third load test on a group of nine steel pipe piles in Beaumont clay was conducted by Brown et al. (1987). Single free-head pile deflections and moments were estimated using the Evans and Duncan procedure, and amplified to values for the group using the simplified procedure discussed above. Comparison of the measured and calculated values showed that the group deflections and moments were in good agreement.

A fourth load test on the same nine-pile group was conducted by Brown et al. (1988) after excavating the

Beaumont clay and compacting sand around the piles. Analysis of the group behavior using the simplified procedure yielded values of group deflections and maximum bending moments that were conservative. This may be due to the fact that the cyclic nature of the loads could have led to densification of the sand and thus reduced values of group deflections and moments.

It can be concluded based on the results of the analysis of the four case histories that the newly developed simplified procedure provides a method of analyzing pile groups that gives either fairly accurate values of group deflections and moments, or values that are conservative.

Studies were also made to develop performance factors for load factor design of axially loaded driven piles and drilled shafts. An overall performance factor that is applied to the resistance side of the LFD equation can be obtained through reliability analysis. Statistics for methods of calculating pile and drilled shaft capacities and statistics for the loads were obtained. Reliability indices were calculated for these methods to determine the levels of reliability inherent in current designs. Target reliability indices were then selected and used to obtain performance factors for several methods of estimating pile and drilled shaft capacities.

The probability of failure of groups of piles and drilled shafts was also examined. Through an example of a four pile group (Rojiani, 1989), it was found that the probability of failure can differ greatly depending on whether the capacities are correlated or uncorrelated, and whether the group behaves as a series or a parallel system.

5.1 Recommendations for Future Research

5.1.1 Deep Foundations Under Lateral Load

The case histories analyzed have shown that the simplified procedure for fixed-head piles and drilled shafts can be used effectively to analyze and design laterally loaded groups of deep foundations. However, out of the four case histories, only one was a fixed-head group of piles. Additional load tests on groups of fixed-head piles would provide valuable additional information.

The simplified procedure does not indicate the distribution of load among the piles in a group. Evans and Duncan (1982) and Brown et al. (1987 and 1988) have shown that in a laterally loaded group, the piles in the leading row carry more load than the rear piles whereas methods based on the theory of elasticity indicate symmetrical distribution of loads (eg. Focht and Koch, 1973). Further research into the mechanism of load transfer through the

soil and cap in pile groups is required so that a more reliable method for estimating load distribution among piles can be developed.

Although no distinction is correctly made between groups of piles and drilled shafts in analyses of lateral load effects, the two different methods of installation for piles and drilled shafts can result in significantly different post-construction in situ stresses and soil properties. Improved models of soil behavior that account for installation effects are required in order to develop more reliable methods for estimating the behavior of deep foundations under lateral loads.

5.1.2 Deep Foundations Under Axial Load

A shortage of load test data has prevented a comprehensive review of the reliability of methods for estimating drilled shaft capacities in cohesionless soils. Additional well-instrumented and well-documented load tests will be valuable to the profession as they will allow a better assessment of the current state-of-the-art.

Groups of piles or drilled shafts with uncorrelated capacities can have widely divergent values of probability of failure depending on whether the group is assumed to be a series or a parallel system. Studies on quantifying the

degree to which pile or drilled shaft capacities in a group are correlated versus uncorrelated, and on quantifying the tendency of a group to behave as a series or a parallel system are needed before fully rational assessments of the probability of failure can be made.

REFERENCES

- American Association of State Highway and Transportation Officials, "Standard Specifications for Highway Bridges", Fourteenth Edition, 1989.
- American Concrete Institute, "Building Code Requirements for Reinforced Concrete", ACI, Detroit, 1983 and 1989.
- American Institute for Steel Construction, "Load and Resistance Factor Design Specification for Structural Steel Buildings", 1986.
- American Society of Civil Engineers, "Minimum Design Loads for Buildings and Other Structures", ASCE Standard 7-88, ASCE, 1990, 94 pp.
- Ang A.H.S. and Tang W.H., "Probability Concepts in Engineering, Planning and Design", Vol. 2, John Wiley and Sons, New York, 1984, 562 pp.
- Baecher G.B., Marr W.A., Lin J.S and Consla J., "Critical Parameters for Mine Tailings Embankment", Report to U.S. Bureau of Mines under contract J0215028, U.S. Dept. of Commerce, National Technical Information Service, 1983, 282 pp..
- Bazaraa A.R.S., "Use of the Standard Penetration Test for Estimating Settlements of Shallow Foundations on Sand", PhD Thesis, Univ. of Illinois Urbana-Champaign, Dept. of Civil Eng., 1967.
- Beatty C.I., "Lateral Test on Pile Groups", Foundation Facts, Vol. VI, No. 1, 1970, pp. 18-21.
- Beredugo Y.O., "An Experimental Study of the Load Distribution in Pile Groups in Sand", Canadian Geotechnical Journal, Vol. 3, August 1966, pp. 145-166.
- Bienawski Z.T., "Rock Mechanics Design in Mining and Tunneling, A.A. Balkema: Rotterdam/Boston, 1984, 272 pp.
- Bogard D. and Matlock H., "Procedures for Analysis of Laterally Loaded Pile Groups in Soft Clay", Proc., Specialty Conf. on Geotechnical Eng. in Offshore Practice, ASCE, April 1983, pp. 499-535.

- Bolton M., "Limit State Design in Geotechnical Engineering", Ground Engineering, Vol. 14, No. 6, September 1981, pp. 39-46.
- Briaud J.L. and Tucker L., "Coefficient of Variation of In Situ Tests in Sand", Probabilistic Characterization of Soil Properties, Proceedings sponsored by the ASCE GED, May 1984, pp. 119-139.
- Brown D.A. and Reese L.C., "Behavior of a Large-Scale Pile Group Subjected to Cyclic Lateral Loading", Geotechnical Engineering Report GR85-12, Geotechnical Engineering Center, Bureau of Engineering Research, Austin, Texas, May 1985, 399 pp.
- Brown D.A., Reese L.C. and O'Neill M.W., "Cyclic Lateral Loading of a Large Scale Pile Group", ASCE, JGED, Vol. 113, No. 11, November, 1987, pp. 1326-1343.
- Brown D.A., Morrison C. and Reese L.C., "Lateral Load Behavior of Pile Group in Sand", ASCE, JGED, Vol. 114, No. 11, November, 1988, pp. 1261-1276.
- Canadian Geotechnical Society, "Canadian Foundation Engineering Manual", 2nd Edition, Bitech Publishers Ltd., 1985, 460 pp.
- Carter J.P. and Kulhawy F.H., "Analysis and Design of Foundations Socketed into Rock", EPRI Report No. EL-5918, New York, 1988, 158 pp.
- Danish Geotechnical Institute, "Code of Practice for Foundation Engineering", 3rd Edition, DS 415, Bulletin No. 36, 1985, 53 pp.
- Davisson M.T., "High Capacity Piles", Innovations in Foundation Construction, Soil Mech. Division, Illinois Section, ASCE, Chicago, 1973, pp. 81-112.
- Deere D.V., "Geological Considerations", Chapter 1 in Rock Mechanics in Engineering Practice by K.G. Stagg and O. C. Zienkiewicz, John Wiley and Sons, Inc., New York, 1968, pp 1-20.
- Donald I.B., Sloan S.W. and Chiu H.K., "Theoretical Analysis of Rock Socketed Piles", Proc., Int. Conf. on Structural Foundations on Rock, Sydney, Balkema: Rotterdam, 1980.

- Duncan J.M., "Class Notes for Deep Foundation Course - CE 5530", Virginia Polytechnic Institute and State University, Spring 1988.
- Ellingwood B., Galambos R.V., MacGregor J.G. and Cornell C.A., "Development of a Probability Based Load Criterion for American National Standard A58", National Bureau of Standards, Dept. of Commerce, Washington D.C., Special Publication 577, 1982, 222 pp.
- Esrig M.I. and Kirby R.C., "Advances in General Effective Stress Method for the Prediction of Axial Capacity for Driven Piles in Clay", Eleventh Annual Offshore Technology Conference, Procs. Paper No. OTC 3406, May 1979, pp. 437-443.
- Evans L.T., "Bearing Piles Subjected to Horizontal Loads", Symposium on Lateral Load Tests on Piles, ASTM, STP 154, 1953, pp. 30-35.
- Evans Jr. L.T. and Duncan J.M., "Simplified Analysis of Laterally Loaded Piles", UC Berkeley Rept. No. UCB/GT/82-04, July, 1982, 245 pp.
- Feagin L.B., "Lateral Pile-Loading Tests", Transactions, ASCE, Vol. 63, No. 8, 1937, pp. 236-254.
- Feagin L.B., "Lateral Load Tests on Groups of Battered and Vertical Piles", Symposium on Lateral Load Tests on Piles, ASTM, STP 154, 1953, pp. 12-20.
- Fellenius B.H., Samson L. and Tavenas F., "Geotechnical Guidelines - Pile Design", Public Works Canada, Marine Works Sector, Ottawa Ontario K1A 0M2, Canada, August 1989.
- Flaate K., "Effects of Pile Driving in Clays", Canadian Geotechnical Journal, Vol. 9, February 1972, pp. 81-88.
- Fleming W.G.K., Weltman A.J., Randolph M.F. and Elson W.K., "Piling Engineering", Surrey University Press, Glasgow, 1985, 380 pp.
- Focht J.A. and Koch K.J., "Rational Analysis of the Lateral Performance of Offshore Pile Groups", Proc. of the Fifth Annual Offshore Technology Conference, Houston, Texas, Vol. 2, Paper OTC 1896, 1973, pp. 701-708.
- Gleser S.M., "Lateral Load Tests on Vertical Fixed-Head and Free-Head Piles", Symposium on Lateral Load Tests on Piles, ASTM, STP 154, 1953, pp. 75-93.

- Grigoriu M.D., Kulhawy F.H., Spry M.J. and Filippas O.B., "Probabilistic Site Strategy for Transmission Lines", Foundations for Transmission Line Towers (GSP-8), ASCE, 1987, pp. 1-14.
- Grouni H.N. and Nowak A.S., "Calibration of the Ontario Bridge Design Code 1983 Edition", Canadian Journal of Civil Engineering, Vol. 11, No. 4, Nov. 1984, pp. 760-770.
- Hansell V.C. and Viest I.M.V., "Load Factor Design for Steel Highway Bridges", AISC Engineering Journal, October, 1971.
- Heins C.P. and Firmage D.A., "Design of Modern Steel Highway Bridges", John Wiley and Sons, New York, 1979, 463 pp.
- Holloway D.M., Moriwaki Y., Finno R.J. and Green R.K., "Lateral Load Response of a Pile Group in Sand", Proc., 2nd Int. Conf. on Numerical Methods in Offshore Piling, I.C.E., London, 1981, pp. 441-456.
- Horvath R.G. and Kenney T.C., "Shaft Resistance of Rock Socketed Drilled Piers", Proc., Symposium on Deep Foundations, ASCE, Atlanta, Georgia, 1979, pp. 182-214.
- Horvitz G.E., Stettler D.R. and Crowser J.C., "Comparison of Predicted and Observed Pile Capacity", Proc. Cone Penetration Testing and Experience (ASCE), St. Louis, Missouri, October 1981, pp. 413-433.
- Jamiolkowski M., "Behavior of Laterally Loaded Pile Groups", Proc., 6th European Conf. on Soil Mech. and Found. Eng., Vol. 2, Int. Society for Soil Mech. and Found. Eng., London, March 1976, pp. 165-169.
- Kim J.B. and Brungraber R.J., "Full-Scale Lateral Load Tests of Pile Groups", ASCE JGED, Vol. 102, No. GT1, January 1976, pp. 87-105.
- Kishida H., "Ultimate Bearing Capacity of Piles Driven into Loose Sand", Soils and Foundation, Vol. VII, No. 3, 1967, pp. 20-27.
- Kulhawy F.H., Trautmann C.H., Beech J.F., O'Rourke T.D. and McGuire W., "Transmission Line Structure Foundations for Uplift-Compression Loading", EPRI Rept. EL-2870, Electric Power Research Institute, 1983.

- Kulkarni K.R., Chandrasekaran V.S. and King G.J.W., "Centrifugal Model Studies on Laterally Loaded Pile Groups in Sand", Proc. Eleventh Int. Conf. on Soil Mech. and Found. Eng., San Francisco, Vol. 1, 1985, pp. 1113-1116.
- Liao S.S.C. and Whitman R.V., "Overburden Correction Factors for SPT in Sand", JGED, ASCE, Vol. 112, No. 3, March 1986, pp. 373-377.
- Lunne T. and Christoffersen H.P., "Interpretation of Cone Penetrometer Data for Offshore Sands", Norwegian Geotechnical Institute Publication 156, 1985, pp. 1-12.
- Manoliu I., Botea E. and Constantinescu A., "Behavior of Pile Foundations Submitted to Lateral Loads", Proc., 9th Int. Conf. on Soil Mech. and Found. Eng., Tokyo, Vol. 1, 1977, pp. 637-640.
- Matlock H. and Reese L.C., "Foundation Analysis of Offshore Pile Supported Structures", Proc. Fifth Int. Conf. on Soil Mech. and Found. Eng., Vol. 2, 1961, pp. 91-97.
- Matlock H., Ingram W.B., Kelley A.E. and Bogard D., "Field Tests of the Lateral Load Behavior of Pile Groups in Soft Clay", Proc., 12th Annual Offshore Technology Conf., OTC 3871, Houston, Tx, May 1980.
- McClelland B. and Focht J.A. Jr., "Soil Modulus for Laterally Loaded Piles", Transactions, ASCE, Vol. 123, 1958, pp. 1049-1063.
- Meyerhof G.G., "Safety Factors in Soil Mechanics", Canadian Geotechnical Journal, Vol. 7, No. 4, November 1970, pp. 349-355.
- Meyerhof G.G., "Bearing Capacity and Settlement of Pile Foundations", JGED, ASCE, Vol. 102, No. GT3, March 1976, pp. 197-228.
- Moses F. and Ghosn M., "A Comprehensive Study of Bridge Loads and Reliability", Report No. FHWA/OH-85-005, Dept. of Civ. Eng., Case Western Reserve Univ., January 1985, 189 pp.
- Nogami T., "Dynamic Stiffness and Damping of Pile Groups in Inhomogeneous Soils", ASCE STP on Dynamic Response of Pile Foundations: Analytical Aspect, 1980, pp. 31-52.

- Nogami T., "Dynamic Group Effect in Axial Response of Grouped Piles", ASCE, JGED, Vol. 109, No. GT2, February 1983, pp. 228-243.
- Nogami T. and Chen H.L., "Simplified Approach for Axial Pile Group Response Analysis", ASCE, JGED, Vol. 110, No. GT9, September 1984, pp. 1239-1256.
- Nottingham L. and Schmertmann J., "An Investigation of Pile Capacity Design Procedures", Final Report D629 to Florida Dept. of Transportation from Dept. of Civil Engineering, Univ. of Florida, Sept. 1975, 159 pp.
- O'Halloran J., "The Lateral Load Capacity of Timber Pile Groups", Symposium on Lateral Load Tests on Piles, ASTM, STP 154, 1953, pp. 52-57.
- O'Neill M.W., "Group Action in Offshore Piles", Proceedings of the Conference on Geotechnical Practice in Offshore Engineering, University of Texas at Austin, April 1983, pp. 25-64.
- O'Neill M.W., "Reliability of Pile Capacity Assessment by CPT in Overconsolidated Clay", Proc. In Situ '86, Blacksburg, Virginia, June, 1986, pp. 237-256.
- O'Neill M.W., Ghazzaly O.I. and Ha H.B., "Analysis of Three-Dimensional Pile Groups with Non-Linear Soil Response and Pile-Soil-Pile Interaction", Proc. of the 9th Annual Offshore Technology Conference, Houston, May 1977, pp. 245-256.
- O'Neill M.W. and Hawkins R.A., "Pile-Head Behavior of Rigidly Capped Pile Group", Transportation Research Record, Transportation Research Board, Washington D.C., 1983.
- O'Neill M.W., Hawkins R.A. and Mahar L.J., "Load Transfer Mechanisms in Piles and Pile Groups", ASCE, JGED, Vol. 108, No. GT12, December 1982, pp. 1605-1623.
- O'Neill M.W. and Tsai C.N., "An Investigation of Soil Nonlinearity and Pile-Soil Pile Interaction in Pile Group Analysis", Research Rept. No. UHUC 84-9, Dept. of Civil Eng., Univ. of Houston, Nov. 1984, prepared for US Army Engineer Waterways Experiment Station, Vicksburg, Miss.

- Ontario Highway Dept., "Ontario Highway Bridge Design Code", 2nd Edition, Ministry of Transportation and Communication, Highway Engineering Division, Toronto, Ontario, 1983, 357 pp.
- Orchant C.J., Kulhawy F.H. and Trautman C.H., "Reliability-Based Foundation Design for Transmission Line Structures", Vol. 2: Critical Evaluation of In Situ Test Methods, Report No. EPRI EL-5507, Cornell Univ., Ithaca, New York, October, 1988.
- Peck R.B., "Rock Foundations for Structures", Proc. ASCE Specialty Conf. on Rock Engineering for Foundations and Slopes, Boulder, Colorado, 1976.
- Peck R.B., Hanson W.E. and Thornburn T.H., "Foundation Engineering", Second Edition, John Wiley and Son, Inc., New York, 1974, 514 pp.
- Poulos H.G., "Behavior of Laterally Loaded Piles: II - Pile Groups", ASCE, JSMFD, Vol. 97, SM5, May 1971, pp. 733-751.
- Poulos H.G. and Davis E.H., "Pile Foundation Design and Analysis", John Wiley and Sons, 1980, 397 pp.
- Prestressed Concrete Institute, "PCI Design Handbook - Precast and Prestressed Concrete", 3rd Edition, Prestressed Concrete Institute, 20 North Wacker Dr., Chicago Il 60606, 1985.
- Quiros G.W. and Reese L.C., "Design Procedures for Axially Loaded Drilled Shafts", Research Rept. 176-5F, Project 3-5-72-176, Center for Highway Research, Univ. of Texas, Austin, December 1977, 156 pp.
- Randolph M.F. and Wroth C.P., "An Analysis of Vertical Deformation of Pile Groups", Geotechnique, Vol. 29, No. 4, 1979, pp. 423-439.
- Reese L.C., "Laterally Loaded Piles: Program Documentation", ASCE JGED, Vol. 103, No. GT4, April 1977, pp. 287-305.
- Reese L.C., "Handbook of Design of Piles and Drilled Shafts Under Lateral Load", U.S. Dept. of Commerce, National Technical Information Services, 1984, 360 pp.
- Reese L.C. and O'Neill M.W., "Drilled Shafts: Construction Procedures and Design Methods", FHWA Publication No. FHWA-HI-88-042 or ADSC Publication No. ADSC-TL-4, August 1988, 564 pp.

- Reese L.C. and Wright S.J., "Drilled Shaft Manual-Construction Procedures and Design for Axial Loading", Vol. 1, U.S. Dept. of Transportation, Implementation Division, HDV-22, Implementation Package 77-21, July 1977, 140 pp.
- Reese L.C., Wright S.G. and Aurora R.P., "Analysis of a Pile Group Under Lateral Loading", Laterally Loaded Deep Foundations: Analysis and Performance, ASTM STP 835, J.A. Langer, E.T. Mosley and C.D. Thompson, Eds., ASTM, 1984, pp. 56-71.
- Robertson P.K. and Campanella R.G., "Intepretation of Cone Penetration Tests, Part 1 and Part 2, Soil Mechanics Series No. 60, Dept. of Civ. Eng., Univ. of British Columbia, May 1983, 80 pp.
- Robertson P.K. and Campanella R.G., "Axial Capacity of Driven Piles in Deltaic Soils Using CPT", Proc. First Int. Symposium on Penetration Testing, Orlando, Florida, March, 1988, pp. 919-928.
- Rojiani K.B., "Class Notes for Reliability of Structures Course - CE 5984", Virginia Polytechnic Institute and State University, Spring 1989.
- Rosenblueth E. and Esteva L., "Reliability Basis for Some Mexican Codes", ACI Publication SP-31, 1972, pp. 1-41.
- Savelly J.P., "Probabilistic Analysis of Intensely Fractured Rock Masses", Proc. of the International Society for Rock Mechanics, Vol. 1, Montreal, 1987, pp. 509-514.
- Schmidt H.G., "Group Action of Laterally Loaded Bored Piles", Proc., 10th Int. Conf. on Soil Mech. and Found. Eng., Vol. 2, Stockholm, 1981, pp. 833-837.
- Seed H.B., "Evaluation of Soil Liquefaction Effects on Level Ground During Earthquakes", ASCE, JGED, Vol. 105, No. 2, Feb. 1979, pp. 201-255.
- Seed H.B. and De Alba P., "Use of SPT and CPT Tests for Evaluating the Liquefaction Resistance in Sands", Proc. In Situ '86, Blacksburg, Virginia, June 1986, pp. 281-302.
- Sidi I.D., "Probabilistic Prediction of Friction Pile Capacities", PhD Thesis, Univ. of Illinois Urbana-Champaign, Dept. of Civ. Eng., 1986, 314 pp.

- Simpson B., Pappin J.M. and Croft D.D., "An Approach to Limit State Calculations in Geotechnics", Ground Engineering, Vol. 14, No. 6, September 1981, pp. 21-28.
- Skempton A.W., "The Bearing Capacity of Clays", Proc. of the Building Research Congress, London, England, Vol. 1, 1951, pp. 180-189.
- Skempton A.W., "Standard Penetration Test Procedures and the Effects in Sands of Overburden Pressure, Relative Density, Particle Size, Ageing and Overconsolidation", Geotechnique 36, No. 3, 1986, pp. 425-447.
- Snyder R. and Moses F., "Load Factor Design for Substructures and Retaining Wall", FHWA Rport No. 79-S0862, 1978, 153 pp.
- Stas C.V. and Kulhawy F.H., "Critical Evaluation of Design Methods for Foundations Under Axial Uplift and Compression Loading", EPRI Report No. EL-3771, November, 1984, 198 pp.
- Tang W.H., "Uncertainties in Offshore Axial Pile Capacity", Proc., Found. Eng.: Current Principles and Practices, Evanston, Illinois, ASCE, June 1989, pp. 833-847.
- Tang W.H., Woodford D.L. and Pelletier J.H., "Performance Reliability of Offshore Piles", 22nd Annual Offshore Technology Conference, Houston, Texas, Paper No. OTC 6379, 1990, pp. 299-308.
- Terzaghi K. and Peck R.B., "Soil Mechanics in Engineering Practice", Second Edition, John Wiley and Sons, New York, 1967, 729 pp.
- Tomlinson M.J., "Pile Design and Construction Practice", A Viewpoint Publication, London, 1987, 415 pp.
- Touma F.T. and Reese L.C., "Behavior of Bored Piles in Sand", ASCE JGED, Vol. 100, No. GT 7, July 1974, pp. 749-761.
- Vanmarcke E.H., "Probabilistic Modeling of Soil Profiles", ASCE JGED, Vol. 103, No. GT11, November, 1977, pp. 1227-1246.
- Vanmarcke E.H., "Random Fields, Analysis and Synthesis", MIT Press, Cambridge, Massachusetts, 1983, 382 pp.

- Vesic A.S., "Experiments with Instrumented Pile Groups in Sand", Performance of Deep Foundations, ASTM STP 444, ASTM, 1969, pp. 177-222.
- Vijayvergiya V.N. and Focht J.A.Jr, "A New Way to Predict Capacity of Piles in Clay", Fourth Annual Offshore Technology Conference, Houston, Texas, Paper No. 1718, 1972, pp. 865-874.
- Whitaker T., "Experiments with Model Piles in Groups", Geotechnique, Vol. VII, December 1957, pp. 147-167.
- Woodward-Clyde Consultants, "Foundation Investigation and Test Program; Locks and Dam 26, Mississippi River, Alton, Illinois", Report Prepared for St. Louis District, U.S. Army Corps of Engineers, 1979.
- Wu T.H., Tang W.H., Sangrey D.A. and Baecher G.B., "Reliability of Offshore Foundations - State of the Art", ASCE JGED, Vol. 115, No. 2, February, 1989, pp. 157-178.
- Yazdanbod A., Sheikh S.A. and O'Neill M.W., "Uplift of Shallow Underream in Jointed Clay", Proc. ASCE, Foundations for Transmission Line Towers, Ed. by Briaud J.L., Atlantic City, New Jersey, April 1987, pp. 110-127.
- Yokel F.Y., "Design Criteria for Shallow Foundations", U.S. Dept. of Commerce, National Institute of Standards and Technology, Gaithersburg, Maryland, November 1989, 49 pp.

APPENDIX A

PGROUPD: A computer program for estimating lateral deflections and maximum bending moments in laterally loaded groups of fixed-head piles and drilled shafts

A1 Introduction

PGROUPD is a computer program written in Microsoft Quick Basic that can be used to calculate the following: (1) lateral deflections of single fixed-head piles or drilled shafts, (2) maximum bending moments in single fixed-head piles or drilled shafts, (3) lateral deflections of groups of fixed-head piles or drilled shafts, and (4) maximum bending moments in groups of fixed-head piles or drilled shafts. The program utilizes the Evans and Duncan (1982) procedure for analyzing laterally loaded single piles and drilled shafts, and the Focht and Koch (1973) procedure for calculating deflections of laterally loaded groups of piles and drilled shafts. The maximum bending moments in groups of piles and drilled shafts are estimated by softening the soil (reducing ϕ' in sands or S_u in clays) until the single pile deflection matches the deflection of the group (Duncan, 1988).

A2 System Requirement

This program runs on any IBM or IBM compatible computer using DOS.

A3 Program Execution

The program is interactive and user friendly. The following procedure is used to run the program:

- 1) Insert the PGROUPD program disk in drive A.
- 2) Type "PGROUPD" followed by "Carriage Return" to run the program.
- 3) Follow the instructions on the screen. The user can select one of several options: (a) create a data file, (b) review a data file, (c) run the program, or (d) return to DOS.
- 4) Upon completion of the execution, select 4 to return to DOS.

A4 Program Operation

The program consists of four modules - a main program and three subroutines: CREATE, REVIEW and PGROUPD. CREATE is the subroutine for creating new data files. REVIEW is the subroutine for reviewing and editing existing data

files. PGROUPD is the subroutine that performs the analysis of laterally loaded piles. The flow diagram for PGROUPD is shown in Fig. A1.

A4.1 Description of Input Data

The program reads the following parameters from the data file:

- 1) Title of the job
- 2) Soil type (sand or clay)
- 3) Lateral load per pile (P_S) - For a group of piles, divide the total lateral load acting on the group by the number of piles.
- 4) Pile width or diameter (D)
- 5) Length of pile (Z)
- 6) Young's modulus of pile (E_p)
- 7) Moment of inertia of pile (I_p)
- 8) Number of piles (N_{pile})
- 9) Coordinates of piles - The user has the option of specifying either the coordinates of every pile, or the number of rows of piles, number of piles per row, and the center-to-center pile spacing if the piles are uniformly spaced. In the latter option, the program will automatically generate the pile coordinates internally based on the information given.

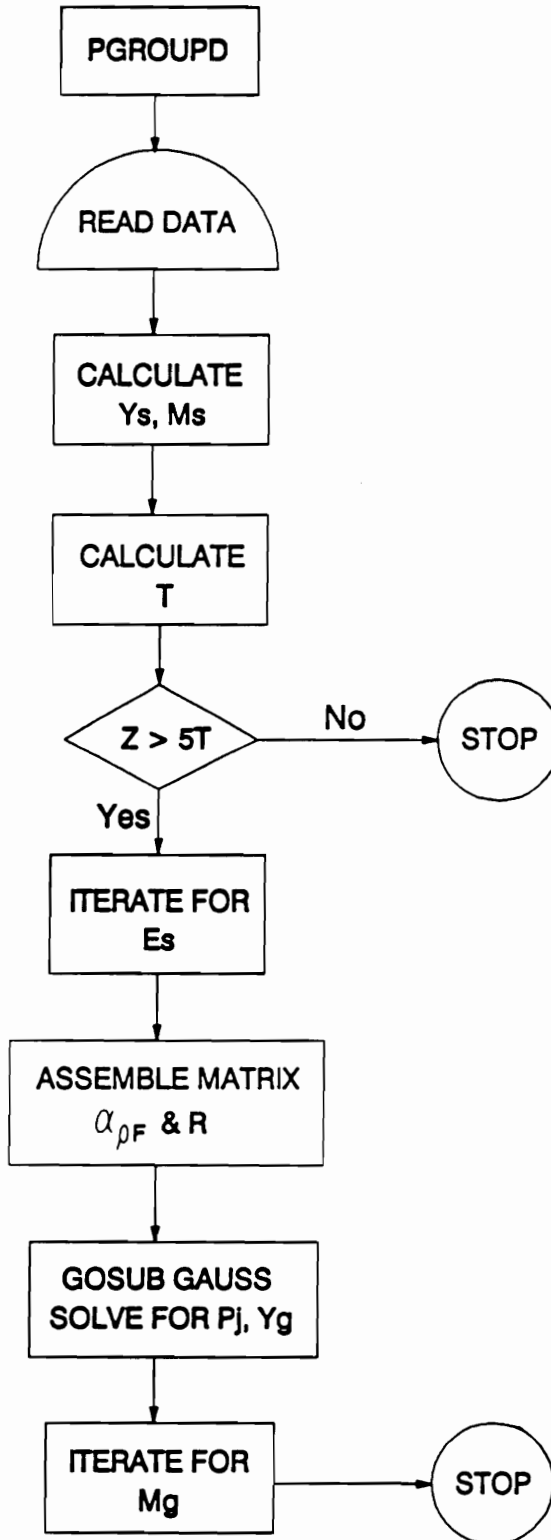


Figure A1 Flow Diagram for Program "PGROUPD"

The orientation of the lateral load is always along the x-direction, which is along the direction of the rows of the piles. If the option of specifying pile coordinates is selected, then they should be specified such that the direction of loading is oriented in the x-direction. If the option of specifying the number of rows of piles, number of piles per row and the pile spacing is chosen, they should be specified such that the direction of loading is oriented along the rows.

Consistent units should be used for all the input data.

A4.2 Estimation of Deflections and Maximum Bending Moments in Single Fixed-Head Piles

The Evans and Duncan procedure for calculating deflections of and maximum bending moments in single fixed-head piles has been described in Section 3.2.1. Single pile deflections are estimated using Fig. 3.1 for sand and Fig. 3.2 for clay. Equations for these curves have been determined by regression analysis and incorporated in the program. These equations are as follows:

$$\text{For sand } \frac{Y_S}{D} = 1.33 \left[\frac{P_S}{P_C} \right] + 149 \left[\frac{P_S}{P_C} \right]^2 \quad (A1)$$

$$\text{For clay } \frac{Y_S}{D} = 0.107 \left[\frac{P_S}{P_C} \right] + 20.3 \left[\frac{P_S}{P_C} \right]^2 \quad (A2)$$

Maximum bending moments are estimated using Fig. 3.10 for sand and Fig. 3.11 for clay. Equations for these curves have also been determined by regression analysis and incorporated in the program. The equations are as follows:

$$\text{For sand } \frac{M_S}{M_C} = 0.482 \left[\frac{P_S}{P_C} \right] + 17.4 \left[\frac{P_S}{P_C} \right]^2 \quad (\text{A3})$$

$$\text{For clay } \frac{M_S}{M_C} = 0.235 \left[\frac{P_S}{P_C} \right] + 2.93 \left[\frac{P_S}{P_C} \right]^2 \quad (\text{A4})$$

A4.3 Estimation of the Characteristic Length of the Soil-Pile System (T)

The Evans and Duncan procedure and the Focht and Koch procedure apply only to long piles (i.e. pile length greater than $5T$, where T is the characteristic length of the soil-pile system). The characteristic length of the soil-pile system (T) can be calculated using the single pile deflection (Y_S) and the following equation (Matlock and Reese, 1961):

$$T = \left[\frac{Y_S E_p I_p}{0.93 P_S} \right]^{1/3} \quad (\text{A5})$$

The criterion that the piles must be long is checked before proceeding with the analysis. If the piles are not long, the program will stop running, and warn the user of the

problem. Alternate design procedures are needed for short piles.

A4.4 Iteration for Soil Modulus

It was discussed in Section 3.3.1 that the group deflection estimated using the Focht and Koch procedure is sensitive to the relative stiffness factor (R), which in turn is sensitive to the soil modulus (E_S). Therefore, one of the most critical part of the analysis is the selection of the value of soil modulus. One advantage of using this program is that an iterative routine described in Section 3.3.1, is incorporated in the program to estimate the soil modulus. The procedure requires the value of the influence factor, $I_{\rho F}$, from Fig. 2.14. Equations for the curves of $I_{\rho F}$ versus the pile flexibility factor ($K_R = E_p I_p / E_S Z^4$), have been obtained through regression analysis. The general form of the equation is as follows:

$$I_{\rho F} = A_0 + A_1 \log_{10} K_R + A_2 (\log_{10} K_R)^2 + A_3 (\log_{10} K_R)^3 + A_4 (\log_{10} K_R)^4 \quad (A6)$$

where A_0 , A_1 , A_2 , A_3 and A_4 are constants. Their values for pile length to diameter ratios (Z/D) of 10, 25, 50 and 100 are given in the table below. For intermediate values of

pile length to diameter ratios, $I_{\rho F}$ is obtained by interpolation in the program.

Z/D	A ₀	A ₁	A ₂	A ₃	A ₄
10	1.11	-0.166	0.159	-0.0529	-0.0677
25	1.30	-0.281	0.193	-0.0280	0.0
50	1.41	-0.363	0.326	0.0463	0.0105
100	1.51	-0.362	0.335	0.0296	0.00975

A4.5 Assembly of the Matrix of Coefficients, $\alpha_{\rho F}$ and R

Equations 3-10 and 3-14 provide a set of ($N_{\text{pile}} + 1$) simultaneous equations which can be solved using matrix techniques. The unknowns are the group deflections (Y_g) and the lateral forces in the piles (P_j). The coefficients in the matrix consist of the interaction factors, $\alpha_{\rho F}$ and the relative stiffness factor, R. R is calculated using Equation 3-12, whereas $\alpha_{\rho F}$ is obtained from Fig. 2.15. Equations for $\alpha_{\rho F}$ versus K_R have been obtained by regression, and they have the following general form:

$$\alpha_{\rho F} = B_0 + B_1 \frac{D}{s} + B_2 \left[\frac{D}{s} \right]^2 + B_3 \left[\frac{D}{s} \right]^3 + B_4 \left[\frac{D}{s} \right]^4 \quad (\text{A7})$$

Values of B_0 , B_1 , B_2 , B_3 and B_4 for values of Z/D of 10, 25 and 100, θ of 0° and 90°, and K_R of 10^{-5} and 0.1, are given in Table A1, where θ is the angle between the direction of

Table A1: Regression coefficients B_0 , B_1 , B_2 , B_3 and B_4

	B_0	B_1	B_2	B_3	B_4
$\theta = 0^\circ$, $K_R = 0.1$ $Z/D = 10$	0.0174	3.02	-7.45	10.8	-6.98
$\theta = 0^\circ$, $K_R = 10^{-5}$ $Z/D = 10$	0.00149	0.938	0.282	-0.570	0.0
$\theta = 0^\circ$, $K_R = 0.1$ $Z/D = 25$	0.0824	4.08	-16.2	33.6	-22.7
$\theta = 0^\circ$, $K_R = 10^{-5}$ $Z/D = 25$	-0.00691	1.77	-1.11	0.0	0.0
$\theta = 0^\circ$, $K_R = 0.1$ $Z/D = 100$	0.244	2.31	-7.68	15.4	-12.1
$\theta = 0^\circ$, $K_R = 10^{-5}$ $Z/D = 100$	0.0394	3.16	-6.56	5.62	0.0
$\theta = 90^\circ$, $K_R = 0.1$ $Z/D = 10$	0.00996	1.55	-1.43	0.0	0.0
$\theta = 90^\circ$, $K_R = 10^{-5}$ $Z/D = 10$	0.0383	-0.500	7.31	-19.6	17.2
$\theta = 90^\circ$, $K_R = 0.1$ $Z/D = 25$	0.0472	2.32	-4.99	4.15	0.0
$\theta = 90^\circ$, $K_R = 10^{-5}$ $Z/D = 25$	0.0249	0.0698	5.98	-17.4	15.7
$\theta = 90^\circ$, $K_R = 0.1$ $Z/D = 100$	0.164	2.05	-6.60	13.4	-11.3
$\theta = 90^\circ$, $K_R = 10^{-5}$ $Z/D = 100$	-0.0203	2.93	-11.1	25.3	-21.8

loading and the line joining the centers of the interacting piles, j and k . For intermediate values of Z/D , θ and K_R , $\alpha_{\rho}F$ is obtained by interpolation.

A Gauss elimination routine is used to solve for the values of Y_g and P_j ($j = 1$ to N_{pile}).

A4.6 Iteration for the Maximum Bending Moment in the Pile Group

Duncan (1988) proposed that the maximum bending moment in the most severely loaded pile in a pile group can be estimated by first obtaining the lateral group deflection through the Focht and Koch procedure, and then softening the soil by reducing S_u for clays or ϕ' for sands, until the group lateral deflection matches the single pile deflection. The corresponding value of maximum moment in that single pile gives a reasonable approximation of the maximum bending moment in the most severely loaded pile in the pile group.

Using softened shear strengths, single pile deflections can be calculated using the Evans and Duncan procedure, described in Section A4.2. The single pile deflections are estimated with the aid of Equation A1 for sand or Equation A2 for clay. A trial and error routine is used in the program to obtain the value of the shear strength, that results in a match between the deflection of the single pile

in a softened soil and the group deflection. Using the value of the "softened" shear strength, the maximum bending moment in a single pile is then estimated with the aid of Equation A3 for sand or Equation A4 for clay. This value of moment is a reasonable approximation of the maximum bending moment in the group.

VITA

Phillip S.K. Ooi was born in Penang, Malaysia, on September 19, 1961. He attended the University of Leeds, England where he received a Bachelor of Science degree in Civil Engineering in July, 1983. In September, 1984, he graduated with a Masters Degree in Civil Engineering from the Massachusetts Institute of Technology.

From 1985 to 1987, he worked as a geotechnical engineer in the design office of the Drainage and Irrigation Department, under the Ministry of Agriculture in Kuala Lumpur, Malaysia. In 1987, he also worked as a lecturer in the Department of Civil Engineering at the University of Malaya, Kuala Lumpur, Malaysia.

Phillip returned to graduate school at Virginia Tech in August, 1987, to study for a doctorate in Civil Engineering. Upon graduating, he will work as a geotechnical engineer with GEI Consultants, Inc. in Winchester, Massachusetts.

Phillip Ooi